LONG-TERM STABILITY OF SORBED PHOSPHORUS BY DRINKING-WATER TREATMENT RESIDUALS: MECHANISMS AND IMPLICATIONS

By

KONSTANTINOS CHRISTOS MAKRIS

A DISSERTATION PRESENTED TO THE GRADUATE SCHOOL
OF THE UNIVERSITY OF FLORIDA IN PARTIAL FULFILLMENT
OF THE REQUIREMENTS FOR THE DEGREE OF
DOCTOR OF PHILOSOPHY

UNIVERSITY OF FLORIDA
2004

This Ph.D dissertation is dedicated to my family: Xristos, Aikaterini, Demetrios and Viktoria.

ACKNOWLEDGMENTS

This Ph.D dissertation is dedicated to my parents Xristos and Aikaterini who devoted their whole life to their children. Their love and support were the spring that gave me the strength to pursue a Ph.D. I also dedicate this dissertation to my brother Dimitrios and my sister Victoria. My siblings have been the best friends I ever had, and their professional success has motivated me to try even harder.

I am truly indebted to my mentors and advisors, Drs. W.G. Harris, T.A. Obreza, and G.A. O'Connor. They comprised a tremendous spectrum of knowledge and personalities that blended inside of me. Without their support and belief in me I would not have been able to graduate. Also, the rest of my committee (Drs. H. El-Shall, H. Elliott, and D. Rhue) were always there for me and made major contributions to my research. Special acknowledgments are given to Dr. Elliott for having the patience and willingness to serve on my committee even though he is a Professor at Penn State University. I would also like to thank Drs. Sartain, Kizza, and Ma for their continuing support.

TABLE OF CONTENTS

page

LIST OF TABLES

LIST OF FIGURES

Abstract of Dissertation Presented to the Graduate School
of the University of Florida in Partial Fulfillment of the
Requirements for the Degree of Doctor of Philosophy

LONG-TERM STABILITY OF SORBED PHOSPHORUS BY DRINKING-WATER TREATMENT RESIDUALS: MECHANISMS AND IMPLICATIONS

By

KONSTANTINOS CHRISTOS MAKRIS

August 2004

Chair: Willie G. Harris
Cochair: Thomas A. Obreza
Major Department: Soil and Water Science

Drinking-water treatment residuals (WTRs) are amorphous metal hydroxides with significant phosphorus (P) retention capacities, and offer significant potential to cost-effectively control soluble P losses in P-impacted sandy soils. The long-term stability of WTR-immobilized P, however, is unknown and is of major concern to regulatory agencies. We studied the sorption/desorption capacities, kinetics, and mechanisms involved in the reaction of P with three Fe-based and four Al-based WTRs. Three approaches to "compress" long-term effects and simulate them experimentally, were used: a) monitor the longevity of the WTR effect on soil P extractability (5.5 years after WTR application) at two sites (Holland, MI); b) study the physical nature of the WTRs, because micropores may severely restrict P desorption; and c) use heat incubations at elevated temperatures (46, 70 C) to hasten reactions that occur over decades in the field.

Phosphorus sorption capacities of the WTRs were a function of oxalate-extractable Fe and Al, % C, and porosity, as expressed by the ratio of specific surface areas measured

with N_2 and CO_2. Phosphorus desorption from the WTRs was minimal. Intraparticle diffusion in micropores of WTRs was the main mechanism of P sorption as inferred by multiple lines of solid-state and chemical assessments for two P-loaded WTRs, which is consistent with the minimum P desorption. In effect, P diffuses to the interior of particles where it is retained tenaciously.

Monitoring of soil P levels with time in two WTR-amended soils showed that P extractability did not significantly increase 5.5 years after WTR application. In parallel, 2 years of heat incubation suggested that P sorbed on WTRs was not released with time, or with increasing incubation temperature. Field and heat incubation data coupled with the fact that intraparticle P diffusion in micropores was the main mechanism, were consistent with irreversible P sorption and imply that WTR-immobilized P is stable in the long term.

CHAPTER 1
INTRODUCTION AND LITERATURE REVIEW

Intense agricultural activities have resulted in current elevated phosphorus (P) inputs in soils. Poorly P-sorbing soils are abundant in Florida and other eastern states of the USA. The low P-sorbing capacities, accompanied by high water tables and coarse-textured particle sizes make these soils vulnerable to P losses (He et al., 1999). The main P pathways to surface waters are lateral and vertical movement of P dissolved in water moving towards the water bodies. Increased P loading of Lake Okeechobee in FL has resulted in algal blooms and subsequent decrease in the Lake's water quality. The lake's watershed has a prolonged history of using P sources such as P fertilizers, manures and biosolids to increase soil fertility and crop yields. However, P-source application is typically based on crop N requirements, which provides P in excess of crop needs. This excess P is either sorbed by a soil's reactive solid phase or is lost through surface runoff or subsurface leaching to the groundwater. Drinking-water treatment residuals (WTRs), a byproduct of processes producing potable water, have potential to mitigate the low P sorption capacities of acidic soils and reduce environmental risks associated with P loss from these soils.

Drinking-WTRs are primarily amorphous masses of metal oxides or $CaCO_3$, that also contain sediment, activated carbon and polymer removed from the raw water during water purification process for drinking purposes (Elliott and Dempsey, 1991). Potable water production is usually achieved with the use of three methods; sedimentation-flocculation, ion exchange and reverse osmosis. Sedimentation-flocculation is the most

conventional water treatment method, which makes use of metal salts combined with synthetic polyelectrolytes such as surfactants and polymers. Addition of Fe, Al, or Ca salts to raw water removes colloids, color, sediment and contaminants from surface and groundwater supplies intended for potable water use. Iron and / or Al salts are commonly used by the waste and drinking water treatment industry to remove P and As from solution (Maurer and Bollet, 1999). In a basic pH environment, Fe or Al salts will hydrolyze to form amorphous iron or aluminum (hydr)oxides, which exhibit dramatic affinity for soluble P. Iron and aluminum (hydr)oxides sorb oxyanions like P and As (Livesey and Huang, 1981) through adsorption and precipitation reactions. WTRs produced where the primary coagulant was Al, Fe or lime, are referred to as Al- or Fe- or Ca-based WTRs. Iron- and Al-based WTRs are the most commonly produced. There are over 1000 drinking water treatment plants in USA that use alum salt [$Al_2(SO_4)_3 \cdot 14H_2O$] as a coagulant for contaminant and color removal (Prakash and Sengupta, 2003).

More than 2 million tonnes of WTRs are generated each year (Prakash and Sengupta, 2003). There are several methods of disposal: (i) directly to a receiving stream; (ii) to sanitary sewers; (iii) to a landfill, assuming that the residual contains no free draining water; and (iv) by land application (Chwirka et al., 2001). Land application is the focus of this project since it combines economic and environment-friendly benefits. WTR are specifically exempt from the 40 CFR Part 503 land disposal regulations. However, in case of land-applying mixtures of water and wastewater residuals, the Part 503 rule applies to the combined residuals.

Land application can function as a means of WTRs disposal and as a means of immobilizing P in poorly P-sorbing soils. Depending on the coagulant used, WTR

contain from 5 to 15% total Al or Fe in the form of an insoluble hydroxide (ASCE, 1996). These metal hydroxides are mixed with other suspended inorganic particles and natural or synthetic organic matter. Metal hydroxides in WTRs are usually amorphous and they should be characterized by small particle size, and greater specific surface area (SSA), than the corresponding crystalline phases (Bohn et al., 1979). Oxides' small size, coupled with their high surface area, makes them reactive and efficient sorbents for oxyanions (O' Melia, 1989). The high amorphous Al/Fe content of WTRs would be expected to increase a soil's P sorption capacity (Elliott et al., 1990).

Alum salt addition to soils or wastes high in P is the current common practice to reduce soluble P levels. Moore and Miller (1994) and Shreve et al. (1995) found that alum and $FeCl_3$ salt additions to poultry litter reduced soluble P in surface runoff from litter-amended soils. Recently, WTRs were proposed as cost-effective amendments to reduce soluble P in systems high in P. Research found that WTRs can immobilize P susceptible to leaching or soil surface runoff. Gallimore et al. (1999) and Peters and Basta (1996) studied the effect of WTR application to poultry litter-amended soils. They showed that WTRs significantly reduced soluble P in surface runoff. Codling et al. (2000) and Ippolito et al. (1999) observed a positive linear relationship between increasing WTR rate and grass yield after co-mixing of WTRs and biosolids. Brown and Sartain (2000) showed that a 2.5 % (by weight) Fe-WTR application rate significantly reduced P leaching from applied fertilizer P with minimal negative impact on crop P uptake.

A concern with land-applied WTRs is the potential for induced plant P deficiencies (Basta et al., 2000). Studies have shown that WTRs application > 10g WTR kg^{-1} (~20 Mg

WTR ha^{-1}) reduced tissue P concentrations, but did not induce other nutrient deficiencies or toxicities (Elliott and Singer, 1988; Heil and Barbarick, 1989; Cox et al., 1997). Harris-Pierce et al. (1994) reported minimal negative effects of co-applied WTRs (5.6 to 22.4 Mg ha^{-1}) and biosolids (11.2 Mg ha^{-1}) on native rangeland vegetation. Another land-application concern that has been raised is the potential toxic effects of dissolved Al towards various aquatic and benthic organisms. Gallimore et al. (1999) found that land application of WTR at rates of 11.2 and 44.8 Mg ha^{-1} did not increase dissolved solids or dissolved Al in surface runoff. Haustein et al. (2000) reported no significant increase of dissolved Al in surface runoff of Al-WTR amended soils (2.2 to 18 Mg ha^{-1}). The long-term stability of P associated with WTRs is also a concern, and properties pertinent to long-term P retention are addressed in this dissertation. The ultimate goal of land-applying WTR is to protect the surface and subsurface water quality as well as to provide financial savings to water treatment plants paying for landfilling or stock-piling WTRs.

Drinking-water treatment plant facilities use different water sources and different coagulants. Thus, they produce WTRs with different elemental compositions and contaminant sorption capacities. Dayton et al. (2003) reported a wide range of P sorption capacities for several Al-WTRs tested in a field experiment. Reduced P levels found in runoff depended on the P sorption capacity of the WTRs. Runoff-P reduction effectiveness was ascribed to WTRs' high P sorption capacities (Dayton et al., 2003). WTRs have considerable P sorption capacities as previous work on FL-produced WTRs showed; WTRs exhibited P retention capacities ranging from 3500 (Fe-WTR) to 5000 (Al-WTR) mg kg^{-1} (O'Connor and Elliott, 2000). An Al-WTR from Bradenton, FL sorbed essentially all of the added P (6000 mg kg^{-1}), suggesting that it can dramatically

reduce soluble P levels when applied to a poorly P-sorbing soil amended with different P sources. The adsorption maximum of the WTR could not be determined, but it was greater than 6000 mg P kg^{-1}.

Once sorbed, P desorption from WTRs needs to be addressed. Preliminary P desorption experiments on the Al-WTR, Bradenton, FL showed that the cumulative percent of P desorbed was less than 1%, suggesting that the Al-WTR had the potential to be an ultimate P immobilizer (O' Connor and Elliott, 2000).

Phosphorus desorption from metal oxides is usually slower than P sorption and decreases with increasing sorption time (Anderson et al., 1996). Ion desorption from soil oxide phases depends on the amount of the adsorbent and the type and concentration of the adsorbate. A considerable amount of phosphate was desorbed from the Bh horizon of a Pomona soil in Florida, in the presence of 5 mM oxalate at pH 4.5 (Bhatti, 1995). Ligand exchange and dissolution of soil mineral surfaces were the two mechanisms responsible for P release, in the presence of oxalate. The P released was not allowed to reprecipitate with soluble Al or Fe due to the formation of stable soluble complexes of oxalate with Al or Fe. Villapando and Graetz (2001) found that for low and medium citrate-dithionite-bicarbonate-extractable (CDB) Al contents of Bh horizons (up to 70 mmol kg^{-1}) nearly all of the P sorbed onto soil Al oxides was desorbable. Spodic horizons of soils high in CDB-Al content (> 100 mmol kg^{-1}) exhibited little P desorbability.

Synthetic and pure mineral / oxide phases show a stronger retention of oxyanions than the soil oxide phases. Research has shown that the amount of P sorbed on goethite is partially reversible (Strauss et al., 1997). Galvez et al. (1999b) suggested that at 0-3 % P / Fe loads, P adsorption on hematite led to P occlusion in its structure. Acid dissolution of

hematite depended on the amount of sorbed P; the presence of P markedly increased the time needed for hematite dissolution. Also, they observed that acid-desorbed P remained largely in solution. Strauss et al. (1997) found the rate of P desorption from goethite tended to decrease following increases (incubation for a week at 40 C) in the oxide crystallinity (greater surface area). Higher phosphate loading on the surface of oxides influences the degree of P desorbability. On an average, higher P loading resulted in smaller P adsorption energy that led to increases in soluble P concentrations (Parfitt, 1979).

Some authors argue that aging of WTRs significantly reduces P sorption capacities (Heil and Barbarick, 1989). Age, crystallinity, size, and processing methods are considered as the main factors that influence WTRs effectiveness in reducing soluble P. Surface area is a physical parameter that could sufficiently characterize the aging of a material. Diakonov et al. (1994) observed decreases in specific surface area (SSA) of aged goethite [FeO(OH)] and hematite (Fe_2O_3) with time. Goldberg et al. (2001) observed changes in the surface area of amorphous Al hydroxides after 9 d, at room temperature as they transformed towards a more crystalline phase (gibbsite). Changes in specific surface area of hydroxides could affect sorption/desorption of oxyanions. Increases in crystallinity of mineral phases may reduce SSAs of amorphous hydroxide phases. Thus, fewer sites are available for sorption. Phosphorus sorption to Fe, Al amorphous oxides are greater than to the corresponding crystalline oxide phases (Bache, 1963). Strauss et al. (1997) showed that P sorption stopped within a day for well-crystallized goethite samples. Less crystalline goethite continued to slowly sorb P even after three weeks. Sorption of P on metal hydroxides is initially rapid, but then decreases

with increasing equilibration time (Fuller et al., 1993; Raven et al., 1998; O'Reilly et al., 2001; Bache, 1964; Muljadi et al., 1966b-c). Oxide surfaces have different types of surface adsorption sites, with different affinities for adsorbates (Davis et al., 1978). Pierce and Moore (1982) found that for up to 1mg L^{-1} initial arsenate concentrations, the adsorption isotherm of As on ferrihydrite could be described by the Langmuir model. At greater adsorption densities (up to 50 mg L^{-1} initial arsenate concentration) data were better fitted with a linear model, suggesting a two-site type of As adsorption.

WTRs can play a significant environmental role when applied to poorly P-sorbing soils like the soils of Lake Okeechobee Basin, Florida. These soils contain low levels of Fe and Al hydroxides in upper (A and E) horizons, which makes some soils prone to P leaching and runoff. Aluminium (hydr)oxides are the major short-range ordered colloids responsible for P retention in some acid FL soils (Villapando and Graetz, 2001). They found that Al associated with soil organic matter (SOM) was the major P sorbent in Bh horizons of Spodosols. Zhou et al. (1997) reported a significant correlation between P sorption capacity of Bh horizons of Florida Spodosols with their Al content, but there was no such correlation with Fe (hydr)oxides.

Long-term sorption mechanisms and kinetics of P by WTRs are not well understood, and long-term P behavior is usually interpreted in the context of metal hydroxides' behavior, which assumes similar reactivities (Bolan et al., 1985). Time constraints in conducting long-term field experiments (> 20 years) to test the stability of soil metal hydroxides inhibit improved understanding of the fate of sorbed P in soils. Laboratory experiments are usually designed to simulate what takes place in the field, but caution needs to be taken when extrapolating the results to the field. Thermal treatment

can accelerate natural weathering and transformation reactions of mineral phases (Martinez et al., 2001). Thus, I hypothesized that moderate (<80 C) heat treatment of WTR could be used as an experimental technique to hasten the aging of metal-oxide-containing WTRs. One could then monitor changes in morphological and chemical long-term parameters of thermally-treated WTRs that might affect oxyanion desorbability from WTR and WTR-amended soils.

No work on long-term P retention of WTRs and WTR-amended soils exists in the literature. This dissertation aimed to address the long-term stability of sorbed P by WTRs. Three approaches were designed to tackle the long-term P sorption mechanisms and reactivity of WTRs and WTR-amended soils. The first approach dealt with the physicochemical properties of the WTRs and their implications for long-term P sorption performance, both from a macroscopic and a microscopic point of view. The second approach dealt with heat incubations at elevated temperatures (46 and 70 C) of synthetic Al and Fe hydroxides, WTRs, and WTR amended soils in an attempt to hasten reactions that could take decades to occur in the field. The third approach was to monitor the longevity of a WTR application effects on extractable P in two MI soils 5.5 years after the one-time WTR application. Appropriate hypotheses were formulated as follows:

- **H1**. WTRs are characterized by significant internal surface area and porosity that explain a time-dependent P sorption.
- **H2**. WTRs should ultimately immobilize P for as long as the particles remain intact due to desorption hysteresis arising from diffusion constraints.
- **H3**. Elevated temperatures would increase the degree of crystallinity of P-treated particles, and concurrently decrease P extractability.

The overall objectives were to determine mechanisms and pathways of P sorption by WTRs, and to interpret the mechanisms in terms of the long-term stability of sorbed P.

CHAPTER 2
GENERAL AND PHOSPHORUS-RETENTION CHARACTERISTICS OF SEVEN DRINKING-WATER TREATMENT RESIDUALS

Introduction

Great efforts have been concentrated to reduce P concentrations in surface runoff and leaching from poorly P-sorbing soils. Land application of drinking-water treatment residuals (WTRs, waste products of drinking water purification) seems to be a cost-effective alternative for effectively sorbing excess levels of labile P. Drinking-WTRs are primarily amorphous masses of either Fe or, Al (hydr)oxides or $CaCO_3$, that also contain sediment, activated carbon, and polymer removed from raw water. WTRs are produced during the drinking water purification process (Elliott and Dempsey, 1991). Addition of Fe, Al, or Ca salts to raw water removes colloids, color, sediment and contaminants from surface and groundwater supplies intended for potable water use.

Land application could function as a means of WTRs disposal, and as a means of immobilizing P in poorly P-sorbing soils. The high amorphous Al or Fe content of the WTRs, would be expected to increase a soil's P sorption capacity (Elliott et al., 1990). Research has found that WTRs can immobilize P susceptible to leaching or soil surface runoff. Gallimore et al. (1999), and Peters and Basta (1996) studied the effect of WTRs application to poultry litter-amended soils. They showed that WTRs significantly reduced soluble P concentrations in surface runoff. Codling et al. (2000) and Ippolito et al. (1999) observed a positive linear relationship between increasing WTR rate and grass yield after co-mixing of WTR and biosolids. Brown and Sartain (2000) showed that a 2.5 % (by

weight) Fe-WTR application rate significantly reduced P leaching from applied fertilizer P, with minimal negative impact on bermudagrass P uptake.

In the short-term, WTRs can dramatically reduce soluble P concentrations in soils and runoff from areas amended with different P-sources (Haustein et al., 2000; Ippolito et al., 1999; Gallimore et al., 1999), but little is known about the long-term P retention of WTRs and WTR-amended soils. The long-term stability of sorbed P by WTRs is a question of major concern to state and federal environmental agencies. Physicochemical properties assessment of WTRs is needed to better characterize the nature of P retention by WTRs.

Approaching the Problem

A flow diagram was constructed to show the sequence of techniques used to characterize P sorption capacities of the WTRs (Figure 2-1). Phosphorus sorption capacities and the degree of P desorbability of WTRs were obtained at room temperature by conducting P sorption and desorption isotherms, respectively. Cross-sectional P distribution within WTR particles was assessed using scanning electron microscopy coupled with energy dispersive x-ray spectrometry (SEM-EDS). Electron microprobe wavelength-dispersive spectrometry enabled quantified P migration into WTR particles. Monolayer P adsorption capacities of WTRs were calculated based on reported P adsorption values for crystalline goethites and gibbsites having specific surface areas (SSAs) similar to the WTRs used here.

Porosity and SSA of the WTRs were determined using Hg porosimetry, and BET-N_2 analyses. Mercury porosimetry provides quantitative analysis of macropores up to 184 μm in diameter, but has limited use in identifying micropores (<20 Å; 1 nm = 10 Å). The smaller pore diameter limit measured by Hg porosimetry is approximately 18 Å. BET-N_2

surface area analysis is able to access pore widths theoretically equal to the thickness of one nitrogen molecular layer (3.54 Å). However, in the case of microporous materials having pore diameters less than 15 Å, kinetics and activation energy issues might cause under-equilibration of measured adsorption points and underestimation of surface area calculations. The N_2 gas sorption at 77 K is hindered by the diffusion of the gas molecules to overcome energy barriers associated with diffusion into micropores of a few molecular layers.

Carbon dioxide has been used as an alternative adsorbate to N_2 for micropore volume and surface area determinations of carbon molecular sieves, activated carbons (Vyas et al., 1994; Guo and Chong Lua, 2002), clay minerals (Altin et al., 1999), and soil organic matter (De Jonge and Mittelmeijer-Hazeleger, 1996). Despite the fact that CO_2 has similar molecular dimensions as N_2 (2.8 Å for CO_2 and 3 Å for N_2), but the elevated temperatures (273 K for CO_2 versus 77 K for N_2) and higher absolute pressures (CO_2 vapor saturation pressure is 26,140 mm Hg versus 760 mm Hg for N_2) used for CO_2 facilitate the access of micropores by CO_2 molecules (Garrido et al., 1987). Therefore, SSA was also determined using CO_2 sorption to assure that surfaces associated with pores accessible by phosphate ions were accessed by the probe gas molecule.

Total C elemental content of WTRs varies, but it can be as much as 150 to 200 g kg^{-1} (O'Connor et al., 2001). A wide pore and particle size distribution should characterize the formation of WTRs, as coagulated particles of variable size and composition destabilize the suspension, and flocculate out of solution. Low molecular organic acids might be trapped in the small pores of the WTRs, thus, being the rate-limiting factor for the diffusion of water and phosphate molecules into micropores-

associated with organics. Dinitrogen molecules (77 K) should require a significant amount of activation energy to diffuse through such small pores. Using CO_2 as the adsorbate at a higher sorption temperature (273 K) enabled quantification of micropores (< 1.5 nm) that could contribute to prolonged three-dimensional P sorption by WTRs.

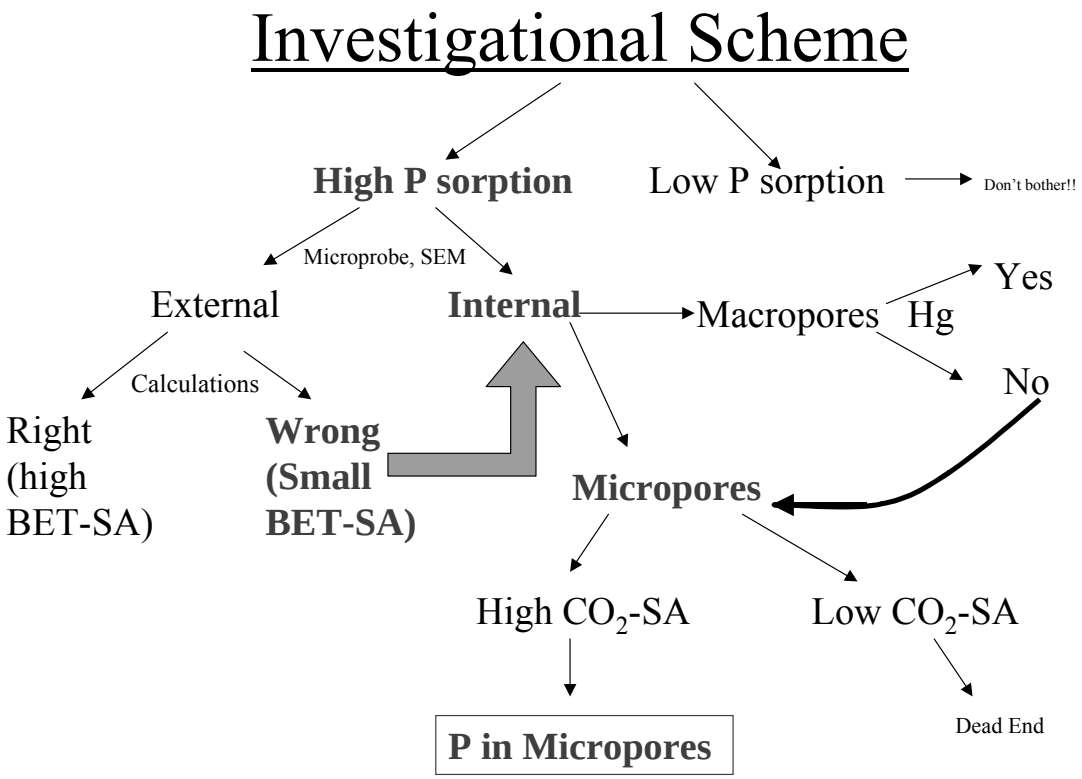

Figure 2-1. Approach used to assess the pathways of P sorption by WTRs.

Materials and Methods

Seven WTRs were used in this study: four were Al-based, and three were Fe-based. The Al-WTRs were obtained from two water treatment plants in Florida (Bradenton and Melbourne), one plant in Holland, MI, and one plant in Lowell, AR. The Bradenton material was obtained from the Manatee Co. water treatment plant in Bradenton, FL. Additions of alum and a small amount of a copolymer of sodium acrylate and acrylamide,

produced the Al-WTR (Dr. McLeod, Bradenton Water Treatment facility, personal communication, 01/20).

The Melbourne material was obtained from the Lake Washington water treatment plant, and was produced using alum combined with quicklime (CaO), acrylamide with sodium acrylate copolymer, and powdered activated carbon (PAC). The process produces ~15,000 tonnes WTR yr^{-1} (Hoge et al., 2003). The PAC may provide with additional sorption sites, but its concentration (by mass) was only 3 % of WTR produced. The Melbourne material was selected because it has been used in a large-scale (5,265 ha) restoration effort converting muck farmland to marsh habitat to reduce external P loading to Lake Apopka, FL. A total of 60,000 wet tonnes of WTR were hauled and applied to the site. Subsamples of the WTR were transferred to our laboratory from the initial stockpile in 1997 that was land-applied. Another important Al-WTR used came from the Holland, MI water treatment plant. This material is produced by alum addition to raw water. The material was used in a field experiment at Holland, MI to evaluate the longevity (5.5 years) of WTR effects in waste-amended soils high in soil test P levels. Subsamples were transferred to our laboratory from the initial stockpile in 1998 that was land-applied (Jacobs and Teppen, 2001).

The fourth Al-WTR came from the Beaver Water treatment plant in Lowell, AR. This material was successfully used to reduce runoff-P in rainfall simulation plots of soils (Haustein et al., 2000) with high soil test P levels. However, a different batch than the one used by Haustein et al. was shipped to us, as was later evidenced by differences in chemical composition.

All Fe-based WTRs were collected from Florida water treatment plants. The Hillsboro River water treatment plant in Tampa, FL processes the raw colored water by reacting with liquid iron sulfate to produce Fe-WTR. The material is distributed by the Kemiron company as *Fe-humate*®, and it is a valuable iron micronutrient source. Another Fe-based WTR came from the Taylor Creek Surface water treatment plant, Cocoa Beach, FL, where iron sulfate is coupled with PAC (100 tonnes) and polymer (7 tonnes) additions, annually. The Panama City surface water treatment plant in Florida provided us with an Fe-WTR, where iron sulfate is used as the coagulant. WTRs were sampled from stockpiles that were formed within 1 year of WTRs production. All WTRs were allowed to air-dry, and were subsequently passed through a 2-mm sieve.

Analytical Methods

General Physicochemical Properties

The pH and soluble reactive P of WTRs were measured in a 0.01 M KCl solution at a 1: 10 solid: solution ratio, after 40 d reaction. Total C and N were determined by combustion at 1010 C using a Carlo Erba NA-1500 CNS analyzer. The WTRs were analyzed for total P, Fe, and Al by ICP following digestion according to the EPA Method 3050B (USEPA, 2000). Oxalate extractable P, Fe, and Al were determined by ICP after extraction at a 1: 60 solid: solution ratio, following the procedures of McKeague et al. (1971). Oxalate-extractable Fe and Al represents noncrystalline and organically complexed Fe and Al present in the solid (McKeague et al., 1971).

Preliminary experiments were conducted to determine the effect of filter size and centrifuge speed on the P concentrations in solution. The fine colloidal material of the WTR might contribute significantly to soluble P concentrations when using 0.45μm filters (Anderson et al., 1996). Use of 0.1 and 0.01 μm filters helped to test this

hypothesis. Also, centrifuge speeds (4000, 8000 and 16000 rpm) were tested to assure that all of the colloidal material settled, and did not interfere with soluble P measurements. Typical QA / QC protocols of matrix spike (5 % of the set) recoveries were used in all the experiments. Method reagent blanks, certified check standard analyses, and new standard curves for each set of samples were used.

Screening Design

The Plackett-Burman screening experimental design or Plackett-Burman design is especially useful in the early stages of research projects to identify the most significant variables from a plethora of variables that would require excessive time and cost if studied using a one-at-a-time approach (Mason et al., 1989). In this study, a total of 8 variables were used with 12 experimental runs (Table 2-1) to identify the 2- to 3 most significant factors that would affect P sorption by WTRs, and thus, should be studied in a more detailed fashion later (Table 2-2). Three experimental runs were used as "dummy" variables, indicating that they are the basis for the calculation of the variance of the experimental design. The effect of variables was calculated:

$E_i = [\Sigma response_{(+)} - \Sigma response_{(-)}] / n$
The variance was calculated:
$\sigma^2 = \Sigma E_d^2 / n$,
where E_d = effect of dummy variable, and n=number of dummy variables.

The decision to accept or reject the significance of variables was based on the comparison of calculated t values with the critical t value $t_{11, 0.1} = 1.78$ (90 % confidence level, df = 11). Comparing the absolute calculated t values with the critical t value of 1.78 led to acceptance of variables with a higher t value and rejection of the variables with lower t values.

Table 2-1. Blackett-Burman design with 8 variables

	Factor numbers										
Run	1	2	3	4	5	6	7	8	9	10	11
1	+	+	-	+	+	+	-	-	-	+	-
2	+	-	+	+	+	-	-	-	+	-	+
3	-	+	+	+	-	-	-	+	-	+	+
4	+	+	+	-	-	-	+	-	+	+	-
5	+	+	-	-	-	+	-	+	+	-	+
6	+	-	-	-	+	-	+	+	-	+	+
7	-	-	-	+	-	+	+	-	+	+	+
8	-	-	+	-	+	+	-	+	+	+	-
9	-	+	-	+	+	-	+	+	+	-	-
10	+	-	+	+	-	+	+	+	-	-	-
11	-	+	+	-	+	+	+	-	-	-	+
12	-	-	-	-	-	-	-	-	-	-	-

Table 2-2. Plackett-Burman variables used in the P sorption study

	Variables	Low Level (-)	High Level (+)
1	pH	4	7
2	Equilibration time	1day	10 days
3	Dummy*		
4	P load	0 ppm P	800ppmP
5	Ionic strength	0.001 M KCl	0.01 M KCl
6	Oxalate	0 ppm	5 mM
7	Dummy		
8	Arsenic	0 ppm As	0.1 ppm As
9	Silicate	0 ppm Si	0.35 ppm Si
10	Type of WTR	Fe, Panama City, FL	Al, Lowell, AR
11	Dummy		

* Dummy variables used to calculate the variance of the experimental runs

Phosphorus Sorption by WTRs

P adsorption maxima of the WTRs were determined with a batch equilibration test, based on the work of O'Connor and Elliott (2000). Representative air-dried (< 2 mm) samples of the WTRs were reacted for 1, 10, 20, 40 and 80 days of reaction with P solutions that resulted in P loads of 2,500 to 10,000 mg P kg^{-1} in a 1:10 WTR:0.01 M KCl suspensions. The same tests allowed determination of P sorption capacities and kinetics of P retention by the materials at 23 C±2. The selection of the above range of P

loads was based on preliminary sorption experiments. Initial P concentrations far exceed those typically found in P-enriched soils, but were selected to account for cases where repeated annual P-source applications or dairy-impacted systems occur. The pH was not controlled and suspensions were not shaken during the equilibration period. No mechanical energy (shaking) was applied to the samples since shaking is not a field process and preliminary work revealed no significant difference in P sorption after 10 days between shaken and no-shaken samples. We also wanted to avoid the possible generation of surfaces due to abrasive forces during shaking. Following the reaction periods, suspensions were centrifuged, filtered (0.45 μm), and analyzed for P, Al and Fe by inductively coupled plasma atomic emissions spectroscopy (ICP-AES).

Following the sorption step, the supernatants were removed and WTR-containing tubes were filled with 5 mM oxalate solution (1:10 WTR:solution ratio) to test the ability of a common soil organic ligand to desorb P from the WTR (Bhatti et al., 1998). Suspensions were reacted again for 1, 10, 20, 40 and 80 d, without shaking or pH control. The amount of P desorbed was calculated as the difference between P sorbed and P measured in solution after the desorption step, accounting for entrained solution P.

Results and Discussion

WTRs Characterization

The WTRs were analyzed for selected chemical properties (Table 2-3). The pH of Al-WTRs was acidic (5.4- to 6.8), except for the Holland WTR that had a pH of 7.4. The KCl-P represented only a small fraction of total P, and ranged from 0.2- to 0.7 %. The KCl-extractable P is considered the most available pool of P and varies among different P sources. The very low amounts of KCl-P in WTRs implied that they may be sinks for P immobilization in poorly P-sorbing soils.

Total C values for the Al-WTRs varied (from 3.4 % for the Holland material to 22.5 % for the Melbourne material). The Lowell and Bradenton materials were intermediate in C concentration (7.6 and 16.2 %, respectively). Total C measured values agreed with the range of organic C found in 21 Al-WTRs (2.3- to 20.5 %; Dayton et al., 2003). Total C determinations may overestimate organic C content since the combustion method (temperature 1010 C) measures both organic and inorganic C. All Al-WTRs had C: N ratios between 11 and ≤C:N≤25, (except for the Bradenton material that had C:N of 27) indicating that there was a significant N pool that could be used by plants, if WTRs were land applied. A C:N ratio of ~25 is commonly used as the value where mineralization and immobilization of an organic amendment are in balance.

Total P in of the Al-WTRs ranged from 0.8 g P kg^{-1} for Lowell and Holland to 1.1 for the Melbourne and 3.1 for the Bradenton WTRs. Total P values were typical of Al-WTRs (0.3- to 4.0 g P kg^{-1}; Dayton et al., 2003). Total P in WTRs comes from the raw water purified in drinking water treatment plants and becomes a part of the WTR structure.

Total Al ranged from 37 g Al kg^{-1} for the Holland material to 103 g Al kg^{-1} for the Lowell WTR. Melbourne (87 g Al kg^{-1}) and Bradenton (92 g Al kg^{-1}) were intermediate but typical of Al-WTRs (15- to 177 g Al kg^{-1}; Dayton et al., 2003). X-Ray diffraction analysis (data not shown) suggested that amorphous Al hydroxides dominated all WTRs, with no apparent crystalline components. Oxalate extractable P, Fe, and Al are usually associated with the amorphous phase of the particles. Oxalate-extractable Al values were close to total Al (80- to 98 % of the total), suggesting an amorphous nature of the Al-WTRs.

All Fe-based WTRs were acidic; Cocoa had the lowest pH (3.9) followed by Panama (5.6), and Tampa (6.3). Similarly to Al-WTRs, KCl-P represented only a small fraction of total (0.2- to 2 %). Total C values were 9.4 % for the Panama and 20.6 % for the Cocoa material. Tampa Fe-WTR was intermediate (14.1 % C). Total C in the Fe-WTRs were also within the range of organic C values measured in 21 Al-WTRs (2.3- to 20.5 %; Dayton et al., 2003). All three Fe-WTRs had C:N ratios equal to 19, suggesting an abundant N pool for plant uptake.

Total P content of the Fe-WTRs ranged from 0.3 g P kg^{-1} for Panama and 0.7 for Cocoa to 3.2 for the Tampa WTR. Total Fe ranged from 242 g Fe kg^{-1} for the Cocoa material to 251 g Fe kg^{-1} for the Tampa, and 311 g Fe kg^{-1} for the Panama WTRs. Total Fe measurements were above typical values found for WTRs (50 to150 g kg^{-1}, ASCE, 1996). Large total values may not necessarily correlate well with elemental bioavailability or increased P sorption capacities. Gallimore et al. (1999) concluded that the amorphous rather than the total Al content of WTRs determines their effectiveness in reducing runoff-P.

X-ray diffraction analysis (data not shown) suggested that amorphous Fe (hydr)oxides dominated all Fe-WTRs, with no apparent crystalline Fe (hydr)oxides. Iron-based WTRs had reduced oxalate-extractable Fe values as a percentage of total compared with the Al-WTRs (45- to 64 %). This difference might suggest reduction in P sorption effectiveness of the Fe-WTRs compared with Al-WTRs.

Screening Design

The Blackett-Burman design was used as a preliminary experimental design to identify with minimum cost and effort the two or three most important variables that

might influence P sorption by WTRs. Selected variables from this design could be studied in a greater detail later.

Table 2-3. General chemical properties of seven WTRs.

Source	Form	pH	KCl-P (mg kg^{-1})	C (%)	N (%)	Total (g kg^{-1})			Oxalate (g kg^{-1})		
						P	Al	Fe	P	Al	Fe
Tampa, FL	Fe-Based	6.3	6.21 ±0.8	14.1 ±0.6	0.8 ±0.04	3.2 ±0.1	9.8 ±0.1	251 ±5.6	2.6 ±0.05	6.0 ±0.1	161 ±8.0
Panama City, FL	Fe-Based	5.6	6.31 ±0.1	9.4 ±0.1	0.5 ±0.01	0.3 ±0.01	1.5 ±0.03	311 ±14	0.2 ±0.08	1.3 ±0.1	195 ±4.1
Cocoa City, FL	Fe-Based	3.9	6.25 ±0.1	20.6 ±0.2	1.1 ±0.01	0.7 ±0.02	2.2 ±0.04	242 ±3.5	0.14 ±0.03	nd[#]	108 ±2.98
Holland, MI	Al-Based	7.4	5.62 ±0.05	3.4 ±0.02	0.3 ±0.05	0.8 ±0.02	37 ±0.8	8.7 ±0.2	0.57 ±0.09	29 ±4.01	2.3 ±0.3
Lowell, AR	Al-Based	6.8	5.26 ±0.01	7.6 ±0.2	0.7 ±0.02	0.8 ±0.05	103 ±6.1	20.7 ±1.9	0.5 ±0.01	89 ±1.4	5.8 ±0.5
Bradenton, FL	Al-Based	5.4	5.08 ±0.04	16.2 ±0.8	0.6 ±0.02	3.1 ±0.04	92 ±0.04	6.2 ±0.04	2.98 ±0.0	91 ±0.1	5.2 ±0.2
Melbourne, FL	Al-Based	5.7	2.20 ±0.14	22.5 ±0.6	1.0 ±0.01	1.1 ±0.06	87 ±0.7	5.7 ±0.4	0.6 ±0.06	79.4 ±0.2	3.6 ±0.1

Numbers are the mean of two replicates ± one standard deviation.
[#] not detected.

Based on the screening design experiment, three variables at the 90 % confidence level were accepted as significant factors that affect P sorption by WTRs (Table 2-4). These were the type of WTR (Fe or Al-based), equilibration time (1 or 10 d), and P load. Rejected variables at the 90 % confidence interval were pH (4 vs. 7), typical soil solution arsenate and silicate concentrations, and ionic strength (0.01 vs. 0.1 M KCl). In the

following section, the three selected variables will be studied in great detail by using multi -point sorption isotherms and sorption kinetics for either Al- or Fe-based WTRs.

Table 2-4. Phosphorus sorption data and calculated t-test values for Blackett-Burman design.

Runs	Sorbed P mg kg^{-1}	Sum (+)	Sum (-)	Variable Effect	Variance	t-test (90 %)	Variables	
1	7470	12348	18622	-784		-1.38	pH	
2	2570	19514	11456	1007		1.78	Equilibration Time	accept
3	7737	12615	18355	-718	321880	-1.26	dummy	
4	0	30970	0	3871		6.82	P Load	accept
5	0	14347	16623	-284		-0.50	Ionic strength	
6	0	16356	16922	-71		-0.12	Oxalate	
7	6578	13193	17777	-573		-1.01	dummy	
8	0	14352	16618	-283		-0.50	Arsenic	
9	4307	13456	17514	-507		-0.89	Silicate	
10	2308	21785	9185	1575		2.78	Type of WTR	accept
11	0	16885	14085	350		0.62	dummy	

Phosphorus Sorption by WTRs

Phosphorus sorption / desorption isotherms (at 23 C) were constructed for the WTRs by reaction with P solutions at different P loads (up to 10,000 mg P kg^{-1}). The four Al-based WTRs exhibited high affinity for P (Figure 2-2). At the greatest initial P load (10,000 mg kg^{-1}), the Melbourne material sorbed the greatest amount of P, followed by Bradenton, Lowell, and Holland. Langmuir-sorption maxima were not determined since isotherms did not exhibit an obvious plateau.

P sorption kinetics of WTRs were also monitored. Sorption reactions did not reach equilibrium as sorption kinetics experiments revealed. Kinetic data for all Al-WTRs were best fit to a pseudo second, rather than to a first order reaction rate model, suggesting a biphasic nature of P sorption (Table 2-4). P sorption was initially fast, followed by a slow P sorption stage.

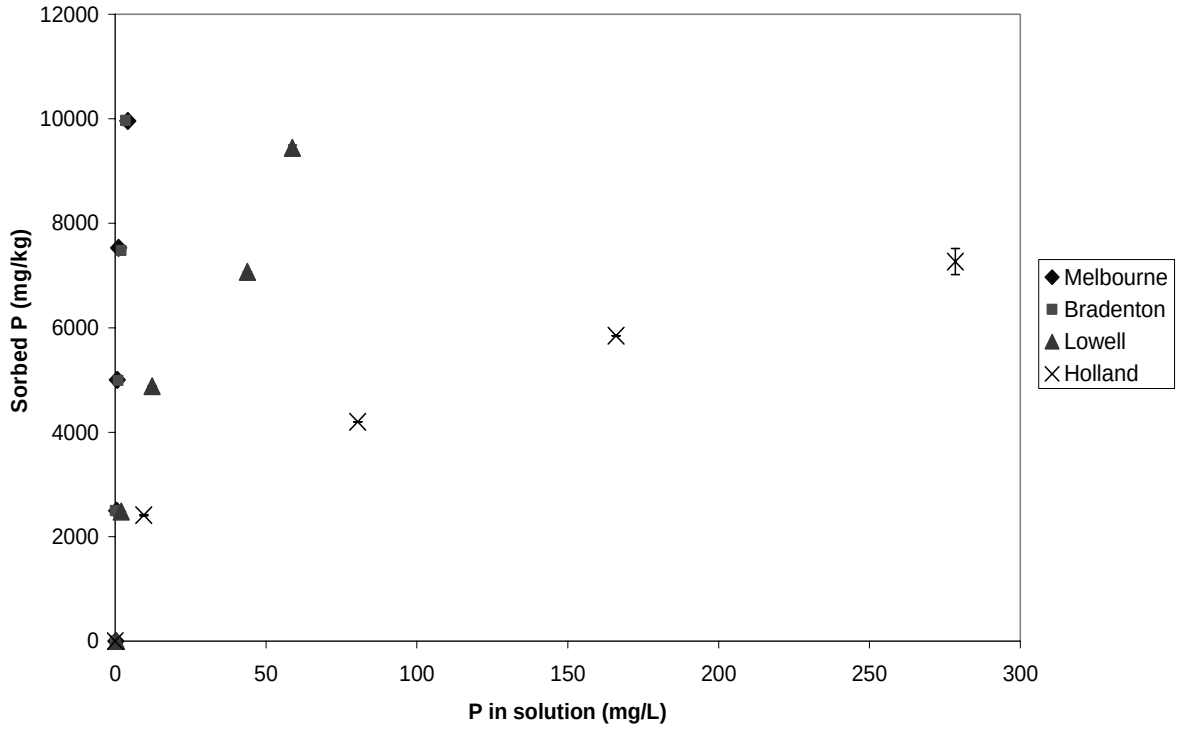

Figure 2-2. P sorption isotherms of four Al-WTRs measured at room temperature after 10 d. No shaking or pH control was applied.

The fast stage of P sorption was ascribed to 1 d sorption data, based on similar data in the literature (Van Riemsdjik and Lyklema, 1980). The slow P sorption stage characteristics varied among WTRs. The pseudo second order reaction rate coefficients increased with the P sorption capacities of the materials. The faster the reaction, as suggested by larger rate coefficients, the greater the amount of P sorbed. The Melbourne material had the largest second order rate coefficient, suggesting little effect of the slow P stage on the overall P reaction with the solid. In parallel, the Melbourne material exhibited the fastest removal of P from solution, depleting all of the added soluble P within 10 d.

The Holland material exhibited the smallest 2nd order rate coefficient, suggesting a greater effect of the slow P sorption stage compared with the other Al-WTRs. The slow P

stage in the Holland material was rate limiting for P sorption. Second order reaction rate coefficients were also positively correlated with calculated P half lives. The greater the rate coefficient, the smaller the time needed to reduce initial P concentrations by half (Table 2-5). Half lives of P for the Al-WTRs ranged from 27 sec for the Melbourne to 10,000 sec for the Holland WTR. Use of P half lives may not be appropriate for materials that exhibit nonlinear reduction of soluble P, like the WTRs.

Table 2-5. Pseudo reaction rate constants and P half-lives in Al-WTRs suspensions after a 1,000 mg P L^{-1} initial pulse input.

Source	Form	1st order rate fit (r^2)	2nd order rate fit (r^2)	2nd order reaction rate k ($L\ s^{-1}\ mg^{-1}$)	P Half-life $t_{1/2}$ (s)
Holland, MI	Al-Based	0.87	0.98	$2*10^{-7}$ #	10,000 *
Lowell, AR	Al-Based	0.86	0.95	$3.4*10^{-5}$	98
Bradenton, FL	Al-Based	0.54	0.94	$1.3*10^{-4}$	29
Melbourne, FL	Al-Based	0.89	0.96	$2.4*10^{-4}$	27

Where the slope of a linear fit to an *n*-order reaction equals: $(n-1)*k_nCo^{n-1}$.
$t_{1/2} = 1 / ((n-1)*k_n*C_o^{n-1}) * (2^{n-1} - 1)$.

Factors causing slow P sorption kinetics by WTRs are unclear. It has been argued that aging of WTRs might affect P sorption capacities. The Melbourne and Holland materials were sampled from solids retention ponds in 1997 and 1998, respectively, and aged in the laboratory under air-dry storage conditions until their use in this study in 2003. Even though the Melbourne sorbed more P than the Holland material, the latter's P sorption capacity was still very high. Aging of the materials in the lab where they were stored (air dried, room temperature) did not seem to affect their P sorption capacities.

Thermogravimetric analysis (Chapter 5) showed that WTRs retained significant amounts of water after air-drying, and even after incubation at 70 C. Thus, the number of sorption sites and particle rigidity should be maintained even under air-dried conditions at room temperature.

During P sorption experiments, Fe and Al aqueous concentrations were also monitored. Aluminium concentrations of Al-WTRs suspensions were below the instrument's (ICP) detection limit (0.03 mg Al L^{-1}). This result suggested no particle dissolution during sorption after 80 d. The pH for all Al-WTRs was not controlled, and by the end of the 10 d sorption experiments, suspension pHs of P-treated samples ranged from 5.8 for the Melbourne to 8.3 for the Holland material.

In general, P sorption increased sorption pH consistent with the exchange of P with structural hydroxyls on external or internal sorption sites. An exception was the Bradenton material that exhibited a decrease in pH with P load (from 5.4 down to 3.9), which increased soluble Al. During P sorption by the Bradenton WTR, no pH decrease was observed after 20 d. Soluble Al increased after 40 d when pH decreased in the P-treated suspensions. However, even after 40 d, dissolved Al as a percentage of the oxalate-extractable Al of the WTR was minimal (only 0.4 %). The reason for the pH drift is unknown. It is noteworthy to mention that all soluble P was removed within 40 d.

At any initial P load, there was a significant negative linear relationship ($r^2 = 0.9$) between the amounts of P sorbed and suspension pH of the untreated WTRs after 1 d (Figure 2-3). After 10 d, the degree of coefficient of determination was decreased by half ($r^2 = 0.45$), suggesting little pH effect on the observed P sorption capacities with time. This result suggests that pH-dependent sorption sites were occupied within a day,

whereas after 10 d all pH-dependent sites were filled, giving rise to internal sorption sites that were diffusion-controlled. O' Connor et al. (2001) performed adsorption envelope experiments with two WTRs and observed no pH-dependency of P sorption after 4d, similar to our results. To fully discern potential pH effects on P sorption by WTRs, composite experiments that take into account P load interactions with pH need to be undertaken.

There was a significant ($r^2 = 0.85$) correlation between the pseudo 2nd order reaction rate coefficients and the amounts of P sorbed at the highest initial load for the Al-WTRs, after 1 d (Figure 2-4). The degree of correlation was lower ($r^2 = 0.54$) for the 10 d contact time. After 10 d, the materials sorbed more than 90 % of initial added P, approaching the plateau of the amount of P that could be sorbed. No interaction between time and 2nd order reaction rate coefficients was evident (Figure 2-4). Initial P load was the limiting factor that determined true P sorption maxima of WTRs. The maximum initial P load of 10,000 mg P $kg^{-1}$is much greater than those found in most natural systems.

After sorption, P desorption was also monitored with a 5 mM oxalate solution. P desorption decreased with increasing desorption time for all Al-WTRs. Decreasing amounts of oxalate-desorbable P suggested non-equilibrium P sorption. This phenomenon was observed for a long-term P desorption experiment of an Al-WTR (Ippolito et al., 2003). Maximum percentages of oxalate-desorbable P (% previously sorbed) were 0.2 % for all Al-WTRs except for the Holland material (1.5 %). The percentages apply to desorption experiments conducted for 10 or 20 d.

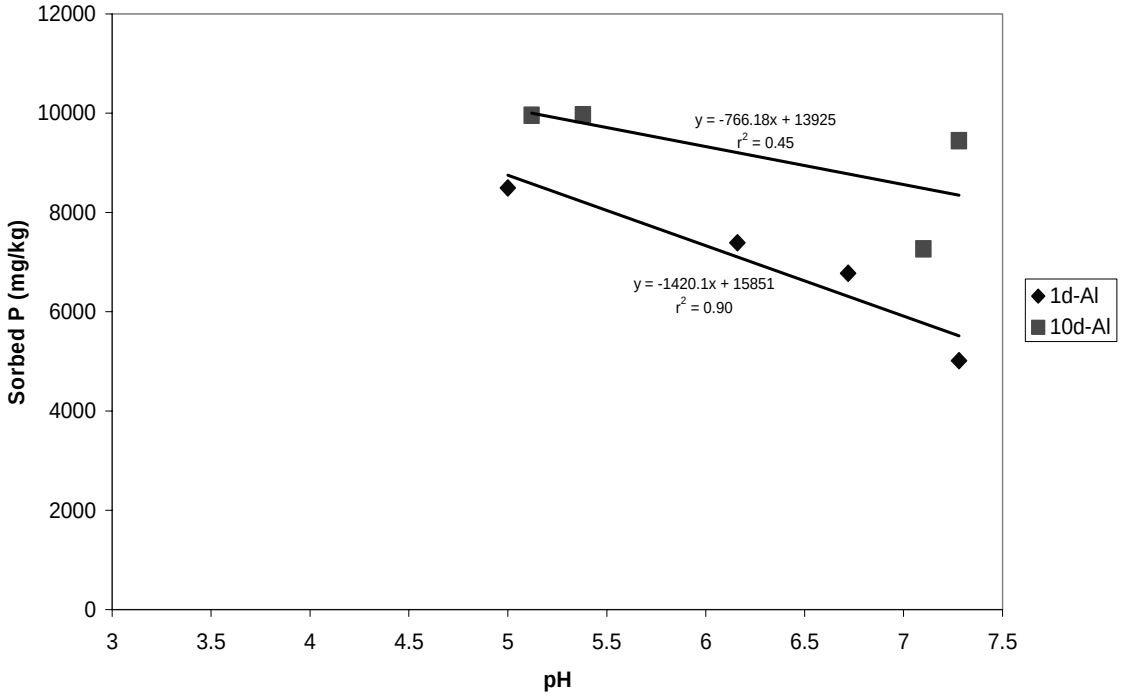

Figure 2-3. Correlation between the pH of the untreated Al-WTRs with the amount of sorbed P at the highest initial P load for the four P-treated Al-WTRs.

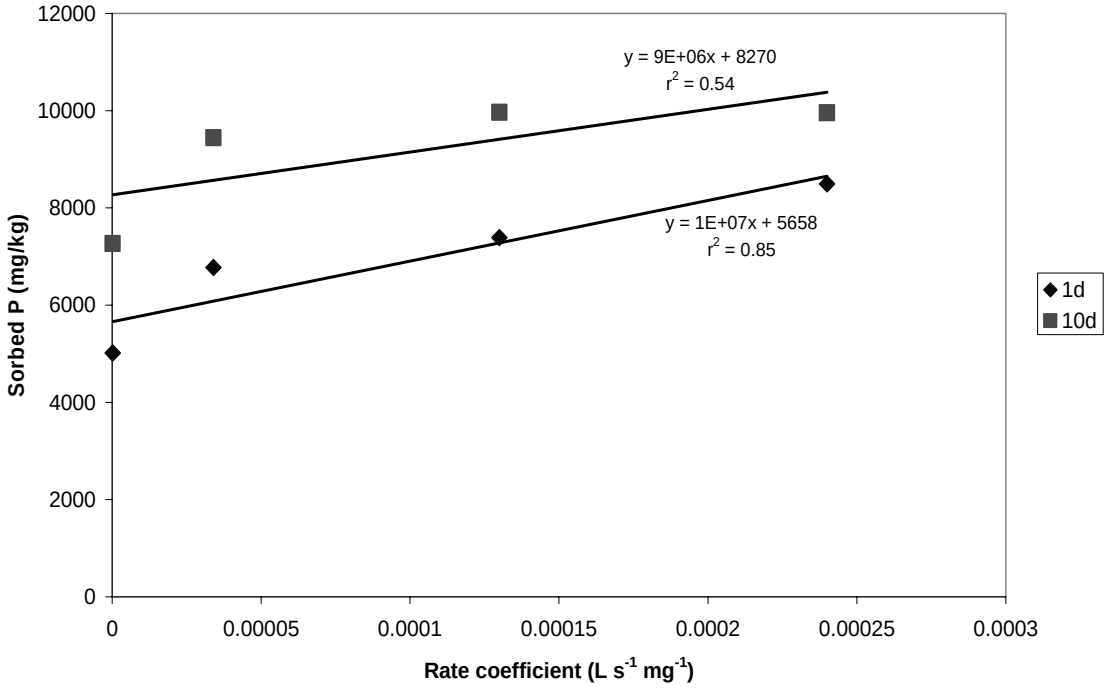

Figure 2-4. Correlation between the pseudo second order rate coefficients with the amount of sorbed P at the highest initial P load for the four Al-WTRs.

As desorption time increased to 80 d, no soluble P (ICP instrument P detection limit 0.3 mg P L^{-1}) was detected for any Al-WTR, suggesting non-equilibrium in the sorption step.

A desorption experiment with an Al-WTR by (Ippolito et al., 2003) showed minimum $CaCl_2$-desorbable P concentrations in solution (0.2 % sorbed P), which agrees with our desorption values. Decreasing amounts of oxalate-desorbable P from WTR particles indicated irreversible sorption. Residual P that was sorbed during desorption came from the entrained solution after sorption. Apparently, P sorbed by Al-WTRs was chemisorbed on WTR surfaces, and resisted desorption with oxalate molecules.

A typical soil solution oxalate concentration of 5 mM was used to desorb P from WTRs (Bhatti et al., 1998). Oxalate was used to mimic natural conditions where land-applied WTRs could release sorbed P via organic ligand mineral dissolution. Butkus et al. (1998) suggested that WTRs may act as P sources when loaded with P. Data from the desorption experiments do not support this suggestion. Rarely occurring P loads that exceed a 1:1 stoichiometric P:Al molar ratios may transform WTRs from a sink to a P source. Such loads are not usually encountered in natural systems.

Similar sorption/desorption experiments were conducted for the three Fe-WTRs. Sorption isotherms at room temperature showed that Tampa Fe-WTR had the greatest affinity for P, followed by Panama and Cocoa Fe-WTRs. Given enough time (80 d), the Tampa material essentially sorbed all P from solution (92 % of initial P load). The Panama WTR sorbed ~ 4,500 mg P kg^{-1} after 80 d. A shorter equilibration time (8 d) may explain the lower P sorption capacity (~3,400 mg P kg^{-1}) of another sample of the Panama material (O'Connor et al., 2002). The Cocoa material sorbed the least amount of P of all WTRs after 80 d (~1,000 mg P kg^{-1}).

Sorption isotherms were non-equilibrium, as sorption kinetics experiments revealed. Except for the Cocoa material, kinetic data for Fe-WTRs were best fit to a pseudo second order reaction rate model, suggesting a biphasic nature of P sorption (Table 2-6). Similarly to Al-WTRs, P sorption was initially fast, followed by a slow stage.

The biphasic nature of P sorption was expressed using a pseudo 2^{nd} order reaction rate coefficient. Rate coefficients increased accordingly to pseudo P sorption capacities of the materials. The faster the reaction, as suggested by larger rate coefficients, the greater the amount P sorbed. However, all Fe-WTRs exhibited smaller P sorption rate coefficients than the Al-WTRs, suggesting a significant effect of the slow P reaction stage on the overall P sorption by the Fe-WTRs.

Of the three Fe-WTRs tested, only the Tampa material reached maximum P sorption capacity levels similar to that achieved with Al-WTRs. Panama and Cocoa materials did not reach these magnitudes even after 80 d. The Cocoa material sorbed the least amount of P, and kinetic data did not fit either a first or a second order reaction model (Table 2-5). The pH of the Cocoa material was more acidic (pH 4) than the other WTRs. A negative linear correlation between P sorption capacities after 1d and pH (r^2 = 0.99) was observed for the three Fe-WTRs. However, a positive linear correlation was observed after 10 or 80 d, possible because of displacement of hydroxyls in solution.

Iron concentrations in solution were also monitored during P sorption. The Tampa and Cocoa Fe-WTRs released a small portion of oxalate-extractable Fe in solution (~1.1 and 0.1 % of total Fe, respectively) during equilibration with 0.01 M KCl in the absence of added P. Panama material did not release any Fe to solution after 80 d.

Table 2-6. Pseudo reaction rate constants and P half-lives in Fe-WTRs suspensions after a 1,000 mg P L^{-1} initial pulse input.

Source	Form	1st order rate fit (r^2)	2nd order rate fit (r^2)	2nd order reaction rate k ($L\ s^{-1}\ mg^{-1}$)	P Half-life $t_{1/2}$ (s)
Tampa, FL	Fe-Based	0.80	0.97	$1.07*10^{-7}$ #	10,000*
Panama City, FL	Fe-Based	0.71	0.77	$5.8*10^{-9}$	184,750
Cocoa City, FL	Fe-Based	0.12	0.12	$1.24*10^{-9}$	1,111,111

Where the slope of a linear fit to *n*-order reaction equals: $(n-1)*k_n*Con^{-1}$.
* $t_{1/2} = 1 / ((n-1)*k_n*C_o^{n-1}) * (2^{n-1} - 1)$.

Supernatants of these samples contained visually-inspected black flocs, probably humic materials, on the water/air interface. The Panama material had the least amount of total C of all the Fe-WTRs, which may be the reason why it did not release any Fe to solution.

Desorbed Fe was gradually removed from solution as P was added to the system. This implies a classic precipitation mechanism for P removal;. However, no Fe was found in supernatants of P-treated WTRs within 1 d. Iron that was desorbed from WTR surfaces after 20 or 40 d (in the absence of added P), reacted with P in solution, resulting in minimum soluble Fe in solution at the highest initial P load.

After sorption, the Fe-WTRs residuals were reacted with a 5 mM oxalate to test P desorbability. Similarly to Al-WTRs, desorbed P amounts decreased with increasing desorption time (10- to 80 d), implying a continuous non-equilibrium P sorption process. The Tampa WTR desorbed the least amount of previously sorbed P (1.3%), followed by Panama (7.3 %), and the Cocoa (8.3 %). There was an inverse trend in percentage of

sorbed and desorbed P. The greatest amount of P desorbed was from Cocoa, which also sorbed the least amount of P of all the WTRs.

Phosphorus Sorption Comparisons between Fe- and Al-Based WTRs

Overall, Al-based WTRs were more effective in sorbing and retaining P than the Fe-based WTRs. Given enough time, all Al-WTRs essentially sorbed all P from solution. Only one Fe-WTR (Tampa) exhibited a P sorption capacity similar to those of Al-WTRs. Reaction between inorganic phosphates and soils or Fe/Al hydroxides is initially fast, becoming slower with time, without reaching true equilibrium (Bolan et al., 1985). The fast reaction is explained by surface-controlled interactions between adsorbent and / adsorbate. The slow reaction can be explained in terms of either intraparticle diffusion (Axe and Trivedi, 2002), formation of a solid solution, or surface precipitation of a new solid phase (Martin et al., 1988). There is a slow P reaction component of the overall P sorption by WTRs, which was more obvious for the Fe-WTRs materials. The slow reaction component suggests a different P sorption mechanism than simple surface ligand exchange of structural hydroxyls for phosphate molecules.

A biphasic nature of P sorption, characterized by an initially fast sorption followed by a slower stage, was observed, with all Fe and Al-WTRs. P sorption isotherms for all WTRs (except two Fe-WTRs-Panama and Cocoa Fe-WTRs) did not exhibit Langmuir isotherm type, showing no apparent plateau formation at any contact time. A second order reaction rate model was the best fit to kinetic data for the WTRs, consistent with suggesting a rate-limiting slow P sorption process. Slow P sorption expressed by rate coefficients calculated from the 2^{nd} order model showed the relative efficiencies of WTRs in reducing soluble P. The larger the rate coefficient, the faster P was depleted from

solution. A significantly higher degree of efficiency of P removal was observed for the Al-WTRs compared with the Fe-WTRs.

Pseudo 2nd order reaction rate coefficients were much smaller for the Fe-WTRs, providing evidence for a slower P sorption stage. A significant ($r^2 = 0.95$) correlation between the rate coefficients and the pseudo P sorption capacities at the highest initial P load in a semi-natural logarithmic plot was constructed for the four Al- and three Fe-based WTRs (Figure 2-5). The natural log-transformed plot was used to accommodate large differences in rate coefficients between the Fe and the Al-WTRs. Despite the large differences in rate coefficients of the WTRs (differences of 4- to 5 orders of magnitude), a linear model seemed to be able to explain differences in pseudo P sorption capacities of a host of WTRs.

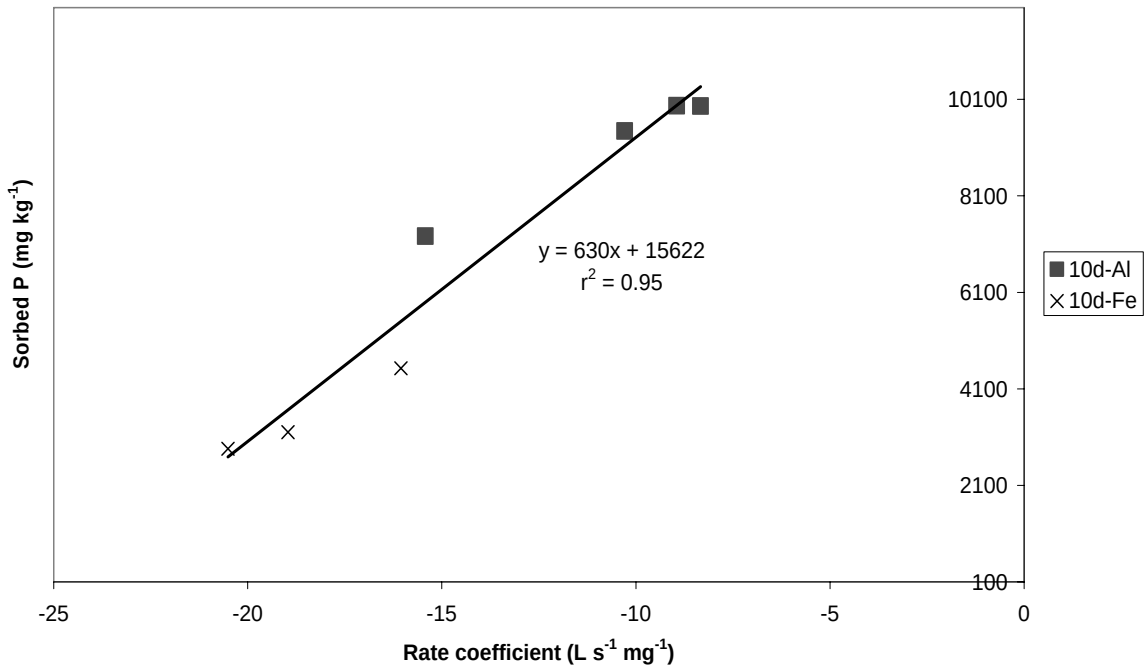

Figure 2-5. Semi (x-axis) ln-transformed plot of the second rate coefficient changes with P sorption capacities after 10 d of reaction for three Fe-WTRs (10 d-Fe) and four Al-WTRs (10 d-Al). The natural logarithmic transformation was utilized to accommodate large differences in the reaction rate coefficients for the 7 WTRs.

Evidently, P sorption limitations that influenced the P sorption capacities and kinetics were greater in Fe-WTRs than in the Al-WTRs.

Traditional measurements of oxalate extractable P, Fe and Al in organic wastes, soils, WTRs and their mixtures have been used to explain trends in runoff-P (Gallimore et al., 1999) and P leaching losses in soils amended with organic P sources and/or WTRs (Elliott et al., 2002). Oxalate extracts non-crystalline forms of Fe and Al and thus are expected to release P bound to Fe and/or Al amorphous hydroxides. Iron-based WTRs were characterized by high oxalate extractable Fe concentrations (108- to 195 g Fe kg^{-1}) and high total C concentrations (9.4- to 20.6 % C). However, oxalate-extractable [Fe+Al] accounted for 50- to 65 % of total [Fe+Al] for the Fe-WTRs, whereas for Al-WTRs it accounted for ranged from 80- to 98 % of total [Fe+Al]. This result suggests a greater reactivity of the Al-WTRs compared with the Fe-WTRs.

Elliott et al. (2002) explained differences in P-fixing capacities of an Al- and a Fe-WTR by their varying reactive Fe- and Al-hydroxide content, as measured by oxalate extraction. Their results indicated that the Al-WTR was more effective in sorbing P than the Fe-WTR. Dayton et al. (2004) found that oxalate extractable Al of 21 Al-WTRs was able to explain differences in runoff-P reductions by WTRs ($r^2 = 0.69$, quadratic model). However, they used smaller (15 h) equilibration times and lower initial P loads than used in this study. All 21 Al-WTRs used by Dayton et al. (2003) were also lower in oxalate extractable Al than the four Al-WTRs tested in this study. Surprisingly, no significant correlation was observed between oxalate extractable Fe +Al concentrations with P sorbed by Fe-WTRs, despite the high oxalate extractable Fe levels. Rate coefficients may explain the presence versus absence of relationships between P sorption capacities and

oxalate extractable Fe +Al for Al-WTRs and Fe-WTRs, respectively. Second order rate coefficients provide sufficient information on the slow P sorption stage that is usually rate-limiting for the overall P sorption.

Forces other than electrostatic, such as hydrophobic, and hydrogen bonding between organic molecules and mineral internal surfaces may be significant and affect the physicochemical nature of WTRs. For example, cationic polyelectrolytes added during the water treatment process account for a significant portion of sorbed P by WTRs (Butkus et al., 1998). Steric effects and hydrophobicities imposed by organic compounds present in WTRs may influence P sorption kinetics and diffusivities, making WTRs a complex system where molecular interactions are not simply electrostatic.

Reduced affinity for P by the Fe-WTRs was most obvious with Cocoa and much less with Panama Fe-WTRs. In the absence of added P, both WTRs had relatively low aqueous pH (3.85 and 5.4 for Cocoa and Panama, respectively). The pH of Cocoa material had an especially acidic pH, but increased upon addition of phosphate, reaching a pH of 5.6. Possibly the low pH of the two WTRs affected organic molecules configuration on the surface of WTRs.

The low pH (of some WTRs) may be responsible for low P sorption capacities, contrary to what would be expected based on pH surface charge effect. Low pH (4- to 5) leaves the majority of surface functional groups unionized, such that molecules may lie flat on the surface and block the free transfer of water or / solutes in and out of pores. Presence of surface functional groups with pKas $\geq$ 5.6 would reduce P accessibility to sorption sites. This may result in retarded solute and water diffusivities and consequently, low P sorption affinities. Preliminary work showed that adjusting the pH to 7 doubled the

P sorption capacity of the Cocoa material. This issue deserves more attention, and research should focus on factors influencing the low P sorption capacities of WTRs.

Oxalate (5 mM) desorbable P from Fe-WTRs was greater than from Al-WTRs, but never exceeded 8.3 % of previously sorbed P even after 80 d. The maximum amount of desorbed P (8.3 %) was exhibited by Cocoa, the least P sorbing material, followed by Panama (7.3 %). All Al-WTRs desorbed ≤ 0.2 % of previously sorbed P after 80 d, except for the Holland material that desorbed 1.5 %, similar to Tampa. Overall, P desorption decreased with increasing desorption time for all WTRs.

Phosphorus desorption from metal hydroxides is usually slower than P sorption, and decreases with increasing sorption time (Anderson et al., 1996). In the absence of competing anions, WTR-desorbed P was less than 1 % of total P during a 48 h equilibration period (O' Connor and Elliott, 2000). Phosphorus depletion from solution after 160 d (80 d sorption+80 d desorption) suggested that P was essentially irreversible bound to WTRs.

P bound to WTRs is apparently not readily released back to solution by a common biologic ligand (5 mM oxalate). However, organic ligand-induced P desorption in soils has been studied. In the presence of oxalate (5 mM), a considerable amount of phosphate was desorbed from B_h horizons of a Pomona soil in Florida (Bhatti, 1995). Ligand exchange and dissolution of the mineral surfaces were the two mechanisms proposed responsible for the P release. P released was not allowed to re-precipitate with soluble Al or Fe due to formation of stable soluble oxalate-Al / Fe complexes. This difference in P desorption by oxalate for WTRs versus soil material (e.g., Bh horizons) suggests that

organic ligand access to the P associated with WTRs is restricted, and that significant P release from WTRs by oxalate requires particle dissolution.

The fact that WTRs showed little metal solubility in 0.01 M KCl electrolyte suggests that they are rigid particles, which may be an advantage with regard to use as a P mitigation amendment, like alum. Alum is used for P reduction in water or animal wastes, and may release significant amounts of Al, posing potential phytotoxic effects, in cases where the pH is low. At pH values ≤ 4, WTRs dissolution may be considerable, and it may release some sorbed P may be released via particle dissolution. Typical oxalate (200 mM) extractions are commonly performed at pH 3, which dissolves noncrystalline Fe and Al components of the WTRs. However, a pH of 3 is rarely encountered in natural systems. Acid soils in humid regions can have pH ≤4.5 and warrant concern about WTR particle stability.However, in this study, this scenario is a worst-case scenario that could release immobilized P in solution. Even the Cocoa material, that had a natural pH of 3.9, did not desorb any Fe in solution after 160 d of oxalate solution in the dark. Potential development of reduced conditions associated with reduction of Fe/Mn hydroxides during the batch experiments must be excluded since no Fe was found in solution.

The large amounts of P sorbed, coupled with minimum oxalate (5 mM)-desorbable P concentrations suggest irreversible P sorption by WTRs. The pronounced hysteresis of P sorption by WTRs prompted further study of the mechanism(s) that may explain the biphasic nature of P sorption, via solid-state characterization techniques. Obviously, WTRs or materials that exhibit a slow P sorption step may not reach equilibrium in 1 to -2 d. Longer contact times may be needed to reach equilibrium. Rate limiting processes

are usually associated with diffusion limitations. Potential diffusion limitations may be associated with a significant amount of internal surfaces.

In the following chapter, we address the magnitude and complexity of internal surfaces that can be present in WTRs, in an attempt to explain slow P sorption by WTRs. Mechanisms and pathways of P sorption by WTRs via solid state characterization will be explored.

CHAPTER 3
PHOSPHORUS IMMOBILIZATION IN MICROPORES OF DRINKING WATER TREATMENT RESIDUALS

Introduction

Few data are available on the long-term P retention by WTRs, or soils amended with WTRs, or metal salts. To fully understand interactions between P and soil constituents, the effect of time needs to be considered (Scheidegger and Sparks, 1996). P sorption kinetics by metal hydroxides and soils are well characterized and generally show a fast sorption phase, followed by a slower reaction rate where sorption does not reach true equilibrium (Bolan et al., 1985). The fast reaction is ascribed to low-energy external surface sites, where ligand exchange is believed to be the main mechanism of adsorption (Bolan et al., 1985). The slow reaction between P and metals with metal hydroxides proceeds for days or months, and has been attributed to surface precipitation reactions (Van Riemsdijk and Lyklema, 1980; Nooney et al., 1998) or intraparticle diffusion into micropores (Axe and Trivedi, 2002).

Surface precipitation has been envisioned to occur either above (Dzombak and Morel, 1990) or below (Li and Stanforth, 2000) supersaturation with respect to the precipitating species. Ler and Stanforth (2003) considered another type of surface precipitation where dissolution of the adsorbent provides a continuous supply of metals to precipitate with P in solution. This phosphate "burial" may result in decreased P availability with time. Metal-P precipitation would be favorable for long-term retention, especially if a stable crystalline metal-P phase were formed. Intraparticle diffusion of

metal contaminants in metal hydroxides has well been documented (Axe and Trivedi, 2002). Diffusion-limited sorption in micropores was the rate-limiting step in Cu and Zn sorption by amorphous metal hydroxides during an "infinite bath" batch experiment (Axe and Trivedi, 2002).

Preliminary investigations of the Fe- and Al-based WTRs revealed a discrepancy between macroscopic P sorption data and P "parking area" based on N_2 specific surface area (SSA) measurements. In effect, the N_2-based "external" SSA was insufficient to account for sorbed P. This led to the hypothesis that P sorption on these WTRs was a 3-dimensional process that involved internal surface area. The objectives of this study were to (i) document 3-dimensional P distribution in WTR particles with respect to duration of loading and (ii) assess physiochemical properties of WTRs that elucidate P sorption mechanisms and implications for the stability of sorbed P.

Materials and Methods

Solid-State Characterization of WTRs

Following the P desorption stage (chapter 2), WTR particles were allowed to air dry for solid-state characterization. A cold field emission scanning electron microscope (*JEOL, JSM6330F*), coupled with an energy dispersive X-ray spectrometer (SEM-EDS) was used to locate P sorbed by the WTR particles. For a more quantitative treatment, electron microprobe wavelength-dispersive spectroscopy (EMPA-WDS, *JEOL, Superprobe 733*) was used to determine P distribution in WTR particles. Air-dried WTR particles from the sorption experiments, and thin sections thereof were used.

Particle size distributions of the two WTRs were generated with a particle size analyzer (Coulter, LS230). The instrument measures particle sizes from 40 nm to 2,000 μm by laser diffraction. The instrumentation is based on the principle that light is

scattered and diffracted at certain angles based on particle size, shape, and optical properties. Calculations assume that the light scattering pattern is due to single scattering events by spherical particles.

Thin cross sections were prepared by embedding WTR particles in a low vapor pressure resin (*Torr Seal, Varian, Lexington MA, USA*), and mounting them for polishing. Water-based mechanical polishing, using variable size silicon carbide abrasive papers (240-600 x), was applied to particles to minimize micro- morphological formations on the surface irregularities. Surface smoothness was confirmed by examination of the particles under a microscope. Samples were then carbon-coated to minimize charge localization phenomena before analysis. Electron microprobe analysis was conducted on flat surfaces avoiding artificial cracks due to polishing, either near particle edges, or interiors of the thin sections. The interior of the particles was designated to be approximately 60 μm on a straight-line distance away from the edge of the thin section.

Elemental compositions of the edges and interiors of particles treated with and without P for 80 d, were obtained. An extra time level of P-treated particles for 1 d was used to study the kinetic effect of P sorption. Ten to fifteen particles per treatment were used, and data were analyzed statistically. A completely randomized 3-factorial design was used to compare differences between treatment means of treatments at the 95 % confidence interval, using the Design-Expert statistical software (Design-Expert, 2001).

Surface Area and Porosity Analyses

The WTRs were treated with P (1,000 mg P L^{-1}), or left untreated for 80 d in a 1:10 solid: 0.01 M KCl solution ratio. Specific surface area characterization of the WTRs was performed after the completion of the sorption experiment. Specific surface areas of the WTRs were measured using N_2 and CO_2, respectively, as adsorbates in a volumetric

apparatus (Quantachrome Autosorb-1, *Quantachrome Corporation*, Boynton Beach, FL) after outgassing at 70 C for 4 h. Dinitrogen and CO_2 gas sorption experiments were performed in a liquid N_2 (77 K), and ethylene glycol baths at 273 K using a thermostat, respectively. Gas sorption was performed by introducing a certain amount of gas into the sample holder at a specific pressure, and temperature for 5 minutes. Pressure was increased incrementally and when the pressure difference was less than $8*10^{-4}$ atm, it would proceed to the next pressure point, or, the procedure was repeated. This procedure resulted in great precision but long experimental times (≥ 30 h per 30 points per sample). Micropore (CO_2) volume of the WTRs was calculated using the Dubinin-Radushkevich (DR) model (Eq. 3-1):

$$\log V = \log(Vo) - \frac{BT^2}{\beta}\left[\log\frac{P_0}{P}\right]^2 \qquad [3\text{-}1]$$

where V is the volume sorbed at standard pressure and temperature ($cm^3\ g^{-1}$ STP), V_0 is the micropore capacity ($cm^3\ g^{-1}$ STP), P_0 is the vapor saturation pressure of CO_2 (26,140 mm Hg), P is the equilibrium pressure (mm Hg), B is a constant representing adsorption energy, and β is the affinity coefficient of CO_2 gas relative to P_0. The monolayer capacity V_0 is obtained by plotting the *log V* against $\left[\log\frac{P0}{P}\right]^2$. The intercept of the linear plot is the monolayer micropore volume of CO_2 gas sorbed in the micropores. The model assumes that the pore size distribution is Gaussian, volume filling instead of layer-by-layer adsorption on the pore walls, and the degree of filling in micropores is a function of the negative differential free energy of adsorption. Micropore monolayer SSA was calculated with the Dubinin-Radushkevich-Kawazoe (DRK) equation, a special case of the DR equation. The DRK equation assumes layer-by-layer gas sorption on the walls, so

the only modification to Eq. 3-1 is that instead of the volume sorbed, the amount of gas sorbed was used.

Mercury Intrusion Porosimetry

Macroporosity of the WTR particles was assessed with the Hg intrusion technique. This technique uses a maximum pressure of 4,083 atm (60,000 psi) to intrude Hg into pores as small as ~ 1.8 nm, and is usually applied for meso- and macro-porous materials since it can quantify pores up to 184,000 nm in diameter. The method assumes the value of contact angle and surface tension of Hg, but no specific pore geometry has to be defined. Mercury does not wet most surfaces, so pressure has to be applied to enter pores. The greater the applied pressure, the smaller the pore size intruded by Hg. This mechanism is different than the N_2-BET method where the smallest pore sizes are accessed first at the lowest relative pressures. Specific surface area of the sample is obtained by relating the total surface area of the WTR particles to the pressure-volume work required to force Hg into the pores.

Results and Discussion

WTR Characterization

X-ray diffraction analysis (data not shown) verified the amorphous nature of both WTRs, with no apparent crystalline Fe and/or Al components. Sorption experiments revealed large P sorption capacities for both Al and Fe WTRs (Chapter 2). In brief, the Fe-WTR sorbed nearly all of the added P (10,000 mg P kg^{-1}), reaching 9,100 mg sorbed P kg^{-1}, after 80 d. The Al-WTR exhibited faster P sorption kinetics and sorbed essentially all of the added P within 10 d. Results from single day P sorption experiments showed that the Fe-WTR sorbed 2,000 mg P kg^{-1}, and the Al-WTR 7,200 mg P kg^{-1}.

Particle size distributions were generated for both WTRs and confirmed the broad size range distribution of the < 2 mm WTR particles (Figure 3-1). The broad size distribution was suggested by the large amounts (% number distribution) of small particles (1- to 10 μm for the Al-WTR, and 0.1- to 10 μm for the Fe-WTR), and a small amount of large volume particles (% volume distribution), in the range of greater than 100 μm.

The dramatic affinity for P and relatively slow P sorption kinetics of the WTRs led us to suspect a sorption mechanism other than ligand exchange with structural hydroxyls on particle exterior surfaces. High P sorption capacity and the pronounced hysteresis prompted further study of the nature of P sorption mechanism via solid-state characterization techniques.

Solid-State Characterization

It was hypothesized that given enough residence time, and initial P load, three-dimensional P sorption would occur. To test this hypothesis, solid-state surface analysis techniques, such as SEM-EDS, and EPMA-WDS were used.

Scanning electron secondary images for both untreated WTRs were similar (Figure 3-2). Images showed the irregular shape and variable size of WTR particles. Particle surfaces ranged from rough to fairly smooth. Elemental spectra (SEM-EDS) verified the presence of P, Al and Fe, as well as Si, Ca, and Na. SEM-EDS dot maps of whole particles showed relatively uniform elemental distributions for both untreated (no P added) and P-treated samples (data not shown). The P in untreated WTRs comes from the original raw drinking water.

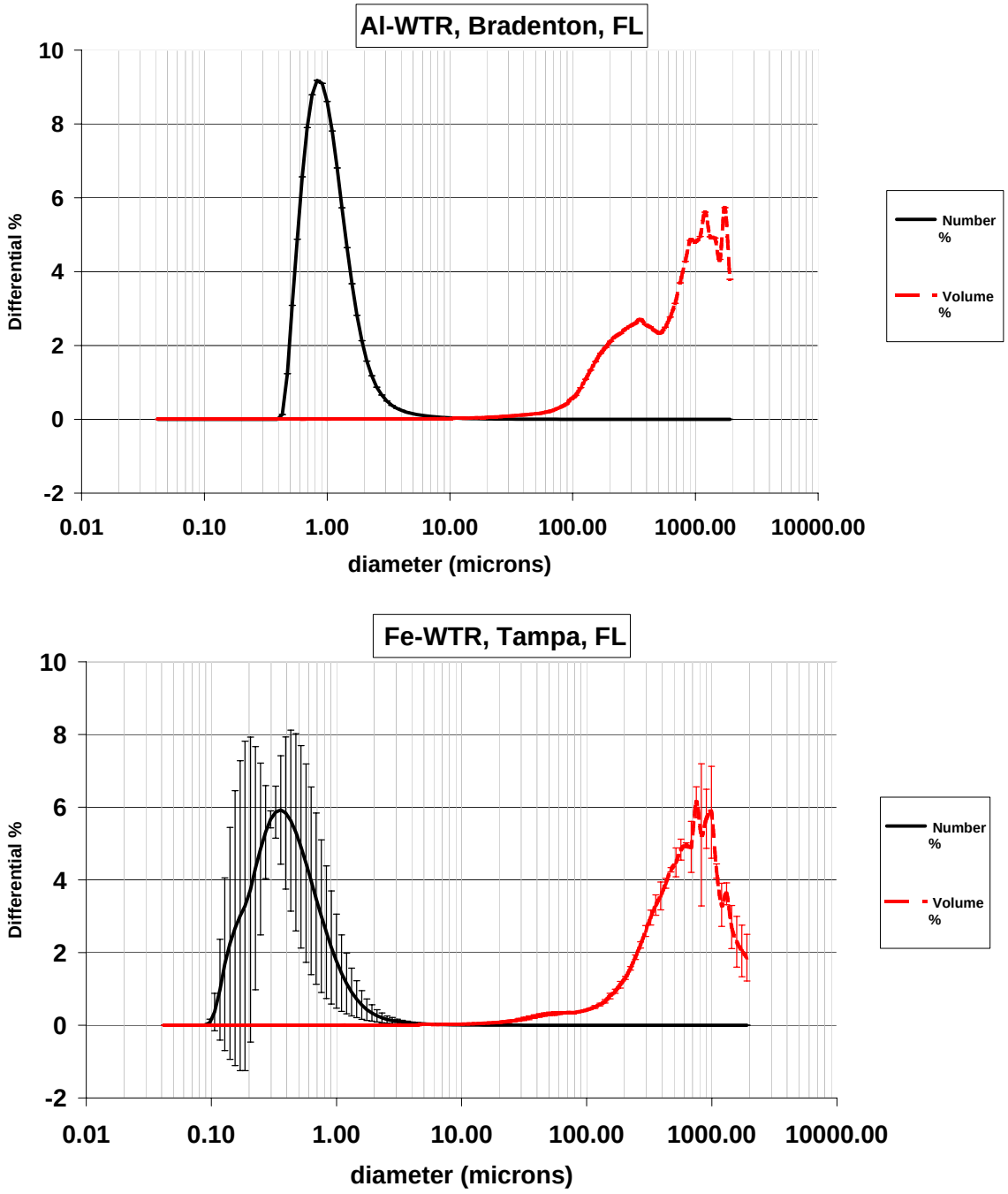

Figure 3-1. Semi-log normal particle size distributions based on laser diffraction, of WTR particles less than 2 mm.

Similar uniform P distribution, but greater dot intensity, was also observed for P-treated particles after 80 d. No clustering of P (zones of obvious P precipitation) was evident. Bertrand et al. (2001) used secondary ion mass spectrometry (SIMS) on goethite and calcite loaded with 2,950 and 930 mg P kg^{-1}, respectively, to study the association of P with the minerals. SIMS analysis, coupled with image analysis, showed that P was evenly distributed on the goethite surface, but clustered on the calcite, suggesting adsorption for the former and precipitation for the latter.

The majority of the studies involved with high P loads and increased equilibration times of P sorption on relatively crystalline metal hydroxide surfaces suggested a P surface precipitation mechanism. However, in our case, no discrete metal -P phases were found on the surfaces of WTRs in this study. The prolonged P sorption coupled with surface area calculations implied a three-dimensional P sorption by WTRs similar to that observed by Bertrand et al. (2001). The hypothesized mechanism is that P diffuses into the interior of WTR particles via solution to reach meso- and micropore domains. To test this hypothesis, thin cross-sections were prepared that allowed monitoring the profile depth P distribution in the WTR particles over time.

No discrete surficial metal-P phases were detected with SEM-EDS spectroscopy, and hypothesized that P diffuses into particles to reach meso- and micro- pore domains. SEM-EDS dot maps of cross-sections from both WTRs qualitatively supported an intraparticle sorption mechanism, showing that P was evenly distributed within the particles (Figure 3-3), except for some near edge P zonation in Fe-WTR particles after P treatment.

Figure 3-2. Scanning electron secondary images of the Al- and Fe-based WTRs. (A) secondary image of representative Al-WTR particles; scale bar = 200 µm. (B) Magnified secondary image of a portion of image (A); scale bar = 100 µm. (C) secondary image of representative Al-WTR surfaces; rough and smooth surfaces; scale bar = 20 µm. (D) Magnified secondary image of the rough surface of the Al-WTR particle from image (C); scale bar = 2 µm. (E) secondary image of representative Fe-WTR particles; scale bar = 200 µm. (F) Magnified secondary image of a portion of image (E); scale bar = 100 µm. (G) secondary image of representative Fe-WTR surfaces; rough and smooth surfaces; scale bar = 20 µm. (H) Magnified secondary image of the rough surface of the Fe-WTR particle from image (G); scale bar = 2 µm. Images D and H show surface porosity, but magnification is not large enough to show microporosity.

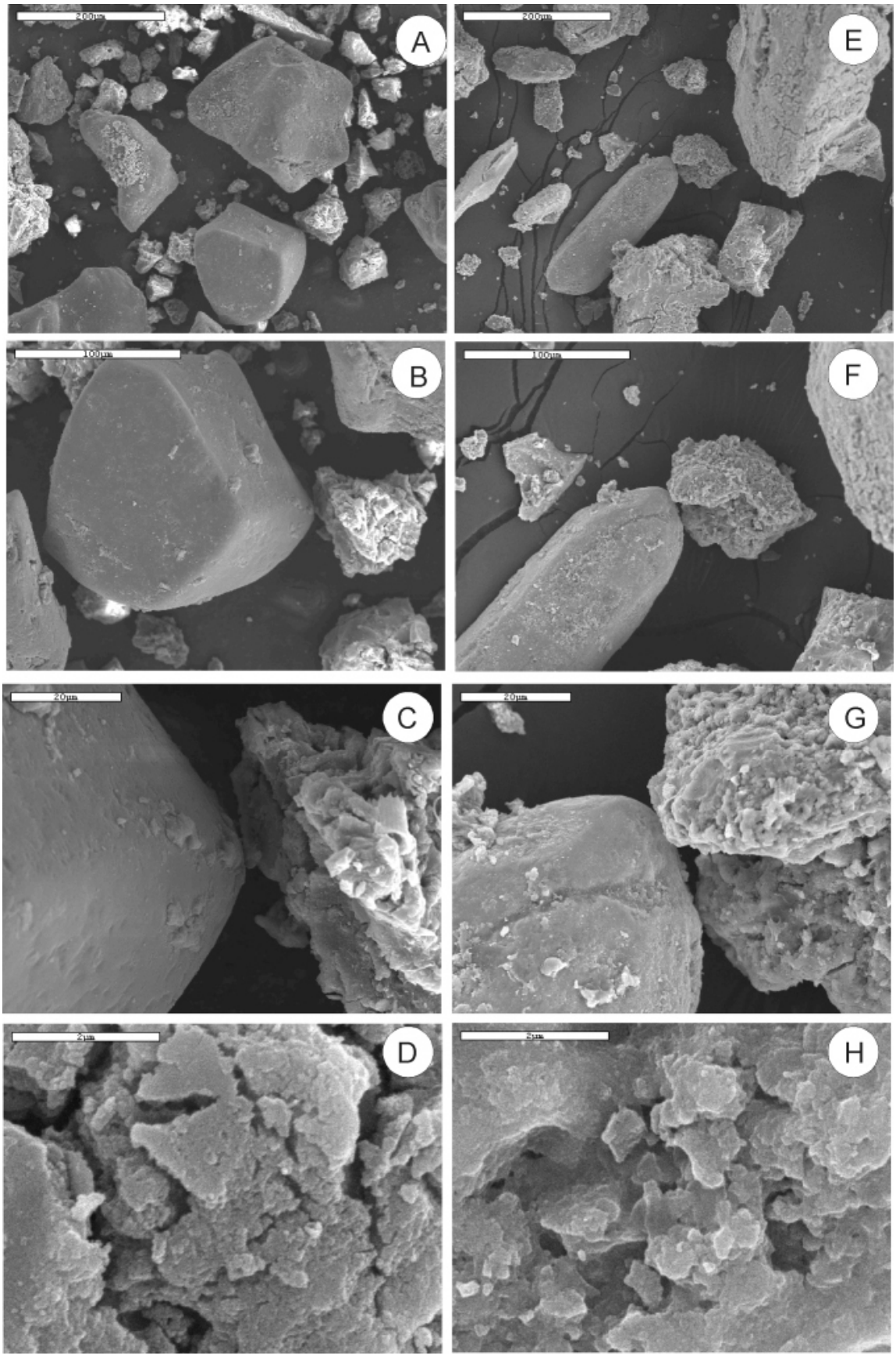
A
E
B
F
C
G
D
H

Cabrera et al. (1981) found that P reacted for a longer time with lepidocrocite than goethite. Lepidocrocite consists of crystals forming aggregates connected by micropores, which may facilitate P diffusion to distant sorption sites. Torrent et al. (1992) used goethites (SSA 25 to 182 $m^2 g^{-1}$) to characterize P sorption after reaction for 4 months. Slow P sorption was correlated with oxalate (200mM)-extractable Fe and microporosity. Strauss et al. (1997) conducted P desorption after loading goethites with P. Release of Fe from P-loaded goethites was much slower than Fe from untreated goethites. Strauss et al. (1997) claimed that the ease of accessibility of sorbed P to the extractant and reaction time were the predominant factors that influenced P desorption. The more P is diffused and associated with micropores, the less P will be desorbed. Madrid and De Arambarri (1985) studied P sorption on two mesoporous iron hydroxides, for reaction times of 0.5 to 12 d. During the desorption step, readsorption of phosphate occurred up to 3 % of the P sorbed, as a result of a continuous slow sorption step. They speculated that the presence of cylindrical mesopores were responsible for the slow P adsorption.

To further confirm the intraparticle P diffusion in WTRs, we used a more quantitative instrumentation than SEM-EDS. EMPA-WDS analysis has been used in soil science to quantify elemental composition in sediments (Rao and Berner, 1995), and more specifically, to assess P distribution in soil samples (Harris et al., 1994; Agbenin and Tiessen, 1994; Qureshi et al., 1969).Measurements were made near the particle edges and within interior regions. The interior of the particles was designated approximately 60 μm on a straight-line distance away from the edge.

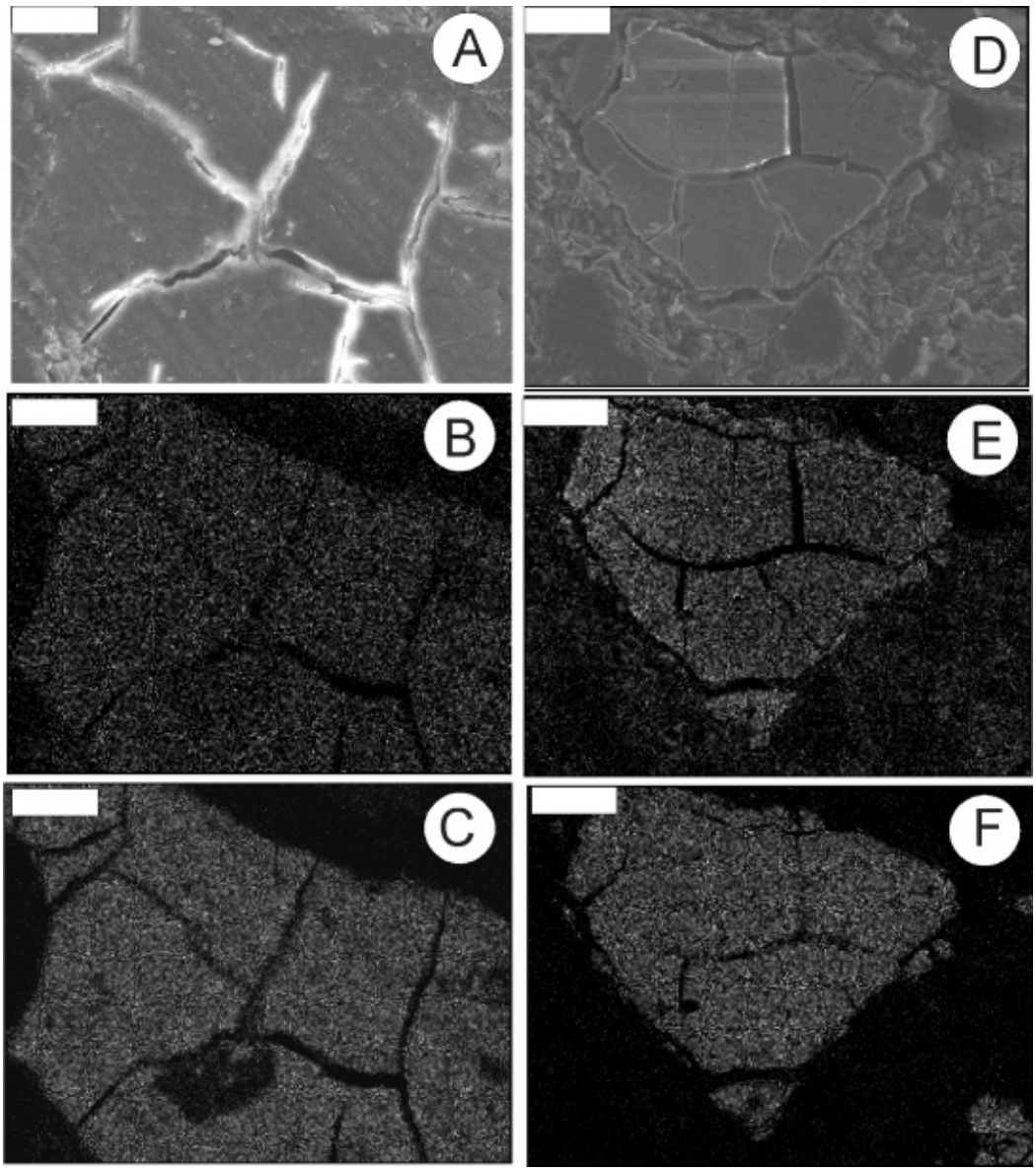

Figure 3-3. Scanning electron secondary images (A, D) and the corresponding P and metal dot maps (B,C, E and F) of thin cross-sections after 80d P treatment for both WTRs. (A) secondary image of a representative Al-WTR cross-section; scale bar = 20μm. (B) P dot map of the secondary image in (A). (C) Al dot map of the secondary image in (A). (D) Secondary image of a representative Fe-WTR cross-section; scale bar = 20μm. (E) P dot map of the secondary image in (D). (F) Al dot map of the secondary image in (D). P dot maps of cross-sections for both WTRs show uniform P distribution, with no evidence for surface precipitation. Rarely, and only for the P-treated Fe-WTR, there were indications of zonal P enrichment near the particle edge.

Cross-sectional P distribution analysis of the P-treated WTRs showed significant ($p<0.001$) increases in the relative P concentrations in the interior of the particles (approximately 60 μm inside) with time (from 1 to 80 d) (Figure 3-4). Phosphorus concentrations of 80 d-treated particles were significantly greater than 1d-treated particles, both at the edge and interior (Figure 3-5). Average P concentrations for P-treated particles were slightly greater near the edge, but edge versus interior differences were not statistically different. Data for the Al-WTR were similar (not shown). Ippolito et al. (2003) used EPMA-WDS dot maps to assess P distribution in a P-treated Al-WTR equilibrated for 211 d. Dot maps showed no evidence for P surface precipitation, but a uniform amorphous Al-P association throughout the particles (Ippolito et al., 2003).

EPMA-WDS work suggests that P diffuses towards the interior of the WTR particles rather than accumulating significantly at the particle surface as by precipitation. This form of sorption may have favorable implications for P immobilization. Strauss et al. (1997) conducted P desorption experiments after loading goethites with P. The ease of accessibility of sorbed P to extractant and reaction time were the main factors that influenced P desorption. These authors proposed a micropore diffusion mechanism but did not perform pore size distributions or SSA determinations that would substantiate this explanation.

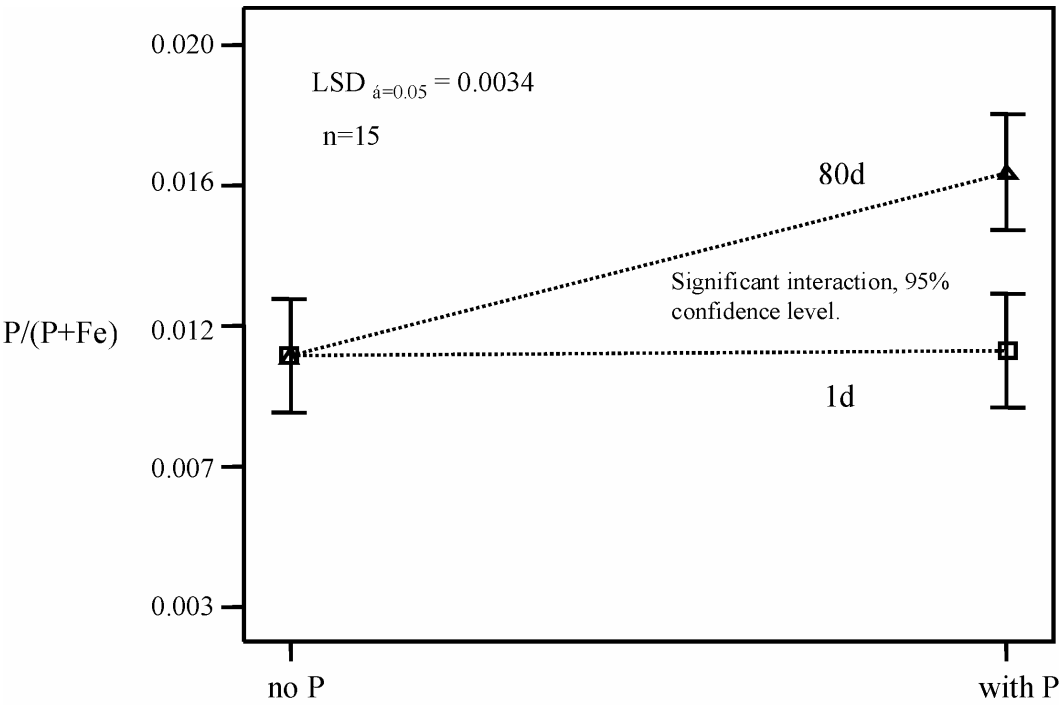

Figure 3-4. Electron microprobe analysis of the thin cross-sections of P-treated and untreated Fe-WTR particles. Error bars denote the least significant difference at the 95 % confidence level. Data for the Al-WTR were similar.

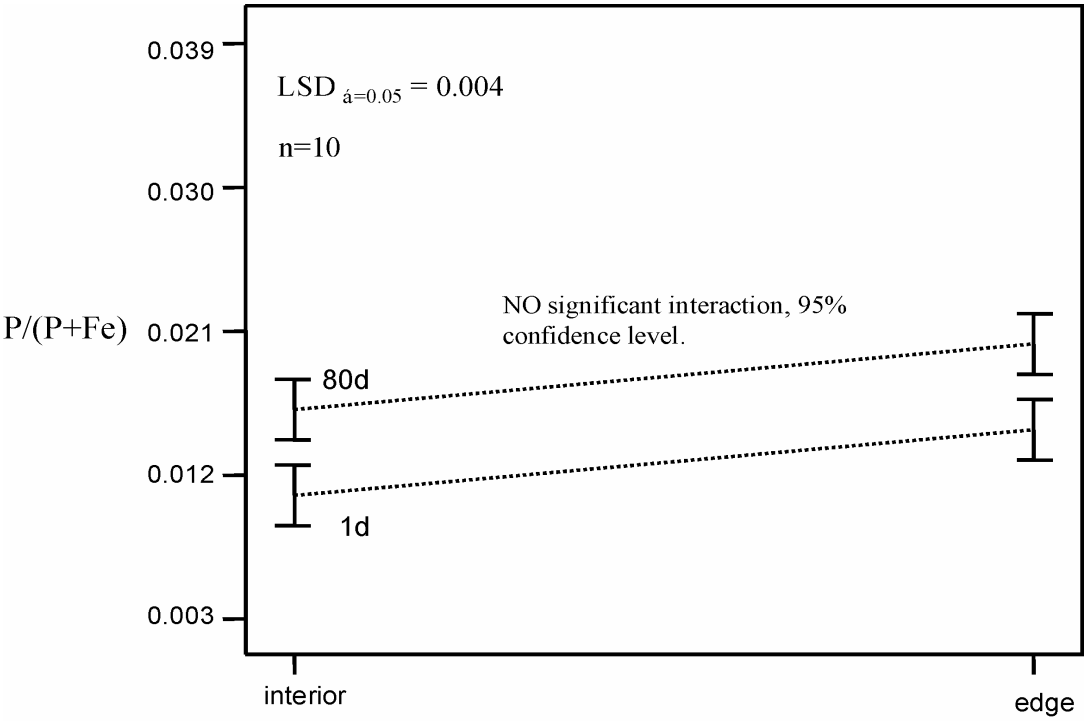

Figure 3-5. Changes in relative P concentration with P location (edge versus interior) and time (1 and 80 d) of P-treated (10 g P kg^{-1} initial load) thin cross-sections of the Fe-WTR. Interior was designated ~ 60 µm away from edge.

Mercury Intrusion Porosimetry

WTRs were subjected to Hg intrusion porosimetry to assess the macroporosity of the materials. Assuming that the BET-N_2 SSA value of ~ 4 m^2 g^{-1} was correct, the Fe-WTR should be a relatively non-porous material. However, the P sorption capacity of the Fe-WTR greatly exceeded the P monolayer adsorption capacity, implying a sorption mechanism other than simple ligand exchange with surface hydroxyls. We hypothesized that macro- and meso-pores facilitated P intrusion of the WTR particles. BET-N_2 analysis is not capable of measuring macropores (> 50 nm). Mercury porosimetry revealed a low volume of macropores for both WTRs; most of the pore volume accessed by Hg was in the pore size range of mesopores (2- to 20 nm) (Figure 3-6). Total pore volume intruded by Hg for the Fe-WTR was very low. Hg intrusion-based SSA of the Fe-WTR was also low (~ 2.5 m^2 g^{-1}), and close to the value measured by the BET-N_2 method (3.7 m^2 g^{-1}) (Figure 3-7). Similarly, Hg intrusion-based SSA of the Al-WTR (33 m^2 g^{-1}) was very close to the BET-N_2 SSA value (37.5 m^2 g^{-1}). Mercury porosimetry data showed that both materials lack a significant network of macropores.

Micropore Surface Areas of the WTRs

The hypothesis was tested that sorbed P by WTRs mostly resides in micropores that probably originated during WTRs formation. This hypothesis would mean that external particle surface area would be insufficient to account for the observed P sorption. Calculations were based on SSA analyses conducted with both N_2 and CO_2 gases. The calculations were used to match the existing P sorption capacities of the WTRs, with the measured SSAs. One day was operationally chosen to represent the P adsorption stage, or the so-called short term P capacity, based on the work of Van Riemsdijk and Lyklema (1980).

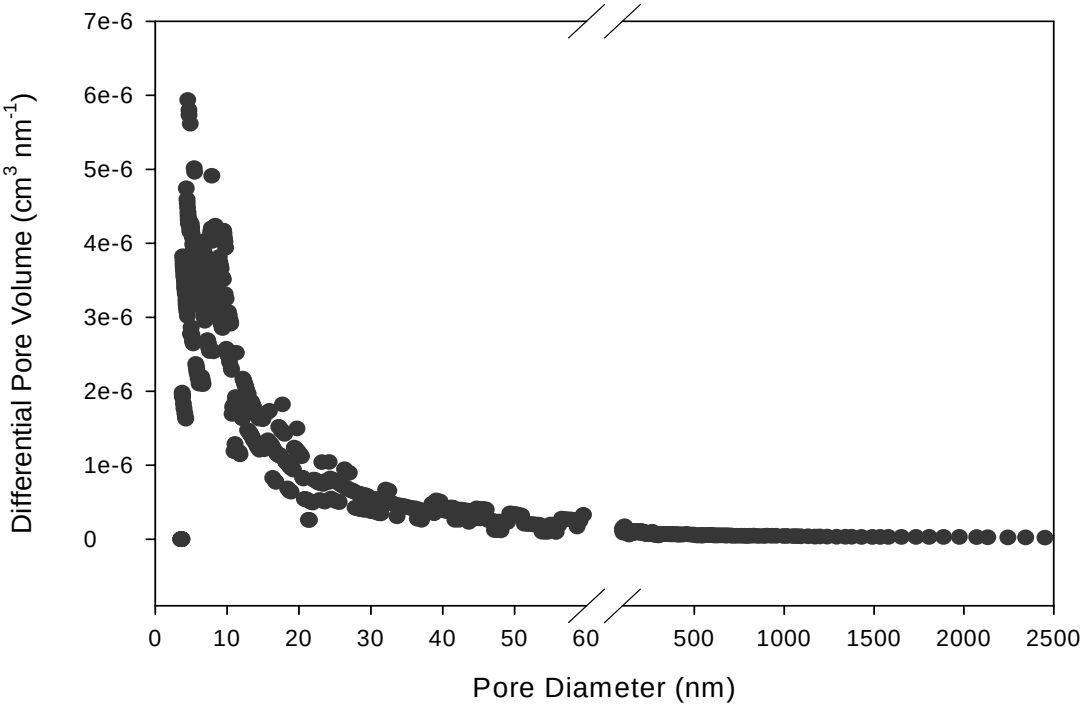

Figure 3-6. Mercury pore volume distribution of the Fe-WTR. Data for the Al-WTR were similar.

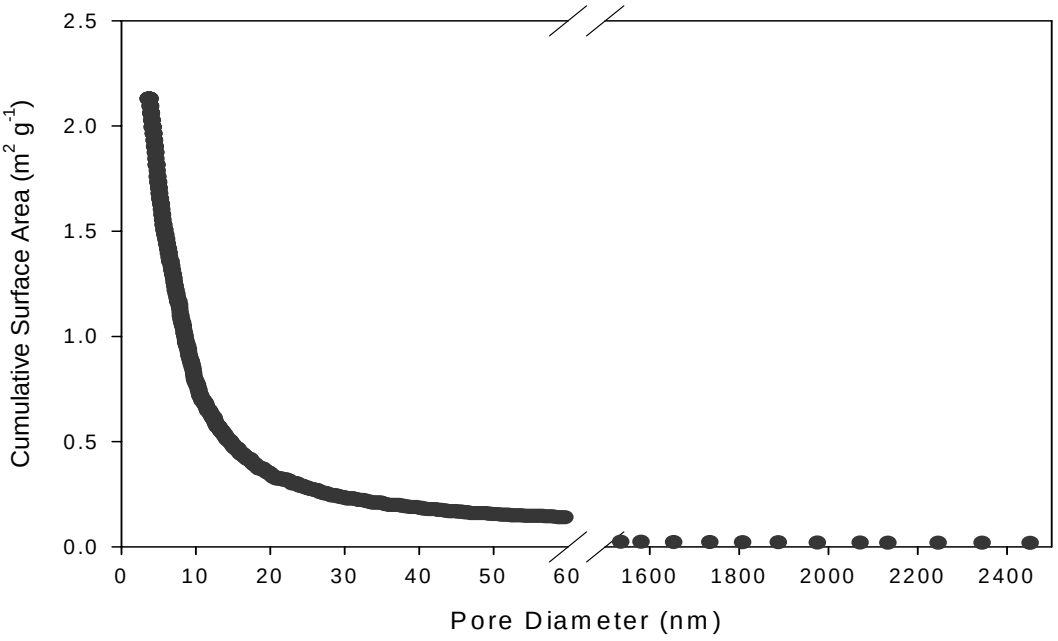

Figure 3-7. Cumulative surface area of the Fe-WTR, based on Hg porosimetry.

Short-term P sorption capacity of the Fe-WTR was 2 g P kg^{-1} and the SSA was 3.7 ± 0.2 m^2 g^{-1}, resulting in a phosphate adsorption density of 1.7 x 10^{-5} moles PO_4^{-3} m^{-2}. For the Al-WTR, the short-term P sorption capacity was 7.7 g P kg^{-1} WTR, the SSA was 37.5 ± 0.7 m^2 g^{-1}, and the phosphate adsorption density was 6.6 x 10^{-6} moles PO_4^{-3} m^{-2}.

Tamura et al. (2001) determined surface hydroxyl site densities of metal oxides with wide SSA values (0.9 to 245 m^2 g^{-1}) treated with di-, tri, and tetravalent metals, and reported a similar density of 2.6x10^{-5} moles of sites m^{-2} for trivalent metal hydroxides. Assuming ligand exchange to be the predominant P adsorption mechanism during short-term (1 d) P sorption, Fe-WTR phosphate density (1.7x10^{-5} moles PO_4^{-3} m^{-2}) was reasonably close to the value reported by Tamura et al. (2001). However, the Al-WTR phosphate density (6.6x10^{-6} moles PO_4^{-3} m^{-2}) was lower, consistent with its higher BET-N_2 SSA. Data indicated that sorbed P exceeded the monolayer P adsorption capacities of both WTRs. Based on the above phosphate densities, we calculated the parking area occupied by a single phosphate molecule:

Parking Area (m^2 / PO_4 molecule) = 1 / (S_{max} avogadro#)*
Where S_{max} is the maximum adsorption capacity in moles P m^{-2}.

The parking area of a PO_4 molecule per WTR N_2-based unit surface area was 9.5 x 10^{-20} and 2.5 x 10^{-19} m^2 per PO_4 molecule sorbed by the Fe-WTR and the Al-WTR, respectively. Iron-WTR sites occupied by phosphate molecules after 80 d (based on sorption of 9 g P kg^{-1}) was also calculated using the parking area equation. The resulting SSA was 16.8 m^2 g^{-1}, which exceeded the BET-N_2 SSA of the untreated Fe-WTR (3.7 m^2 g^{-1}). Similarly, the estimated SSA of phosphate molecules for the Al-WTR after 80 d (10 g P kg^{-1}) was 48.7 m^2 g^{-1}. BET-N_2 SSA of the P-treated Al-WTR for 80 d was 25 m^2 g^{-1}.

Total P uptake by the Fe-WTR was 7.9 mg PO_4 m^{-2}, based on a P sorption of 9 g P kg^{-1} WTR, and SSA of 3.5 m^2 g^{-1} after 80 d. Similarly, total P uptake by the Al-WTR was estimated to be 1.23 mg PO_4 m^{-2} based on P sorption of 10 g P kg^{-1} WTR, and SSA equal to 25 m^2 g^{-1} after 80 d. Mean P adsorption monolayer capacities of goethites varying in crystallinity and SSAs after single day sorption at pH 6 were 0.239 mg PO_4 m^{-2} (Torrent et al., 1992), and 0.095 mg PO_4 m^{-2} for gibbsites (van Riemsdijk and Lyklema, 1980). A goethite with SSA similar to the Fe-WTR had a P adsorption monolayer capacity of 0.270 mg PO_4 m^{-2} after 1 d (Torrent et al., 1992). In the case of the Fe-WTR, a different phosphate adsorption density (1.6 mg PO_4 m^{-2}) was observed for suspensions reacted for a day and corresponded to the P adsorption maximum capacity for goethites.

A similar trend was observed by van Riemsdijk and Lyklema (1980), where P sorption densities less than 0.09 mg PO_4 m^{-2} were the result of ligand exchange between surface hydroxyls with phosphates, and densities greater than the monolayer (0.095 mg PO_4 m^{-2}) were ascribed to P precipitation. The data suggested that more PO_4 was sorbed per unit area than feasible based on adsorption densities of Fe and Al hydroxides varying in SSA and elemental composition. This, in turn, suggests that actual WTRs SSA of WTRs is under-estimated by N_2-BET analysis.

Typically, adsorption is considered to be exothermic in nature and increases as temperature decreases. Sorption in narrow pores (micropores or bottle neck-shaped mesopores) may be diffusion-controlled and endothermic, involving significant amounts of activation energy. Apparent underestimation of SSAs via BET-N_2 suggests that dinitrogen molecules do not have the necessary activation energy to overcome energy barriers associated with micropores present in the WTRs. Carbon dioxide gas sorption at

273 K is an alternative to N_2 for micropores that are less than approximately 1.5 nm or 15 Å wide. Carbon dioxide molecules have a greater saturation vapor pressure (26,140 versus 760 mm Hg), and the determination is conducted at greater temperatures (273 versus 77 K). This enables the CO_2 molecules to diffuse through pores-doorways that are a few molecular diameters in width.

CO_2 gas sorption analysis was performed for both WTRs. The isotherm analysis of CO_2 sorption by the Fe-WTR untreated and treated with P for 80 d, revealed mean SSA values of 27.5 and 17.3 $m^2 g^{-1}$, respectively (Figure 3-8). Similarly, the mean CO_2-surface area of the Al-WTR was 105 and 80 $m^2 g^{-1}$, for samples untreated and treated with P for 80 d. The CO_2-SSAs were calculated, based on the DRK method (Table 3-1). Thus P sorption causes reduction in CO_2 -SSA, suggesting that P blocks some pores that would otherwise be accessible to CO_2. A grand canonical Monte Carlo model was used to calculate the micropore volume distribution of the Fe-WTR (Figure 3-9).

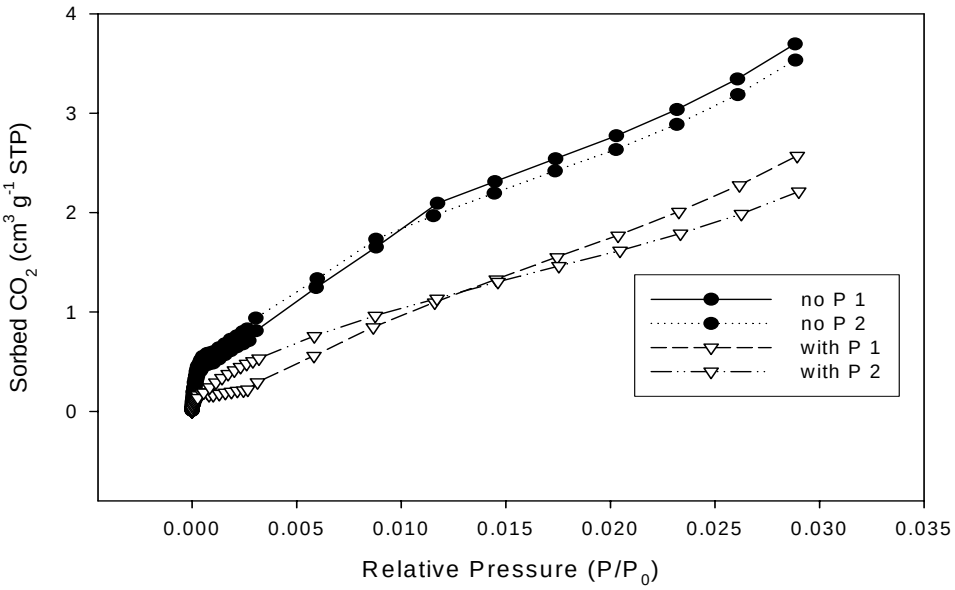

Figure 3-8. Replicated CO_2 gas sorption (273 K) of the Fe-WTR treated with and without P for 80 d.

Table 3-1. Total micropore volume, and CO_2-SSA calculations based on the Dubinin Radushkevich method (DR) of the WTRs treated with and without P for 80 d.

	Treatment	DR micropore surface area ($m^2\ g^{-1}$)	Linear regression fit R^2 (%)	Total micropore volume ($cm^3\ g^{-1}$)
Fe-WTR	No P	27.5 ± 0.71*	99	0.012 ± 0.0004
	With P	17.3 ± 0.99	99	0.008 ± 0.0004
Al-WTR	No P	104.9 ± 10.4*	99	0.042 ± 0.008
	With P	79.9 ± 9.5	99	0.034 ± 0.004

* average of two replicates ± one standard deviation.

Phosphate sorption in micropores shifts the pore size distribution to larger size micropores since phosphate occupies micropores from 0.4 to 0.8 nm (Table 3-1). These SSA values represent only surfaces associated with pores up to 1.5 nm, therefore the surface area values are not external, but micropore associated.

The decrease in CO_2-SSA values after P- treatment is roughly consistent with the surface areas previously estimated to be occupied by phosphate molecules. That is, the sum of the two values for both WTRs was higher than the N_2-values, but not unrealistically high. To prove this, we conducted some simple calculations. The CO_2-SSA for the treated-with-P Fe and Al-WTRs were 17.3 and 79.9 $m^2\ g^{-1}$, respectively. We assumed that micropores blocked by phosphate molecules are inaccessible to CO_2 molecules. If the above values are added to the calculated SSA of phosphate molecules occupying the Fe and Al –WTR sites, (which were 16.65, and 48.7 $m^2\ g^{-1}$, respectively), then the sum (33.95, and 128.6 $m^2\ g^{-1}$ for the Fe and the Al-WTR, respectively) falls close to the CO_2-SSA for the untreated Fe and Al-WTRs (27.5 and 104.9 $m^2\ g^{-1}$,

respectively). The error associated with the calculations is 23 and 22 % of the CO_2-SSA for the untreated Fe and the Al-WTRs, respectively.

The underestimation of BET-SSA based on P sorption capacities of both WTRs could be explained by the inability of N_2 molecules to access the micropores present in the WTRs. Kaiser and Guggenberger (2003) found that the BET-N_2 SSA of a host of soils varying in organic carbon content was inversely related to the soil C content. Sorption of soil organic matter at the mouth of micropores formed by two domains of a mineral may hinder N_2 molecular diffusion into the micropore, and thus, underestimation of the true SSA (Kaiser and Guggenberger, 2003).

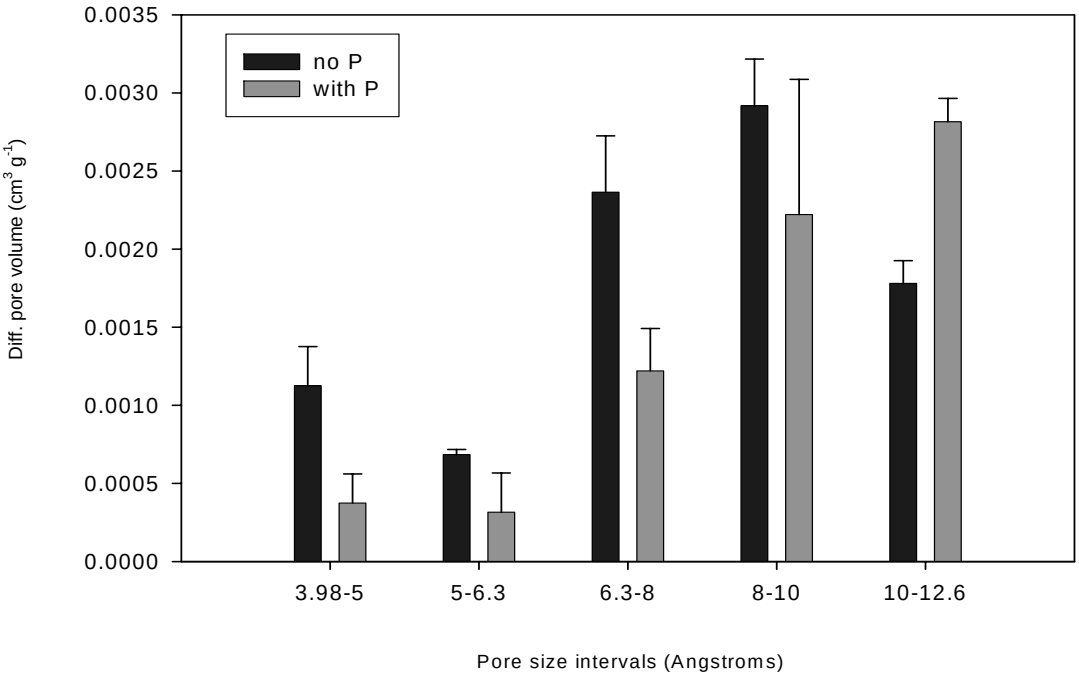

Figure 3-9. Pore size distribution of the Fe-WTR treated and untreated with P for 80 days.

The CO_2 molecules can diffuse and occupy such micropores that N_2 can not. Phosphate molecules may reside in micropores (< 1.5 nm) that are inaccessible by traditional BET-SSA measurements. Micropore accessibility is consistent with time-

dependent P sorption and hysteresis, since they could limit diffusion rates. Micropore-bound P would likely resist desorption, which favors long-term stability of sorbed P by WTRs.

The calculations seem reasonably accurate taking into account the complex organo-mineral nature of WTRs. More specifically, the elemental heterogeneity of the WTRs coupled with their wide pore size distribution, would affect the consistency of the calculations. Near-surface characteristics (surface roughness) could influence the sorption of N_2 and CO_2 gas molecules under dry conditions during BET measurements (Huang et al., 1996). However, phosphate sorption in aqueous solutions would not have encountered such problems since phosphate is a polar hydrophilic compound that could access micropores without being restricted by the presence of water molecules, as this might happen with non-polar organic compounds (Huang et al., 1996).

Another factor that might influence the accuracy of the calculations is the uncertainty behind the monolayer P adsorption capacities of the WTRs (fast reaction). The amount of P adsorbed within a day was used to calculate the amount of P required completing a monolayer on the external surface of the WTRs (Van Riemsdijk and Lyklema, 1980; Torrent et al., 1990).

Total elemental C content of WTRs varies, but it can be as much as 15- to 20 % (O'Connor et al., 2001). Recent studies have shown the importance of microporosity of soil organic matter (SOM) in regulating hydrophobic organic contaminant (HOC) availability and transport (Xing and Pignatello, 1997; Xia and Ball, 1997). SOM was recently recognized as a dual-functional sorbent for HOCs; consisting of as a soft or rubbery state, as well as a hard or glassy C state (Huang et al., 1997; Ran et al., 2002).

The hard C or condensed organic domain is believed to exhibit nonlinearity in the sorption of HOCs by SOM. Ran et al. (2002) showed that the condensed microporous C domain of a peat and two river sediments was responsible for the nonlinear sorption of HOCs. Ran et al (2002) further speculated using CO_2 gas sorption that HOC sorption within the micropores of SOM is a pore filling process based on their micropore volume calculations.

A bimodal sorption character of organic contaminants in soils, sediments, and aquifer materials has been extensively documented (Huang et al., 1996; Farrell et al., 1999). The bimodal sorption consists of an initially fast reaction, followed by a slow rate of reaction that could last from weeks to months until reach equilibrium is reached. The slow fraction of sorption has been attributed to intraparticle diffusion in meso- and micro pores of mineral particles (Axe and Trivedi, 2001), and / or to diffusion of contaminants within soil organic matter.

Phenathrene sorption to meso- and micro-porous silica gels, and to non-porous kaolinite, alumina and quartz samples reached equilibrium within minutes, indicating that little phenathrene was sorbed by the internal porosity of the gels (Huang and Weber, 1996). The non-polar nature of phenathrene may be a significant factor that negatively affected its pore diffusion in inorganic matrices (Huang and Weber, 1996).

In an attempt to explain slow-desorption processes on mineral solids, Farrell et al (1999) used glass beads and silica gels to assess the desorbabilities of chloroform, trichloroethylene, and perchloroethylene in unsaturated columns of silica particles with water-filled micropores. The particles were previously left to react with the organics for a period up to 3 months. The desorption-resistant fraction increased with increasing contact

time during the sorption step. They suggested that silica precipitation blocked the micropores, thus retarding organic desorption rates. Riley et al. (2001) were able to attribute the slow desorption of phenathrene from porous silica gels to micropore effects.

Low molecular organic acids might be trapped in the small pores of the WTRs, regulating the diffusion and bioavailability of water and phosphate molecules. Thus, for N_2 molecules to diffuse through such small pores, greater activation energy would be required to overcome resistant at organically constricted pore openings (Gregg and Sing, 1982). The use of CO_2 as the adsorbate at a higher sorption temperature (273 K) may have enabled access of pores having widths less than 1.5 nm that apparently contributed to the prolonged three-dimensional P sorption by the WTRs.

To test the organic blockage hypothesis, and further confirm the validity of our CO_2 measurements, synthetic Al hydroxides with and without P, as well as a non-porous sea sand, were subjected to CO_2 gas sorption analysis. Both Al hydroxides and the sea sand were free of organic C (data not shown). Specific surface areas for the Al hydroxides, calculated with both N_2 and CO_2, were expected to be similar. The CO_2-SSA of the Al hydroxides co-precipitated with and without P were 53 and 148 $m^2\ g^{-1}$, respectively. The BET-N_2 SSAs of the Al hydroxides co-precipitated with and without P were 42 and 168 $m^2\ g^{-1}$, respectively. Thus, SSAs calculated based on N_2 and CO_2 gas sorption were similar, consistent with the idea that the absence of organics in the Al hydroxides was responsible for not underestimating SSA measurements using N_2 gas sorption.

De Jonge and Mittelmeijer-Hazeleger (1996) showed that the SSAs of three SOM samples were underestimated by BET-N_2 measurements. CO_2 analysis showed that 95- to

99 % of the SOM surface area is composed of micropores having average width of 0.5 nm. The differences in CO_2 and N_2 SSA values of the WTRs suggested that organic compounds trapped in WTR-micropores regulated the diffusion of gas molecules in and out of WTR micropores of the WTRs. The sea sand "analytical blank" did not adsorb CO_2, confirming its non-porous and organic C-free nature.

Micropores exhibit significantly greater interaction potentials than the meso- or macropores due to the walls proximity. Everett and Powl (1976) calculated that the adsorption energy could be up to 3.5 times greater in a micropore compared with that of an open surface. Desorption of solutes residing in micropores might be limited by the high adsorption enthalpy involved between the adsorbate and the pore-wall residing adsorbent. The strong field forces associated with micropore walls might provide us with a mechanistic explanation of the long-term stability of sorbed P by the WTRs. Micropore-bound phosphates may be anchored by the walls interacting with both sides of phosphate molecules, maximining the bonding sstrength between oxides and P.

Several studies have attempted to explain the slow P sorption by metal hydroxides (Willett et al., 1988; Agbenin and Tiessen, 1995; Madrid and De Arambarri, 1985; Cabrera et al., 1981). All of these studies suggested a mechanism for P diffusion into micropores, mechanism, but none supplied the kind of direct evidence presented in this study. Micropore-bound P should not be released unless dissolution of the WTR particles occurs, such as in strongly acidic conditions (pH < 4). WTR particles maintained structural integrity for 160 d at pH 5- to 7, as monitored by soluble P and metal measurements in 0.01 M KCl (data not shown).

Further studies are needed to predict the time scales over which P will be stable and immobilized by WTRs. Combination of diffusional and thermodynamic models might be useful to address such a complicated issue. Non-linear fits of long-term P sorption kinetics data for of the Fe-WTR to a diffusion model resulted in a calculated P diffusion coefficient on the order of 10^{-15} cm^2 s^{-1} (for details see chapter 7), which is in accordance with slow P diffusion in microporous sorbents (Axe and Trivedi, 2001). Estimated P concentrations after 80 d of reaction 60 μm inside the particle measured with EPMA-WDS were 94 % of predicted values from the diffusion model and the calculated P diffusion coefficient. However, the diffusion model was applied to the idealized case where particles have a specific shape (spheres), and unimodal particle and pore size distributions. The model also assumed that sorption and desorption have the same reaction rates, ignoring hysteretic effects. P diffusion coefficients likely vary with WTR physicochemical properties, which could affect the ease with which phosphate molecules diffuse into the structure.

Our findings provide evidence to support the long-term stability of sorbed P by similar Fe- and Al-based WTRs, when land-applied to P-sensitive ecosystems. To the best of my knowledge, intraparticle P diffusion, using other than wet chemical methods, has not been documented for WTR particles. Future work should include investigations on other WTRs varying in physicochemical properties to determine P retention characteristics.

Predicting Long-Term P Sorption Capacities of WTRs

I also utilized SSA and porosity measurements to improve the understanding of the biphasic nature of P sorption by WTRs, we also utilized. We hypothesized that organic compounds inherently present in WTRs may impose steric and diffusion restrictions to

solute diffusion towards the interior of particles. Traditional BET-N_2 measurements showed the large difference in SSAs among the untreated (no P added) WTRs (Figure 3-10). Lowell Al-WTR had the greatest BET-N_2 SSA of all WTRs tested (100 m^2 g^{-1}), followed by materials from Panama >Bradenton >Holland >Tampa >Cocoa. P sorption by WTRs reduced N_2 SSAs for all WTRs except for Lowell and Holland materials, where P treatment had no effect on SSAs. However, BET-N_2 SSAs did not correlate well (r^2 = 0.1) with pseudo P sorption capacities of the materials estimated by reacting materials at an initial P load of 10 g P kg^{-1}, and contact time of 40 d.

Underestimation of P sorption capacities may be responsible for the lack of correlation between the amount of sorption sites determined with the BET method and the amount of P sorbed by WTRs. True P sorption capacities had not been attained due to limited initial P load (maximum initial load of 10,000 mg kg^{-1}). Another explanation would be that N_2 molecules were unable to reach all sorption sites due to diffusional restrictions. Based on BET-N_2 values, De Jonge and Mittelmeijer-Hazeleger (1996) showed that SSAs of three SOM samples were underestimated. WTRs contain variable, but significant amounts of C (3.4- to 21 %) that could affect the magnitude of BET-N_2 SSAs.

We hypothesized that low molecular weight organic acids along with higher molecular weight humic acids might be trapped in small pores of WTRs, regulating the diffusion of water and phosphate molecules. Thus, for N_2 molecules to diffuse through such small pores, greater activation energy is required to jump through these doorways (Gregg and Sing, 1982). Using CO_2 as the adsorbate at a higher sorption temperature

(273 K) we were able to access micropores having widths less than 1.5 nm or 15 Å. Micropore CO_2-based SSAs were calculated based on the DRK method (Figure 3-11).

CO_2-based micropore SSAs were greater than the corresponding BET-N_2 SSAs, except for Lowell and Holland materials. Lowell and Holland had the lowest levels of total C, suggesting little influence of organics on the degree of accessibility of sorption sites either by CO_2 or N_2. Lack of significant diffusion limitations for these two materials were also obvious for P-treated samples, which did not show reduced SSAs. However, the other materials showed a significant decrease in micropore SSA when P was added, suggesting a micropore blocking effect of phosphate molecules (Figure 3-11).

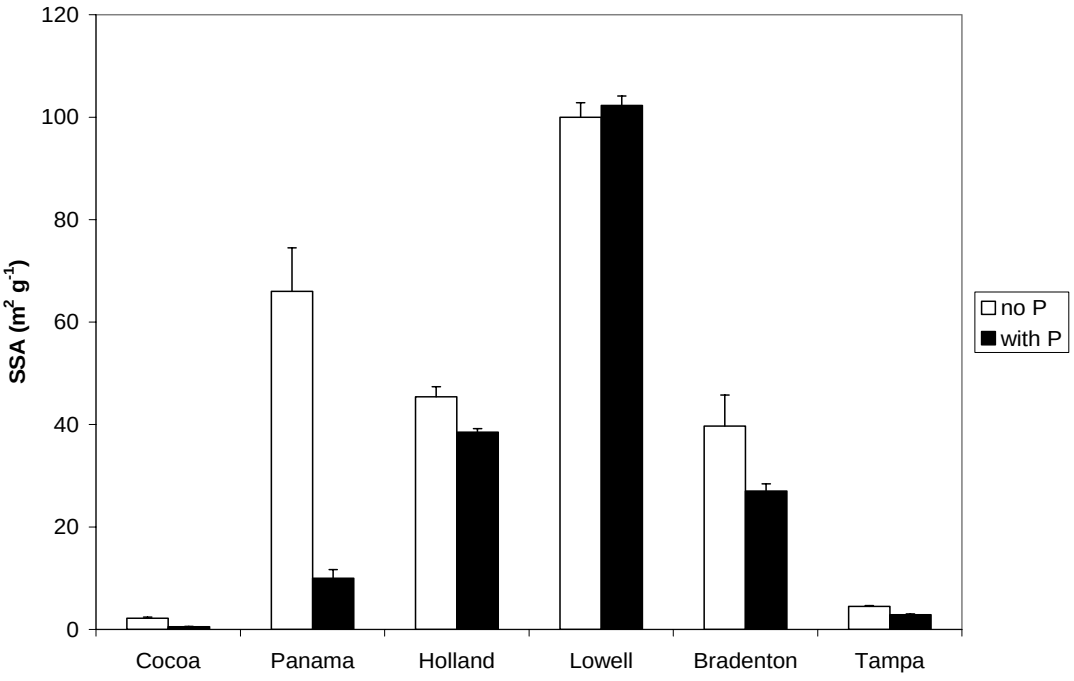

Figure 3-10. BET-N_2 SSA measurements for untreated and P treated (10 g P kg^{-1} initial load) for 40 d. Error bars denote one standard deviation of two replicated runs.

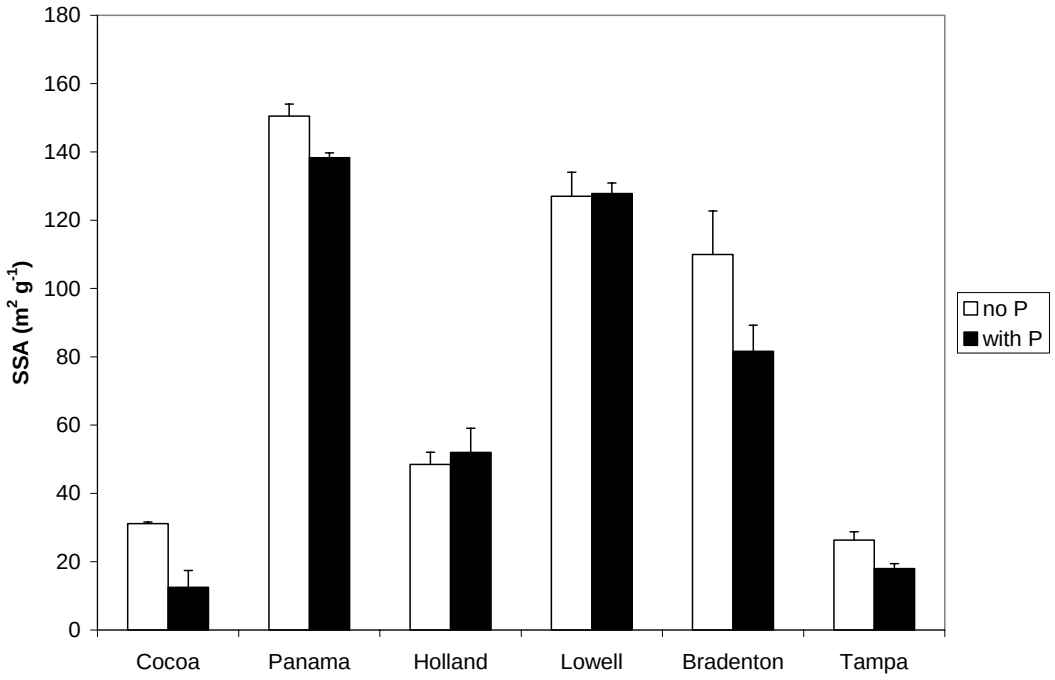

Figure 3-11. Micropore CO_2 SSA measurements for untreated and P treated (10g P kg^{-1} initial load) for 40 d. Micropore SSAs were calculated with the DRK method. Error bars denote one standard deviation of two replicated runs.

The CO_2 and N_2 SSA values of WTRs were not similar, suggesting a significant role of organic compounds trapped in WTR-micropores regulating the diffusion of gas molecules in and out of micropores. A strong correlation ($r^2 = 0.86$) was observed for total C and the N_2 / CO_2 SSA ratios for the WTRs (Figure 3-12).

Materials with low total C content (Holland and Lowell) showed no discrepancy in the amounts of N_2 and CO_2 sorbed (N_2 / CO_2 ratio close to 1). As total C increased, so did the difference in SSAs measured by CO_2 and N_2 ($CO_2 > N_2$). It seems that the presence of organic C imposed diffusion restrictions in N_2 sorption, but not to CO_2 molecules. This behavior resulted in decreased N_2 / CO_2 SSA ratios with total C in WTRs. A similar trend was observed for native grassy or forest Chicago soils in the work of Ravikovitch et al. (2003). They proposed using N_2 / CO_2 SSA ratios to characterize and predict various

soils' behavior in sequestration processes involving humic substances (Ravikovitch et al., 2003).

Data from SSA analyses for the two WTRs extensively characterized (Tampa and Bradenton materials) showed that CO_2-SSA better estimated pores associated with P than N_2-SSA. Dinitrogen-based SSAs may be greater than external SSA since they can also access micropores. However, CO_2 molecules can access micropores in the lower size range of micropores (0.35-1.2 nm) that N_2 diffusion may be severely restricted. Thus, CO_2 molecules may access micropores accessed by phosphates, or ultramicropores that can not be accessed by phosphates (micropores smaller than 0.7 nm) (Rodriguez-Reinoso and Linares-Solano, 1988). Ultramicropores may be associated with carbon structures that are indigenous in the WTR internal network. Thus, CO_2-based SSAs may be overestimating the effective SSA that may be accessed by phosphates. As we noted earlier in this chapter, there was a 23 % over-estimation of the CO_2-SSA for the two materials when compared with parking area-based SSA calculations.

Prediction of the long-term P sorption capacities of the complex WTRs may not be straightforward, and seems to require information collected from both N_2- and CO_2-based SSAs. Despite the fact that CO_2 better explained P sorption, there was not perfect correspondence either. In effect, I attempted to utilize the N_2 / CO_2 SSA ratios to predict the long-term capacities of the WTRs. The presence of organics could only retard P diffusion towards internal sites, since they would not serve as sorption sites for phosphate molecules. Thus, normalizing P sorption capacities after 40 d to C content of WTRs may provide a means of predicting their long-term P sorption capacities.

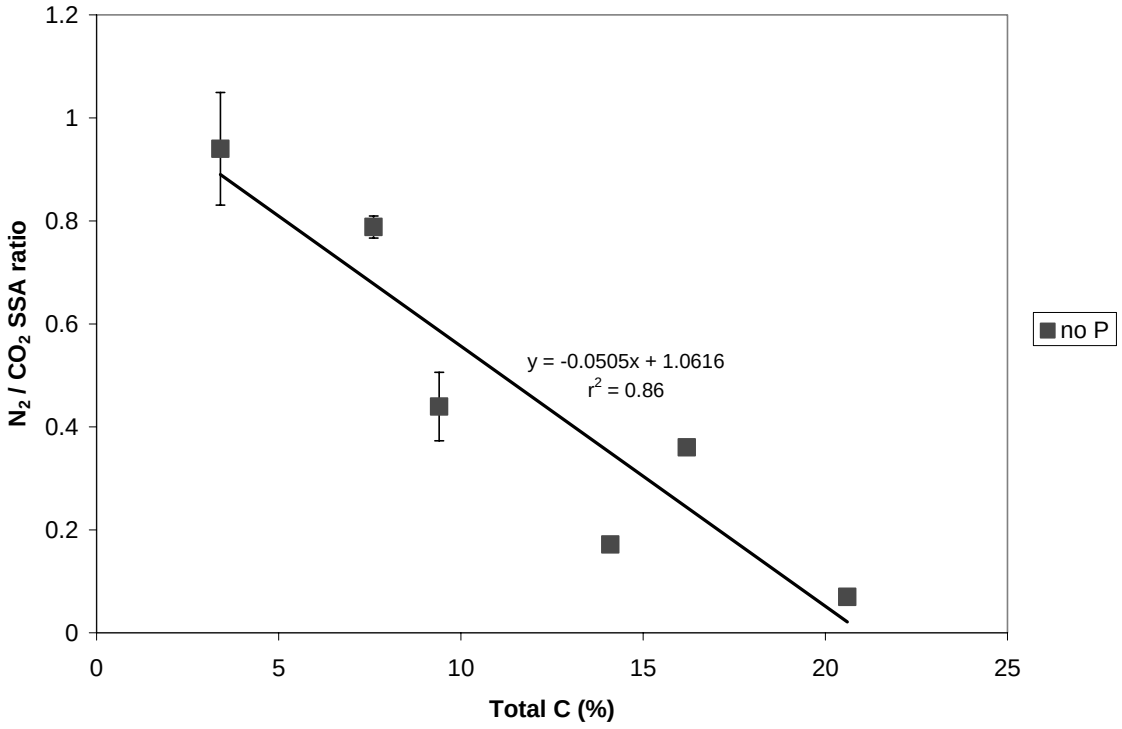

Figure 3-12. Correlation between the SSA ratio of BET-N_2 and CO_2 gas with total C of the untreated (no P) WTRs tested in this study. Error bars denote one standard deviation of two replicates.

As shown in Figure 3-13, there is significant (*$p<0.001$*) positive linear relationship between the normalized to C content of WTRs amount of P sorbed after 1 or 40 d with the N_2 / CO_2 SSA ratios of the untreated WTRs. Measuring three independent variables, total C, and N_2 and CO_2 SSAs, we were able to explain 87 % of the variability in the long-term measured P sorption capacities of the WTRs after 40 d. The number (6) of WTRs used in this model was limited, but covers a span of WTRs significantly varying in total C, Fe and Al contents. Accordingly, SSAs of the WTRs varied an order of magnitude.

Assuming easy access to instrumentation that measures surface area, SSAs measured with N_2 or CO_2 may take a few hours, and total C may take even shorter time.

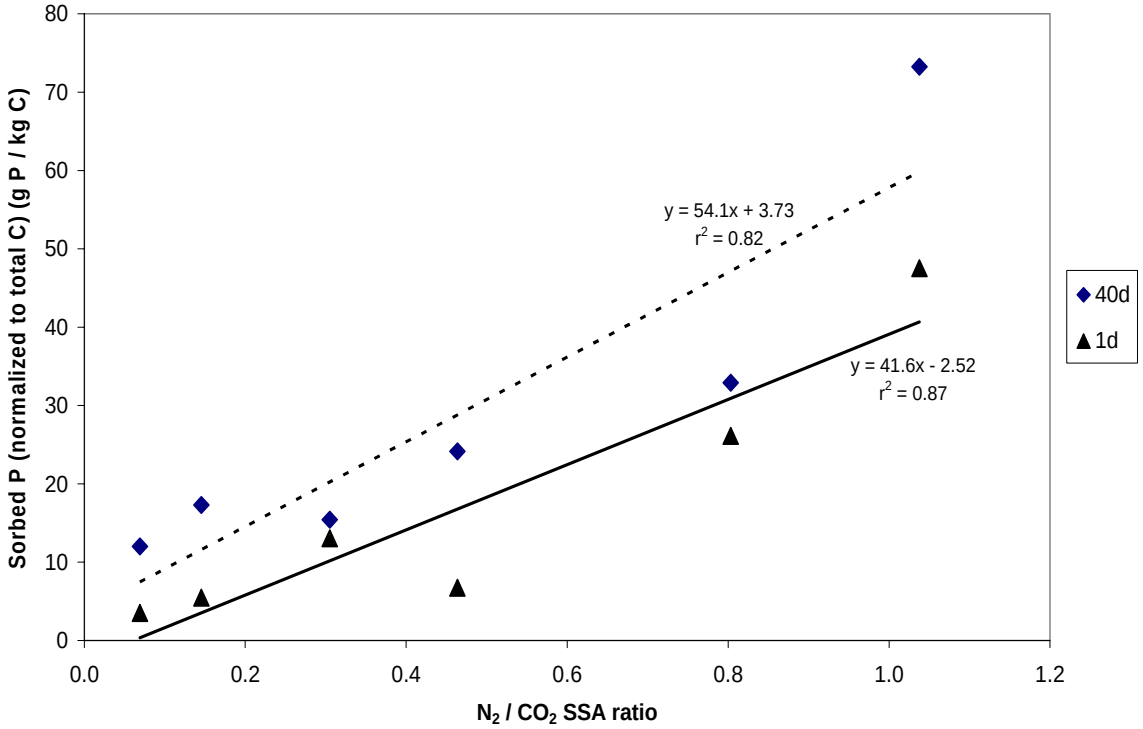

Figure 3-13. Correlation between the SSA ratio of BET-N_2 and CO_2 gas with long-term (40 d) pseudo P sorption capacities of WTRs. Initial P load (2,500 mg P kg^{-1}).

This may help in accurately predicting P sorption capacities of WTRs, avoiding long-term batch equilibration times. This model seems encouraging, but further validation using WTRs from different facilities around the nation may be needed.

CHAPTER 4
LONGEVITY OF WTR EFFECTS ON SOIL P EXTRACTABILITY FROM TWO MICHIGAN SOILS HIGH IN P

Introduction

In the previous chapters, seven WTRs exhibited dramatic P sorption capacities and slow P sorption kinetics. Short-term experiments with WTRs have shown their efficacy in reducing soluble P concentrations in runoff (Dayton et al., 2003) and leaching (Elliott et al., 2002) events. The time constraints needed to conduct long-term field experiments are the major drawback to understanding the long-term fate of sorbed P in WTR-amended soils. Long-term stability issues are also complicated by the complexity of WTRs, which comprised of amorphous masses of Fe and Al or Ca oxyhydroxides, and often high in organic C content.

Amendments high in Fe or Al content, such as alum salts or some biosolids relatively high in total Al and Fe have been field-applied to reduce soluble P levels and to monitor the longevity of the effect. During a 3-year study, Self-Davis et al. (1998) grew tall fescue grass in plots treated with alum-amended poultry litter. There was no differences in soil water-soluble P and Mehlich III-P values for the treated plots when compared with an un-fertilized control. However, water-soluble P in the untreated poultry litter plots increased each year (Self-Davis et al., 1998).

During a 4-year study, Lu and O'Connor (2001) showed that biosolids applied to a poorly P-sorbing soil initially increased P sorption, but the effect leveled off near the end of the study. There was a parallel decrease in oxalate-extractable Fe and Al, which was

attributed to losses of Fe and Al from the A horizon to the spodic horizon, and not to changes in Fe or Al forms. Hetrick and Schwab (1992) showed that long-term P fertilization (> 40 yr) of a Smolan silt loam resulted in increased P activities that appeared in equilibrium with variscite (crystalline aluminum phosphate) and tricalcium phosphate. Apparent equilibria with amorphous aluminum hydroxide and hydroxyapatite were observed for the un-fertilized control. There are no reports of long-term field data from WTR-amended soils that monitor P extractability.

Data from one of the few, if not the only one, nationally found, long-term WTR field application experiments was used in this study (Jacobs and Teppen, 2000). We hypothesized that (i) WTR application should significantly reduce soil P extractability over time, and (ii) aging of WTR in the field would promote crystallization of the WTR, which would inhibit P desorption over a long period of time. Our objective was to demonstrate the long-term effectiveness of a Al-WTR in reducing P extractability in soils with a prolonged history of poultry manure applications.

Materials and Methods

Two field sites (sites 1 and 2) were selected in 1998 for evaluation of drinking-WTR application (effectiveness in reducing soluble P) in soils with "having very high" soil test P levels. Both sites had a long-term history of poultry manure applications. Soil at site 1 was a Granby (Sandy, mixed, mesic Typic Endoaquolls) fine sandy loam with a "very high" Bray P1 soil test levels of about 300 mg P kg^{-1}. Soil at the second site was a Granby loamy sand with a "very high" Bray P1 soil test levels of about 600 mg P kg^{-1}. Field corn (*Zea mays L.*) was planted at each site.

An Al-WTR (Holland, MI) was applied in spring 1998 at a rate of 114 dry Mg ha^{-1}. Soils were disked twice at each site to mix the WTR with soil. The field at site 1 (WTR1)

was chisel plowed and field cultivated prior to planting corn on May 5, 1998. The field at site 2 (WTR2) was moldboard plowed before planting corn on May 4, 1998. Both sites were rototilled in April/May, 2000 prior to planting to promote more thorough mixing of WTR and soils.

Surface soils were initially sampled in fall 1998, about 6 months after Al-WTR application in spring 1998 by compositing 20 cores of 2.54 cm long length from the top 20 cm depth. Similar soil surface samples were collected in the fall of subsequent years (1999-2003). Soils were air-dried and passed through a 2-mm sieve.

Phosphorus and aluminum extractability in soils was monitored as a function of four factors: field equilibration time, WTR treatment (with / without WTR addition), and oxalate extractant concentration. Two oxalate concentrations in buffered solutions were used: 5 and 200 mM (McKeague et al., 1971) at a 1:60 soil: solution ratio, shaken for 4 h in the dark, filtered (0.45 μm), and analyzed for P and Al by ICP. Selected soil samples were analyzed for total P, Fe, and Al by ICP following digestion according to the EPA Method 3050B (USEPA, 2000). Water -soluble P in soils was determined by shaking soil samples with deionized water at a 1:10 soil: solution ratio for 24 h, as modified from Sparks et al. (1996). Water soluble P was analyzed colorimetrically with the method of Murphy and Riley method (1968). Differences between treatments were statistically analyzed as a randomized factorial design using Design Expert (Design-Expert software, 2001), at the 95 % confidence level used as the criterion to statistically separate means.

Results and Discussion

Surface soil samples were collected from sites 1 and 2 before, and every year after the Al-WTR application in the spring of 1998 until Fall 2003. Oxalate (200 mM) extractable P for both treatments (control and WTR-amended) decreased with time in the

field (Figure 4-1). No significant effect of WTR application was detected at either site by simply using the oxalate-200 mM P data. Oxalate-extractable P reduction with time could not be directly attributed to P sorption by WTR, since similar decreases were also observed in the control plots. Jacobs and Teppen (2000) suggested vertical movement/loss of colloidal P in the coarse-textured (fine sandy loam) plots of site 1.

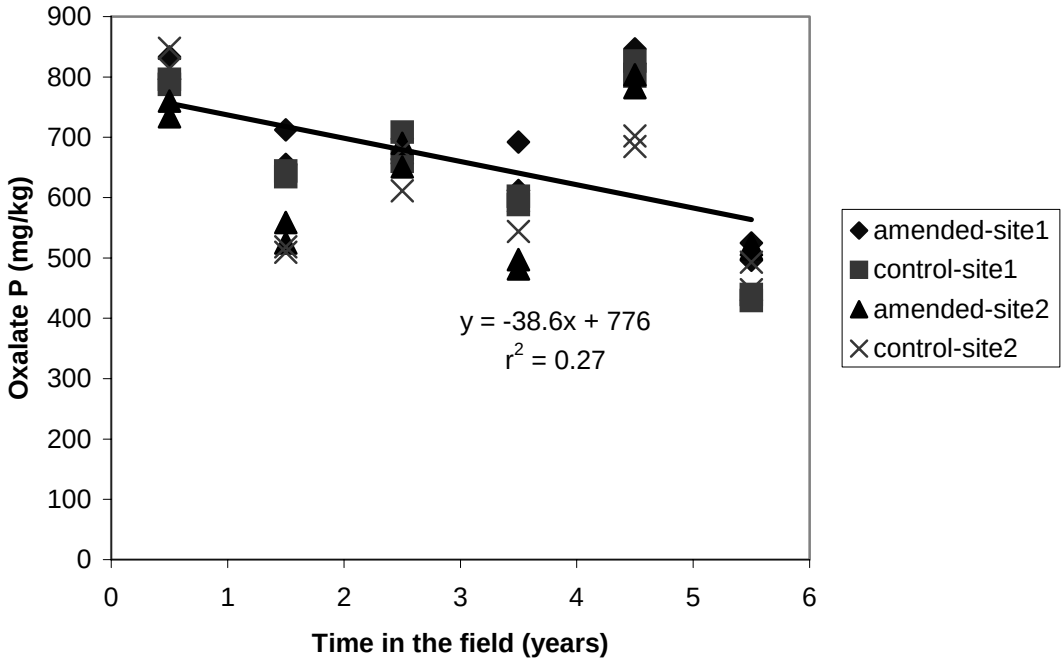

Figure 4-1. Changes in oxalate (200 mM) extractable P concentrations with time for sites 1 and 2. Statistical analysis showed that there was a significant ($p < 0.01$) effect of time, but no treatment effect. A common linear trend line was fit to all data for both sites.

Total soil Al and Fe analyses paralleled the decreasing trend of oxalate (200 mM) P from 1998 to 2003 in the untreated and WTR-treated plots of both sites (Figure 4-2). Total Fe and Al concentrations decreased in both control and WTR-amended plots with time at both sites. However, site 1 exhibited a considerable decrease in total Al and Fe at the last sampling point (5.5 years after WTR application). This decrease was significant at the 95 % confidence limit and there was a significant ($p<0.001$) interaction between

time and treatment (WTR) for both sites. Total Al and Fe decreases with time in the field could be attributed either to soil mixing / compositing or to sampling variability.

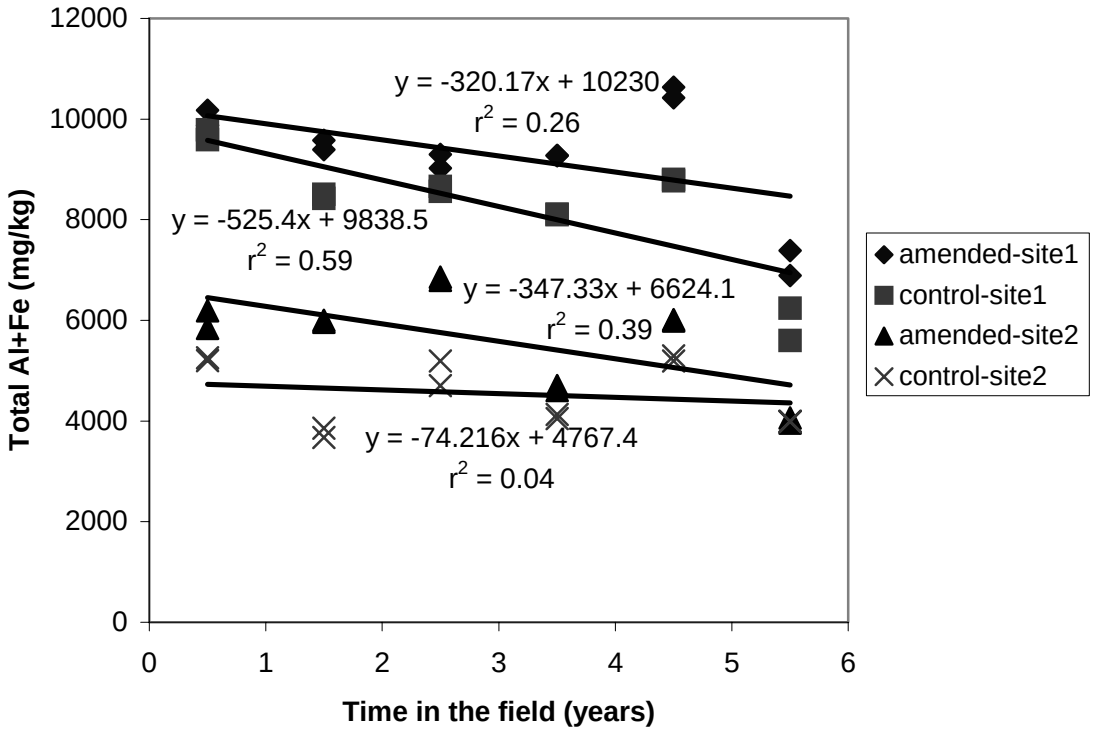

Figure 4-2. Changes in total Fe and Al concentrations with time for sites 1 and 2. Statistical analysis showed that there was a significant ($p<0.001$) interaction between time and treatment (WTR).

Iron and Al hydroxides, especially Al coming from the Al-WTR, is the major sorbent for oxyanions in soils, such as P. Changes in sorbent pool with time could influence a sorbent's P sorption capacity. Thus, reductions in sorbent (total Fe and Al) pool for both sites prompted us to normalize the data by dividing oxalate-extractable P by the corresponding oxalate Fe and Al values. This normalization is defined as the P saturation index (PSI) (Elliott et al., 2002). PSI is calculated as the ratio of oxalate-extractable (200mM) values of P divided by the corresponding sum of Fe+Al, in mmoles. A change point of PSI = 0.1 has been assigned for Florida sandy soils amended with

animal wastes, above which there is a high probability risk for P release from soil (Nair et al., 2004). PSI values for both sites were calculated and data were statistically analyzed to evaluate subtle differences observed between treatments.

For site 1, PSI values of the WTR-amended plots did not significantly differ at the 95 % confidence level from control (no WTR) plots (Figure 4-3). Aging in the field had no effect on PSI values for WTR-amended plots even 5.5 years after WTR application. PSI values remained approximately constant (0.2) throughout the monitoring period. PSI values were lower in site 1 than site 2 suggesting little potential for P release from WTR-amended or unamended plots of site 1. Native total soil Al and Fe levels in site 1 were high (10,000 mg Fe+Al kg^{-1} soil) and may be responsible for the absence of a WTR effect.

For site 2, PSI values were at least double those of site 1 for both control and WTR-amended plots (Figure 4-4) because site 2 had about twice the soil test P and one-half the total Fe and Al of that in site 1. Control plots of site 2 had relatively high PSI levels (~0.8), which suggest that site 2 could contribute significant amounts of P in runoff events. WTR treatment significantly ($p<0.001$, $\alpha=0.05$) decreased PSI values six months after application, but thereafter had little impact. The magnitude of PSI values in the WTR-amended plots was approximately 40% less than that of the controls. However, there was no significant effect of time suggesting little potential for P release from WTR-amended plots. Low native total soil Al and Fe concentrations may have contributed to the positive WTR effect on reducing P extractability. Site 1 had relatively

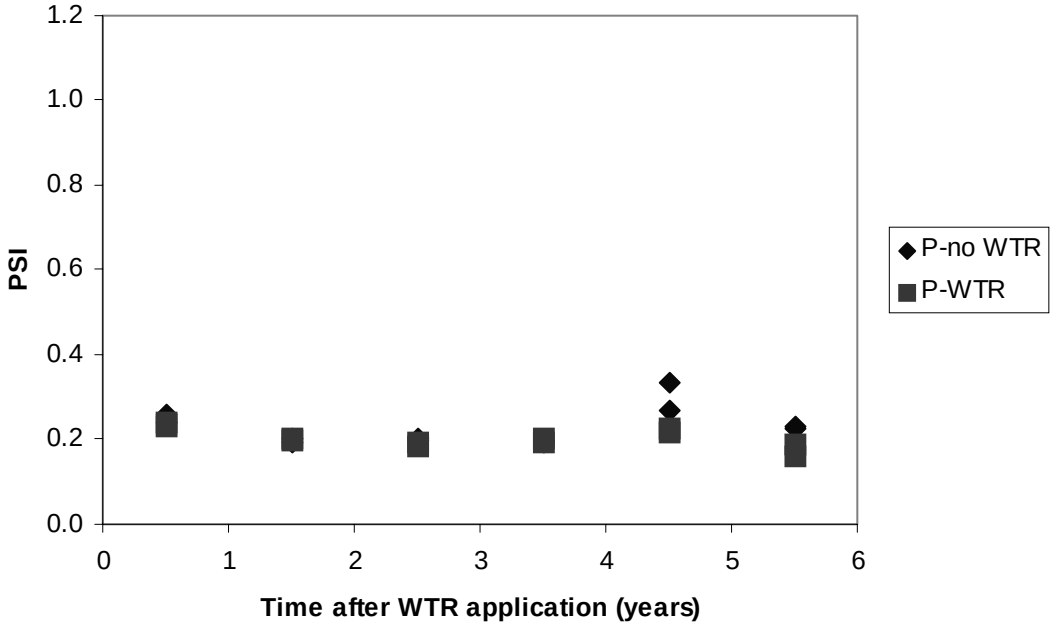

Figure 4-3. PSI changes with time for site 1. No trend lines are presented since there was no statistically significant effect of WTR or time.

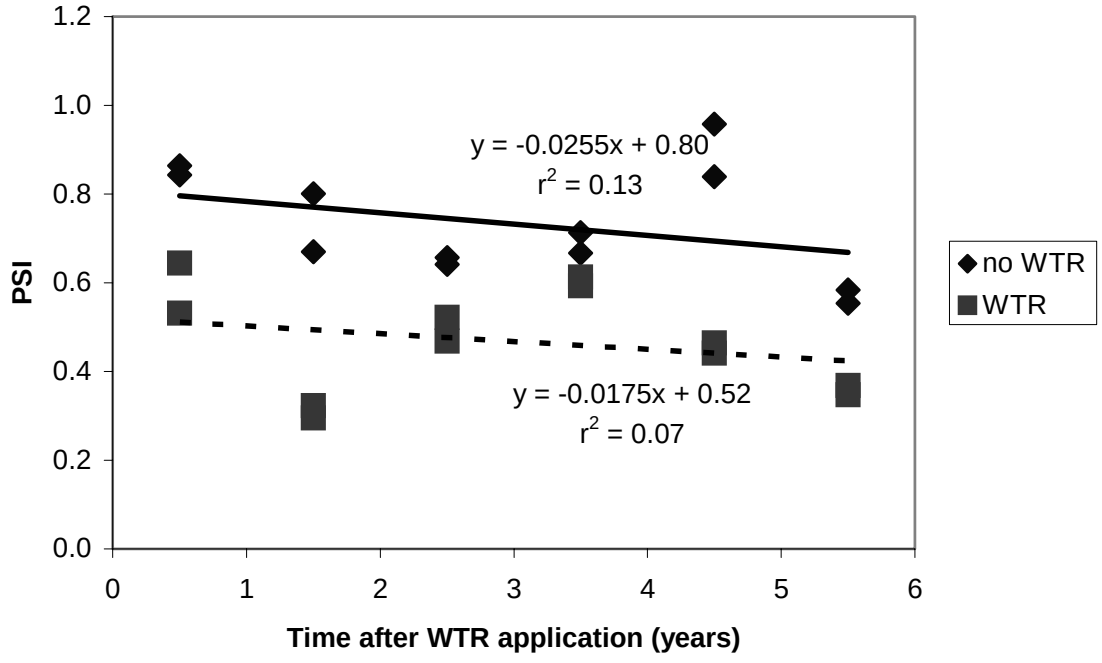

Figure 4-4. PSI changes with time for site 2. Regression lines are presented only for statistically significant effects (WTR load; no time effect).

large amounts of native total Al and Fe, thus, WTR application rate was not sufficient to significantly increase total soil Al.

Measures of P extractability, such as PSI, are best interpreted when compared with measures of P availability. Water soluble P (WSP) is considered as an environmental P availability test (Codling et al., 2000). Codling et al. (2000) conducted WSP measurements in soil samples collected from poultry farms and amended with 25 Mg ha^{-1} application rate of a Al-WTR. The WSP levels were significantly reduced (below 10 mg kg^{-1}) after 2 weeks of incubation with Al-WTR. In the MI study, WSP levels were measured in surface soil samples obtained 5.5 years after WTR application. WSP levels in the untreated plots did not change with time, and were ~30 and 40 mg P kg^{-1} for sites 1 and 2, respectively (Figures 4-5 and 4-6). Site 2 had greater amounts of WSP due to greater soil test P levels, consistent with the greater soil test P levels (double those of site 1). The invariant WSP values for the control plots suggests that both unamended soils could serve as significant (and constant) sources of soluble P in runoff events for many years.

Plots amended with the Al-WTR had significantly lower WSP levels than the untreated controls for both sites. In site 1, WTR application resulted in significant WSP reduction from ~30 to 20 mg P kg^{-1} six months after WTR application (Figure 4-5). WSP levels continued declining reaching equilibrium approximately 3 years after WTR application (~10 mg P kg^{-1}). Stabilization of WSP levels in the WTR-amended plots of site 1 roughly coincided with the thorough rototilling that occurred 2 years after WTR application to improve contact of WTR and soil particles. Stabilized WSP concentrations

at site 1 were < 1 mg P L^{-1}, suggesting that WTR application can significantly reduce water quality impacts of high-P soils.

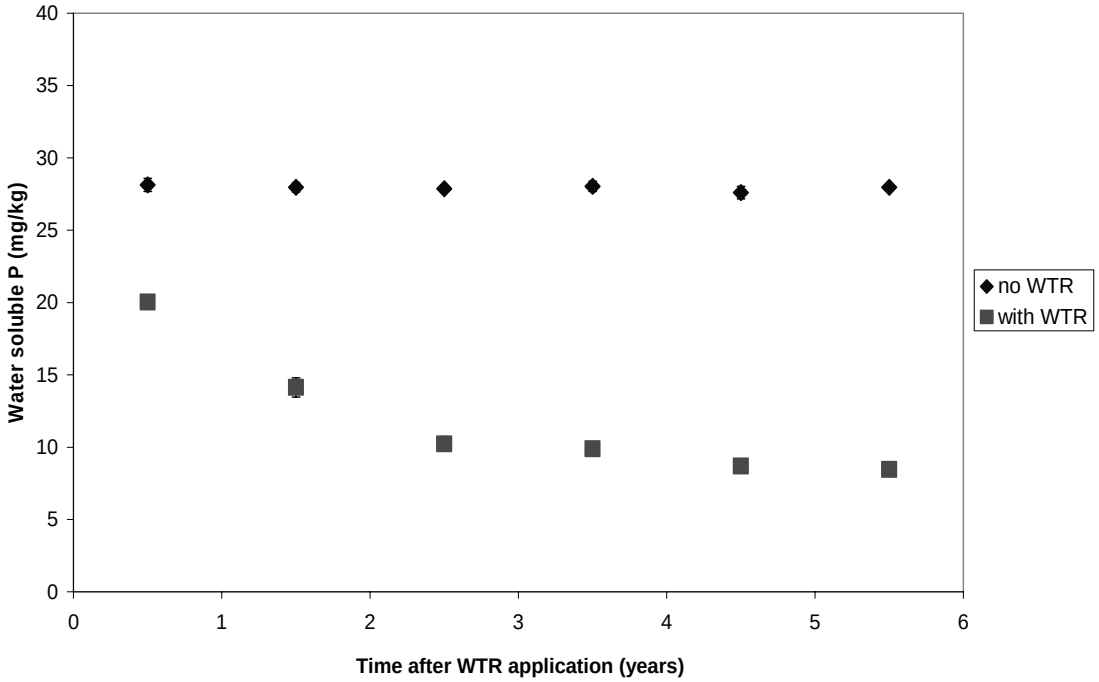

Figure 4-5. Changes in water soluble P levels in site 1with time in the field of soil samples from plots amended with and without WTR. Error bars denote one standard deviation of two replicates.

Similar results were obtained at site 2; unamended controls were relatively high in WSP concentrations (~37 mg P kg^{-1}). WSP concentrations were invariant throughout the monitoring period (5.5 years). WTR application significantly decreased WSP with time (Figure 4-6). WSP levels were reduced six months after WTR application but they continued decreasing through 4.5 years. Thereafter, WSP reduction stabilized at levels in the order of ~ 20 mg P kg^{-1}. WTR reduction continued for at least 3 years before WSP reach a minimum value for site 1 and 4.5 years for site 2. The mean PSI for control soils (no WTR) was significantly greater than that of the WTR-treated soils. Site 2 had double the soil test P values of site 1. WTR application in a soil with high WSP levels resulted in

~50 % reduction. WSP data show that there was poor contact between soil and WTR particles, and also, that WTR was characterized by slow P sorption kinetics that took from 2.5 to 4.5 years, depending on the native soil P levels.

The kinetic character of P sorption and sorption capacities of WTRs has been documented in previous chapters of this thesis. P sorption experiments with the same Al-WTR that was applied to these sites showed the dramatic P sorption capacity of the material and slow P kinetics that were also obvious in the field. WTR effectiveness continues for years assuming minimal changes in physical nature of the WTR particles.

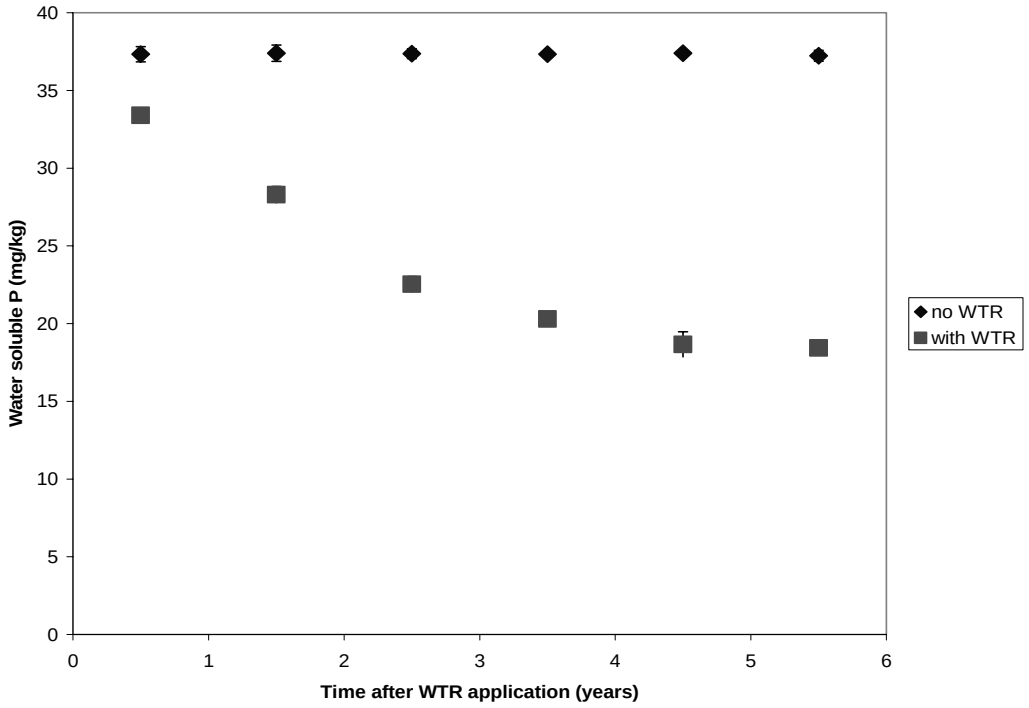

Figure 4-6. Changes in water soluble P levels in site 2 with time in the field of soil samples from plots amended with and without WTR. Error bars denote one standard deviation of two replicates.

In an effort to associate soil P levels with the potential for P losses via runoff, we attempted to correlate WSP with PSI measures. There was a positive linear correlation (r^2 = 0.53) between PSI and WSP values for both sites of the WTR-amended soil samples

(Figure 4-7). The greater the PSI, the larger the WSP for the two MI sites. There was no correlation between PSI and WSP for the untreated plots of both sites. The absence of correlation may be due to the fact that oxalate-based PSI measurements are inappropriate for the unamended plots of both sites.

Oxalate extraction is appropriate for soils that Fe and Al hydroxides dominate their chemistry. Both sites were heavily manured, thus, their chemistry must be dominated by Ca and Mg compounds. Untreated plots of site 2 had elevated PSI values (0.8-1) that are much higher than the threshold value of 0.1 established for P-containing waste amended soils (Nair et al., 2004). Untreated plots of site 1 had slightly higher PSI values (0.2-0.25) than the threshold value of 0.1. WTR application may have shifted soil chemistry for both sites from Ca/Mg to Al-dominated. WTR application reduced PSI and consequently WSP levels suggesting minimal risk of P losses via surface runoff.

Data from both sites suggest that WTR additions impact soluble P levels rapidly, but that the full impact requires 3 (site 1) to 4.5 (site 2) years. Site 2 had twice the initial soil test P as site 1, so WTR impacts were delayed, but WSP was reduced at both sites by ~50 % with time. As with the total and oxalate data collected from these samples, there was no evidence for release of WTR-immobilized P with time from either site. The WSP data, however, are clearly more sensitive measures of labile soil P status and clearly demonstrate impacts of WTR in controlling soluble P in highly P-impacted soils.

The WSP data, thus, support our earlier hypothesis that there is little danger that WTR-immobilized P will released to solution. This is an important finding in state and federal efforts to assess the long-term stability of sorbed P by WTRs applied in the field.

Given the minimal changes in P extractability in the field samples, there appears to be little fear that WTR-immobilized P will be released over time.

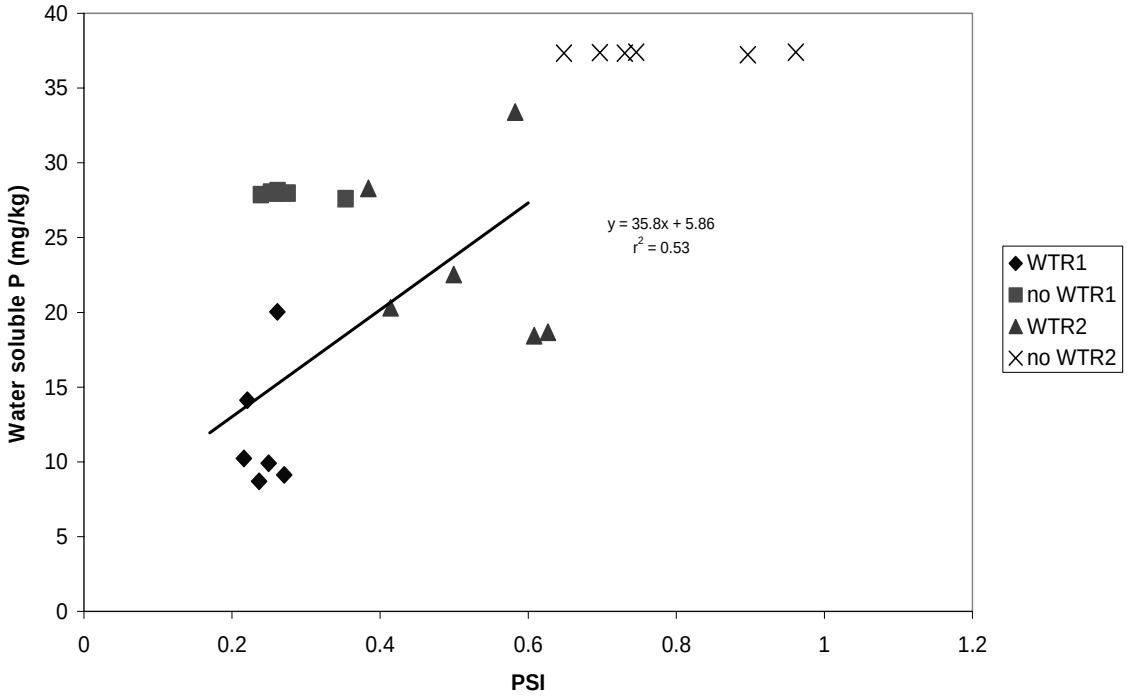

Figure 4-7. Correlation between PSI and water soluble levels for WTR-amended and unamended plots of two MI soils. Linear trendline is fit to data from the WTR-amended plots for both sites.

CHAPTER 5
LONG-TERM INCUBATION OF SYNTHETIC IRON AND ALUMINIUM HYDROXIDES, DRINKING-WATER TREATMENT RESIDUALS (WTRs), AND SOILS AMENDED WITH WTRs

Introduction

Iron and Al oxyhydroxides are abundant in soils and play a key role in contaminant transport and reactivity. They are usually colloidal (less than 2 μm), vary in crystallinity, and they are characterized by large SSAs. In soils, metal hydroxides are the product of the weathering of primary and secondary minerals and exist as mineral coatings, or discrete phases. Thermodynamic stabilities of Fe and Al hydroxides regulate the fate and availability of nutrients and contaminants.

Current surface complexation models provide a reasonable explanation of near-equilibrium processes in natural water bodies (Tessier et al., 1996). However, no chemical model explicitly considers the sorbent as a dynamic system (Ford et al., 1997). Amorphous Fe and Al oxyhydroxides can be metastable, and they could transform with time to thermodynamically stable phases.

Amorphous Al hydroxides transform to more crystalline phases via dissolution / reprecipitation. Amorphous Al hydroxides show the lowest solubility around pH 5.1. Solubility increases rapidly below that pH and increases less rapidly in alkaline conditions. Alkaline media enhance dissolution / reprecipitation phenomena, and boehmite may form (pH 7-8). A general rule is that increasing pH and temperature, increases crystal growth (Okada et al., 2002). At pH < 5.1, gibbsite readily forms because conversion rates from boehmite to bayerite to gibbsite are fast (Okada et al., 2002).

Amorphous Fe hydroxides transform to more crystalline phases either by dissolution / reprecipitation (goethite) or by structural re-arrangements (hematite). Two types of amorphous Fe hydroxides exist: The first forms by fast hydrolysis around pH 7 (OH / Fe ~3) and shows two broad XRD peaks (two-line). The second type is produced by forced acid hydrolysis of a $Fe(NO_3)_3$ solution at OH / Fe = 0 and elevated temperature (12 min at 80 C), and has six or seven XRD peaks (six-line) (Schwertmann et al., 1999). Amorphous iron hydroxides intermediate in structure and crystallinity may form as a result of different preparation conditions and different crystallization methods (Schwertmann et al., 1999).

Both 2- and six-line ferrihydrites can transform to crystalline Fe compounds (goethite and hematite). At relatively high water content of metal hydroxide suspensions, increasing temperature or pH towards the zero point of charge (ZPC) of ferrihydrites (pH 7- to 8) favor formation of hematite over goethite. Hematite formation is favored by dehydration at pH values where the solid has the lowest solubility and the greatest potential for coagulation / aggregation. Baltpurvins et al. (1996) found that when pH increased from 7 to 9, the transformation of ferrihydrite to a mixture of goethite and hematite accelerated. The effect of time was also significant; at pH 9 and 20 C, 50 % of the ferrihydrite was transformed to a more crystalline solid phase in 40 d, whereas at pH 7 and 20 C, 360 d were needed to transform 50 % of the amorphous Fe phase to a more crystalline state.

Goethite formation is usually favored under conditions of dissolution / reprecipitation phenomena. In low water activity or dry systems, transformations still occur, but at a lower rate since ion mobility is restricted. Air-dried two-line ferrihydrite

may transform to hematite at room temperature after 20.4 years (Schwertmann et al., 1999). Internally adsorbed water facilitates the conversion process, even at low water content (100- to 150 mg g^{-1} water). However, in dry systems, hematite will form in less than 20 years at temperatures close to or above (300 C) (Schwertmann et al., 1999). Hematite formation is more sensitive to temperature changes than is goethite formation (Schwertmann and Cornell, 1991).

Iron or Al amorphous hydroxides are abundant in soils and usually contain impurities, such as, inorganic and organic ions that may influence physicochemical properties of the solids. Specific adsorption of anions on ferrihydrite largely retards its transformation to a more crystalline solid phase (Baltpurvins et al., 1996). Hsu (1979) found that phosphate was the most important inorganic ligand in inhibiting crystallization of Al-hydroxides followed by: silicate > sulfate > chloride > nitrate > perchlorate. Hsu (1982) found that aging of Al phosphate precipitates at room temperature for 5 years did not result in formation of variscite except under extreme conditions (low pH and, high Al, and P concentrations).

Violante and Huang (1985) found that Al precipitation products formed in the presence of phosphate at pH 8.2 and aged for 5 months at 20 C was mostly an x-ray amorphous material, regardless of changes in P / Al molar ratios (0.05- to 3 %). Phosphates were effective in distorting the formation of crystalline Al phases (Violante and Huang, 1985). Crystallization of ferrihydrite, as evidenced by oxalate extractions, occurred at arsenate loads up to 29.5 g As kg^{-1} after 125 d incubation at 40 C. Arsenate was stabilized into the goethite/hematite structure. Greater arsenate loads retarded ferrihydrite crystallization.

Similarly, Barron et al. (1997) reported that small amounts of phosphate could retard the crystallization of ferrihydrite at alkaline pH and reduce the growth of goethite crystals in the [001] direction. Galvez et al. (1999a) showed that in the absence of phosphate, ferrihydrite was transformed to hematite and goethite mixtures incubated for 2 years at 25 C or 2 months at 50 C. When P was added, the degree of ferrihydrite transformation was largely retarded, and at P / Fe ratios >1.5 %, oxalate extractable-Fe / total Fe was close to 1, suggesting no formation of a crystalline phase. Biber et al. (1994) observed decreased dissolution rates of iron oxides in the presence of sorbed phosphate on the oxide surface. Willett and Cunningham (1983) found that phosphate stabilized the surface of ferrihydrite at a wide range of pH and E_h values.

Sorption of inorganic ligands by Fe and Al hydroxides could inhibit or reduce organic ligand-promoted dissolution of mineral oxides. Phosphate and arsenate sorption on goethite and lepidocrocite (γ-FeOOH) inhibited dissolution at circumneutral pH values, but enhanced dissolution at pH < 5 with EDTA solutions (Bondietti et al., 1993). The authors attributed this behavior to the kind of metal surface complex present: mononuclear complexes (especially bidentate) accelerated dissolution, whereas binuclear bidentate complexes inhibited dissolution. Greater energy was needed to remove sorbed P or As from the two surface Fe atoms.

Spectroscopic work by Fendorf et al. (1997) showed that different Fe-As surface complexes formed on goethite, depending on the As surface coverage. At low surface As coverage, monodentate complexes prevailed, whereas high surface coverages (θ = mol As / mol Fe; log θ = -2.05) favored bidentate complexes were predominant. Arsenate could form bidentate surface complexes on goethite, thus reducing the tendency of

organic anions to promote the oxide's dissolution (Eick et al., 1999). Eick et al. (1999) studied the effect of arsenate (up to 5 mM) on oxalate- (5 mM) -promoted dissolution of goethite. Goethite dissolution rates decreased with increasing arsenate surface coverage at pHs from 3- to 7, except at pH 6.

In soils, organic matter (OM) can inhibit crystallization of amorphous Al hydroxides by forming soluble or insoluble OM-Al-PO_4 bridging complexes (Stevenson and Vance, 1989). Grossl and Inskeep (1991) showed that soluble organic acids (citrate, oxalate) prevented crystal growth by blocking surface sites on the newly formed Ca-P precipitates. Low molecular weight organic ligands, such as like oxalate, are commonly encountered in soils. Oxalate dissolution of mineral particles has been documented in the literature (Fox et al., 1990). Bhatti et al. (1998) suggested that the failure of Al and Fe to re-precipitate after being released from a Spodosol Bh horizon by 5 mM oxalate was due to formation of stable Al-oxalate complexes. It has been postulated that ligand exchange is the main mechanism of phosphate desorption with low concentrations (5 mM) of oxalate in soils (Bhatti et al., 1998).

Horanyi (2002) summarized the adsorption mechanism of oxalate by hematite and alumina in high ionic strength (0.5 M, electrostatic interactions were excluded) acid media: protonation of the oxide surface, followed by specific adsorption of the anionic form of the organic acid. At pH values lower than the pKa of the organic acid, adsorption decreased significantly. Molis et al. (1997) studied the sorption of oxalate, acetate and other low MW organic acids (10^{-5} to 10^{-1} M) on Al hydroxides at circumneutral pH. At low ligand concentrations, adsorption occurred through inner-sphere complexation on Al surface hydroxyl sites. At higher ligand concentrations, the surface charge was reversed,

resulting in excess electrons that weakened the Al-O-Al bonds and promoted release of soluble Al-OC complexes.

Structural changes of amorphous metal hydroxides may be reflected by changes in crystallinity or SSA. Increasing crystallinity of metal hydroxides results in bigger crystallites characterized by lower SSA compared with their corresponding amorphous phases. Diakonov et al. (1994) observed decreases in SSAs of goethite [α-FeO(OH)] and hematite (α-Fe_2O_3) with time. Goldberg et al. (2001) observed changes in SSAs of amorphous Al hydroxides during a 9 d period, at pH 4- to 5, and room temperature, that coincided with the formation of gibbsite. Amorphous Al oxides were unstable relative to gibbsite and thus dissolved and recrystallized into the more stable gibbsite with time. Prolonged aging (200 d) at room temperature of Cu-noncrystalline alumina resulted in gibbsite formation with concurrent ejection of sorbed Cu (Martinez and McBride, 2000). The speculated effect of SSA reduction (crystallization) on Cu exclusion from internal sites was not explored via SSA measurements.

Metal hydroxides have comparable, but less complex elemental composition than Fe-, or Al-based WTRs. Using amorphous metal hydroxides as model compounds to monitor their transformation towards long-range ordered particles would help us interpret trends observed with the “dirty” WTRs. We hypothesized that metal hydroxides and WTRs would have similar reactivity and behavior. Heating amorphous metal hydroxides could hasten transforming reaction rates and could be used as an experimental technique to study long-term structural changes (Sorensen et al., 2000; Martinez and McBride 1998, 1999).

Contrasting theories exist for the solubility of aged suspensions composed of ions sorbed onto Fe and Al oxyhydroxides. The classic theory of aging processes supports the idea of structural reorganization of an amorphous solid phase by ion incorporation into the solid, forming a "solid solution" (Spadini et al., 1994). Solubility of long-range ordered oxides is usually orders-of-magnitude less than that of the amorphous solid, and the vulnerability of these oxides to microbially-induced Fe reduction is also reduced (Postma and Jakobsen, 1996). Ion partitioning is envisioned to be irreversible, unless dissolution of the host mineral occurs.

Artificial aging may be induced by heat input, which increases the translational energy of atoms, and thus, weathering transformation rates. Martinez and McBride (1998) synthesized aged (200 d) Cd, Cu, Pb and Zn coprecipitates with amorphous Fe hydroxides, and incubated at 70 C for 2 months. Aging decreased Cd and Zn, but not Cu solubility. Despite Cu movement towards the surface of the coprecipitate at increased aging time (up to 2 years at 23 C), decreased Cu solubility resulted from the coprecipitation of Cu with alumina, at pH 6 to 7.5 (Martinez and McBride, 2000). Aging induced the transformation of an initially non-crystalline alumina to more crystalline phases, including gibbsite.

Cobalt and Cd were incorporated into ferrihydrite after 5 months of aging at room temperature (Ainsworth et al., 1994). Metal cation solubility decreased and coincided with decreases in oxalate-extractable Fe (Ainsworth et al., 1994). Heat treatment (70 C) of a Pb-treated Egmont soil resulted in reduced Pb availability (Martinez et al., 2001). The authors attributed the soil's Pb retentive behavior to increased concentrations (64 %)

of imogolite, which could account for physical adsorption of Pb into micropores (intercalation).

The classic theory of decreasing metal solubility in aged metal hydroxides does not apply to all metals. Martinez et al. (1999) demonstrated that Pb sorbed by soil oxides and ferrihydrite [$Fe(OH)_3$ x H_2O] was released into solution after heat incubations at 70 C for 2 months. Baig et al. (1996) studied the solubility of carbonated apatites at different temperatures (50, 70, and 95 C). Apatite's degree of crystallinity decreased, and its solubility increased, with decreasing temperature of synthesis and increasing carbonate content. Ford et al. (1997) synthesized ferrihydrite in contact with Pb solutions at 40-70 C for 2- to 6 weeks. Lead was excluded from the solid phase as a result of reduced sorption sites, due to formation of goethite.

Sorensen et al. (2000) used SEM-EDS and BET-N_2 measurements to show that SSA decreases with temperature were due to increasing crystallinity of Fe hydroxides after drying at 50 C. Further heating at temperatures up to 900 C induced the transformation of amorphous Fe (hydr)oxides to hematite. Despite the formation of the more stable hematite, elevated temperatures significantly reduced Cd and Pb retention capacity of the hematite. Recently, Martinez et al. (2001) studied Pb solubility at 70 C after prolonged aging (1.5 years) of suspensions of a Brazilian Oxisol and a volcanic soil containing non-crystalline aluminosilicates and oxides of Fe and Al. Crystallization of Fe amorphous phases towards goethite proceeded, and Pb was released into solution. Similar trends were observed for long-term biosolids-amended NY soils (20 years).

Heat incubations of the metal hydroxides (70 C) would help us explain potential transformations observed during the incubation of WTRs and WTR-treated soil samples.

Loading metal hydroxides with phosphates may be useful to study P desorption from heat incubated particles, and make assessments about the long-term P stability. In addition, metal phosphates have recently attracted much attention in their use as catalysts or ion exchangers for heavy metals (Sahu and Parida, 2002). Aluminum phosphates have been used to remove heavy metals (Co, Ni, and Cu) from aqueous solutions (Mishra et al., 1998). Aluminum phosphates are also used as adjuvants in licensed human vaccines as the stimulant for the immune response (Burrell et al., 2001). Aluminium phosphate adjuvants are commonly prepared at 1:1 P:Al molar ratios, similar to our experiments.

Our overall objectives were to characterize the physicochemical nature of heat-treated (70 C) metal hydroxides, and to determine the effect of time, and P load on structural properties of the metal hydroxides. Iron and Al oxyhydroxides incubation data should compliment data from studies of incubated WTRs and WTR-amended soils and aid in interpretations designed to assess the long-term stability of sorbed P.

Materials and Methods

All reagents were of analytical grade and were used without further purification. Solutions were prepared in double-distilled water using Pyrex glass vessels. Amorphous gels of Fe and Al were prepared with and without P, according to methodology described by Goldberg et al. (2001). Briefly, P was added to metal chloride solutions ($FeCl_3$, or $AlCl_3$) to achieve 1:1 (P: metal) molar ratio in the final suspension. Mixtures were reacted for 1 hour at 23 C, with mild continuous stirring. Suspensions were slowly brought up to pH 8 with the aid of 1.08 N NaOH. This process enabled the metals to form hydroxide gels that precipitated out of solution. Resulting gels were separated by centrifugation at 4000 rpm for 15 min, and were then washed with deionized water. Double-distilled water was used to bring all suspensions to the same volume (500 mL);

the suspensions were covered with Al foil and placed in incubators at 70 C. Suspension moisture was not controlled, and all physisorbed water was evaporated within 3 weeks of incubation. The selection of the incubation temperature (70 C) and the lack of moisture control resembled the WTRs incubation conditions.

Subsamples were collected from the incubated samples during a 24-month period. Aggregates were gently crushed with mortar and pestle, and then were extracted with oxalate (5 and 200 mM) extractions were performed (McKeague et al., 1971). Oxalate extractable P, Al, and Fe were unaffected by solid: solution ratio (1:60 versus 1:300) or filter size (0.45 versus 0.1 μm) changes. Thus, a 1:300 ratio, and 0.45 μm filter size were used. Following oxalate extraction, suspensions were centrifuged at 4000 rpm for 15 min, filtered, and analyzed for P, Al, and Fe by a Perkin-Elmer Plasma 3200 Inductively Coupled Plasma Spectrometer (ICP).

To assess changes in crystallinity of the hydroxides due to incubation at elevated temperature, powder XRD analyses were conducted using monochromatic CuKα radiation at 35 kV and 20 mA. The 2θ diffraction angle (2°- to 50 or 70°) was scanned at a rate of 2° (2θ) min^{-1}. Thermogravimetric (TG) measurements were conducted using a thermal analysis apparatus in air at a heating rate of 5 C min^{-1} to 70 C where isothermal weight loss was monitored for 2 or 10 h. BET-N_2 SSAs were determined by a N_2 adsorption/desorption method at liquid N_2 temperature (77 K) using a surface area analyzer (Autosorb-1, Quantachrome Inc. Boynton Beach, FL, USA). Prior to N_2 adsorption/desorption measurements, all samples were outgassed at 70 C for 4 h using He as the eluent.

For the WTRs, subsamples (< 2 mm) that reacted for 40 d with P solutions at a P load of 10,000 mg P kg^{-1} in 1:10 WTR: 0.01 M KCl suspensions were utilized for the incubation experiments. The pH was not controlled and the suspensions were not shaken during the equilibration period. After P sorption, WTR particles were air-dried, and placed in incubators maintained at 23, 46, and 70 C. Non-treated (no added P) WTR samples were also included in the incubation experiment. P-treated and untreated samples of six WTRs were incubated in the lab for 2 years. Another set of air-dried WTRs was left at 23 C as a control treatment for the incubation experiments. The heat treatment was applied in an effort to encourage structural changes that might mimic long-term weathering reactions in the field. We hypothesized that elevated temperatures would provide the necessary activation energy for structural rearrangements with time. These changes in particle conformation, towards a lower free energy of the system, would either exclude or occlude sorbed P by the Al-WTR.

Subsamples of WTRs incubated for 2 years at 70 C were subjected to oxalate (5 and 200 mM) extractions, and analyzed for P, Fe and Al with ICP. Particle size separation (wet sieving) showed that medium sand was the predominant size fraction in the materials used for extensive TG analysis (Tampa Fe-WTR and Bradenton Al-WTR). Air-dried particles were subjected to a heating rate of 5 C min^{-1} up to 70 or 150 C. The temperature was then kept constant for 2 and 10 h, after which the samples were brought to room temperature and relative humidity conditions for 2 and 10 h.

Soils amended with WTRs present the most complex and realistic system studied to ascertain long-term P stability of sorbed P by WTRs applied to soils. Soil samples from two different sites were utilized. The first set of soil samples came from Holland, MI,

which is a long-term field experiment to monitor the longevity of WTR effect in reducing soluble P levels in soils (see chapter 4). The other set of soil samples came from a joint effort of South Florida Water Management District and the USEPA to study the effect of WTR application to a sandy soil in Kirton Ranch (KR), Okeechobee, FL, amended with different P sources. Surface soils samples from both sites were collected and transferred to our Gainesville, FL laboratory for the incubation studies.

Air-dried field soil samples from the Holland, MI sites 1 and 2 were incubated in the lab at 46 and 70 C, for 2 years. Another set of the air-dried soil samples was left at 23 C as a control treatment for the incubation experiments. The heat treatment was applied in an effort to encourage intraparticle structural changes that might mimic long-term weathering reactions in the field. Subsamples of the soil samples incubated for a year at elevated temperatures were subjected to oxalate (5 and 200 mM) extractions, and analyzed for P and Al with ICP.

Unamended soil samples from the A horizon of the KR, Okeechobee site were collected and transferred to the laboratory, where they were air dried and sieved (2mm). Soil samples were amended with 2.5 % (by wt.) air-dried Al-WTR. Phosphorus was added as TSP solution at three rates: zero, low, and high to roughly mimic field study rates. The “low rate” of 43 mg P kg^{-1} is slightly greater than the rate recommended for pasture grass raised for hay. The “high” P rate equals 100 mg P kg^{-1} soil. Fertilizer-P was dissolved in 0.01 M KCl and added to generate a solid: solution ratio of 1: 10. Two replicates were used and a total of twelve samples were studied. The experimental design was a complete randomized design:

no P, no WTR	low P, no WTR	high P, no WTR
no P, WTR	low P, WTR	high P, WTR

The soil-WTR suspensions were reacted for 7d at room temperature, without stirring. The suspensions were then centrifuged and supernatants were decanted. The residues were thoroughly mixed, divided into three portions (~100 g each), and put in incubators at 23, 46, and 70 C. No attempt was made to control soil moisture during incubation. Subsamples were removed from incubators 1, 6, 14, 18 and 24 months of incubation.

Results and Discussion

Aluminium hydroxides were coprecipitated, with and without P, and incubated at 70 C for 24 months. Stability transformations of incubated aluminium hydroxides coprecipitated with and without P were monitored via oxalate extractions. Oxalate (200 mM) extractable Al of the untreated (no P) samples was significantly less than for the P-treated samples. Extractability of Al for the untreated samples decreased over the 1st week of incubation, gradually decreased up to 3 months of incubation, and thereafter stabilized (Figure 5-1). No significant changes in oxalate (200 mM) -extractable Al with time were evident when P was coprecipitated with Al at a 1:1 molar ratio (Figure 5-1). Similarly to Al, oxalate -extractable P levels of the P-treated Al gels remained constant throughout the incubation period (24 months).

Oxalate extractions of the Fe oxyhydroxides gave contrasting results to the Al system (Figure 5-2). Oxalate (200 mM) extractable Fe of the untreated (no P) samples remained constant throughout the incubation period (24 months) at 70 C, and was greater than for the P-treated samples. When P was coprecipitated with Fe, P and Fe extractability increased only slightly during the 1st week and was stabilized thereafter, showing no changes after 24 months at 70 C.

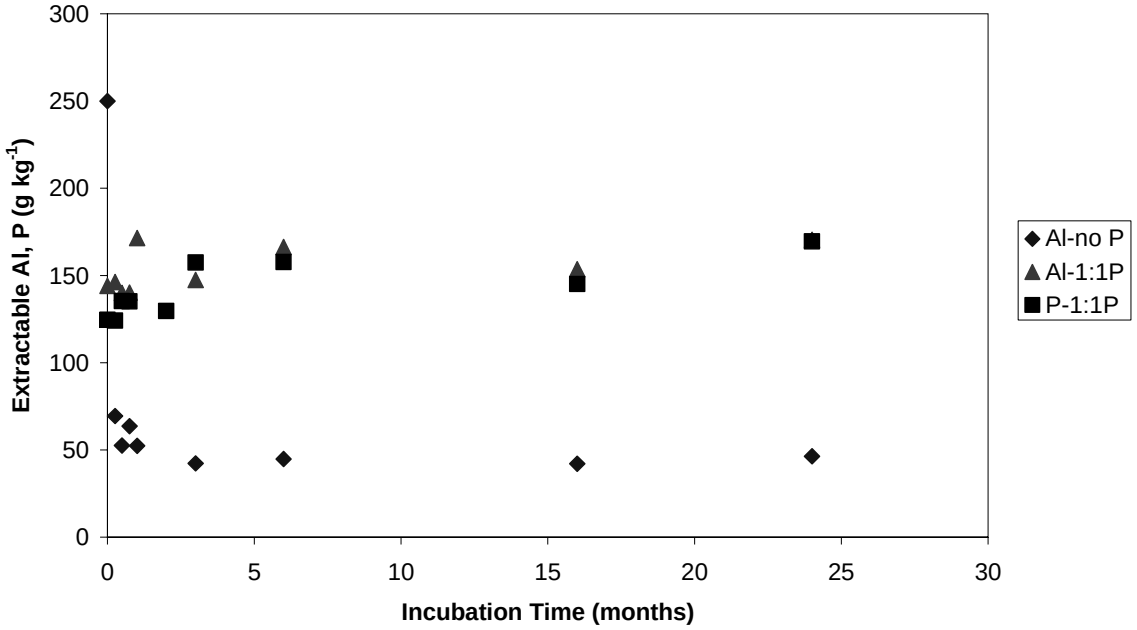

Figure 5-1. Changes in oxalate (200 mM) extractable Al and P of P-treated and untreated Al hydroxides incubated for 24 months at 70 C. Error bars denote one standard deviation of the mean (n=2), and their size is smaller than the legend.

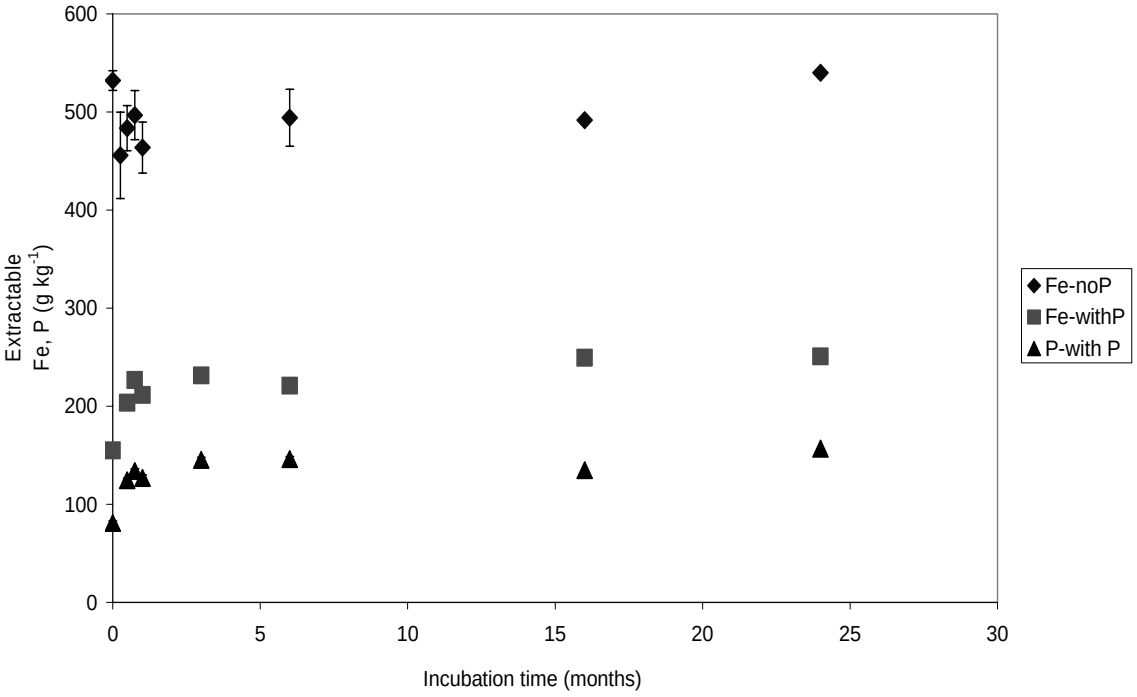

Figure 5-2. Changes in oxalate (200 mM) extractable Fe and P of P-treated and untreated Fe hydroxides incubated for 24 months at 70 C. Error bars denote one standard deviation of the mean (n=2), and their size is smaller than the legend.

Particle surface transformations are difficult to detect using a high concentration of oxalate (200 mM), especially in the 1:1 P:metal systems. The oxalate treatment almost completely dissolved Fe and Al particles and extracted > 90 % of total P. The insensitivity of the 200 mM oxalate treatment in extracting P led us to use a milder extractant (5 mM oxalate). Oxalate (5 mM)-extractable Al for the untreated Al hydroxides followed the decreasing trend of the 200 mM oxalate treatment with incubation time at 70 C (Figure 5-3). However, oxalate (5 mM)-extractable Al for the P-treated Al hydroxides was very low compared with the 200 mM treatment (~0.6 g Al kg^{-1}) and paralleled oxalate- (5 mM) P (~ 4 g P kg^{-1}). Oxalate (5 mM)-Al was much lower than 200 mM since 5 mM is considered a milder extractant that selectively extracts P mainly from external surfaces.

Oxalate (5 mM) P and Al in P-treated Al gels remained relatively constant through 24 months of incubation at 70 C. Overall, 5 mM oxalate extraction was lower in magnitude and consistent with trends observed with 200 mM. Interestingly, a trend not seen in the oxalate (200 mM) extractions of the P-treated samples was that P addition stabilized the Al hydroxide surface by significantly lowering Al extractability compared with the untreated gels (Figure 5-3). Biber et al. (1994) observed decreased dissolution rates of Fe hydroxides in the presence of sorbed phosphate.

In the case of Fe oxyhydroxides, oxalate (5 mM) Fe for the untreated Fe gels remained unchanged after 24 months of incubation at 70 C, despite an initial slight

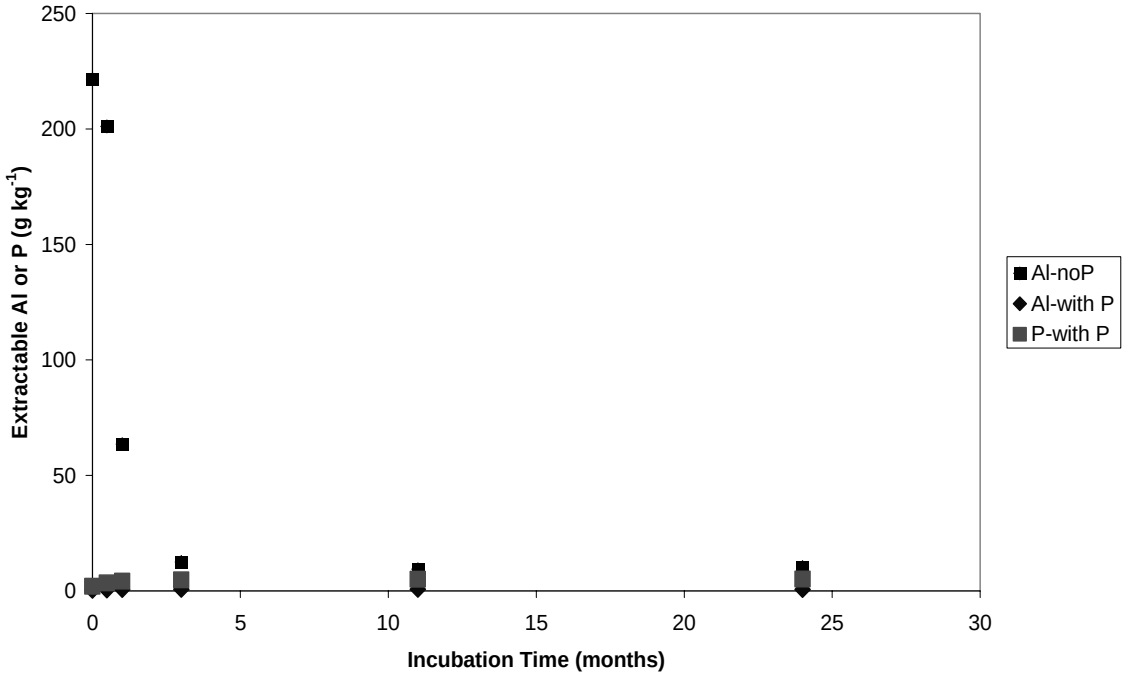

Figure 5-3. Changes in oxalate (5 mM) extractable Al and P of P-treated and untreated Al hydroxides incubated for 24 months at 70 C.

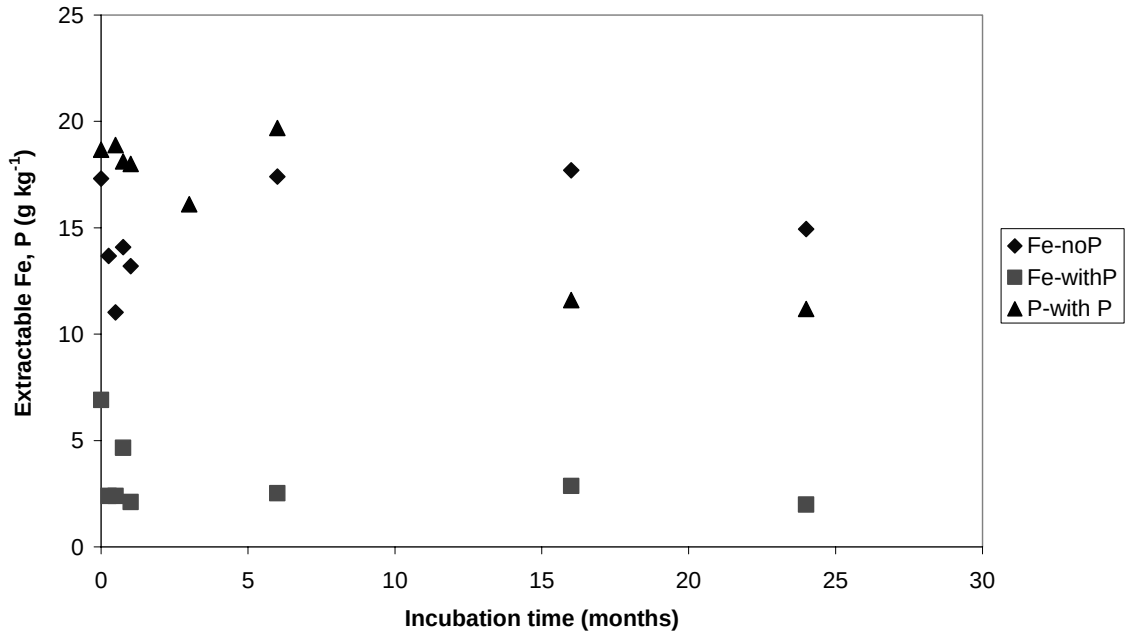

Figure 5-4. Changes in oxalate (5 mM) extractable Fe and P of P-treated and untreated Fe hydroxides incubated for 24 months at 70 C.

decrease in oxalate-Fe (Figure 5-4). When P was added (1:1 P/Fe molar ratio), oxalate (5 mM) Fe decreased within the 1st month of incubation and remained constant thereafter (Figure 5-4). Contrary to Al gels, oxalate (5 mM) P did not parallel oxalate Fe since it remained constant the first 6 months of incubation and decreased thereafter.

X-ray diffraction analyses were conducted on both Al and Fe amorphous gels during their incubation at 70 C. At time zero, both P-treated and untreated Al hydroxides were amorphous (Figure 5-5). Incubation at 70 C of the untreated Al gels for a month was sufficient to induce some degree of long-range order as evidenced by a broad peak (Figure 5-6) that was tentatively assigned to pseudoboehmite (Okada et al., 2002). There was no further increase in crystallinity even after 24 months of incubation at 70 C.

Phosphorus-treated Al oxyhydroxides remained amorphous throughout the incubation period of 24 months. It seems that P addition poisoned Al crystallization of the particles as was observed with the untreated Al gels. Galvez et al. (1999a) showed that at P / Fe atomic ratios less than 3 %, crystallization of ferrihydrite proceeded normally, whereas at ratios greater than 3 % phosphate inhibited the iron hydr(oxide) crystallization. This study's P-treated samples (1:1 P/metal molar ratio) of both Fe and Al hydroxides inhibited structural transformations that were observed in the absence of P.

In the case of Fe oxyhydroxides, incubation time and temperature had no significant effect on crystal growth for either P-treated or untreated samples, which remained amorphous throughout the incubation period (Figure 5-7). The x-ray pattern of the untreated Fe hydroxides resembled six-line ferrihydrite and was mostly amorphous.

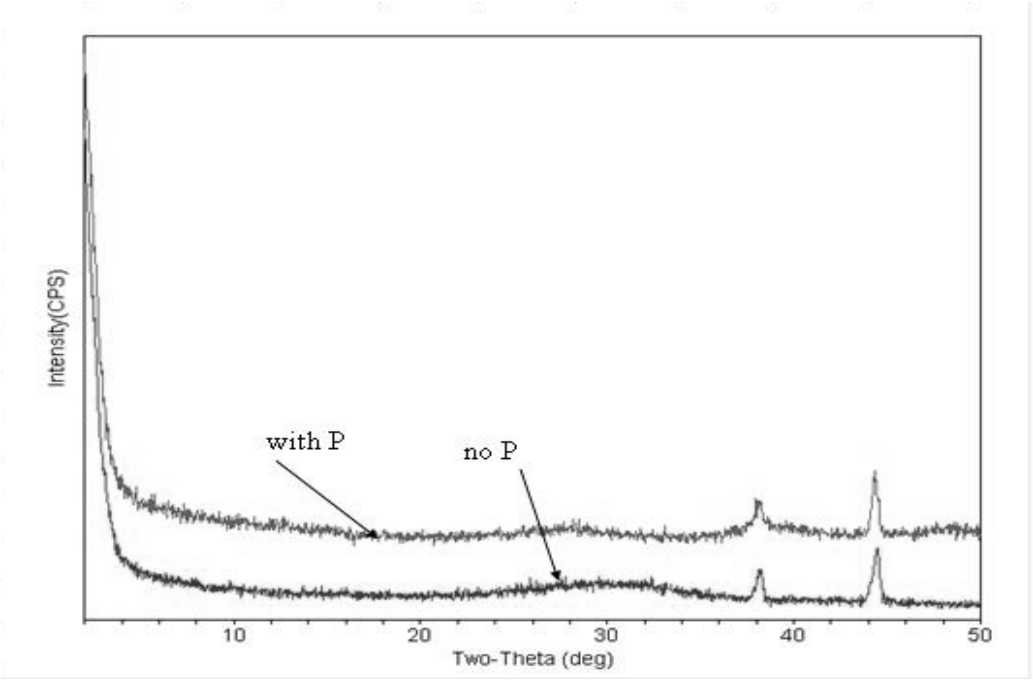

Figure 5-5. X-ray diffraction analysis of P-treated and untreated Al hydroxides before placing them into incubators (time zero). Both treatments (P-treated and untreated) were amorphous. The two sharp peaks around 40 two-theta degrees came from the mount.

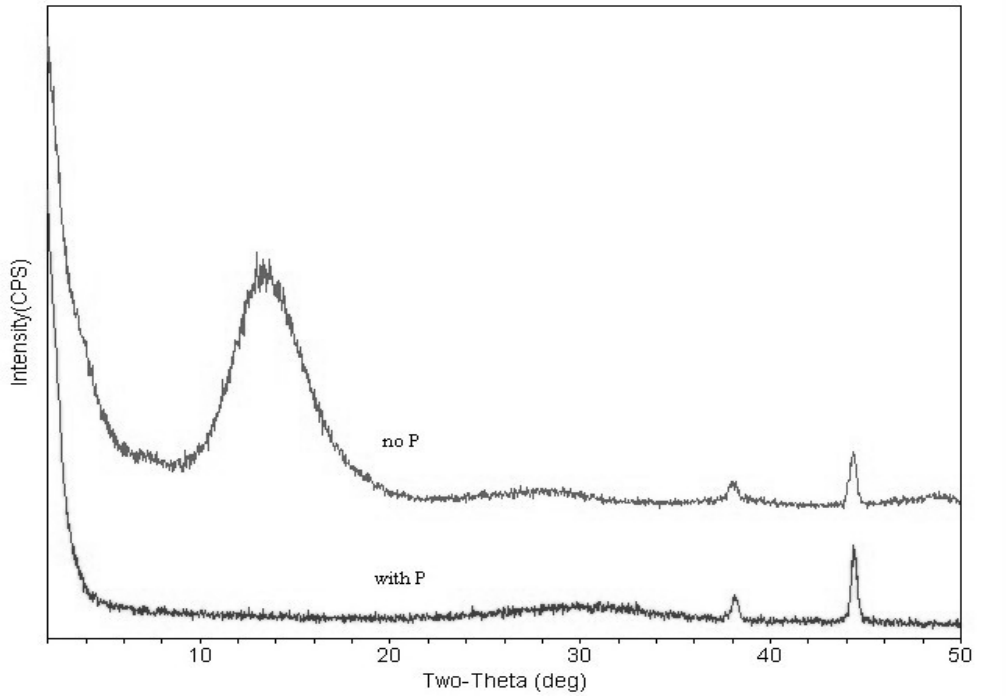

Figure 5-6. X-ray diffraction analysis of P-treated and untreated Al hydroxides 1 month after incubation at 70 C. Untreated samples showed the formation of pseudoboehmite. Further incubation at 70 C for 24 months did not result in major changes to the peaks.

Although the amorphous nature of the P-treated samples was expected, based on evidence for P poisoning of crystallization, the fact that untreated Fe oxyhydroxides remained amorphous was surprising. The method used was initially conducted for Al hydroxides (Goldberg et al., 2001), but should work for Fe hydroxides as well. However, preparation conditions were different than the typical two-line and six-line ferrihydrite preparation (Schwertmann et al., 2001).

The majority of changes in P and Al extractabilities occurred within the first 2 months of incubation with the untreated Al hydroxides, but little changes were observed with the Fe hydroxides. Incubated suspensions were allowed to air-dry, and free bulk water evaporated within a 2-week incubation at 70 C. One might doubt the effectiveness of low water heat incubations as a means to accelerate soil particle transformations towards more crystalline phases. An example of this type of transformation is goethite = hematite + water (Langmuir, 1971). Removing water from soil particles with the aid of heat input usually results in lowering the water activity; the remaining water should be strongly bound to soil particles. Al substitution into goethite particles results in lowering the water activity, so stabilization of goethite particles might occur that prevents transformation towards more crystalline Fe phases (Yapp, 1983).

The effect of drying on mineral transformations and degree of crystallinity has been assessed for uranium oxides. Sowder et al. (1999) found no significant differences in XRD patterns for air-dried metaschoepite, either at room temperature or at 65 C. They also observed a positive effect of dehydration (65 C) on metaschoepite transformation to a secondary weathering phase of the U (VI) oxide hydrates. Dry heating of the metaschoepite resulted in the formation of a more crystalline dehydrated schoepite.

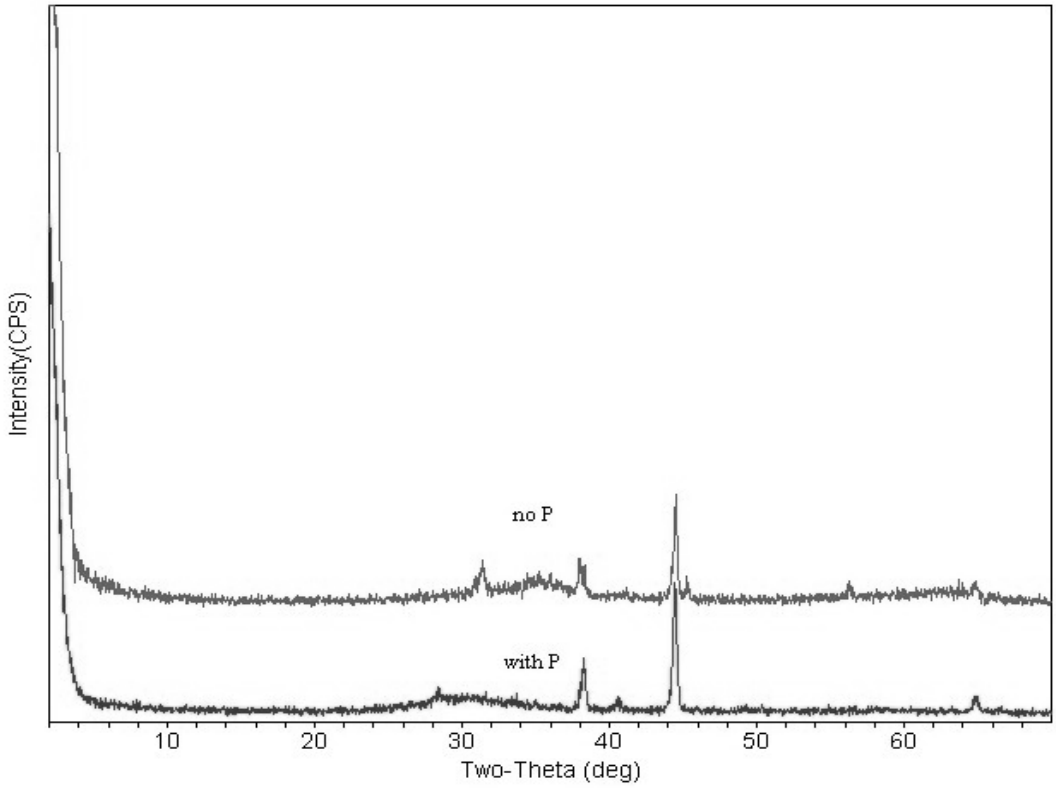

Figure 5-7. X-ray diffraction analysis of P-treated and untreated Fe hydroxides one month after incubation at 70 C. Both untreated and P-treated samples were amorphous. Further incubation at 70 C for 24 months did not result in major changes of the peaks shown here. The two sharp peaks around 40° 2θ come from the mount. Sharp peak of the untreated sample around 32 two-theta degrees comes from remaining salt (NaCl).

Weidler (1997) synthesized two-line ferrihydrite to study the effect of temperature and humidity on BET-SSA and crystallinity of ferrihydrite. Weidler observed that for samples allowed to become wetted during the outgassing procedure, (series A) hematite was formed around 120 to 130 C. Ferrihydrite samples with constant decreasing humidity (water loss 150 mg g^{-1}, up to 150 C) during outgassing (series B) showed no hematite formation. Interestingly, BET-SSA for series B ferrihydrite samples remained constant up to 120 C, whereas BET-SSA for series A decreased as temperature increased from 100 C and beyond. Schwertmann et al. (1999) reported that two-line ferrihydrite kept for 9-12 years in water at temperatures of 4 to 30 C was transformed to hematite especially at the

highest temperature (30 C). In the case of low water activity, Schwertmann et al. (1999) reported that an air-dried two-line ferrihydrite stored for 20 years at room temperature was partially transformed to hematite. In the absence of bulk water, restricted mobility of atoms will influence the transformation rate.

Schwertmann et al. (1999) speculated that a gradual structural transformation is expected with dry heating. Campbell et al. (2002) observed that dry heating induced transformation of Si-ferrihydrite towards Si-incorporated hematite. This transformation was dependent upon the Si load and temperature. Thus, structural transformations can also occur in low water activity systems at relatively high temperatures (> 50 C). Further, we will discuss isothermal TG data for air dried metal hydroxides and WTRs that suggest the presence of hysteretic internally found water molecules. Meso- and micro-pore bound water may play a key role in structural transformations during heat incubations of air-dried particles.

Surface Area and Porosity of the Al and Fe Hydroxides

At time zero of incubation (right before starting the incubations), untreated Al gels were fully hydrated and characterized by large BET-N_2 SSA since they were mostly amorphous (607 m^2 g^{-1}) (Figure 5-8). A N_2 gas adsorption isotherm showed increased gas sorption at low relative pressures (less than 0.1 P / P_o) indicative of microporosity (less than 2 nm) (Gregg and Sing, 1982). The isotherm also revealed the hysteretic behavior of the untreated Al gels when subjected to desorption. The hysteresis at the higher relative pressures of the isotherm suggests the abundant presence of mesopores in the untreated Al gels that formed during the coprecipitation process (Gregg and Sing, 1982).

Incubating the untreated (no P added) Al hydroxides at 70 C resulted in significant BET-N_2 SSA decreases (Figure 5-8). Incubation (70 C) of the untreated Al hydroxides

for 1 month resulted in drastic reduction of SSA measurements from 607 to 168 $m^2 g^{-1}$ (Figure 5-8). Further incubation for 24 months resulted in a minor decrease in SSA values. This trend is corroborated by similar kinetic trends observed with oxalate extractions as well as the XRD data. It seems that pseudoboehmite formation was achieved within 1 month of incubation at 70 C and little changes in crystallite size and SSA occurred thereafter. SSA decreases may have resulted from the combination of physi-sorbed water losses and structural rearrangements, due to heat input (70 C). Structural rearrangements of the untreated Al hydroxide particles, as evidenced by SSA decreases, suggest particle transformations towards a more ordered phase. Interestingly, after 1 month of incubation, mesoporosity of the untreated Al hydroxides before incubation (time zero) was no longer obvious since N_2 desorption was no longer hysteretic as evidenced by the overlap of adsorption and desorption points (Figure 5-8).

In the case of P-treated Al hydroxides, BET-N_2 gas sorption was overall lower in magnitude than the untreated particles (Figure 5-9). Isotherms showed lower microporosity, but a greater macroporosity as evidenced by the large upward direction of the curve at relative pressures P/P_0 of 0.8-1. Observed hysteretic N_2 gas desorption in untreated Al particles was not shown in P-treated samples, where adsorption and desorption points fell on top of each other (Figure 5-9) suggesting absence of mesopores. It seems that P coprecipitation with the metal resulted in micropore occupation by phosphates and distortion of the structure, making it more open, and higher in macropore content. At 70 C, incubation time at 70 C had little effect on N_2 gas adsorption isotherms after 24 months (Figure 5-9).

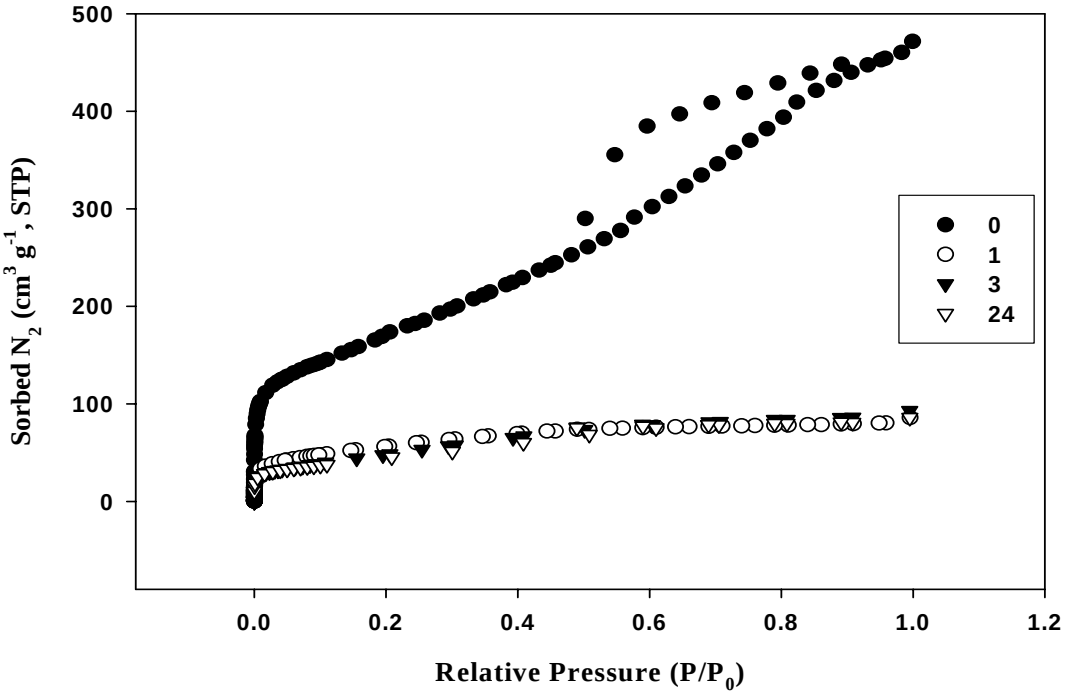

Figure 5-8. Changes in N_2 gas adsorption / desorption isotherms of the untreated Al hydroxides after different incubation times (0 to 24 months) at 70 C.

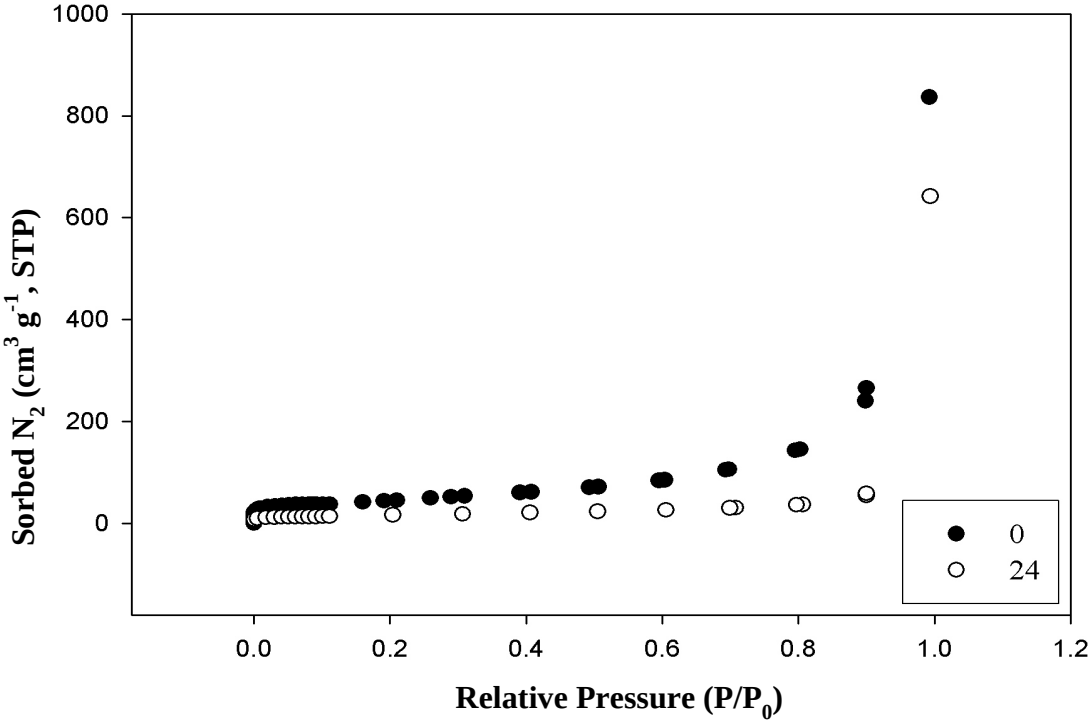

Figure 5-9. Changes in N_2 gas adsorption / desorption isotherms (-196 C) of the P-treated (1:1 P/Al molar ratio) Al hydroxides performed after different with incubation times (0 and 24 months) at 70 C.

These data are in accordance with XRD analyses that showed no evidence of crystalline Al-P components after isothermal (70 C) incubation of the P-treated Al particles for 24 months had no effect on particle crystallinity. SSAs of P-treated particles decreased with time, but not as significantly as untreated particles (Figure 5-10). Decreases in SSA of a material do not necessarily reflect increases in crystallinity. Phenomena such as particle shrinkage due to dehydration may be responsible for the observed SSA decreases in the P-treated particles. P-treated particles showed significantly lower SSA values compared with untreated particles. This feature might explain why we observed lower oxalate (5 mM) Al concentrations when P was coprecipitated with the Al hydroxides.

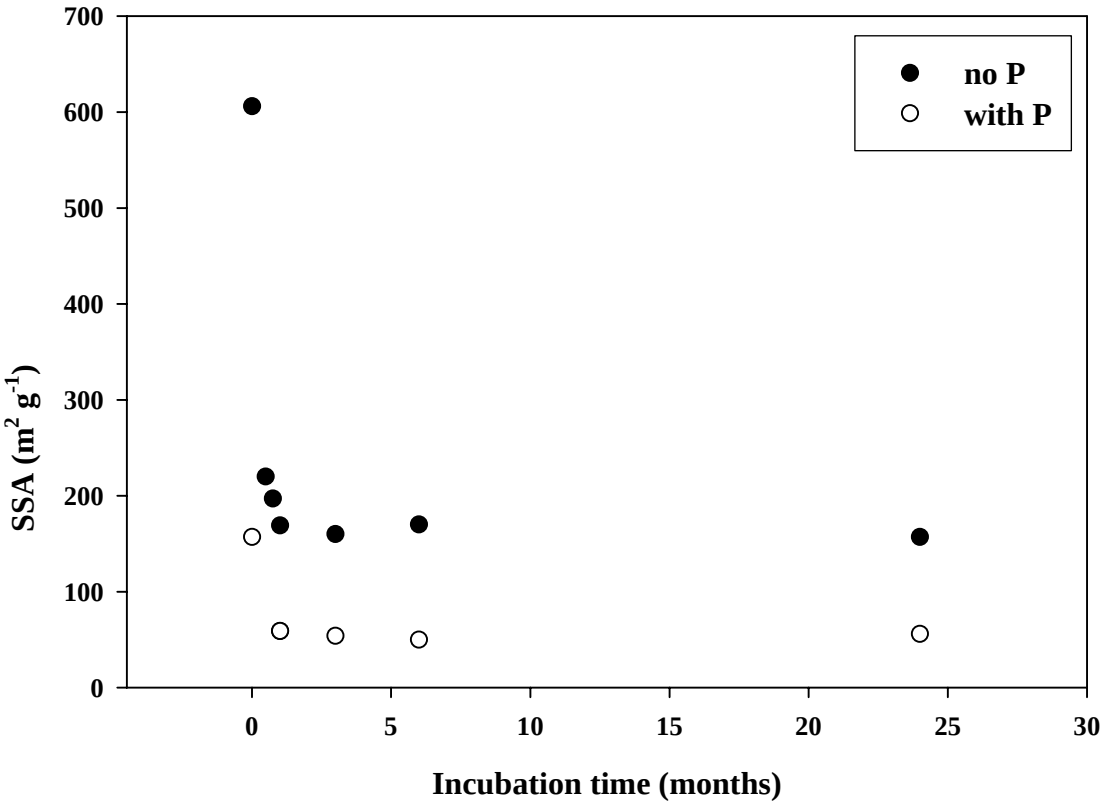

Figure 5-10. Temporal change of BET-SSAs with time of synthetic Al hydroxides coprecipitated with (1:1 P:Al ratio) or without P, and incubated at 70 C.

Amorphous metal oxides can be metastable and transform to more crystalline and thermodynamically stable phases with time. We hypothesized that micropores play a key role in the long-term transformations of amorphous metal hydroxides. The identification and quantification of micropores in the Al untreated hydroxides was accomplished using a model that accounts for large interaction potentials involved between pore walls in close proximity (< 1.5 nm). The Kelvin equation is widely used, but its applicability is limited to pores greater than 2 nm. Below this pore size, liquid cannot be considered a fluid with bulk properties due to large capillary forces between pore walls (Saito and Foley, 1991; Horvath and Kawazo, 1983).

The SF model developed by Saito and Foley (1991) assumes cylindrical micropores with structure similar to zeolites or molecular sieves. The SF model was applied to Al hydroxides to evaluate their micropore size distribution. The SF pore size distribution of the untreated Al hydroxides revealed the predominance of micropore diameters around 10 Å (1nm = 10 Å) (Figure 5-11). At time zero, micropores were abundant but were significantly reduced after 1 month of incubation at 70 C (Figure 5-11). This trend was consistent with oxalate extractions, SSA decreases, and increases in the crystallinity of the untreated Al hydroxide, as evidenced by XRD analyses. As crystallite size increases, its SSA decreases and micropores decrease at the apparent expense of crystal growth.

When P was coprecipitated with Al (1:1 P/Al molar ratio), micropore volume measured by the SF method was significantly lower than the untreated Al hydroxides and showed a decrease in micropore volume after 24 months of incubation at 70 C (Figure 5-12). Phosphorus-treated micropore size distributions also showed also a predominant size around 1 nm, similarly to untreated pore distributions.

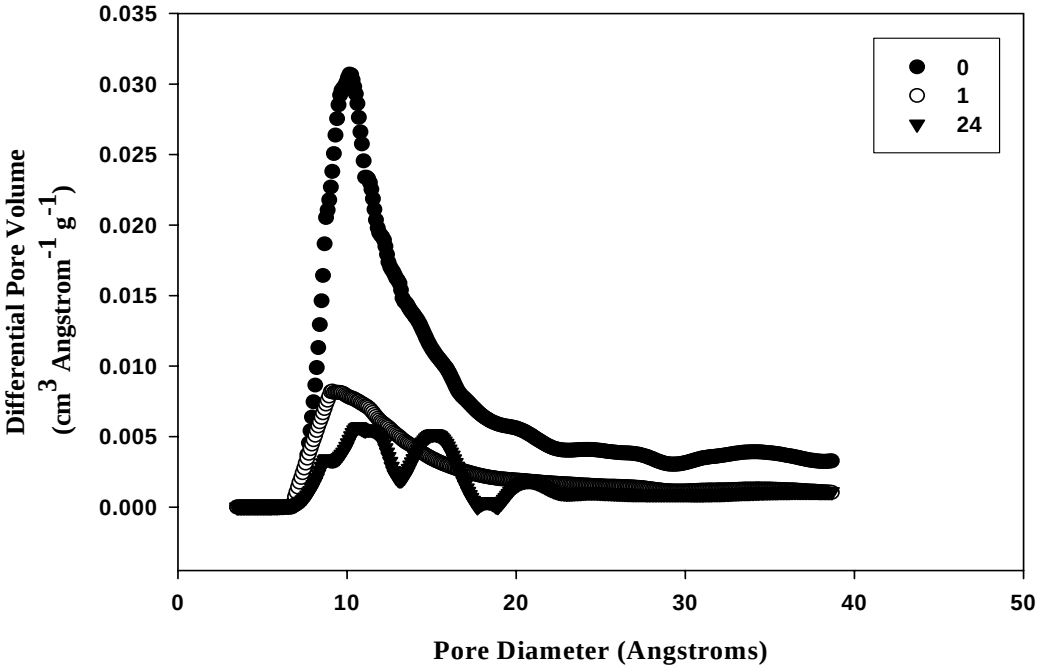

Figure 5-11. Pore size distribution of the synthetic untreated Al hydroxides incubated at 70 C for 24 months.

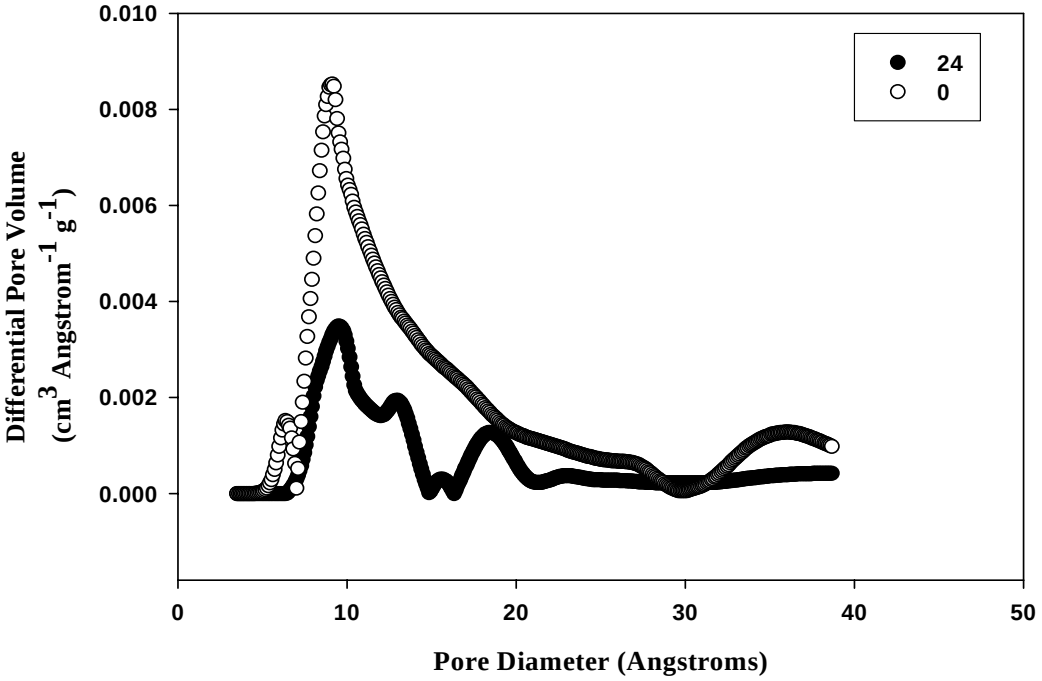

Figure 5-12. SF micropore size distribution of the P-treated Al hydroxides incubated at 70 C for 24 months.

Iron Hydroxides-Results

Similar SSA and porosity analyses were also conducted for the Fe hydroxides coprecipitated with or without P and incubated at 70 C for 24 months. Results from the N_2 gas adsorption isotherms of the untreated Fe gels showed increased microporosity character and hysteretic desorption, suggesting the presence of mesopores (Figure 5-13). Hysteretic desorption was observed at all incubation times (from time zero to 24 months of incubation at 70 C). The amount of gas adsorbed decreased within 1 month of incubation and did not change thereafter, similarly to the untreated Al gels. However, no evidence of crystalline Fe components was found using XRD.

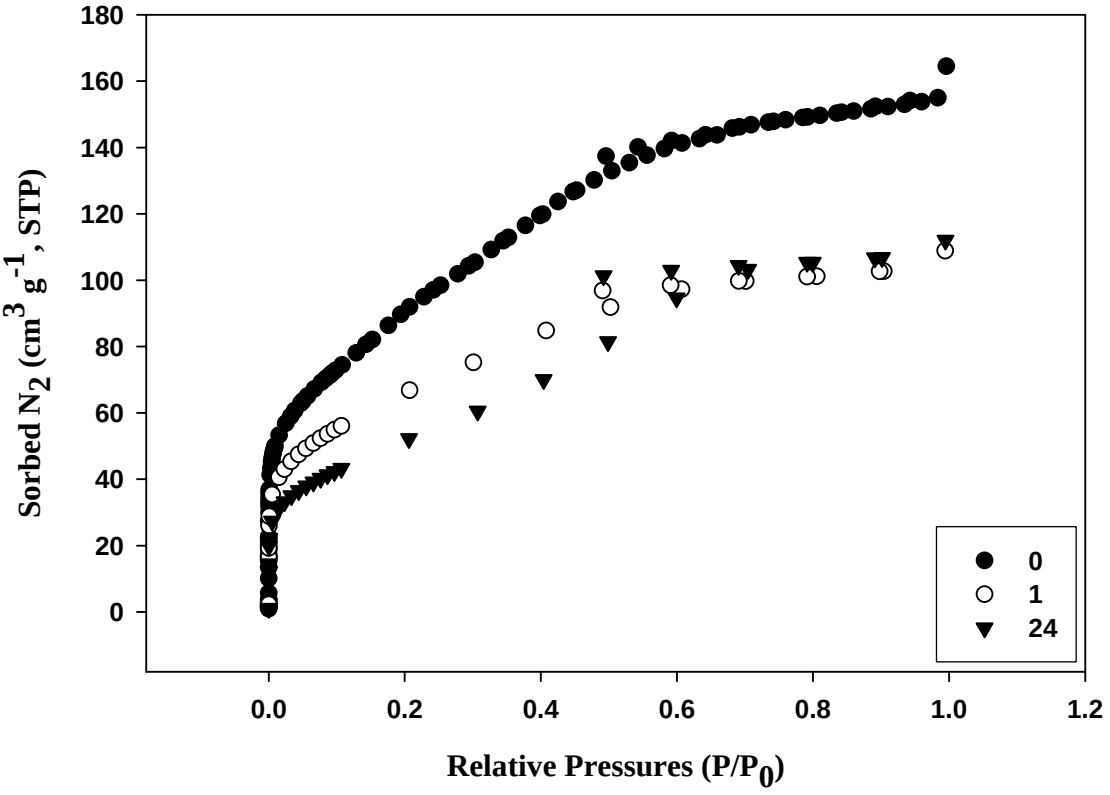

Figure 5-13. Changes in N_2 gas adsorption / desorption isotherms (-196 C) of the untreated Fe hydroxides performed after different with incubation times (0 to 24 months) at 70 C. Hysteretic desorption was observed for all incubation times, where sorption data did not coincide with desorption points.

When P was coprecipitated with the Fe salt, gels formed were highly amorphous and showed lower microporosity than the untreated, based on the lower amount of N_2 sorbed at relative pressures less than 0.1 P/P_0 (Figure 5-14). Isotherms also showed the large proportion of macropores based on the upward direction of the curve at relative pressures > 0.8. Specific surface areas were reduced with incubation time and macropores disappeared after 6 months of incubation.

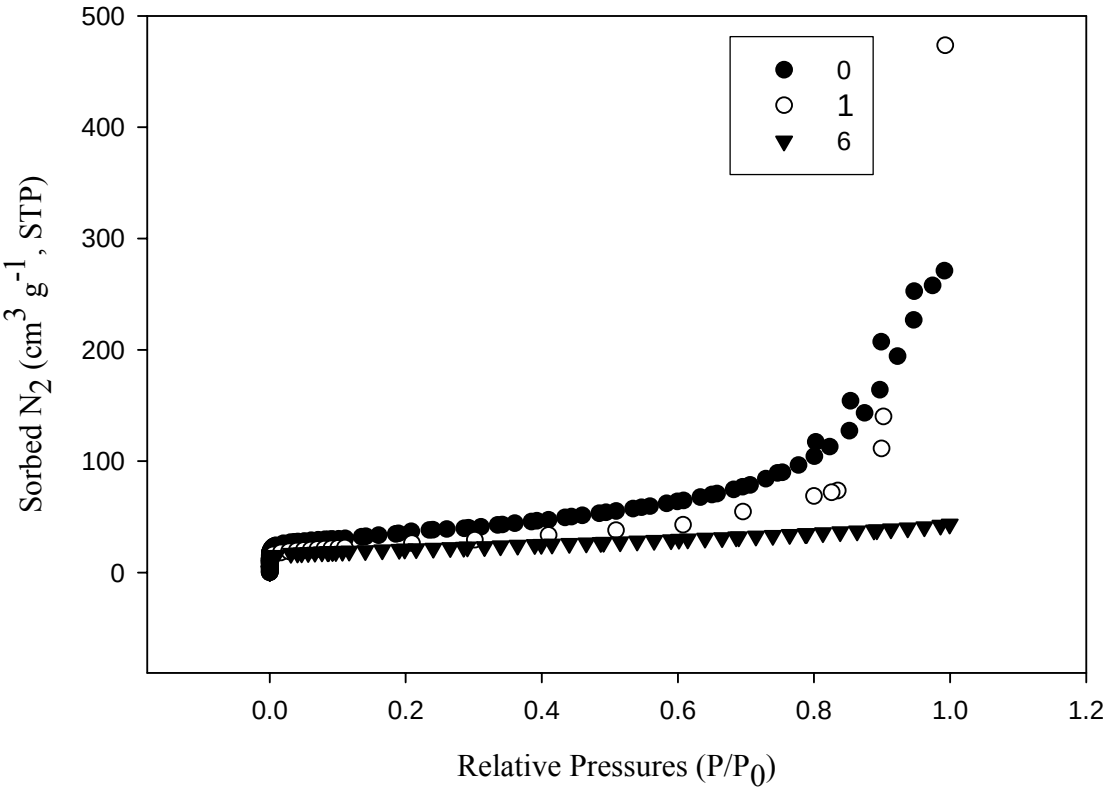

Figure 5-14. Changes in N_2 gas adsorption / desorption isotherms (-196 C) of the P-treated Fe hydroxides performed after different with incubation times (0 to 24 months) at 70 C. Isotherms 24 months after incubation at 70 C resembled the isotherm showed above for 6 months. Hysteretic desorption was observed only for time zero treatment, where sorption data did not coincide with desorption points.

Disappearance of macropores was coincident with diminishing SSA with time for both P-treated and untreated Fe hydroxide particles (Figure 5-15). The kinetic effect of SSA decreases was independent of P treatment and was not accompanied by increases in

crystallinity. SSA stabilization in the Fe hydroxides took more time (6 months) versus 1 month for the Al hydroxides, and was independent of P load. Stabilization of SSA decreases was not correlated with increases in crystallinity for the Fe hydroxides, but only for Al hydroxide particles.

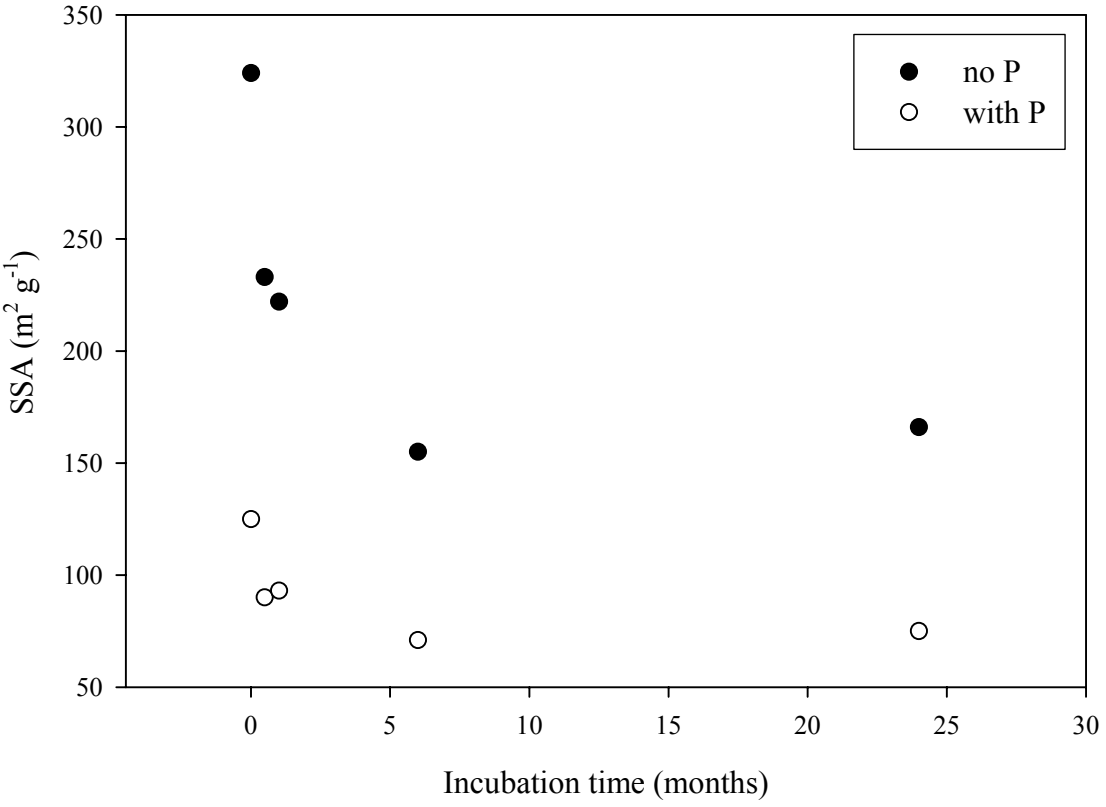

Figure 5-15. Changes in BET-SSAs with time of synthetic Fe hydroxides coprecipitated with (1:1 P:Al ratio) or without P, and incubated at 70 C.

Pore size distributions of the untreated Fe hydroxides were also determined based on the SF model (Figure 5-16). At time zero, untreated Fe hydroxide particles showed a predominant micropore size distribution, which was significantly reduced within 1 month of incubation. Micropore volume reduction was stabilized 6 months after incubation at 70 C with no changes thereafter. Pore size distributions of the P-treated Fe hydroxide particles exhibited pore volumes lower in magnitude than the untreated particles (Figure

5-17). Most of the porosity was found in micropore size range, similar to the untreated particles. A significant portion of micropore volume was lost within 1 month of incubation. Micropore volume was stabilized 6 months after incubation.

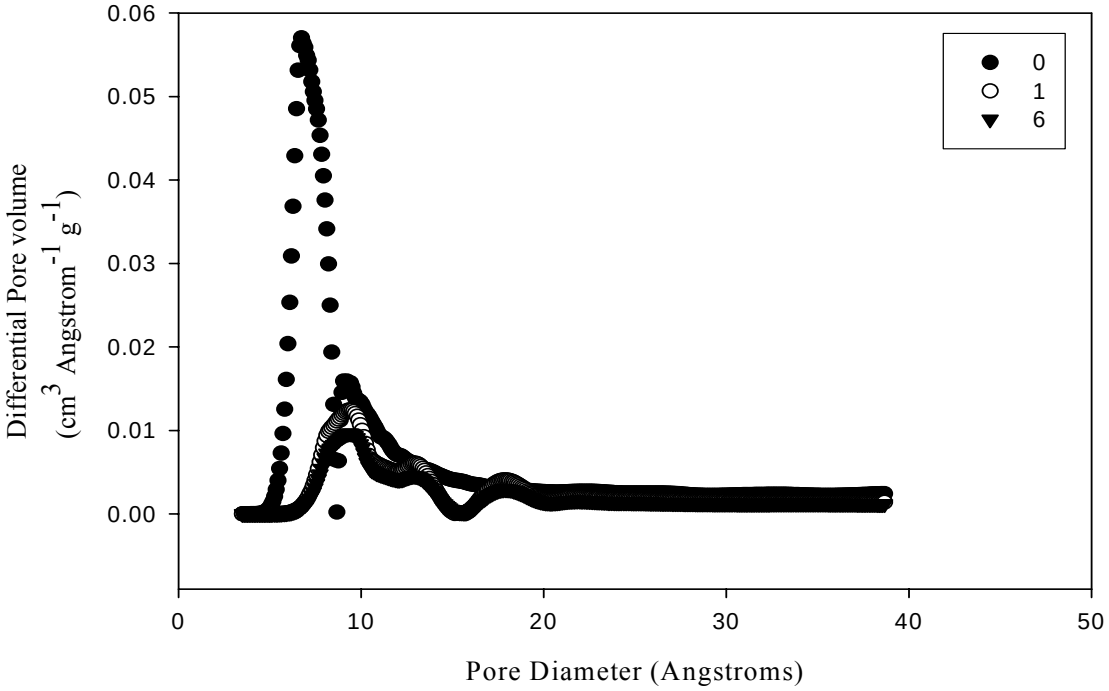

Figure 5-16. Pore size distribution of the synthetic untreated Fe hydroxides incubated at 70 C for 24 months. Only 6 months of incubation are shown here since there was no difference between 6 and 24 month time periods.

To further confirm the presence of phosphate in micropores of the Al hydroxides, CO_2 gas sorption at 0 C was performed. Micropores less than 1.5 nm in diameter that encounter diffusional restrictions can be determined by CO_2 adsorption at 0 C. The CO_2 analysis of the untreated Al hydroxide incubated for 6 months revealed that micropore SSA of the untreated sample was 148 m^2 g^{-1} (90 % of the BET-N_2 SSA value) (Figure 5-18).

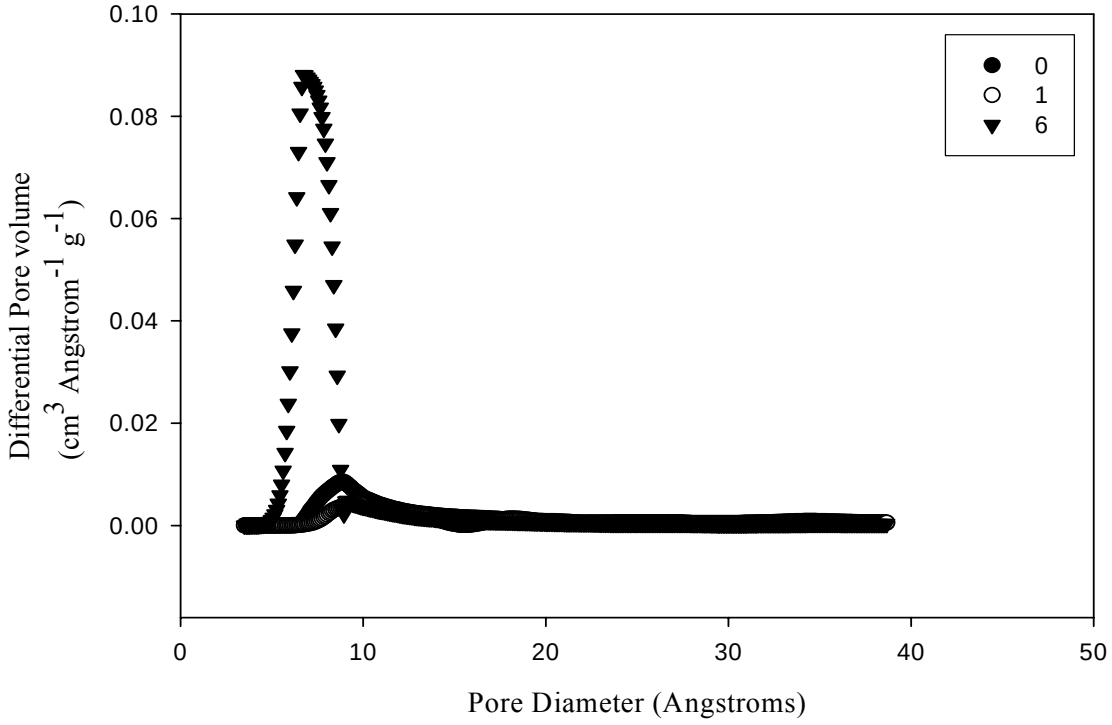

Figure 5-17. Pore size distribution of the synthetic P-treated Fe hydroxides incubated at 70 C for 24 months. Only 6 months of incubation are shown here since there was no difference between 6 and 24 month time periods.

A significant decrease in SSA of the CO_2 isotherm was observed in P-treated particles (1:1 P/Al molar ratio) (Figure 5-18). This result supports the idea of micropore blockage by phosphate molecules. Micropore CO_2 SSA and pore volume distributions further confirmed the reduction in SSA of micropores with diameters of 0.4 to 1.2 nm (4 to 12 Å) (Figure 5-19). Both SSA and pore volume distributions showed a shift in porosity of the Al hydroxides when P was added (1:1 P) from the lower to the highest (1.0 to 1.5 nm) size limit of micropores.

Another line of evidence for microporosity of gels and WTRs was collected from isothermal (70 C) thermogravimetric (TG) weight losses.

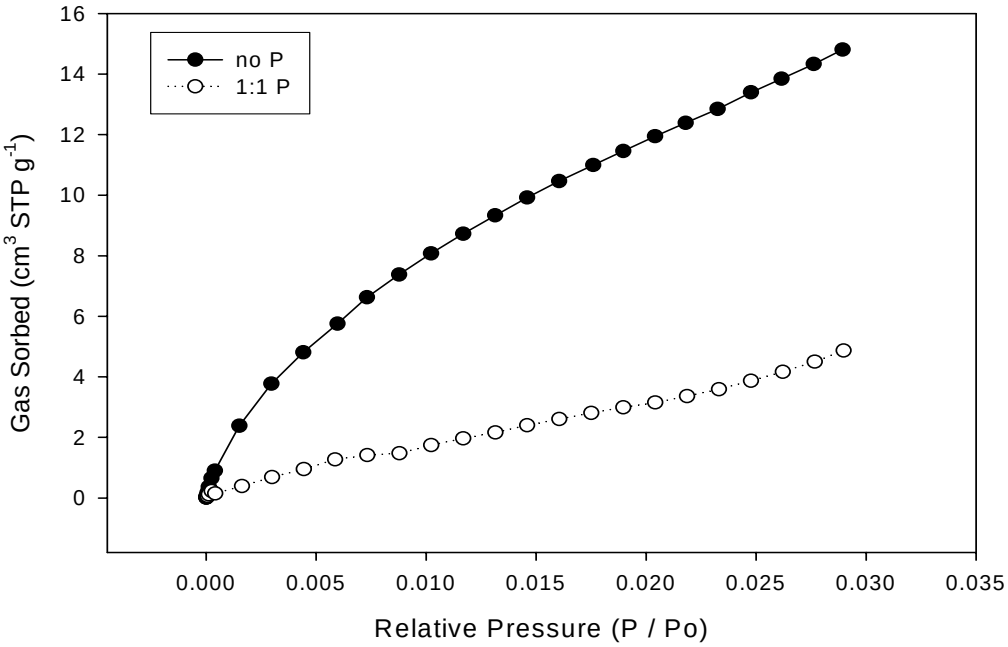

Figure 5-18. CO_2 gas sorption of the Al hydroxides treated with and without P, and heated for 6 months at 70 C.

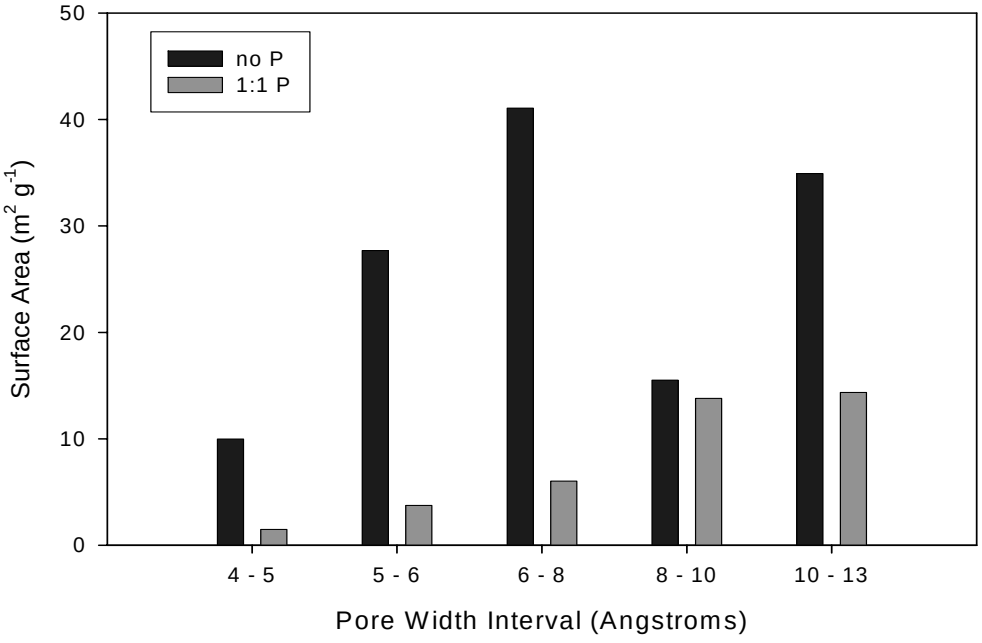

Figure 5-19. Differential SSA distribution of the P-treated and untreated Al hydroxides incubated for 6 months at 70 C.

TG analysis has been used in synthesized hematite particles to assess the structure of micropores in colloidal suspensions (Kandori, and Ishikawa, 2001).Isothermal weight losses of the Al and Fe hydroxides were time dependent, suggesting the presence of "zeolitic" water (Figure 5-20). At time zero of the incubation, the P-treated Al hydroxides showed a gradual decrease in weight within the first 10 h of the TG analysis. The retardation of weight losses at time zero of the incubation may be attributed to the presence of micropores that strongly retained water molecules within their walls. This gradual weight loss (within 10 hours of TG analysis) disappeared for samples incubated for 3 months, showing that kinetically-driven water losses at elevated temperatures are irreversible; this water is probably associated with micropores. As already mentioned, the micropore volume and SSA were reduced after 3 months of incubation.

In our attempts to rehydrate the particles by exposing to open atmosphere, the 3-month incubated samples almost completely recovered the lost water (99 %) with little difficulty to re-gain the water molecules lost during the heating. If a significant amount of micropores were still present, then the water regain should have been much less than 99 % of the original weight. Time zero particles showed partial re-adsorption of water since water lost during heating at 70 C does not have the required activation energy.

Silica precipitation in micropores of silica gels under water-saturated conditions was speculated to be responsible for inhibiting TCE desorption from micropores, based on calculated desorption activation energies from TG plots (Farrell et al., 1999). TG analysis has also been used to study water thermodesorption from microporous activated carbons (Jaroniec et al., 1994). Weight-loss curves contained steps that were attributed to micropores, and broad curves due to the C micro structural heterogeneity.

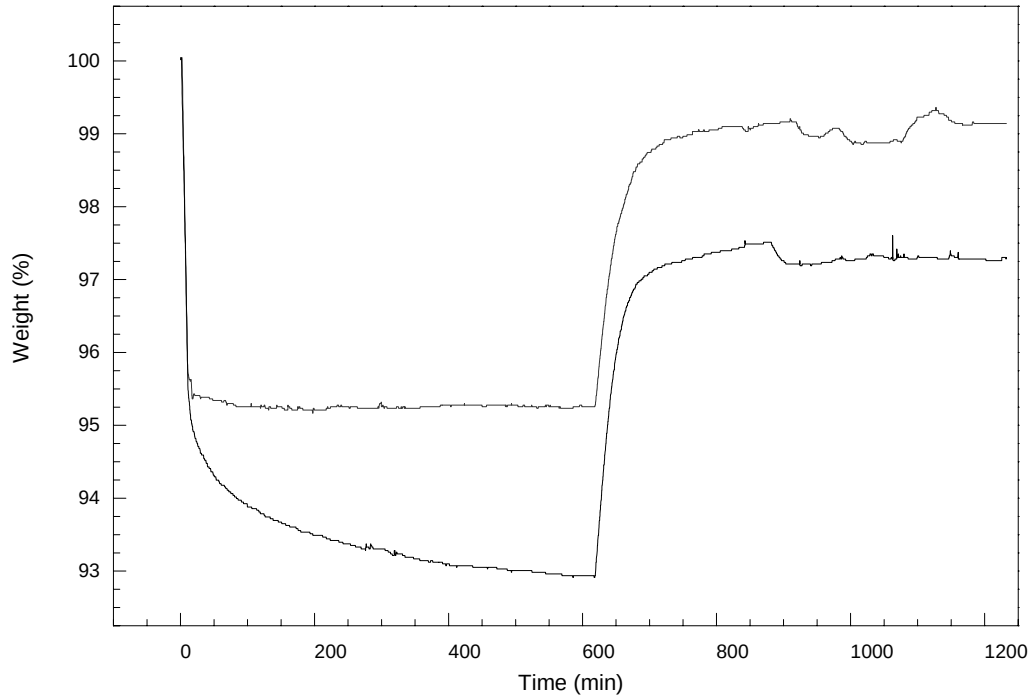

Figure 5-20. Typical TG isothermal (70 C) weight losses during a 600 min exposure for P-treated Al hydroxides at time zero (lower line) and after 3 months of incubation (upper line). After 600 min of heating at 70 C, samples were left open to ambient pressure and temperature for 600 min. Similar trend was observed for the untreated Al or Fe hydroxides.

TG analysis of the untreated and P-treated Al hydroxides showed significant reduction in isothermal weight losses of the P-treated Al compounds (Figure 5-21). We hypothesized that under water-saturated conditions, phosphate molecules preferentially access high-sorption energy sites that are characterized by high desorption activation energies. Thus, water desorption kinetics from these micropores should be very slow due to diffusional limitations impeded by micropore-bound phosphate molecules.

We also conducted isothermal (70 C) weight loss TG experiments for WTRs. Results showed that the Fe-WTR treated with P for 40 d had significantly ($p<0.05$) lower weight loss (6.4 vs. 7.2 %) at the 95 % confidence level, during the isothermal TG step at 70 C, for 10 h when compared with the untreated (no P) Fe-WTR.

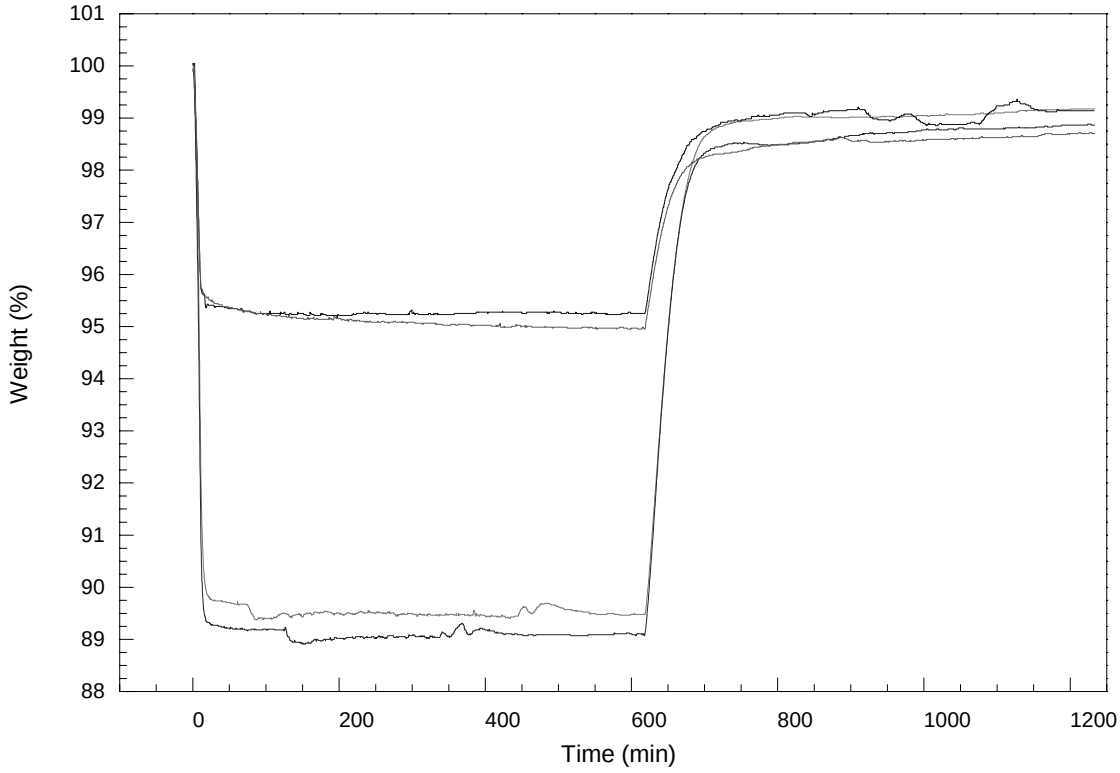

Figure 5-21. Typical TG isothermal (70 C) weight losses during a 600 min exposure for untreated and P-treated Al hydroxides after 3 months of incubation. After 10 h of heating at 70 C, samples were left open to ambient pressure and temperature for 600 min (10 h). The upper two lines are replicates (n=2) of the P-treated particles, and the two lines below are the replicated untreated particles.

The difference in % weight loss between the two samples could be ascribed to a stoichiometric displacement of water by phosphate, during its migration into the particle, and covalent bonding with structural inner-particle Fe sites.

The difference in water loss (%) was 0.8 % or 8,000 mg H_2O kg^{-1}. The amount of P sorbed by the Fe-WTR during a 40 d period was equal to 8,300 mg P kg^{-1}. The amount of P sorbed and water lost by the Fe-WTR particles correlated well (within experimental error), with a 1:2 P:H_2O stoichiometric exchange in the particle structure. The phosphate molecules that resided in micropores might have blocked the pore opening or limited the diffusion of water molecules. The significant increase in water desorption with increasing

temperature to 150 C (12.9 %) for both treated and untreated particles after 10 h of isothermal heating further indicates the diffusional nature of water desorption from pore openings that pose activation energy barriers. The association of phosphate molecules with micropores can only be indirectly inferred from TG data, but these data are consistent with other supporting evidence that micropores of the WTRs are responsible for the high P sorption and stability of sorbed P.

Discussion

A prerequisite for long-range order formation of minerals, such as pseudoboehmite which formed in this study, is dehydration / rearrangement of atoms towards a lower free energy state of equilibrium. Decreases in SSA may be concurrent or follow dehydration / rearrangement processes. Therefore, changes in SSA do not prove *de facto* formation of crystalline components, but may simply denote dehydration phenomena that evaporate water from sites that can be then accessed by N_2 molecules. That was the case for the amorphous Fe hydroxides, which did not develop long-range order components during incubation at 70 C, despite the decreased SSA values. Decreases in SSA of the untreated Fe hydroxides could have been the result of structural rearrangements and particle shrinkage due to dehydration. Oxalate -extractable Fe remained constant throughout the incubation period, paralleling the absence of sharp XRD peaks.

Temperature is an important parameter controlling the transformation of amorphous to crystalline solid phases. Hematite formation is optimum at temperatures >90 C, whereas goethite can be optimally synthesized at temperatures < 40 C (Schwertmann and Cornell, 1991). The temperature used in this study (70 C) seems to be outside the optimum range of hematite formation. Micropore volume and SSA analyses

of both Fe and Al untreated hydroxides showed increased microporosity that tended to decrease accordingly as SSA changed with incubation time.

Phosphorus coprecipitation with Fe or Al resulted in significantly altered the physicochemical properties of the formed gels. Lookman et al. (1997) reacted amorphous Al hydroxide with 3 mM P at room temperature to yield amorphous octahedral aluminum phosphate. Drying this material at 75 C induced the formation of an amorphous tetrahedral aluminium phosphate, but no crystalline phase was formed. After 1 night at 100 % relative humidity, 30 % of the tetrahedral Al was rearranged to its original octahedral coordination. Hsu (1982) found that aging of Al phosphate precipitates at room temperature for 5 years did not result in formation of variscite except under extreme conditions (of low pH, and high Al, /P concentrations). Van Riemsdijk et al. (1975) observed the formation of a crystalline Al-phosphate material (sterretite) from the reaction of low P concentrations and amorphous Al oxide.

Coprecipitation of P with metal salts should have resulted in homogeneous and even distribution of P throughout the particles. SSA analyses suggested that a significant amount of P was located in micropores, resulting in lower SSA values. The occupation or blocking of pores by phosphates probably hinders the movement of N_2 molecules within these pores, thus, lowering SSA values (Vansant, 1990).

An important implication of the data is that P is occluded into the metal hydroxide structure. Oxalate (5 mM) extractions showed that lower P extractability was not the result of increased crystallinity. Increasing bonding strength between Al and Fe with phosphate molecules may have occurred as evaporated water decreased distances between P and metal atoms, creating new and stronger bonds. Ford et al. (1997) found

that goethite was the predominant crystalline Fe phase when ferrihydrite-Mn or Ni coprecipitates were aged at 70 C and pH 6 for 17 d. Following the transformation, Mn and Ni were incorporated into the goethite's structure, but Pb and Cd were not.

Oxalate (5 mM) extraction unlikely the 200 mM treatment leaves most of the micropores intact. Oxalate (5 mM) Al of P-treated particles was very low, contrary to the 200 mM oxalate treatment, implying greater bonding strength of surficial Al and P. Kandori et al. (1992) coprecipitated phosphate with Fe to form goethites of different P concentrations (up to 2 % molar PO_4 / Fe ratio) and monitored weight losses of samples heated between 100 and 300 C as a function of added PO_4. Drastic decreases in weight loss with added PO_4 were observed. At the same time, SSA of the goethite was increased as PO_4 was added to the system. The increase in SSA was attributed to the formation of micropores during the coprecipitation process. However, we observed the opposite; P blocked micropores, apparently reducing the access of these pores by N_2 gas molecules. Also, our system used a higher P load (1:1 P / metal molar ratio) and lower temperature (70 C) than what Kandori et al. (1992) used.

Coprecipitation of P with Fe to form synthetic hematites resulted in partial occupation of micropores of the synthetic hematite (Galvez et al., 1999), but SSA changes were not monitored. The SF model was applied to P-treated Al hydroxides to monitor changes in micropore volume. The average size of micropores found in P-treated samples was the same as with the untreated samples in the present study. However, the micropore volume of P-treated samples was significantly lower than the untreated samples at all incubation times.

It appears that phosphate molecules occupy a significant portion of micropores in the synthesized amorphous Al and Fe hydroxides. Lower micropore volume of the P-treated samples reflected their lower SSA, as compared with untreated SSA values. Incubation of the metal hydroxides at 70 C resulted in significant changes in physicochemical properties that influenced sorbed P stability, and these changes may be used as an interpreting guide for the similar experiments with WTRs.

Heat Incubation of WTRs

Iron and Al hydroxides heat incubation experiments were used to facilitate interpretation of incubation data obtained from WTRs and soils amended with WTRs. WTRs are primarily amorphous masses of Fe or Al or Ca hydroxides with a variable amount of organic C. Similarities in chemical composition between the synthetic gels and WTRs might help us explain trends and transformations observed in lab incubations of the complex WTRs.

Incubations were performed for three Al-WTRs (Holland, Bradenton and Lowell) and three Fe-WTRs (Tampa, Panama, Cocoa). Results were similar, thus, only data for the Holland Al-WTR material are presented here. The Holland material was selected for explanation purposes because it was the least complex of all materials (least total C content and least oxalate extractable Al levels) and showed the clearest trends. This material was also included in a long-term field experiment to test the longevity of WTR effectiveness in reducing soluble P levels in two soils in MI (see chapter 4).

Incubation of the Al-Holland WTR, Holland, MI for 2 years at 70 C did not reduce oxalate (200 mM) extractable P levels with time (Figure 5-22), either with- or without P added to the WTR (initial load of 10,000 mg P kg^{-1}). There was no temperature effect since there was no difference in oxalate P or Al values either at 70 or 46 or 23 C. This

trend was also observed also with the other five WTRs incubated WTRs, but (data are not shown). The slight increase in oxalate-200 mM concentrations (<10 %), however, in the P-treated WTR samples was deemed to have no significance due to the insensitivity of the extracting solution (oxalate-P similar to total P). Oxalate (200 mM) treatment extracted almost all (> 90 % of previously sorbed P) of P added (and sorbed) to WTRs before incubation. Similarly, there was no incubation time effect on 200 mM oxalate-extractable Al in either P-treated or untreated WTR samples (Figure 5-23).

Oxalate-extractable Al was within 10 % of total Al in the P-treated WTR samples, suggesting the formation of a short- range order of P-treated WTR particles. However, elevated incubation temperature (46 or 70 C) significantly decreased oxalate-extractable Al (compared with the 23 C data) in the control (no added P) WTR particles (Figure 5-23). The data suggest a heat-induced structural rearrangement of the particles to more crystalline forms, but changes towards more crystalline structure could not be confirmed via XRD.

Phosphorus loading, significantly ($p<0.001, \alpha=0.05$) increased oxalate-extractable Al (~40,000 mg kg^{-1}, Figure 5-23) compared with the untreated (no P added; 30,000 mg kg^{-1}) WTR. Total Al values increased from 36,000 mg kg^{-1} in the untreated WTR to 41,000 mg kg^{-1} in the P-treated WTR (data not shown). We hypothesize that phosphate sorption improved digestion efficiency of the 3050B method used. Total recoverable Al in an NIST sample increased using USEPA method 3051, when compared with the 3050 method (Chen and Ma, 1998).

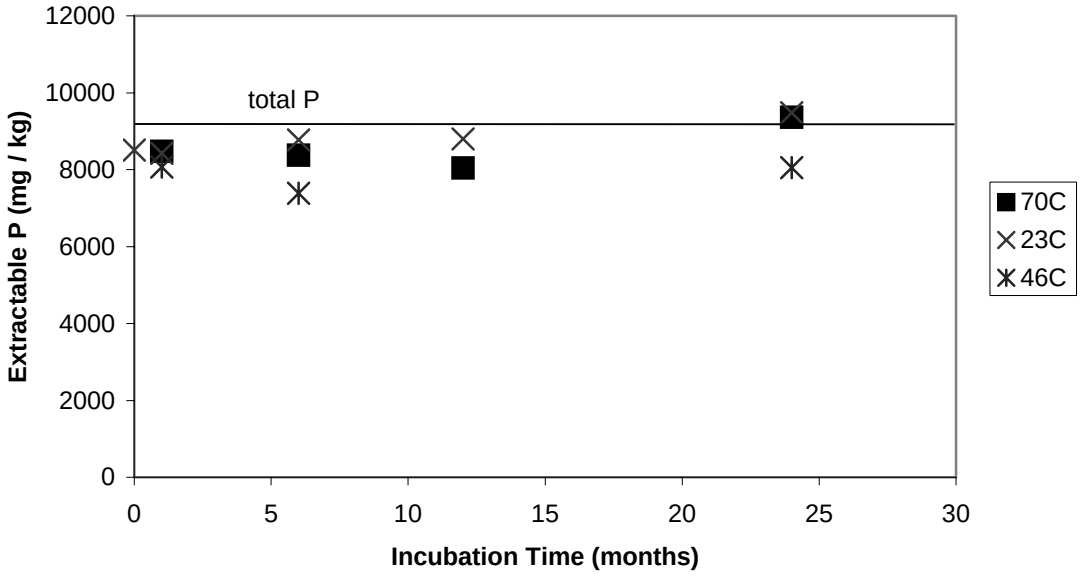

Figure 5-22. Changes in mean (n = 2) oxalate (200 mM)-extractable P concentrations with incubation time and temperature of the P-loaded Al-WTR particles. The point at the origin represents data collected before the P-loaded WTR was incubated. The control (no P) WTR particles showed no changes, and are not shown.

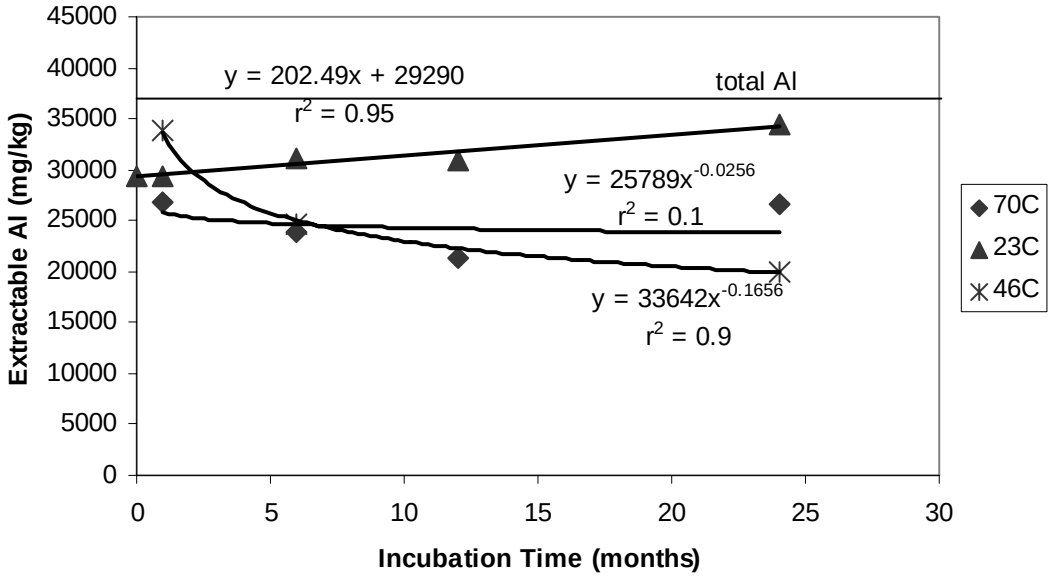

Figure 5-23. Changes in mean (n = 2) oxalate (200 mM)-extractable Al concentrations with incubation time and temperature of the control (no P added) Al-WTR.

P sorption may have opened up the WTR structure, facilitating acid penetration to more recalcitrant sites within the WTR. Oxalate-extractable Al was within 10 % of total Al in the P-treated WTR samples, suggesting short-range-ordered P association with WTR particles, and there was no evidence of an Al-P crystalline mineral phase, using XRD particles. The point at the origin represents data collected before the WTR incubated.

Galvez et al. (1999a) showed that at P / Fe atomic ratios less than 3 %, crystallization of ferrihydrite proceeded normally, whereas at ratios greater than 3 % phosphate inhibited the iron hydr(oxide) crystallization, forming amorphous Fe-P conglomerates. The high P load of the P-loaded WTR (total P/Al ratio = 22 %) in conjunction with its chemically heterogeneous nature of the WTR may have facilitated an amorphous, open Al-WTR structure, making the particles less resistant to 200 mM oxalate dissolution, and poisoning particle crystallization. Oxalate (200 mM) extractable P and Al trends were parallel through the incubation time. P addition seemed to result in distorting WTR particles' internal structure to accommodate the phosphate molecules.

Particle surface transformations due to temperature or sorbate additions would be difficult to detect using a high concentration of oxalate (200 mM), so we also used a lower (5 mM) concentration. The 5 mM oxalate treatment extracted significantly ($p<0.005$) less P and Al than the 200mM treatment. For the P-treated WTR, 5 mM oxalate-extractable P significantly ($p<0.005$) decreased at the end of the 70 C incubation (2 years), at 70 C (Figure 5-24), in contrast to the 200 mM oxalate P data. Decreased oxalate P levels with temperature was observed for all the other WTRs, except the Lowell

Al-WTR. This material had very little oxalate (5 mM) -extractable P levels (< 90 mg kg^{-1}), which may be the reason for the unclear trend.

Decreased P extractability with time at 70 C may be attributed either to intraparticle P diffusion, or external surface transformations towards a long-order range structure. However, XRD analysis suggested no formation of an Al-P mineral crystalline phase. Untreated WTR had oxalate (5 mM) -extractable P levels close to the instrument's detection limit (0.3 mg P / L). Phosphorus indigenous to the WTR (no P added treatment) was incorporated in the internal WTR structure, therefore, most was not accessible to a weak extractant (like 5 mM oxalate). Oxalate (5 mM) extractable Al was reduced after 1 year of incubation at 70 C, whether or not the WTR was treated with P (Figure 5-25). By the end of the 2-year incubation period, oxalate (5 mM) Al levels were similar to that at time zero.

Contrary to the 200 mM-Al data, the magnitude of oxalate (5 mM) -extractable Al of the treated WTR was significantly ($p<0.001$) less than the untreated WTR. This behavior did not seem to be simply a pH effect during the P sorption equilibration period (40 d) since the pH values of the suspensions with (7.44) and without P added (7.45) were similar. We hypothesized that the reduction in oxalate (5 mM) Al with P added compared with the untreated 5 mM oxalate Al was due to potential P migration towards the interior of the particles. P intraparticle diffusion permitted surficial Al atoms to rearrange themselves and attain equilibrium Al-O bond distances similar to the untreated WTR. No incubation time effect on 5 mM oxalate-Al for both P-treated and untreated WTR samples was found.

Incubation data for the Al-WTR suggested that sorbed P would not be released over time (2 years of incubation). These data corroborate information from the actual field soil samples taken 5.5 years after WTR application, which also suggest little P release from WTR amended fields.

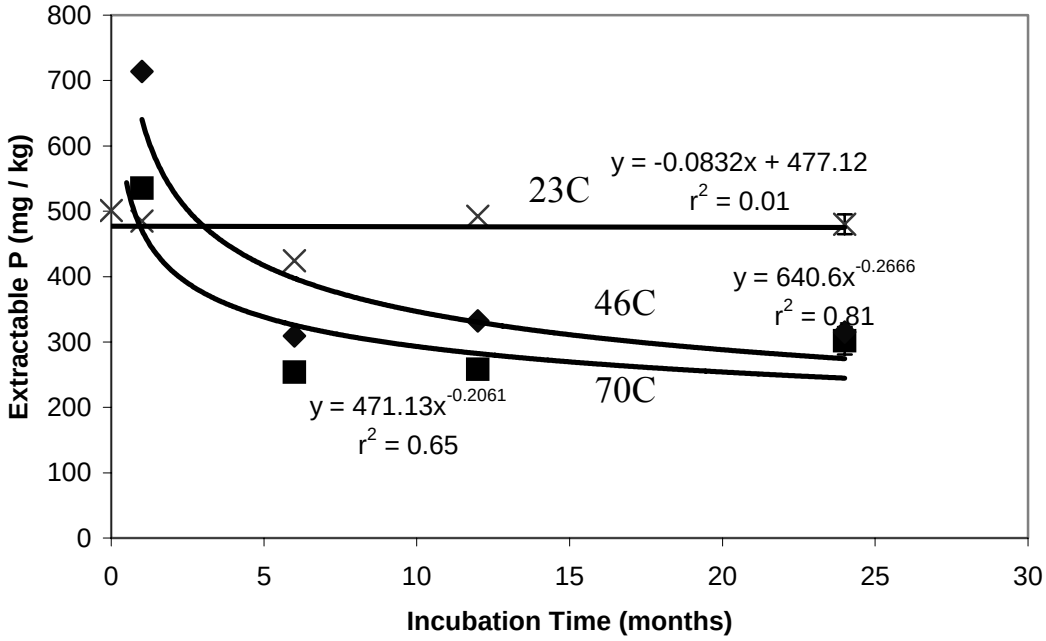

Figure 5-24. Changes in mean (n =2) oxalate (5 mM)-extractable P concentrations with incubation time at 23, 46 and 70 C of the P-treated Al-WTR. The point at the origin represents data collected before the P-loaded WTR was incubated. The untreated WTR had negligible (<0.3 mg P/L) oxalate 5 mM extractable P levels.

Heat Incubations of Soils Amended with WTRs

Heat Incubations of the MI Soils

Soil samples from both MI sites were incubated at 23, 46 and 70 C for 2 years. Oxalate extractions showed that there was no effect of either incubation time or temperature on P and Al extractability in both unamended and WTR-amended plots at both sites (Figures 5-26, and 5-27). Oxalate-extractable P and Al of WTR-treated and

untreated plots at both sites showed little change in concentration with time, even after 2 years of incubation at 70 C.

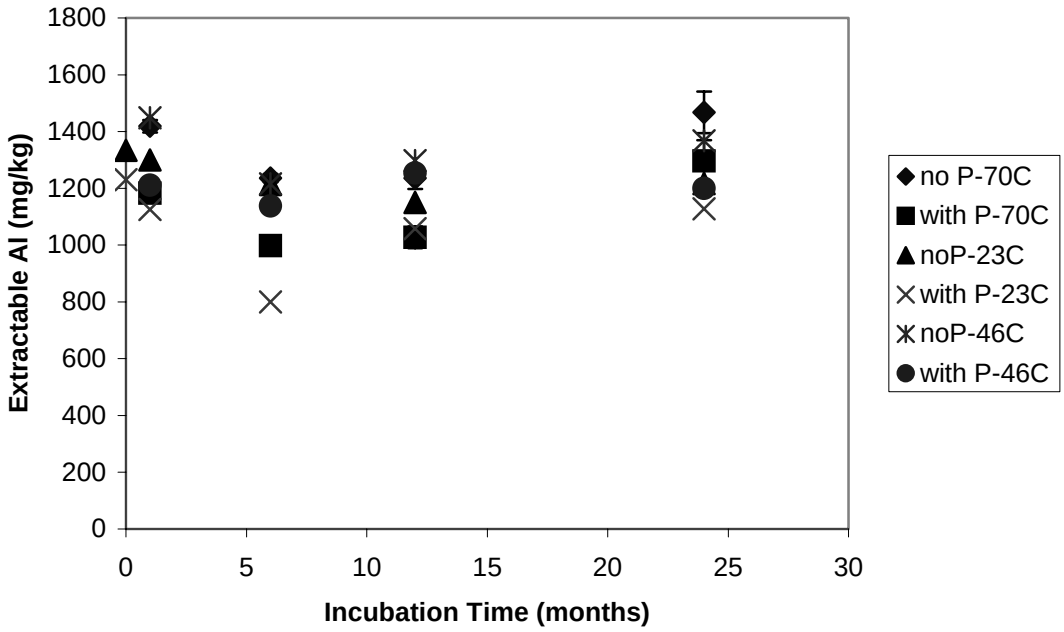

Figure 5-25. Changes in mean (n =2) oxalate (5 mM)-extractable Al concentrations with incubation time at 23, 46 and 70 C of the P-treated and untreated Al-WTR.

Similarly, 5 mM oxalate P and Al data were not influenced by changes in temperature or incubation time (data not shown);. WTR treatment also had no effect either. The WTR that was applied to both sites was also included in the incubations. It was shown above that the Holland Al-WTR exhibited a decrease in 5 mM oxalate P concentrations with incubation time and temperature. The fact that we were not able to detect the above effect on the incubated soil samples remains unclear. It is suggested that the degree of complexity of the soil matrix was masking any structural changes that may have occurred in the WTR that was mixed with soil

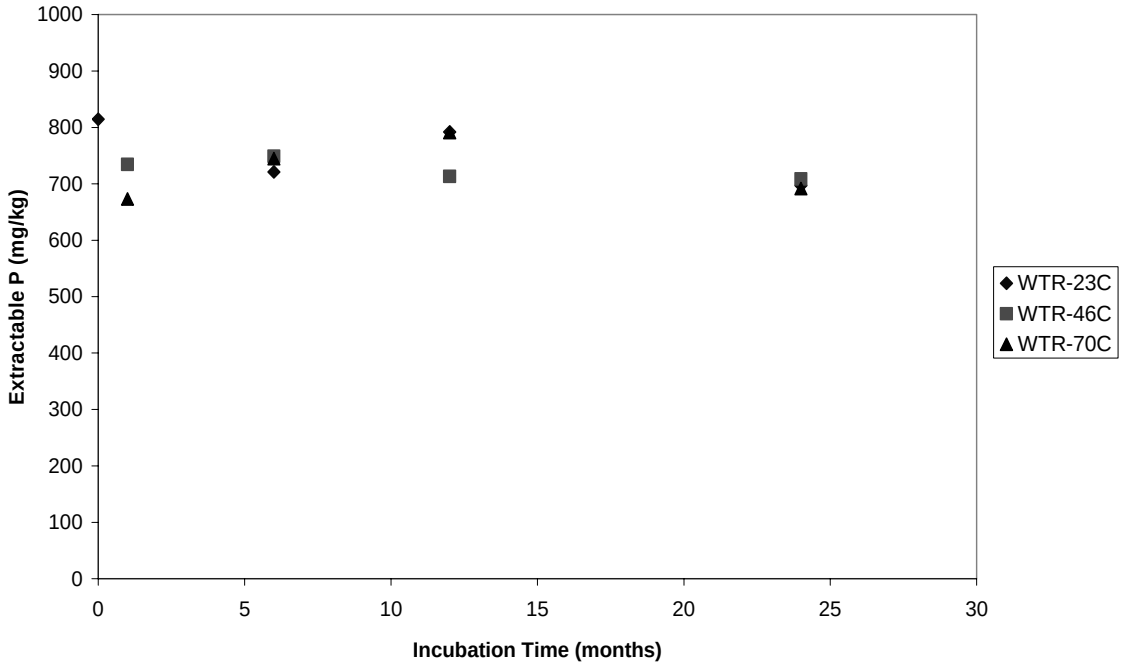

Figure 5-26. Changes in oxalate (200 mM)-extractable P concentrations with incubation time at 23, 46 and 70 C of the WTR-treated soils from site 1 in MI. Site 2 soils exhibited similar behavior.

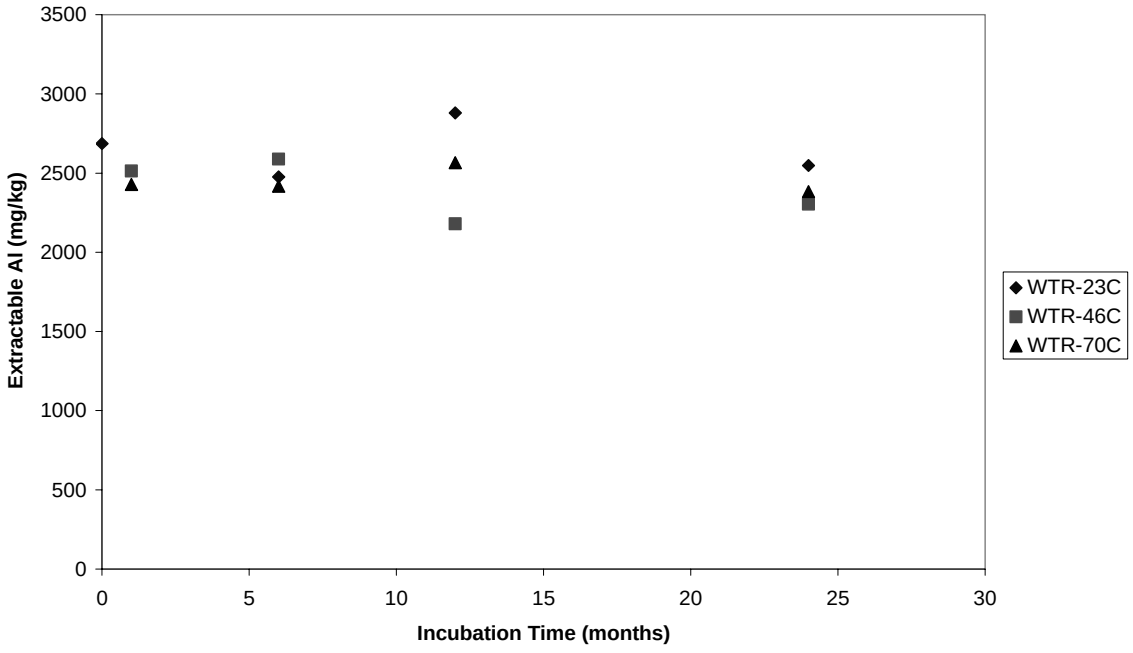

Figure 5-27. Changes in oxalate (200 mM)-extractable Al concentrations with incubation time at 23, 46 and 70 C of the WTR-treated plots of soil from site 1 in MI. Site 2 soil exhibited similar behavior.

The absence of adequate bulk water should not have impeded structural transformations since solid state diffusion processes in micropores has been suggested to occur even in air dry soil samples (Bramley et al., 1992). The common practice of storing soil samples at room temperature will not preserve the soil P status (Bramley et al., 1992).

The WTR incubation data suggested that decreases in 5 mM oxalate P concentrations were the result of diffusion of P molecules towards the particle interior. Ma and Uren (1997) showed that incubation of soil samples for 1 year at temperatures up to 40 C resulted in decreases in Zn extractability that were explained by diffusion -limited sorption of Zn.

Incubation Data for KR-Okeechobee Site

This data set differs from the MI data set in the age of soil samples. Soil samples from MI that were used in the incubations had already been in the field since 1998, whereas this data set involves soil samples that had been equilibrated with P solutions for 1 week. Obviously, soil and WTR particles from the MI site had reacted with P for a much longer time, thus, the P chemical environment should differ between the two sites.

Oxalate extractions were performed on soil samples collected at several time intervals during a 2-yr period. Oxalate-200 mM P concentrations from the untreated (no WTR) soil samples that had not been amended with TSP showed no changes with time or temperature (Figure 5-28). The high (100 mg P kg^{-1}) P treatment showed an interaction of time with temperature. At room temperature, oxalate-P levels did not change with time, but at 70 C there was a significant increase in oxalate-200 mM P levels during 2 yr of incubation. This increase in oxalate-P with time (at 70 C) occurred during the first 6 months of incubation, and stabilized thereafter.

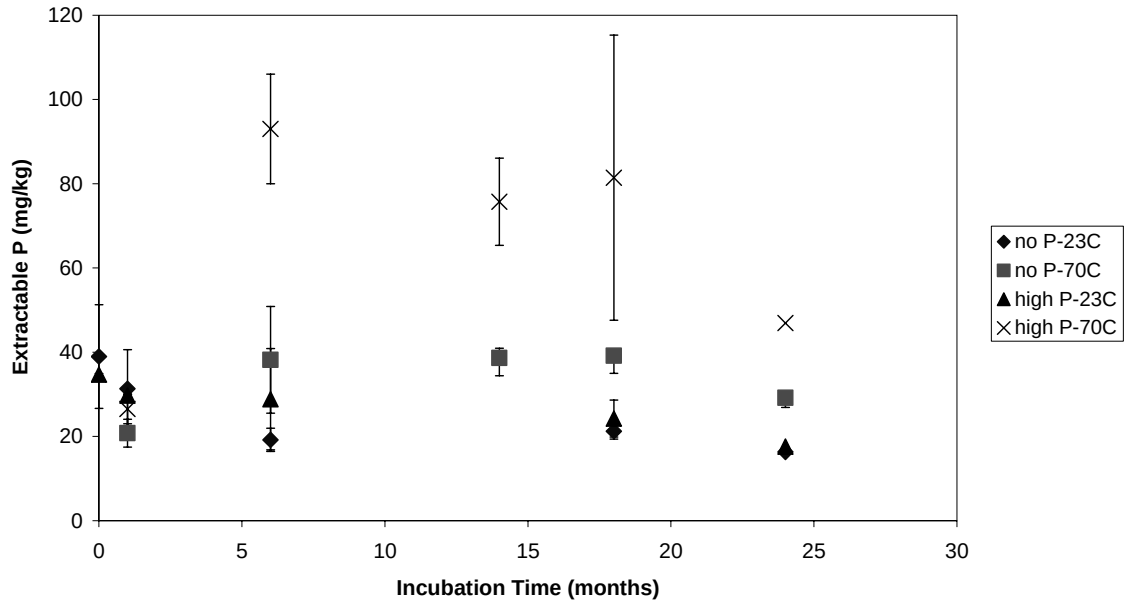

Figure 5-28. Changes in oxalate (200 mM)-extractable P concentrations with incubation time at 23 and 70 C for the untreated (no WTR) soils that either did or did not receive P.

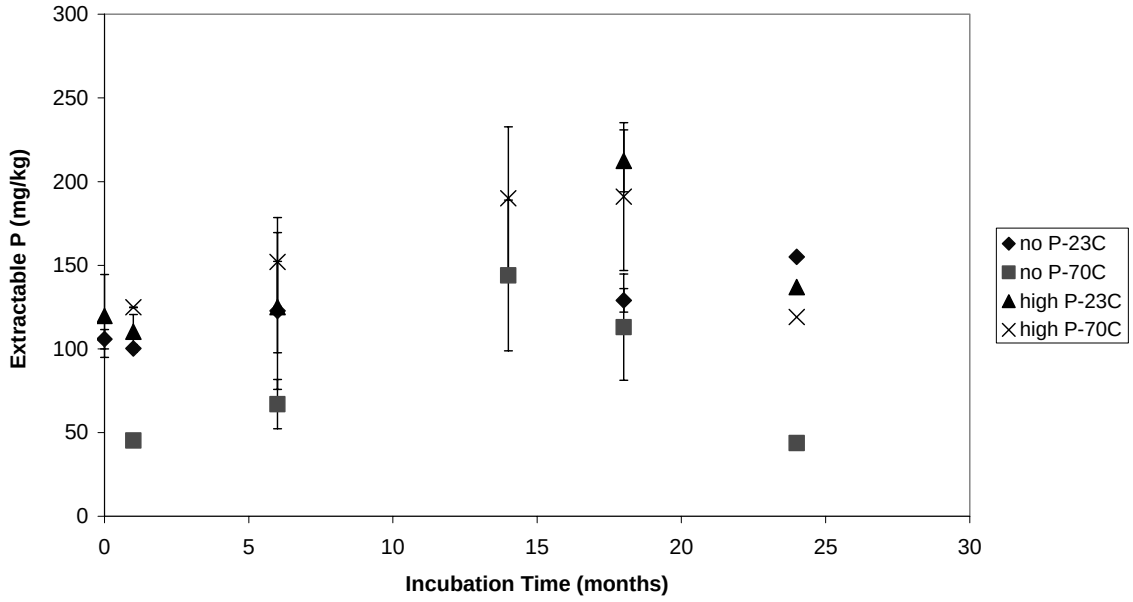

Figure 5-29. Changes in oxalate (200 mM)-extractable P concentrations with incubation time at 23 and 70 C for the WTR-treated soils that either did or did not receive P.

When WTR was applied to the soil samples, there was no significant difference in oxalate-200 mM P data between 23 and 70 C (Figure 5-29). It seems that WTR addition sorbed a significant amount of P added as TSP, and concurrently decreasing soluble P.

Incubation data for the metal hydroxides, WTRs and finally the WTR-amended soils showed that WTR addition to soils may provide significant reduction in soluble P levels that will remain immobilized in the long-term. Incubation at 46 and 70 C for 2 years did not show release of P from WTRs or WTR-amended soils. Data from the long-term field experiment in MI (chapter 4) showed that at least for 5.5 years WTR-bound P was not released to soil solution. It seems that sorbed P will remain indefinitely immobilized unless particle dissolution occurs. However, more incubation data and other chemical or spectroscopic methods are needed to directly quantify the long-term stability of sorbed P in WTR-amended soils.

CHAPTER 6
SUBSTITUTING ALUM WITH ALUMINIUM-BASED DRINKING WATER TREATMENT RESIDUALS TO REDUCE SOLUBLE PHOSPHORUS IN POULTRY LITTER.

Introduction

There is an increasing public demand to reduce phosphorus (P) transport to water bodies at risk of eutrophication from agricultural- P inputs, including land application of animal wastes. Animal wastes contain considerable amounts of P that have a great potential for surface runoff or leaching towards water bodies. Extensive efforts have been focused on finding ways to reduce soluble P in animal wastes. Techniques used to reduce soluble P are divided into three main categories: physical (electrodialysis, reverse osmosis), biological, and (most commonly) chemical methods.

A conventional chemical method to reduce soluble P in animal wastes is the application of a chemical coagulant, like alum (aluminum sulfate) (Moore et al., 1996). Dou et al. (2003) added alum to moist poultry litter (10- to 25 % by weight of litter) and found that P in water extracts was reduced from 80 to 99 % compared with the non-amended control. Sims and Luka-McCafferty (2002) applied alum to 97 poultry houses in a 16-month period. Alum additions decreased litter water-soluble P levels and pH. Lefcourt and Meisinger (2001) added alum and zeolites to dairy slurry waste at rates of 0.4- to 6.25 % by weight. Alum and zeolites reduced soluble P by 90 % and more than 50 %, respectively.

Alum has also been applied to soils high in P, such as those heavily amended with poultry litter. Shreve et al. (1995) observed that adding alum (10- to 20 % by weight) to

soils that had received long-term application of poultry litter resulted in reduced soluble P in runoff, and increased crop yields. Tall fescue grass plots amended with alum-treated (10 % by weight of litter) poultry litter for a period of 3 years showed no differences in soil water-soluble P and Mehlich III-P values when compared with a non-amended control (Self-Davis et al., 1998). However, water-soluble P in the non-treated (no alum) poultry litter plots increased each year (Self-Davis et al., 1998). Alum has also been applied to wetlands to reduce P release from sediments. Alum additions (1.2 % alum) minimized P release from a constructed wetland (Ann et al., 2000).

The established effectiveness of alum in reducing soluble P levels is accompanied by a significant economic cost. A typical broiler house needs 1.8 tonnes of alum per growing season, or 0.1 kg / bird (Moore et al., 1998). Assuming a value of $ 2.6 / kg alum, then ~ $ 4,700 is needed to apply the optimum rate of alum. Not included in the economic analysis, is the cost involved with use of lime, or sodium aluminate that is occasionally applied to bring the pH of the alum solution close to neutral levels.

Drinking water treatment residuals (WTRs) are the by-products of the drinking water purification process in treatment plants. They are a potential alternative to alum as a P mitigating amendment. WTRs are usually disposed of in valuable landfills space, but can be obtained at minimal or no cost from water treatment plants. WTRs are amorphous masses of Al or Fe hydr(oxides) that originate from flocculant additions made during the drinking water purification.

Free-of-charge WTRs are rich in Al, suggesting that they could have an effect similar to alum effect in reducing poultry litter soluble P levels. Research has shown that the high amount of amorphous Fe or Al hydr(oxides) in the WTRs make them efficient P

sorbents (O'Connor and Elliott, 2000). Use of WTRs is an emerging practice to reduce soluble P in systems high in P (O'Connor and Elliott, 2000).

Research has been conducted to evaluate the effectiveness of WTRs as amendments applied to soils high in P as a means of reducing P losses via runoff (Peters and Basta, 1996; Haustein et al., 2000), or leaching (Elliott et al., 2002; O'Connor et al., 2002). Codling et al. (2000) incubated (20 % moisture content, room temperature) poultry litter and litter-amended soils with a Fe-WTR (20 % Fe by weight) for 7 weeks and found that water-soluble P was reduced with time as WTR application rate increased. Dayton et al. (2003) suggested that oxalate extractable Al, and the Langmuir P sorbing maxima of WTRs were the key parameters that explained the significant reduction in runoff-P from WTR-amended soils treated with poultry litter. O'Connor et al. (2002) fertilized a low P sorbing Immokalee soil with 100 mg total P kg^{-1} and incorporated an Al-WTR at various rates of poultry litter. At WTR rates greater than 1 % (dry weight), soluble P levels were significantly reduced over the non-amended control (no WTR).

Alum has been widely used in drinking water and wastewater treatment facilities to promote contaminant, color, and particulates removal. Synthetic organic macromolecules like surfactants and polymers are used in conjunction with alum to promote flocculation and settling of particles in water treatment plants (Hiemenz and Rajagopalan, 1997; Ozacar and Sengil, 2003). The combined use of alum and polyelectrolytes may significantly reduce the cost of drinking water purification. Polymer usage is cost-effective in reducing the alum dosages needed to achieve minimum turbidity levels, thus, making the alum-only process much more expensive (Ozacar and Sengil, 2003).

The combined use of alum and Al-WTRs may be a cost-effective practice to reduce soluble P in manures or slurries when compared with alum-only use, since the WTRs can be cost-free. Complete substitution of Al-WTRs for alum could be practiced in cases of all year -around, abundant WTR availability. In the cases of limited WTR availability, which seems the most probable scenario, a combination of alum / Al-WTR could be used. However, the potential synergistic/antagonistic effects of combining alum with Al-WTRs on the amounts of reduced soluble P are unknown. Preliminary work has shown that WTR particles retain their integrity and do not dissolve except possibly under most conditions, unless they encounter very acidic conditions. The potential detrimental effect of soluble Al concentration on plants can be minimized by using Al-WTRs, since the residual Al concentration in WTR suspensions could be less than 1 mg Al L^{-1} (O'Connor et al., 2002). To the best of our knowledge, no work has been conducted on the combined use of Al-WTRs and alum as a means to reduce soluble P levels in poultry litter.

Also, the mechanism of P removal by WTRs from poultry manure suspensions remains unknown. The multi-component chemical composition of poultry manure poses serious limitations to characterizion of these systems, even with advanced spectroscopic techniques. X-ray absorption near edge structure spectroscopy (XANES) application to alum-treated poultry litter samples suggested that the soluble P removal mechanism was a precipitation of amorphous Al hydroxide followed by P adsorption on the Al hydroxide. No pure Al-P precipitate was found (Peak et al., 2002). However, their P solid phase reference database did not include any organo-Al-P spectra that could be compared with the sample spectra.

The role of dissolved organic carbon (DOC) in regulating P sorption remains unknown and complicated. Increased DOC in manure suspensions may bind to Al^{3+}, creating soluble metal-organic soluble complexes. Recent work with ^{31}P-NMR spectroscopy by Hunger et al. (2004) did not exclude the possibility of organo-Al-P association in alum-treated poultry litter. Hunger et al. (2004) mentioned that P chemical shifts are influenced by cations with which P is complexed to. Inorganic cation-P bonding shows pronounced, sharp chemical shifts, whereas chemical environments that contain organically-complexed cations will show a rather broad P chemical shift (Hunger et al., 2004).

The mechanism by which P is immobilized by WTRs differs from that of alum P fixation. Alum is soluble in water and P inactivation occurs via a co-precipitation Al-P mechanism. Drinking-WTR particles are insoluble in water, and thus, are rigid particles that may immobilize P in pores. Preliminary work in our laboratory has shown that intraparticle P diffusion in the porous Al-WTR structure was the main mechanism behind P sorption (chapter 7). Thus, mechanistic reasons prompted us to test the potential synergistic/antagonistic effects of combining alum with Al-WTR on reduction of soluble P in poultry litter.

It is necessary to determine the relative efficacy of WTR and alum in reducing soluble P in animal wastes if WTRs are to ultimately be used as a cost effective and environmentally friendly alternative to alum. No work has been conducted on the combined use or comparison between Al-WTRs and alum as means to reduce soluble P in poultry litter. The objectives of this study were: a) to compare alum versus Al-WTR effectiveness in maximizing soluble P reduction in poultry litter; and b) to evaluate

evidence for the formation of a mixed, amorphous organo-Al-P precipitate rather than a simple inorganic Al-P phase in alum / Al-WTR treated poultry litter.

Materials and Methods

Ten grams (dry weight) of composted poultry litter were immersed in a 0.01 M KCl solution and left to equilibrate for 1 day. Alum [$Al_2(SO_4)_3 \cdot 14H_2O$, A.C.S. grade, Fisher Scientific Inc. Fair Lawn, NJ] and an Al-WTR from the Bradenton, FL water treatment plant were added to litter suspensions in different weight-based ratios to give a total amendment concentration range of 0 to 25 % of dry litter weight. The Al-WTR was sampled directly from an evaporation pond, air-dried, and passed through a 2-mm sieve. The pH of a 0.01 M KCl solution of the litter and the WTR was measured after 20d reaction (1:10 solid: solution ratio).

Determination of percentage solids was performed by drying the materials at 105 C (Sparks, 1996). KCl-extractable P was measured at a ratio of 1: 10 in a 0.01 M KCl solution after 40 d. Total C and N were determined by combustion at 1010 C using a Carlo Erba NA-1500 CNS analyzer. The WTR and the litter were analyzed for total P, Fe, and Al by ICP following digestion according to the EPA Method 3050B (USEPA, 2000). Oxalate-extractable P, Fe, and Al of the amendments and the suspensions were determined by ICP after extraction at a 1: 60 solid: solution ratio, following the procedures of McKeague et al. (1971). Alum is a well-characterized chemical coagulant, and was not included in the initial characterization.

The calculated combined Al/P molar ratios of the suspensions were based on the oxalate-extractable P value of the litter, the total Al concentration of alum, and the oxalate -extractable Al value in the Al-WTR. Al / P molar ratios ranged from 0.34 to 1.32. Oxalate-extractable WTR-P was ignored since it was low (2.98 g kg^{-1}), and not

labile (data not shown), when compared with the litter oxalate-P. Use of oxalate P to determine molar ratios may be more valid than total, since total P, at least in animal wastes, does not reflects the material's P availability (Burns et al., 2001). Aluminium in alum was assumed to be 100 % extractable with oxalate. The high P sorbing capacity (at least 10 g P kg^{-1} WTR) of the Al-WTR was confirmed by constructing a P sorption isotherm (23 C) by incubating the Al-WTR with inorganic P solutions for 10 d.

Central composite design. A central composite design (Mason, 1989) was used to investigate the main effects and interactions of combining alum and an Al-WTR (Figure 6-1). WTR and /alum weight loads, and contact time were the three factors investigated. Five levels of each factor were used to encompass a range of alum concentrations used to reduce soluble P from poultry litter (Table 6-1). Synergistic or antagonistic effects of alum and the Al-WTR on soluble P levels in litter suspensions were evaluated in experimental units prepared using combinations of the two sorbents (Table 6-2). The central composite design has widely been used in the fields of statistics and engineering but, to our knowledge, has not been applied to agricultural type of experiments (Mason, 1989; Christmas et al., 2002). The major advantage of the central composite design is that multiple variables (3) at five different levels can be evaluated with a limited number of experiments (Christmas et al., 2002). The central composite design identifies the main and interaction effects of the variables, which are not obtained by analyzing one variable at a time. Twenty experimental units were used, consisting of combinations of the five levels for each factor. There were 14 single-run experimental units (dots) plus six

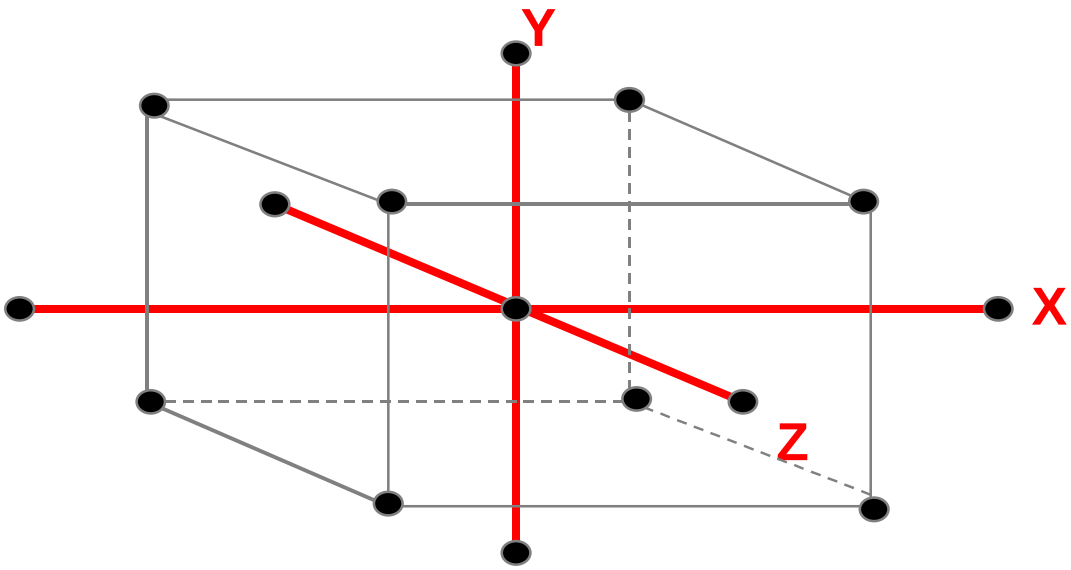

Figure 6-1. Three-dimensional geometric representation of the experimental runs (dots) used in the central composite design. The dot in the center of the cube represents the experimental run that corresponds with the mid-point level of each factor. X,Y,and Z axes represent the three tested factors.

Table 6-1. The five levels of each factor used in the central composite design, five levels each. The equation below is the quadratic polynomial used to describe the main and interactive effects of WTR, alum, and time on the amounts of reduced residual P in poultry litter.

Factors	Levels				
WTR (%)	0	5.1	12.5	20.0	25.5
Alum (%)	0	5.1	12.5	20.0	25.5
Time (days)	0.44	10.5	25.5	40	50

$$y = a_0 + WTR + alum + time + WTR^2 + alum^2 + time^2 + WTR*alum + WTR*time + alum*time.$$

replicated runs for the dot in the center of the cube (Figure 6-1). The design's limited number of runs prohibits the use of traditional statistical methods such as the separation of treatment means technique. The design did not include "control" (no alum, no WTR) samples that we had to run separately in order to include the "controls".

P sorption experiment. Alum with or without WTR, as well as WTR-only, were mixed with 10 grams (dry wt.) of poultry litter in a 1: 10 solid: solution ratio in 0.01 M KCl. Potential pH effects on the magnitude of soluble P in suspensions due to pH differences between alum and WTR solutions were minimized by maintaining the pH at 6.5. The pH of the suspensions was adjusted using micro-quantities of strong acid (HCl for WTR) or base (NaOH for alum). The suspensions were not shaken during the equilibration period that ranged from 0.4 to 50 d. Samples were not shaken to mimic field conditions. We also wanted to avoid WTR particle abrasion due to shaking that could artificially generate new surfaces. Suspensions were equilibrated from 0.4 to 50 d in an attempt to show the long-term P sorption capacity of the Al-WTR. After equilibration, the suspensions were centrifuged, passed through 0.45 μm filters, and analyzed by ICP for P, and Al. Total organic carbon (TOC) in filtered (0.22 μm) solutions was determined using a TOC analyzer.

After the completion of the sorption step, residual material was re-suspended in a 0.01 M KCl solution (1:10 solid: solution ratio) to monitor P desorption from the sorbents. The suspensions were left to react for 0.44 to 50 d, without shaking, or pH control. Following the equilibration period, the suspensions were centrifuged, filtered and analyzed for P, Al, and TOC, as described above.

Table 6-2. The central composite design structure with five levels of three factors, 5 levels each. The runs below represent the dots in Figure 6-1 above. There are 14 single-run dots on the cube in Figure 6-1 plus six replicated runs (total 20 runs) for the mid point in the center of the cube.

Run #	% WTR added	% Alum added	Time (d)
1	12.55	12.55	0.44
2	20	5.1	10.5
3	5.1	5.1	10.5
4	5.1	20	10.5
5	20	20	10.5
6	25.08	12.55	25.25
7	12.55	12.55	25.25
8	12.55	0	25.25
9	12.55	12.55	25.25
10	12.55	12.55	25.25
11	0	12.55	25.25
12	12.55	12.55	25.25
13	12.55	25.08	25.25
14	12.55	12.55	25.25
15	12.55	12.55	25.25
16	5.1	5.1	40
17	20	20	40
18	5.1	20	40
19	20	5.1	40
20	12.55	12.55	50

Results

The poultry litter and the Al-WTR were analyzed for selected chemical properties (Table 6-3). The pH of the materials ranged from 5.4 for the Al-WTR to 7.2 for the poultry litter. The poultry litter had 74 % solids, while the WTR was only 40.6 % solids since it was sampled directly from an evaporation pond. The litter C:N ratio (5.4) was less than average values (~ 10) reported by Sharpley and Moyer (2000). The Al-WTR had a C: N ratio of 27, reflecting the high organic carbon (OC) content of the material (16 %). This value was greater than the median OC value of 6.3% reported by Dayton et al. (2003) for 21 WTRs.

On a dry matter basis, the poultry litter had the greatest amount of total P, (44.9 g kg^{-1}) , which was significantly greater than the average (20 g P kg^{-1}) reported for poultry litter total P by Barnett (1994). The total P value of the WTR was 3.1 g kg^{-1}, slightly greater than another sample of the Al-WTR from Bradenton, FL (2.8 g kg^{-1}, O'Connor and Elliott, 2000). However, this total P value (3.1 g kg^{-1}) was much greater than the median value (1.3 g kg^{-1}) reported by Dayton et al (2003) for a host of WTRs. The poultry litter had little total Al and Fe (0.28 %) since Ca is usually the dominant element (Barnett, 1994). The WTR had 92 g kg^{-1} total Al, falling within the typical range of total Al values for Al-WTRs (50- to150 g kg^{-1}, ASCE, 1996).

X-ray diffraction (XRD) analysis confirmed the noncrystalline nature of the revealed a lack of Al mineral-related crystallinity in the WTR and litter (data not shown). Oxalate -extractable P, Fe, and Al are usually associated with the amorphous phase of the particles. Oxalate P was lower than total P since oxalate values represent the amorphous portion of this element. Poultry litter oxalate-P was 70 % of the total P, suggesting a high

degree of P lability. Oxalate Al plus Fe for the WTR was 96 % of the total Al +Fe, suggesting that WTR is a sink for P.

Table 6-3. Characterization of the poultry litter, and the Al-WTR (oven-dry basis).

Source	Form	pH	% Solids	% C	% N	Total (g kg $^{-1}$) P	Al	Fe	0.2 M Oxalate (g kg $^{-1}$)† P	Al	Fe
Georgia	poultry litter	7.2	74.4$^{@}$ ±1.2	25.8 ±0.8	4.8 ±0.02	44.9 ±2.5	2.4 ±0.3	0.4 ±0.04	31.6 ±1.9	0.5 ±0.08	0.28 ±0.03
Bradenton, FL	Al-WTR	5.4	40.6 ±1.6	16.2 ±0.8	0.6 ±0.02	3.1 ±0.7	92 ±5.4	6.2 ±0.1	2.98 ±0.02	91.1 ±1.3	5.2 ±0.3

$^{@}$ Mean of two samples ± standard deviation
† Solid: Solution 1:60
¶ Following method EPA 3050B digestion

Reduction in KCl-extractable P

In the absence of competing sorbent, either Al-WTR or alum exhibited similar abilities to reduce KCl-extractable P values in litter suspensions after 25 d (2755 and 3024 mg reduced P kg^{-1} litter, respectively). The calculated reduction in soluble P levels was based on the KCl-extractable P concentrations measured in litter-only, and in litter suspensions treated with alum and / or WTR, at different contact times, according to the following equation (Eq. 1):

Reduced P (mg kg^{-1}) = [litter-only P (mg L^{-1}) - litter+sorbents P (mg L^{-1})] * [volume suspension(L) / mass litter(kg)] Eq. [1]

The sorbent-free KCl-P values in the poultry litter fluctuated somewhat with time and appeared to reach equilibrium after 25 d (Figure 6-2). On average, the mean sorbent-free KCl-P in the litter suspensions was approximately 10 % of the initial total P levels in the litter (44,900 mg P kg^{-1}). This percentage of soluble P in sorbent-free poultry litter agrees with published values (Peak et al., 2002). The pH of the suspensions for all

treatments, after the completion of the sorption experiment, ranged from 6.3-6.7. This pH range may have facilitated Ca-P dissolution from litter and release of P into solution.

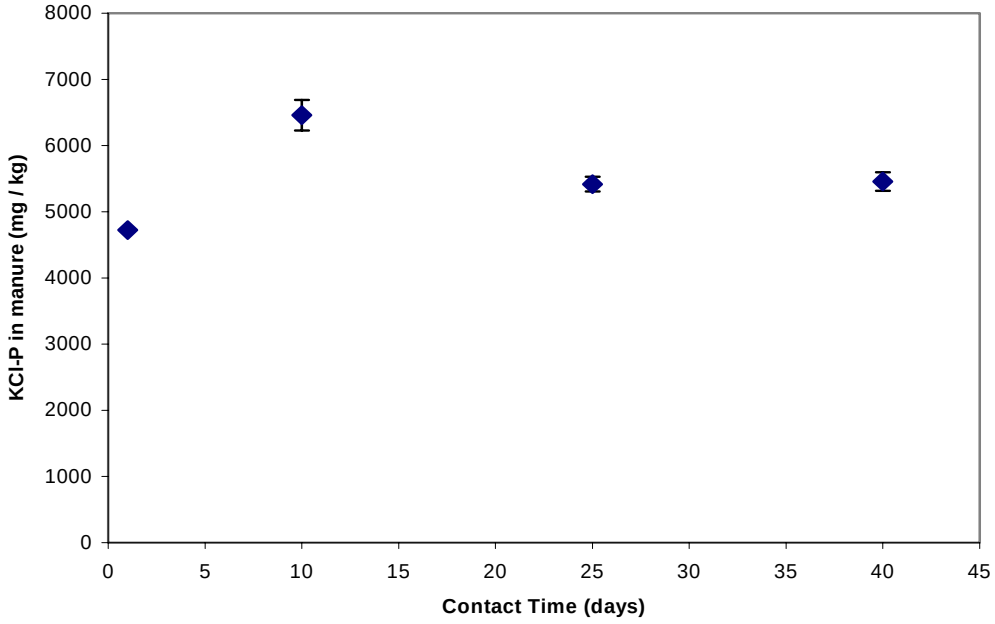

Figure 6-2. Kinetics of KCl-extractable P release in suspensions of poultry litter without alum or WTR in 0.01 M KCl background electrolyte. Data are the mean of two replicates and the error bars represent one standard deviation.

When the two sorbents were added in different weight-based ratios to poultry litter, different amounts of reduced P were observed (Table 6-4). Significant interaction with respect to reduced KCl-P levels ($p<0.02$) was found for alum and Al-WTR (Table 6-5). Three dimensional surface contour plot generated from results of the central composite design illustrated the interaction between alum and Al-WTR with respect to reduced KCl-P levels in litter, after 25.5 d (Figure 6-3). The plot from the model shows a linear response of reduced soluble P levels when combining the two sorbents.

Table 6-4. Reduced soluble P levels in alum/WTR treated poultry litter for all runs of the central composite design. The "control" experimental run, which corresponds with the litter-only suspension, is not included here.

Run #	WTR added %	Alum added %	Time (days)	Reduced KCl-P (mg kg-1litter)
1	12.55	12.55	0.44	3336
2	20	5.1	10.5	4359
3	5.1	5.1	10.5	2554
4	5.1	20	10.5	5769
5	20	20	10.5	5500
6	25.08	12.55	25.25	4693
7	12.55	12.55	25.25	4492
8	12.55	0	25.25	2755
9	12.55	12.55	25.25	4105
10	12.55	12.55	25.25	4721
11	0	12.55	25.25	3024
12	12.55	12.55	25.25	4480
13	12.55	25.0	25.25	5304
14	12.55	12.55	25.25	4798
15	12.55	12.55	25.25	4637
16	5.1	5.1	40	3220
17	20	20	40	5336
18	5.1	20	40	5212
19	20	5.1	40	4587
20	12.55	12.55	50	5032

The lowest sorbent combination (5:5 % WTR:alum, by weight), which is the common alum application rate (10 %; Moore et al., 1996), resulted in significant KCl-P reduction of 2,554 mg P kg^{-1} after 10 d and 3,220 mg P kg^{-1} after 40 d. This increase with time was not significant at the 95 % confidence level, and the magnitude was similar to the alum or WTR-only treatments. Greater sorbent load combinations (up to 25 % load) further reduced KCl-P in the litter/sorbents suspensions to nearly 100 % of the initial KCl-P values measured in the untreated (sorbent-free) litter suspensions.

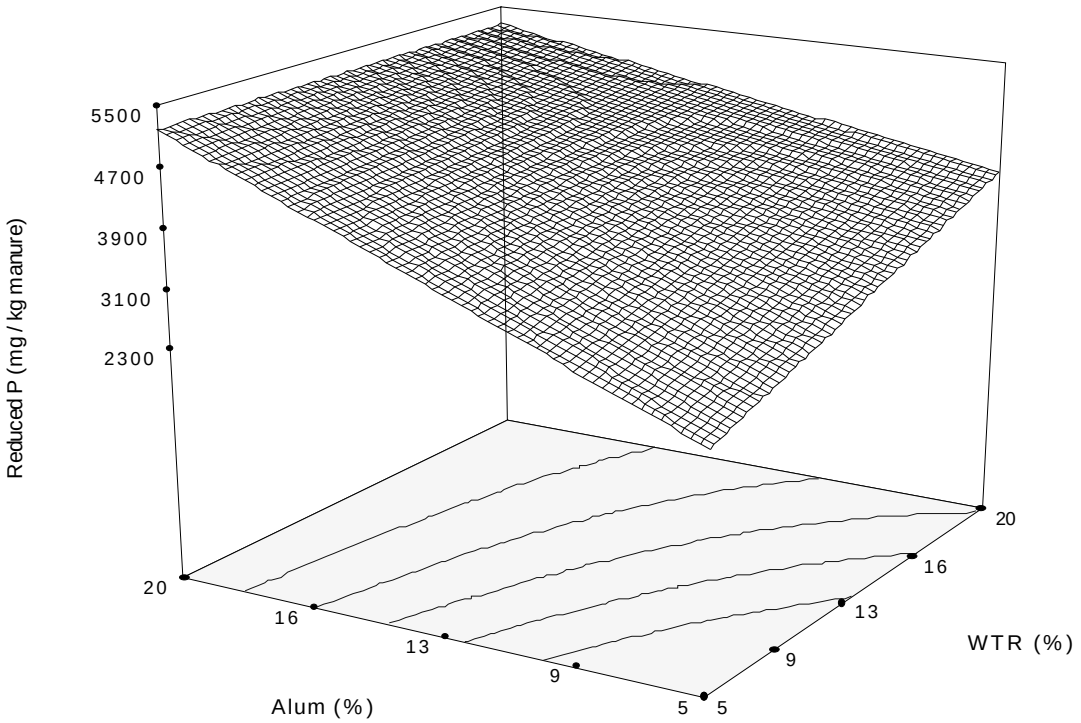

Figure 6-3. Three-dimensional surface contour plot of the WTR and alum effects on reducing soluble P in poultry litter suspensions, at a specific contact time (after 25.5 d).

Based on the ANOVA of the central composite design (Table 6-5), the main effects of WTR and alum, but not contact time, were significant ($p<0.005$). Alum x time, or WTR x time interactions were not significant at the 95 % confidence level. The absence of slow P sorption kinetics is understandable for the alum salt, as all the alum-Al would be expected to immediately react with P in solution. P sorption kinetics for the Al-WTR were fast (no effect of time) because the amount of soluble P present was not large enough to access high sorption energy sites.

A P sorption kinetics experiment using only the Al-WTR (no poultry litter present) showed that 75 % of the initial soluble P load (10,000 mg kg^{-1}) was removed from solution within 1 d, and essentially no P remained in solution after 10 d (data not shown).

However, the litter suspensions had a significant amount of DOC that was not present in the Al-WTR sorption kinetics experiment. Data in the literature suggest that the effectiveness of alum to reduce P in wastewater suspensions depends on the percentage organic C, and the P forms that might be present (Omoike and vanLoon, 1999). Despite possible complications presented due to DOC, alum and the Al-WTR exhibited similar soluble P reducing capacities in poultry litter suspensions.

Table 6-5. Analysis of variance table of the central composite design. A linear equation used to fit the P sorption experimental data.

Source	Sum of Squares	DF	Mean Square	F Value	Prob > F
Model	1.34E+007	3	4.45E+006	20.05	< 0.0001
WTR	2.49E+006	1	2.49E+006	11.23	0.0041
Alum	9.49E+006	1	9.48E+006	42.73	< 0.0001
WTRxAlum	1.37E+006	1	1.37E+006	6.20	0.0242
Residual	3.55E+006	16	2.22E+005		
Pure Error	3.08E+005	5	61,640		
Cor Total	1.69E+007	19			

Std. Dev.	471	R-Squared	0.79
Mean	4390	Adj R-Squared	0.75
C.V.	10.7	Pred R-Squared	0.69

Reduced KCl-P (mg kg^{-1} litter) = 1095+151xWTR (%) + 205*Alum (%) -7xWTRxAlum

A positive quadratic correlation ($r^2 = 0.75$) between the reduced KCl-P levels in suspension and oxalate-extractable Al/P molar ratios was observed for all experimental runs (Figure 6-4). The increasing trend in reduced soluble P concentration appeared to reach a plateau at molar ratios close to 1, which theoretically suggests precipitation as a 1:1 P:Al solid phase. Al / P molar ratios close to 1 coincided with 100 % reduction of KCl-P levels in treated litter suspensions. A several fold excess of Al is usually added to ensure P removal in wastewater treatment plants (Galarneau and Gehr, 1997). Significant reduction in KCl-P levels occurred with Al/P molar ratios close or less than one1,

indicating that avoiding use of excess Al (>1:1 Al:P molar ratio) would be a cost-efficient practice to reduce soluble P in animal wastes.

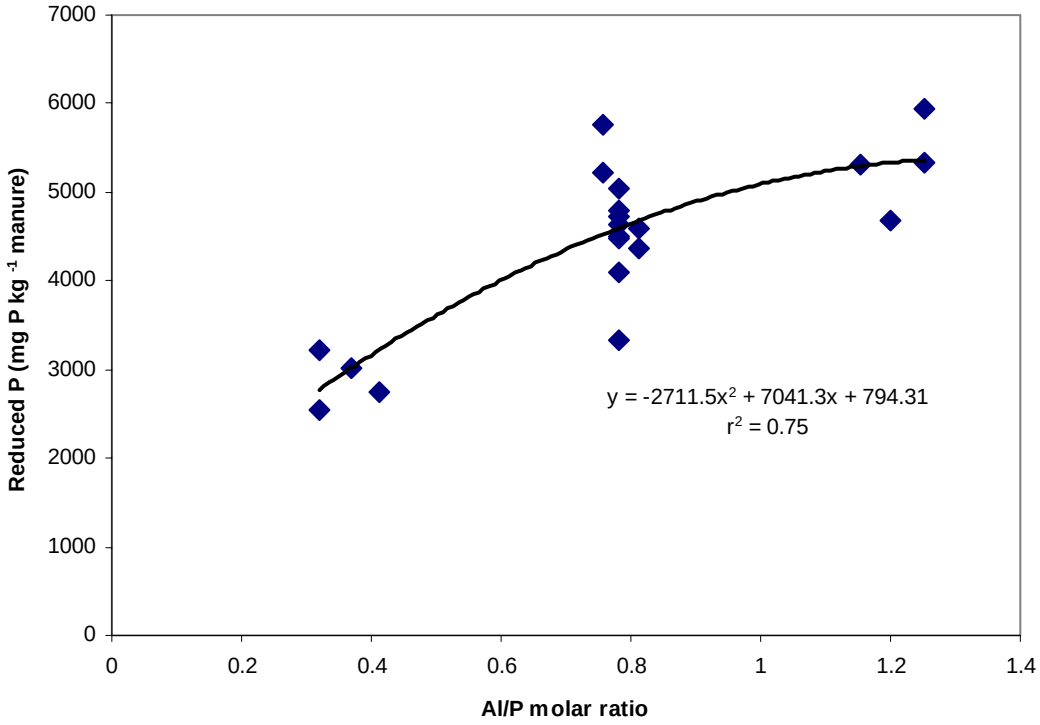

Figure 6-4. Relationship between reduced soluble P in litter suspensions and the oxalate-extractable Al/P molar ratios in all experimental runs of the central composite design.

Aluminium concentrations in solution were also monitored during the P sorption experiment. We assumed that aluminum concentrations would primarily originate from alum and the Al-WTR, with much less from the poultry litter (Table 6-3). Sorbent-free KCl-Al values in the poultry litter increased with time and seemed to reach equilibrium after 25 d of reaction (117 mg Al kg^{-1} litter, data not shown). The WTR particles have limited solubility at circumneutral pH (Elliott et al. 2002), and are expected to contribute even less Al in solution than what litter would supply on its own

A negative linear correlation ($r^2 = 0.46$) was observed between the amount of Al in solution and the amount of reduced KCl-P in all runs (Figure 6-5). After 25 d, either alum- or WTR-only, mixed with the poultry litter, had Al residual concentrations of 5,366 and 99 mg Al kg^{-1} sorbent, respectively. The WTR-only treated litter desorbed little Al (99 mg Al kg^{-1}), suggesting that WTR particles are relatively insoluble with little potential of Al desorbability. Based on thermodynamic considerations at pH of 6.8, minimum Al^{3+} would be present in solution. However, alum-only treated litter suspension at pH 6.8 had the greatest soluble Al concentration of all experimental runs, suggesting that soluble Al was likely organically complexed, and not "free" Al^{3+} in solution. Increased total organic C levels in solution might have complexed Al^{3+}, thus, increasing the concentration of soluble organo-Al complexes. Potential Al toxicity to plants and humans has well been documented in the literature (Barcelo et al., 1996; Desroches et al., 2000). Desroches et al. (2000) found that free or organically-complexed Al in biological fluids was well correlated with prevalence of Alzheimer's disease.

Total organic C (TOC) was measured in supernatants of the suspensions after the completing of the P sorption experiment. It was assumed that TOC was mostly dissolved organic C since the centrifuged supernatants had passed through 0.22 μm filters. There was a negative linear correlation ($r^2 = 0.57$) between the amount of reduced KCl-P and TOC concentrations measured in solution for all experimental runs (Figure 6-6). Increased levels of TOC in suspensions resulted in reduced effectiveness of both sorbents in reducing soluble P levels. Similar behavior has been observed for soils amended with dairy litter (Lane, 2002), where P sorption, by the same Al-WTR used in this study, was significantly reduced.

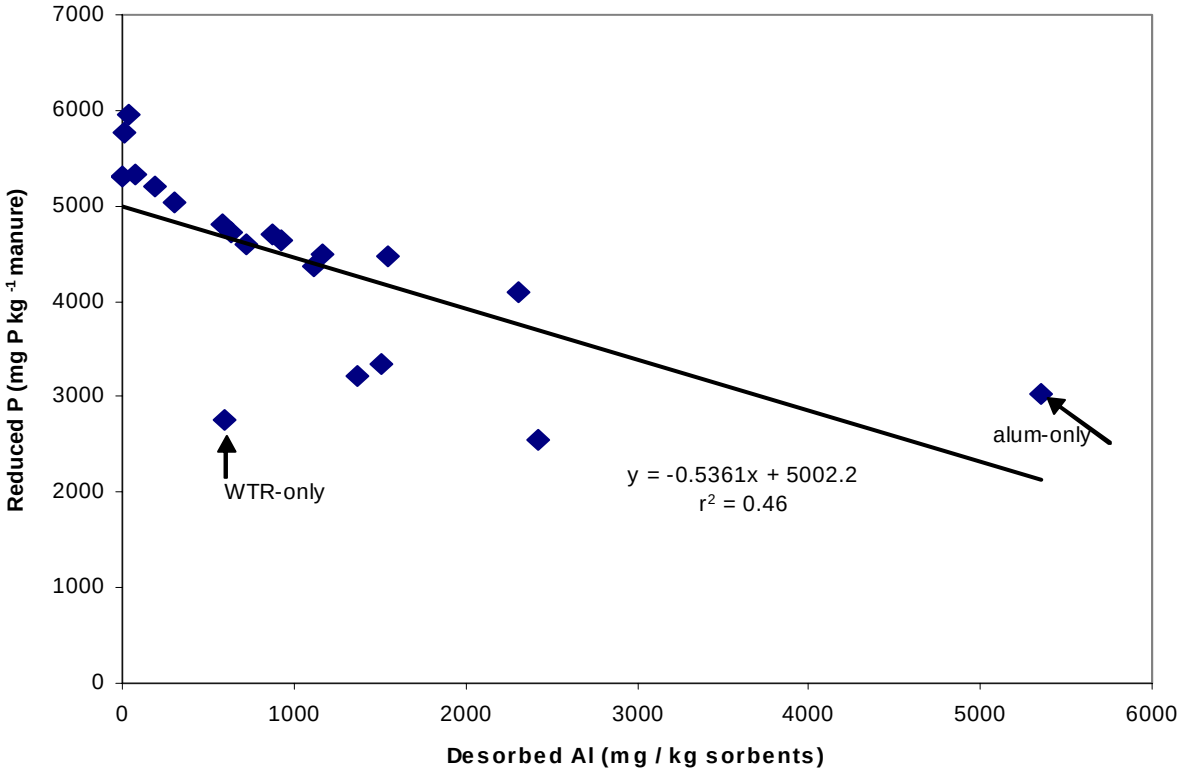

Figure 6-5. Relationship between Al in solution coming from alum and the WTR and the amounts of reduced KCl-P in all experimental runs of the central composite design.

Increased levels of DOC were identified as the main reason for the observed decrease in P sorption. Competition of phosphate and organic acids for sorption sites has been well documented (Eick et al., 1999). DOC from the alum-only treated litter suspension represented the amount of DOC released from the poultry litter (TOC = 23 g C kg^{-1} litter) since alum should have had insignificant residual C levels. WTR-only treated litter had slightly greater TOC levels (25.4 g C kg^{-1} litter plus WTR) than alum-only treated litter, probably due to WTR-associated organic dissolution. Median organic C content of a suite of WTRs was relatively high (6.3 %; Dayton et al., 2003).

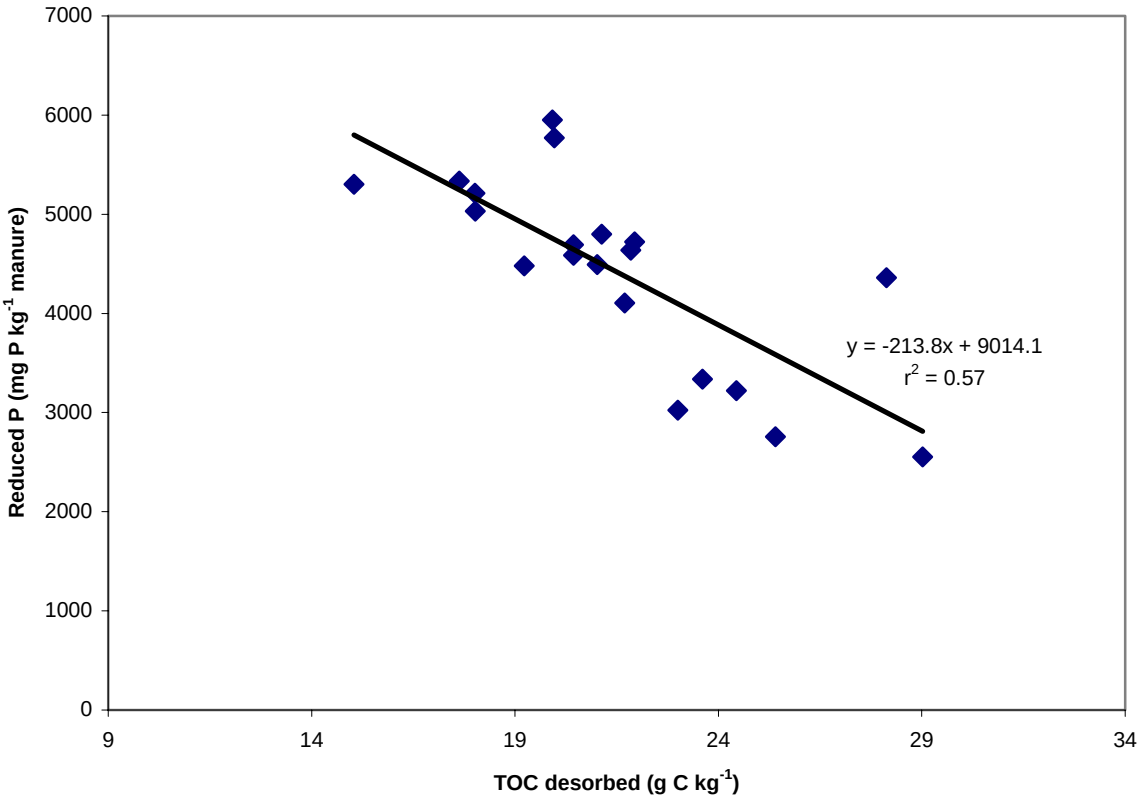

Figure 6-6. Relationship between TOC levels in solution coming from litter and the WTR and the reduced KCl-P in all runs of the central composite design.

WTR-only treated litter had slightly greater TOC levels (25.4 g C kg^{-1} litter plus WTR) than alum-only treated litter, probably due to WTR-associated organic dissolution. Median organic C content in a suite of WTRs was relatively high (6.3 %; Dayton et al., 2003). TOC and Al concentrations in solution seem to behave in parallel, and in accordance with the amount of residual KCl-P measured in suspension. The greater the soluble P reduction by the alum and the WTR, the less the Al and TOC remaining in solution, suggesting some type of a mixed organo-Al-P phase.

XRD-detectable crystalline Al-P inorganic phase peaks were not identified, even after 50 d of reaction of added alum and WTR to poultry litter suspensions. No crystalline inorganic Al-P phase was identified in alum-treated poultry litter using synchrotron-based

techniques at very high water-extractable P based Al/P final molar ratios (11- to 24; Peak et al., 2002).

Possibly an organo-Al-P precipitate forms in the treated poultry litter suspensions. Such a precipitate would be highly amorphous, of very small particle size, and high specific surface area, and likely to pass a 0.22 μm filter. Work by Omoike and vanLoon (1999) showed that co-precipitation of aluminum, tannic acid and orthophosphate produced a precipitate with very small particle size. Ng Kee Kwong and Huang (1981) demonstrated that the specific surface area of aluminum hydroxides was about five times greater in the presence of tannic acid, compared with samples not treated with the organic acid.

Recent work by Prakash and Sengupta (2003) revealed the close association of dissolved Al and DOC in two WTRs tested in a range of pHs (2- to 12). The adsorption edge experiment they performed revealed a U-shaped behavior for both Al and DOC, with minimum concentrations at pH ~ 7. All of our experimental runs had adjusted pH values (6.5), within 2 pH units away from the isoelectric point of a pure Al hydroxide (pH 8- to 9). However, significant amounts of dissolved organics in our system possibly could have reduced the point at which the zeta potential of on the slip plane of the surface of the WTR particles surfaces would be zero. Thus, the pH at which the system would exhibit minimum solubility should be less than the pH we encountered (6.5), which would be consistent with the large soluble Al and DOC levels found in our samples.

A decrease in Al and / or DOC solubility should be manifested as the result of increased net attractive forces between coagulated particles. Precipitation will occur when Al concentrations reach a critical point that neutralizes all the available binding

sites, or when the solubility of the Al-organic acid complexes is exceeded (Gregor et al., 1997).

The Al complexation capacities of several river waters ranged from 6.5 to 9.9 μM at pH 4.7 (0.18 to 0.26 mg Al L^{-1}) (Hawke et al., 1996). Soluble residual Al concentrations in our study (ranging from 0.16 to 59 mg Al L^{-1}) were greater than the above values and support the view that bridging flocculation has occurred as the result of supersaturation.

Omoike and vanLoon (1999) studied the interaction of aluminium, tannic acid, and P at pH values of 6.6 to 7.8, from 5 to 120 min of contact time. The initial concentrations used were 4.3 mg Al L^{-1}, 5 mg P L^{-1}, and 17 mg tannic acid L^{-1}, all of which were much lower than their respective concentrations in our study. Omoike and vanLoon (1999) found that tannic acid addition to an initially formed aluminum hydroxyphosphate solid results in coating the inorganic precipitate. At low tannic acid concentrations, the tannic acid and phosphate are incorporated into the Al hydroxide gel. As the tannic acid concentration increases, a higher concentration of Al remains non-precipitated due to the formation of a soluble Al-tannic acid complex. Increasing the tannic acid concentration resulted in poorer P removal by alum.

Galarneau and Gehr (1997) speculated that a mixed Al hydroxide phosphate precipitate formed during P removal by an aluminum hydroxide suspension within 1 h of reaction (Al/P molar ratios ranging from 2 to 8). Their thermodynamically-based mineral equilibria calculations showed that the minimum P concentration needed to precipitate aluminum phosphate at pH 6, in the absence of organics, is 148 mg P L^{-1}. The above

support the hypothesis that the form by which P is reduced in solution is a mixed precipitate of organo-Al-phosphate.

After the completion of the sorption step, residual materials were re-suspended in a 0.01 M KCl solution to monitor the P desorption from WTR or alum, or their combinations. The Al/P molar ratio of the mixtures influenced the amount of desorbed P (Figure 6-7). There was a weak negative linear correlation ($r^2 = 0.46$) between the Al/P molar ratio and the amount of P desorbed (data not shown). ANOVA analysis of the central composite design for the desorption step showed that WTR, alum, and reaction time, were all significant factors at the 95 % confidence level, but interactions were not significant.

There was a negative linear correlation between the soluble P reduction in litter suspensions, and the P desorbed (% of soluble P reduced during the sorption step) (Figure 6-7). Thus, the greater the Al/P molar ratio, the greater the reduction in soluble P in litter suspensions, and the smaller the amount of P desorbed from the sorbents. For alum- or WTR-only treated litter suspensions, had approximately 35 % of sorbed P was desorbed into solution after 25 d. The impacts of DOC on P desorption by WTRs remains unidentified and additional research is needed to be conducted to clarify the current trends.

Summary and Conclusions

An Al-WTR and alum were compared individually and as mixtures with respect to efficacy in reducing P release from poultry litter. On a per mole Al basis, Al-WTR was nearly as effective as alum in reducing P release at a specific pH (6.5).

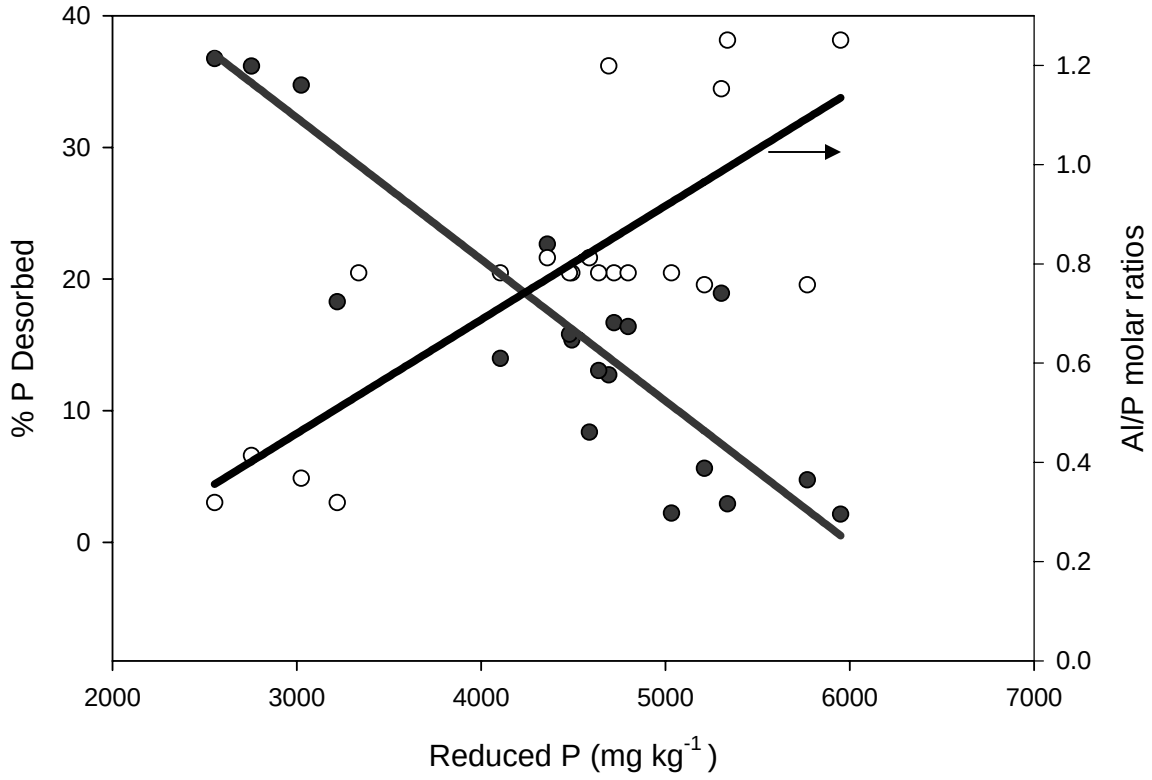

Figure 6-7. Reduced (sorbed) P levels as related to (i) desorbed P as a percentage of reduced (sorbed) P (open circles) and (ii) Al/P molar ratios (closed circles) after the completion of the P desorption in all runs of the central composite design.

The WTR-only treatment resulted in sorption of 22,500 mg P kg^{-1} WTR (52 % of initial soluble P in untreated litter). Sorbent combinations resulted in soluble P reduction that related to increased molar Al/P ratios. No significant synergistic or antagonistic effects occurred with combined alum and Al-WTR, despite different inferred mechanisms of P sorption for WTRs and alum. Soluble Al and TOC concurrently decreased as reduction in P solubility increased, suggesting that at least some of the P released from the litter was in the form of an organo-Al-P mixed solution species, or very fine colloidal phase. The amount of P desorbed from the mixtures decreased with the sorbent load up to a 1.2 Al/P molar ratios.

Two significant advantages of Al-WTRs compared to alum indicated by this study are cost effectiveness, and significantly less release of dissolved Al. However, additional research is needed to document these advantages at field scale and for different WTR sources, as well as to determine the effect of DOC on P desorption from Al-WTR / alum-treated litter.

CHAPTER 7
MODELING INTRAPARTICLE PHOSPHORUS DIFFUSION IN A DRINKING-WATER TREATMENT RESIDUAL AT ROOM TEMPERATURE

Introduction

Reactions between phosphate molecules and soils or Fe, and/or Al hydr(oxides) are initially fast, become slower with time, but never reach true equilibrium (Bolan et al., 1985). The fast reaction is explained by simple Coulombic interactions between adsorbent and adsorbate. The slow fraction of sorption has been attributed to intraparticle diffusion in meso- and micro- pores of mineral particles (Willett et al., 1988), and/or diffusion within soil organic matter (SOM) (Huang and Weber, 1997). SOM is recognized as a dual-functional sorbent possessing a soft or rubbery state, and a hard or glassy C state (Huang and Weber, 1997). The hard C or condensed organic domain is believed to exhibit non-linearity in the sorption of organics by SOM. Total elemental C in WTRs varies, but can be as much as 15 to 20 % (O'Connor et al., 2001).

Previous chapters of this dissertation showed P migration towards internal sites of WTRs exhibiting a slow P sorption character. We hypothesized that intraparticle P diffusion into the porous network of the WTR particles was responsible for the slow P sorption kinetics. Use of the intraparticle diffusion model to fit the sorption kinetic data for the WTR would permit the calculation of an apparent P diffusion coefficient. Matching the calculated P diffusion coefficient with published values from direct determination of diffusion coefficients of solutes into porous sorbents would possibly explain the slow P sorption kinetics by the WTR. Slow sorption into micropores of the

WTR would significantly increase the activation energy of desorption, immobilizing P into the pores of WTRs. Slow P sorption by WTRs may be an indicator of the long-term stability of sorbed P in P-sensitive ecosystems that have been amended with WTRs.

The objectives of this work were to characterize the sorption kinetics and determine the apparent diffusion coefficient of P sorption by a Fe-WTR at room temperature.

Materials and Methods

An Fe-WTR was obtained from the Hillsborough river water treatment plant in Tampa, FL, where $Fe_2(SO_4)_3$ is used as the coagulant. General chemical properties, specific surface area (SSA), and particle size distribution of the WTR can be found in chapter 3 of this dissertation.

Phosphorus Diffusion Considerations

The diffusion process plays a major role in solute sorption/desorption dynamics (Grathwohl, 1998). Slow sorption ascribed to diffusional limitations seems to apply to many types (inorganic/organic) of compounds and sorbents (Pignatello et al., 1993). To model P intraparticle diffusion in the WTR, the continuity equation was coupled with Fick's second law in spherical coordinates (Grathwohl, 1998):

$$Da\left[\left(\frac{\partial^2}{\partial r^2}C(r,t)\right)+\frac{2\left(\frac{\partial}{\partial r}C(r,t)\right)}{r}\right]=\frac{\partial}{\partial t}C(r,t) \qquad \text{(Eq. 7-1)}$$

WTR particles, for modeling purposes, were assumed to be homogeneous spheres. The above partial differential equation assumes that the apparent diffusion coefficient (Da) is constant. The Da can be constant in cases where the adsorption isotherm is linear (independent of concentration) or in cases of small incremental concentration changes; r is the average particle radius where r = 0 at the center of the sphere. Sorption occurred at

ambient constant pressure and temperature in a bath of limited volume. A pulse input of solute (phosphate) was initiated at time zero, followed by monitoring the decrease in aqueous P with time. Initial and boundary conditions involved were:

C =0	t=0	0<r<a	
C = Ceq	t=infinity	r=a	(Eq. 7-2)
∂C/ ∂r = 0	t>0	r=0 (center of sphere)	

The batch experiments were mathematically treated as a "bath of limited volume" (Grathwohl, 1998). The analytical solution of the corresponding partial differential equation (Eq. 7-1), based on the initial and boundary conditions described above, is (Crank, 1975):

$$\frac{M}{Meq} = 1 - \left(\sum_{'n' = 1}^{400} , \frac{6\ \beta\ (\beta + 1)\ \mathbf{e}^{\left(- \frac{q_n^{\,2}\ Da\ t}{a^2} \right)}}{9 + 9\ \beta + q_n^{\,2}\ \beta^2} , \right) \qquad \text{(Eq. 7-3)}$$

Where "M/Meq" denotes the mass of P (M) in the WTR sphere after time t normalized by the mass of P in the WTR sphere at equilibrium (Meq). "Da" is the apparent diffusion coefficient of P ($cm^2\ s^{-1}$). The ratio of the mass of P dissolved in the aqueous phase at equilibrium divided by the mass of P in the WTR particle at equilibrium is denoted as "β". "a" is the WTR particle radius in cm.

The qns are the positive non-zero roots of: $\tan(qn) = \frac{3\ qn}{3 + \beta\ qn^2}$

At large values of n (> 50) the qns approach n*π (Grathwohl, 1998). We assumed that qn = n*π + dqn, where dqn is the differential qn value. We calculated that n had to be at least

equal to 400 terms to get dqn=0.002, thus, qn could be approximated by n*π. Thus, 400 terms were used for the subsequent calculations.

We hypothesized that P sorption is diffusion-controlled and not simply reaction-controlled with hydroxyls on surfaces (external and internal sites). Phosphorus reaction with external and internal sites of the WTR was assumed to be homogeneous, since reaction is not limited on the external solid/liquid interface but involves reaction with pore walls of the interior. As a result, the rate of reaction decreases due to diffusion limitations, although reaction at the micropore walls may be heterogeneous (react with the surface and produce the product, which will diffuse back out (Cussler, 1997). Based on the analytical solution (Eq. 7-3) and the actual P sorption kinetics data, we performed a nonlinear optimization routine with the General Algebraic Modeling System (GAMS software) (Castillo et al., 2001). The GAMS optimization routine fitted the intraparticle diffusion model to the actual data by varying the apparent Da values (one for each size class).

Results and Discussion

The analytical solution (Eq. 7-3) of the diffusion model was used to fit the P sorption data. The percentage number particle size distribution data were pooled in five size classes, and a geometric diameter for each size class was calculated based on the following equation:

$$d = \sqrt{d1d2} \qquad \text{(Eq. 7-4)}$$

where "d1'' is the smallest diameter of the pooled size class and "d2" is the largest diameter of the pooled size class.

Particle size effects on the non-equilibrium diffusion of solutes in porous media have been acknowledged (Wu and Gschwend, 1988). Carta and Ubiera (2003) showed

that particle size distribution effects were significant for modeling of pore diffusion-controlled batch sorption experiments. Thus, the analytical solution (Eq. 7-3) was modified to include the broad range of particle sizes measured. The modified intraparticle diffusion equation was the sum of five terms that corresponded to the geometric diameters of the five pooled size classes weighted by the corresponding % number probabilities. By minimizing the squared residuals between actual and predicted (model) values for all 400 terms x 5 size classes data points, we were able to precisely quantify the apparent P diffusion coefficients (Table 7-1).

The overall mean squared error of the fit was small (5 %), and the model fit the sorption data well (Figure 7-1). "Meq" was assumed to correspond to the maximum amount of P sorbed by the WTR particles (initial pulse input of 10,000 mg P kg^{-1}). Fitted Da values ranged from 10^{-20} to 10^{-15} cm^2 s^{-1} (Table 7-1). There seemed to be an increasing fitted Da with particle radius (Table 7-1). The percentage number of particles within a size class (probability) was assumed responsible for the artificial Da/particle diameter positive trend. In order to calculate a single value for Da based on the actual sorption data, we plotted M/Meq versus the dimensionless time t' (Figure 7-2).

$$t' = t * Da*a^{-2} \qquad \text{(Eq. 7-5)}$$

Figure 7-2 helped us perform a simple calculation to determine the *maximum* apparent P diffusion coefficient. The *minimum* dimensionless time necessary to allow all aqueous P to diffuse into a WTR particle with the most probable (0.73; Table 7-1) measured radius ($4.5*10^{-4}$cm) after 80 d of reaction was 0.15.

Table 7-1. The pooled five size classes from the particle size distribution and its corresponding geometric diameters. The fitted Da are the result of the nonlinear optimization method.

% number	Geometric diameter (cm)	Da ($cm^2\ s^{-1}$) Fitted
0.44	$3.4*10^{-6}$	$1.34*10^{-20}$
17.62	$0.75*10^{-5}$	$6.46*10^{-20}$
73.26	$4.5*10^{-4}$	$2.32*10^{-16}$
8.62	$1.6*10^{-4}$	$2.94*10^{-17}$
0.06	$1.2*10^{-3}$	$1.65*10^{-15}$

We hypothesized that the largest WTR micropore would be equal to the particle radius (Werth and Reinhard, 1997). Substituting into equation (5), we found that the *maximum P* diffusion coefficient for the WTR particles at room temperature was Da = $4*10^{-15}$ $cm^2\ s^{-1}$.

This value is within the range of published diffusion coefficients for microporous oxides. Intraparticle diffusion of heavy metals in model microporous Al and Fe oxides was shown to occur under steady supplement of the metal in solution (Axe and Trivedi, 2001). Axe and Trivedi (2001) reported that cation (Zn, Cu, etc.) diffusion coefficients at "infinite bath" initial and boundary conditions, ranged from 10^{-10} to 10^{-14} $cm^2\ s^{-1}$. The effective diffusion coefficient of phosphate molecules in free liquid solution has been calculated to be $8.9*10^{-6}$ $cm^2\ s^{-1}$ (Valenta et al., 1981).

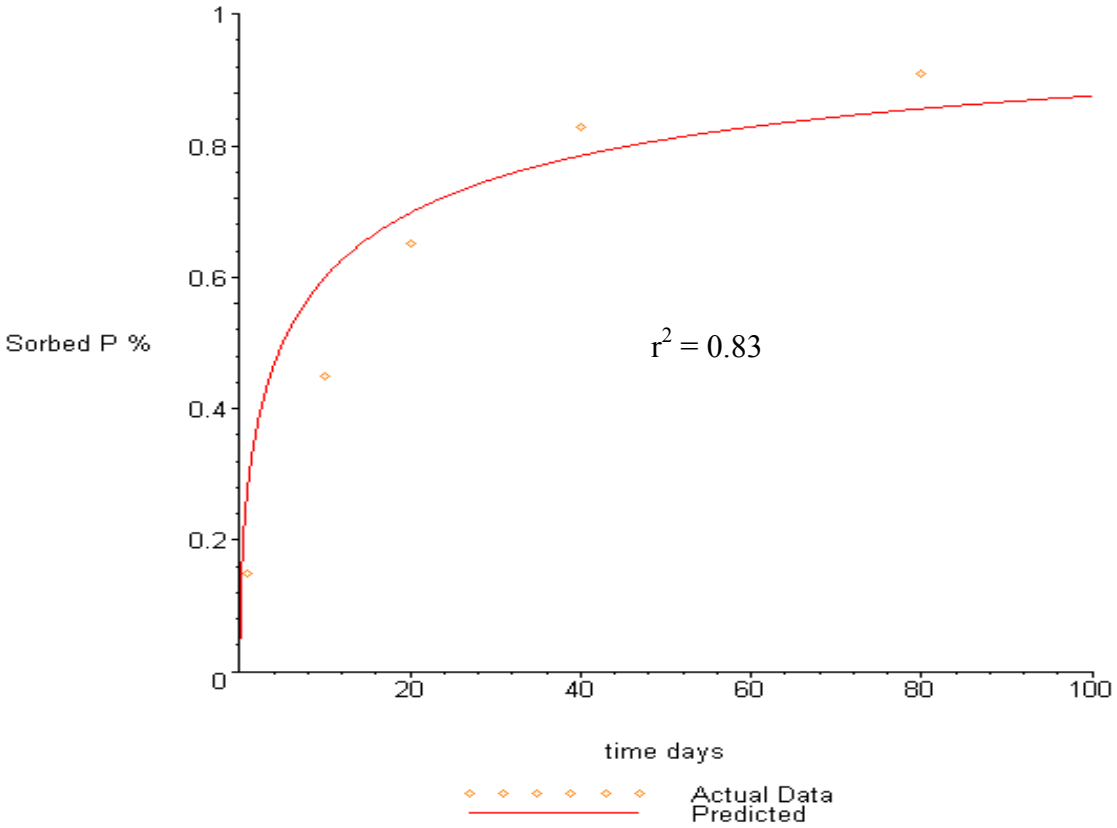

Figure 7-1. Intraparticle diffusion model fit to the P sorption kinetics data for an initial pulse input of 10,000 mg P kg^{-1}.

Several studies have been performed to determine P diffusion coefficients in soils. Direct determination of P bulk diffusion coefficients in soil was in the order of 10^{-13} cm^2 s^{-1} at 298 K (Bhadoria et al., 1983). The P diffusion coefficient measured for an Fe alloy was 10^{-19} to 10^{-17} cm^2 s^{-1} at 550 to 850 K (Valenta et al., 1981). The effective P intraparticle diffusion coefficient into activated alumina at 298 K was measured based on P breakthrough curves, and was on the order of 10^{-15} cm^2 s^{-1} (Hano et al., 1997). Micropore diffusion of organic contaminants in soil is usually on the order of 10^{-16} to 10^{-8} cm^2 s^{-1} (Werth and Reinhard, 1997).

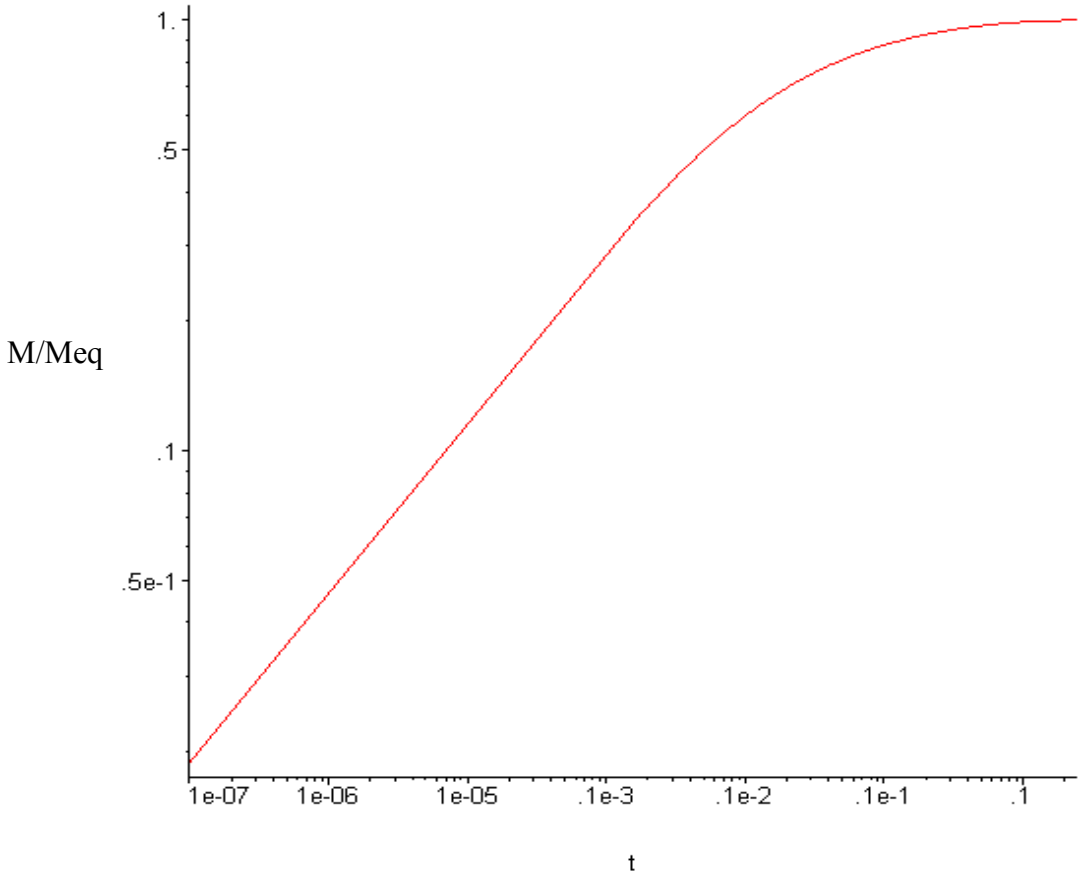

Figure 7-2. Double logarithmic plot of the M/Meq versus the dimensionless time. The trend seems to reach equilibrium at a value of 0.15 dimensionless time.

The calculated maximum apparent diffusion coefficient ($4*10^{-15}$ cm^2 s^{-1}) in this work matches the published effective P diffusion coefficients for sorption into porous sorbents, as determined directly from diffusion experiments.

Conclusions

Land or water application of WTRs to systems high in P is an emerging practice to reduce soluble P in soils or water bodies (lakes, ponds, etc.). The sorption isotherm at room temperature showed that the Fe-WTR removed nearly all of the aqueous P without reaching true equilibrium. Phosphorus sorption kinetics by Fe-WTR exhibited nonequilibrium characteristics even after 80 d of contact.

SSA measured with CO_2 gas (micropore SSA) was significantly greater than BET-N_2 SSA. The observed increase in SSA was attributed to internal surfaces of microporous nature. The high C content present in the WTR was speculated to be responsible for the low BET-N_2 and the high CO_2-SSA measured in the WTR.

An intraparticle diffusion model was used to explain the slow P kinetics. The analytical solution of the appropriate partial differential equation of the intraparticle diffusion model was modified according to the particle size distribution data since the particle size distribution was broad, covering three orders of magnitude.

The sorption data fit well to the diffusion model ($r^2 = 0.83$) when a non-linear optimization routine was used. The maximum value for the apparent P diffusion coefficient was $4*10^{-15}$ cm^2 s^{-1}, which agreed with published values from direct determinations of effective P diffusion coefficients, assuming intraparticle diffusion in porous sorbents. The observed consistency in P diffusion coefficients may provide *indirect* evidence for intraparticle P diffusion into the WTR particles. Calculated P diffusion coefficients may be used to different batches of Fe-WTR from Tampa as well as batches of other WTRs that resemble it in pore size, volume distribution, and organic C content. Phosphorus diffusion coefficients may then be applied to predict the long-term maximum P sorption capacities of WTRs when applied to P-sensitive ecosystems.

CHAPTER 8
ADVANCES IN UNDERSTANDING THE LONG-TERM FATE OF SORBED PHOSPHORUS BY DRINKING WATER TREATMENT RESIDUALS

Past agricultural activities including waste disposal to soils have resulted in elevated phosphorus (P) inputs in many soils. Accumulated P has minimal agronomic impact, but can have serious environmental impacts if the P is mobilized to water bodies. Sandy poorly P-sorbing soils are abundant in Florida, and other eastern states of U.S.A. Low P sorbing capacities, accompanied by high water tables, and coarse-size textures make these soils vulnerable to P losses (He et al., 1999). Lateral and vertical movement of P with water towards the water bodies are the main pathways to surface waters. Increased P loading of streams, lakes, and rivers can cause algal blooms, and subsequent decreases in water quality, which can increase costs associated with drinking water purification.

Drinking-water treatment residuals (WTRs) can cost-effectively reduce excess soluble P levels in soils high in P. Drinking-WTRs are primarily amorphous masses of Fe, Al hydroxides or $CaCO_3$ that may also contain humic/fulvic acids, activated carbon, and polymers (Elliott and Dempsey, 1991). Research has confirmed that WTRs can immobilize P susceptible to leaching or runoff. In the short-term, WTRs can dramatically reduce soluble P levels in soils and runoff from areas amended with different P-sources (Haustein et al., 2000; Ippolito et al., 1999; Gallimore et al., 1999).

However, no information exists on long-term reactions of P with WTRs. Federal agencies need data sets that deal with the long-term stability of sorbed P in soils and

guide management practices on high P soils. Three approaches were designed to tackle the long-term P sorption mechanisms and reactivity of WTRs and WTR-amended soils. The first approach dealt with determining the physicochemical properties of the WTRs and how they affect the long-term P sorption, both from a macroscopic and a microscopic point of view. The second approach dealt with heat incubations at elevated temperatures (46 and 70 C) of synthetic Al and Fe hydroxides, WTRs, and WTR amended soils in an attempt to hasten reactions that could take decades to occur in the field. The third approach monitored the longevity of a WTR effects in two MI soils 5.5 years after a one-time Al-WTR application.

Appropriate hypotheses were formulated as follows: firstly, WTRs are characterized by significant internal surface area and porosity that would explain a time-dependent P sorption; secondly, WTRs could ultimately immobilize P; thirdly, elevated temperatures would increase the degree of crystallinity of P-treated particles, and concurrently decrease P extractability. The overall objectives were to determine mechanisms and pathways of P sorption by WTRs, and to interpret the mechanisms in terms of the long-term stability of sorbed P.

The first approach began with the macroscopic characterization of the WTRs. Long-term sorption isotherms and kinetics of P by WTRs are not well understood, and long-term P behavior is usually interpreted in the context of metal hydroxides' behavior, which assumes similar reactivities (Bolan et al., 1985). WTRs resemble Fe and Al hydroxides in metal composition, and retain significant amounts of water within the porous particles. Total Fe and / or Al concentrations in WTRs are high and usually range from 4-30 %, as it was documented in earlier chapters of the thesis. Thermogravimetric

(TG) analysis (25-1000 C) of the WTRs showed that minimal (<1 %) weight loss occurred up to 70 C at a heating rate of 5 C min^{-1}. Isothermal (70 C, 10 h) weight losses of WTRs were characterized by an initially fast release of water followed by a kinetically driven stage where hysteretic water was slowly released from the interior of the WTR particles. Significant amounts of water prevail in the internal surfaces of the WTRs that could classify WTRs as gels.

WTRs also contain a significant amount of carbon (3-21 %) that may play a role in the overall P sorption by WTRs. The large percent C of WTRs may be responsible for deviations from the ideal metal hydroxide/gel physicochemical behavior. Forces other than electrostatic, such as hydrophobic, and hydrogen bonding between organic molecules and mineral internal surfaces may be significant and affect the physicochemical nature of WTRs. For example, cationic polyelectrolytes added during the water treatment process account for a significant portion of sorbed P by WTRs (Butkus et al., 1998).

Steric effects and hydrophobicities imposed by organic compounds present in WTRs may influence P sorption kinetics and diffusivities, making WTRs a complex system where molecular interactions are not simply electrostatic. Two out of seven WTRs tested (Panama and Cocoa, FL) had the least amounts of sorbed P (2 and 3 g P kg^{-1}), even after 80 d of reaction. It is noteworthy to mention that the Cocoa material had a pH of 4 and the Panama had a pH of 5. We speculate that the low pH of the two WTRs affects organic molecules conformation on the surface of WTRs. The low, relative to the other WTRs, pH may be responsible for the low P sorption capacities. Low pH (4-5) leaves the majority of surface functional groups unionized, thus, organic molecules lay

flat on the surface blocking the free transfer of water / solutes in and out of the particle. This results in retarded solute and water diffusivities and consequently, low P sorption kinetics. This issue deserves more attention, and further research should focus on factors influencing the low P sorption capacities of WTRs. Further work may be needed to characterize the physical and chemical nature of organics present in WTRs and how may influence contaminant sorption.

O'Connor et al. (2001) called for the need for further lab studies on the long-term stability of the immobilized P to compliment the short-term studies they conducted. Long-term P sorption isotherms revealed the huge P sorption capacities of the WTRs, as well as, a non-equilibrium, slow P sorption character. Long-term (up to 80 d) P sorption kinetic data of the WTRs were best fit to a second order reaction rate model. This confirmed the biphasic nature of P sorption by WTRs; an initial fast reaction within one day followed by a slower reaction that in some cases reached equilibrium only after 80 d. Five out of seven WTRs tested, showed dramatic affinity for soluble P, sorbing essentially all of the added P within 10 to 80 d.

Slow P sorption was accompanied by decreasing desorbed P levels with increasing desorption time from 5 to 80 d for all WTRs using a 5mM oxalate solution. Ippolito et al. (2003) reported similar minimal P desorption with another Al-WTR. This suggests that sorption had not reached equilibrium and it was kinetically hysteretic, where the slow state appears to fill faster than it empties (Pignatello and Xing, 1995). The maximum amounts of desorbed P with 5 mM oxalate solution were obtained with the shortest desorption contact time and ranged from 0.2 to 8.3 % of sorbed P. Irreversible P binding by WTRs was suggested from the P desorption experiment. We hypothesized that P

diffusion to distant and less-accessible sites may be responsible for the negligible P desorption. Another explanation could be the large sorption energy potentials involved with micropore walls that demand significant amounts of activation energy to desorb micropore-bound P. Literature on slow P sorption kinetics have divided P reactions with Fe/Al hydroxides into two processes: redistribution of sorbed P into the interior of particles via solid-state diffusion (Bolan et al., 1985), or diffusion in micropores (Cabrera et al., 1981), and second, surface precipitation of a metal-P insoluble phase (Nooney et al., 1998). A first look at the P sorption isotherms suggested formation of a multilayer solid phase on the WTR surface (surface precipitation) based on the upward trend of the isotherm line and the elevated P/WTR loads. Calculations were performed to match the P adsorption monolayer capacities of crystalline and non-porous Fe and Al oxides (goethites and gibbsites) with the total P uptake by WTRs, and the respective BET-N_2 specific surface areas (SSAs). Total P uptake by WTRs was approximately five times greater than what an external surface monolayer formation would explain. However, SEM-EDS surface analysis of P-treated WTRs for 80 d provided no evidence of localized surface precipitation. Similar SEM-EDS work on a P-treated Al-WTR showed no evidence for surface precipitation but rather an amorphous Al-P association throughout the particles (Ippolito et al., 2003). We were also unable to detect a crystalline Al-P phase using x-ray diffraction analysis. It is possible that the high organic carbon content of the WTRs coupled with the chemical heterogeneity of the materials would hinder the formation of a discrete crystalline Al-P phase.

To further study P distribution in the WTRs, we created cross sections of the particles (z-axis depth profiles). Cross-sectional P distribution analysis of the P-treated

WTRs with the aid of an electron microprobe showed significant ($p<0.001$) increases of the relative P concentrations in the interior of the particles (approximately 60 μm inside) with time (from 1 to 80 d). There was no significant difference between the edge and the interior of the particles after 80 d, suggesting an intraparticle P diffusion mechanism to explain the slow P sorption kinetics. Electron microprobe-based dot map analysis on the whole surface of the cross-sections of a P-treated Al-WTR for 211 d showed the uniform distribution of P throughout the particle (Ippolito et al., 2003). Speculated sorption mechanisms were surface P chemisorption, or precipitation of an amorphous Al-P phase. Microprobe spectroscopic analyses of our work utilized further quantitative treatment, instead of visually inspected treatment differences found in dot maps that statistically proved P intraparticle diffusion. Our data provided a new insight in P reactions with amorphous metal hydroxide surfaces that usually dominate P chemistry in acidic soils. P can move in a three-dimensional fashion towards the interior of the WTR particles, having favorable implications for the long-term stability of sorbed P.

An intraparticle diffusion mechanism has been utilized to explain Sr, Cd, and Zn sorption under steady supplement of the metal in solution by microporous amorphous Al and Fe hydroxides (Axe and Trivedi, 2001). Intraparticle diffusion in soils has also been used to explain slow sorption kinetics of organic contaminants (Pignatello and Xing, 1995). P diffusion in metal hydroxides at ambient temperatures and pressures has long been speculated, but no direct evidence has been obtained (Cabrera et al., 1981). To the best of our knowledge, intraparticle P diffusion in natural systems, using other than wet chemical methods, has not been documented for ambient pressure and temperature conditions.

Several studies have attempted to explain the slow P sorption by Fe, Al amorphous hydroxides, or soils with high amounts of metal hydroxides (Willett et al., 1988; Agbenin and Tiessen, 1995; Madrid and De Arambarri, 1985; Cabrera et al., 1981). All of the above studies suggested P diffusion in micropores of metal hydroxides as the reaction rate limiting mechanism, but no direct evidence was presented to support the speculations (no use of spectroscopic techniques, or surface area measurements).

Diffusion of P into the internal surfaces of the amorphous WTRs would not be realistic, unless a significant network of connected pores would exist. We attempted to address this issue by using Hg and N_2 porosimetry to assess macropore and micropore size distributions of the WTRs, respectively. Mercury intrusion porosimetry quantifies macropores, but cannot access micropores. Mercury porosimetry has been successfully used in soils to measure SSAs and correlate them with inorganic (Goldberg et al., 2001) and organic compounds sequestration assessments (Chung and Alexander, 2002). Mercury porosimetry data showed that WTRs had very little macroporosity; most of the pore volume was found in ≤ 5 nm pore widths (meso to micro- pore range).

The BET-N_2 SSAs of WTRs did not correlate with theie high P sorption capacities. We hypothesized that the large organic carbon content of the WTRs was responsible for this. A plethora of high and low molecular weight organics either naturally occurring (humic and fulvic acids), or synthetic (polymers, surfactants) usually added to enhance and accelerate the water purification process, can be found in WTRs. Kaiser and Guggenberger (2003) found that the BET-N_2 SSA of a host of soils varying in organic carbon content was inversely related to the soil C content. Sorption of soil organic matter at the mouth of micropores formed by two domains of a mineral may hinder N_2

molecular diffusion into the micropore, and thus, underestimation of the true SSA (Kaiser and Guggenberger, 2003). We also observed a linear negative correlation ($r^2 = 0.50$) between the total C content and the BET-N_2 SSAs measured for 6 WTRs.

In an attempt to test this hypothesis, we used high-resolution CO_2 gas adsorption to measure micropore-SSAs of the WTRs. Carbon dioxide gas sorption at 0 C has been used to evaluate microporosity in soils high in organic carbon content (Xing and Pignatello, 1997). CO_2 molecules have a greater diffusion coefficient than N_2 molecules since they have approximately 32 times greater saturation pressure and much greater (0 versus –196 C) temperature than what N_2 molecules encounter during the BET method. This permits CO_2 molecules to access micropores associated with organic molecules that N_2 cannot, due to energetic barriers.

CO_2-based micropore SSAs for six out of seven WTRs were greater than the BET-N_2 suggesting the presence of narrow micropores, or constrictions in the pore opening that restrict N_2 diffusion. Garrido et al. (1987) compared N_2 to CO_2 gas sorption by different microporous activated carbons and found that when $N_2 < CO_2$ sorption, there was restricted N_2 diffusion or narrow microporosity. When $N_2 = CO_2$ sorption, microporosity was homogeneous. When $N_2 > CO_2$, microporosity distribution was wider and very heterogeneous. Six out of seven WTRs had $N_2 < CO_2$ SSAs suggesting restricted diffusion of dinitrogen molecules to micropores where the pore opening was partially or wholly covered with organic compounds, or to narrow micropores (bottle shape micropores).

Only two out of the 7 WTRs had similar N_2 and CO_2 SSA (Holland and Lowell Al-WTRs) and also had the lowest carbon content (3.4 and 7.6 %). Low carbon content of

the WTRs could be responsible for this behavior. One-to-one correspondence between SSAs measured by N_2 and CO_2 was found for the low organic carbon WTR or for microporous synthetic Al hydroxides free of organic carbon. As the percent carbon in WTRs increased, so did the discrepancy between the SSAs measured by CO_2 and N_2. Ravikovitch et al. (2003) also observed this interesting trend for non-contaminated Chicago soils.

Micropores may be associated with organic compounds that are either characterized by coiling / patching morphologies which may create tortuous organic micropores that hydrophilic molecules have to diffuse through, or by sorption of organic molecules that may block the mouth of inorganic micropores (Kaizer and Guggenberger, 2003). There was a significant positive correlation (r^2 = 0.85 %) between the CO_2/N_2 SSA ratio and the amount of P sorbed after 40 d normalized to the carbon content of the WTRs. Correlation between the carbon content, CO_2 and N_2 SSAs with the long-term P sorption may prove to be useful to predict long-term P sorption by WTRs. N_2 and CO_2 SSAs methods seem to compliment each other and provide useful information on the physical nature of the materials. Carbon content influences the magnitude of the CO_2 / N_2 ratio, which in turn may give valuable information on the pore size distribution of the WTRs, or other amorphous, high in SSA, materials.

The potential effect of P sorption by micropores on the measured SSAs was also evaluated. Micropore-CO_2 SSAs of the P-treated WTRs were reduced relative to the untreated (no P added) WTRs. Micropore-SSAs' percent reduction was positively correlated to the P sorption maxima of the WTRs after 40d. The reduction in micropore-SSA of the P-treated WTRs was due to micropore blocking by phosphate molecules.

Phosphates sorbed by micropores hindered CO_2 diffusion, thus reduced the micropore volume of CO_2 molecules sorbed per gram of WTR. WTR particles in contact with phosphate molecules in aqueous solution will permit phosphate molecular diffusion via the tortuous pore network of the WTRs. Water flow into the particles carries phosphates that diffuse into internal surfaces, reaching hydrophilic micropores that exhibit high-energy adsorption potentials. Non-uniform distribution of micropores may be responsible for the slow P sorption process, as phosphates access distant internal sorption sites.

P sorption by micropores of the WTRs may satisfactorily explain the reduced P extractability, as the P desorption experiment revealed. Minimum P desorption from the WTRs may be the result of increased micropore energy potentials involved between the pore walls and the sorbed phosphates. The close proximity of micropore walls maximizes the bonding interaction between the sorbent and the sorbate, thus, reducing sorbate availability. Increased amounts of activation energy may be required to overcome energetic barriers associated with micropores. Micropore accessibility is consistent with time-dependent P sorption and hysteretic desorption phenomena, since they could limit P diffusion rates. Similarly, isothermal (70 C) water loss of the WTRs showed a slow hysteretic release of water, being consistent with the idea of micropores. Micropore-bound P would likely resist desorption, which favors long-term stability of sorbed P by WTRs.

Traditional parameters used to explain P sorption capacities in acidic soils and WTRs, such as oxalate- (200 mM) extractable Al and Fe alone, were not sufficient to explain trends observed in the long-term sorption experiments with WTRs. No significant relationship was found between the oxalate (200 mM) extractable Al and Fe and the P

sorption maxima for seven WTRs. P sorption by WTRs never reached true equilibrium, despite the long equilibration times (80 d) and the initial P load (10 g kg^{-1}). Dayton et al. (2003) reported a significant positive relationship between Langmuir P sorption maxima and oxalate extractable Al for twenty-one WTRs. However, the Langmuir P sorption maxima were calculated for shorter equilibration times (15 h) and smaller initial P loads (2.5 g kg^{-1}) than used here. Oxalate-extractable Fe / Al concentrations of WTRs is an important parameter needed to describe long-term P sorption, but not sufficient. Factors that describe the physical nature of the WTRs such as the external and / or internal SSAs, pore size distributions and the carbon content should compliment oxalate extractions to better explain long-term trends of P sorption by WTRs and WTR-amended soils.

Another approach used to study the long-term stability of sorbed P was to directly measure the longevity of a WTR effect on P extractability of WTR-amended soils. Two sites in Holland, MI received a one-time WTR application in 1998, and P extractability was monitored from spring-1998 to fall-2003. For many years before 1998, both sites had received heavy poultry litter applications and they were characterized by high soil test P levels (Bray 1; 300 and 600 mg P kg^{-1}, for sites 1 and 2, respectively).

In both soils, P extractability as expressed by the phosphorus saturation index (PSI, Nair et al., 2004) remained constant 5.5 years after WTR application. Positive WTR effects in reducing PSI values were observed only at site 2 that had half the amount of native total Al measured in site 1. Encouraging was the fact that we observed neither P release, nor crop yield reductions from WTR-amended soils, 5.5 years after initial application (Dr. L. Jacobs, personal communication, 2004). Drinking-WTR effects in

reducing P extractability should be pronounced in soils low in Fe and Al, such as, Florida's sandy soils.

WTR addition in sandy soils, or acidic soils low in total Fe and Al would significantly increase a soil's reactivity by increasing reactive metal concentrations, which would bind soil P. Data from the Holland, MI long-term experiment suggest that WTR-bound P would be stable with time, at least for five and a half years. Phosphorus would become less available with time, as it diffuses towards the micropores of the WTR particles. Micropore-bound P should be the most stable since the pore opening is so small that even enzymes could not access it. Further studies are needed to directly address the long-term WTR effect in larger time scales in fields amended with WTRs.

Need to predict the long-term stability of sorbed P by WTRs beyond 5.5 years of the field study, led us to use indirect methods to simulate long-term reactions. Such methods involved the use of heat incubations at elevated temperatures (46 and 70 C) to hasten reactions that could take decades to occur in the field (Martinez and McBride, 2000). Elevated temperatures would accelerate the aging of P-treated sorbents, such as synthetic amorphous Fe and Al gels, WTRs, and WTR-amended soils. Aged P sorbents would be characterized by increased crystallinity, which in turn would reduce P extractability.

Synthetic amorphous Fe and Al hydroxides were incubated at 70 C as the "clean" model systems that would give the most information from the heat incubations. All of the three incubated systems (synthetic metal hydroxides, WTRs, and soils) were allowed to evaporate free water during heating at 46 and 70 C. Thermogravimetric analysis of the synthetic Fe, Al hydroxides and the WTRs after incubation at 70 C for 2 years showed

that the metal hydroxides and the WTRs retained most of their internal water at 70 C, acting as gels that would permit potential P desorption from internal surfaces. Free water removal from synthetic metal hydroxides or WTRs particles would have no effect on potential P desorption from internal surfaces.

Heat incubations of the Al hydroxides at 70 C for 2 years with no free water resulted in the formation of pseudoboehmite (poorly crystalline boehmite) and decreased oxalate (5 and 200 mM) extractable Al concentrations. The formation of pseudoboehmite was relatively fast (within a month) and crystal growth remained constant thereafter. No effect of temperature and time was observed on the oxalate extractable Fe and degree of crystallinity of the Fe hydroxide particles. Iron hydroxides remained mostly amorphous, as evidenced by the broad peaks, throughout the dry heating incubation period (2 yrs at 70 C), consistent with the literature (Stanjek and Weidle, 1992).

Changes in crystallinity occurred mostly in the Al and much less in the Fe hydroxides, paralleling decreases in BET-N_2 SSAs with time in both systems. Data are in agreement with previous studies; dry heat incubation (125 C) of a two-line ferrihydrite for 47 d did not induce changes in crystallinity, and weight losses were attributed to losses of surface and structural hydroxyls (Stanjek and Weidler, 1992). Similarly, no changes in crystallinity were observed after ten cycles of freezing (-25 C) and thawing (25 C), or cooling (4 C) and warming (25 C) of a two-line ferrihydrite (Hofmann et al., 2004).

The method of using low temperatures to induce crystallization by dehydrating the particles is similar to the one we used and involved the use of elevated temperatures (70 C). Seventy degrees Celsius induced gradual changes in SSA, porosity, and weight losses

of the synthetic metal hydroxides with time. At time zero, the untreated Al hydroxides were mostly microporous in nature. As the particles dehydrated, micropore volume was reduced and micropores were shrinking. As a result, net attractive forces dominated and new chemical bonds were formed, bridging particles together and increasing the XRD coherence length. SSAs were reduced, as the crystallites grew at the expense of micropore SSA, a process similar to Ostwald ripening (Weidler and Stanjek, 1998).

Phosphorus-treated Al hydroxides were also microporous, but were also characterized by a considerable network of macropores. Total micropore volume was significantly less than the untreated Al hydroxides due to phosphate sorption by the micropores. Coprecipitation of phosphates may be responsible for the distortion of the unit cell as they opened up the structure creating macropores that were not observed in the absence of P.

Phosphorus-treated and untreated WTRs were also heat incubated at 23, 46 and 70 C for two years. P extractability of the heat incubated (46 and 70 C) WTRs as monitored by using a 5 mM oxalate solution was reduced over the 23 C treatment. However, 200mM oxalate, which is the traditional concentration used, was deemed ineffective in selectively extracting P from the WTRs, as it extracted greater than 90 % of total. Reductions in the magnitude of the oxalate (5 mM) extractable P levels of the heat treated (46 and 70 C) WTRs did not parallel increases in crystallinity, or decreases in the oxalate-extractable Fe or Al concentrations.

X-ray diffraction did not show the formation of a crystalline phase. Oxalate (5 mM) Fe or Al levels did not parallel decreases in oxalate (5 mM) P levels. This may be attributed to an intraparticle P diffusion mechanism, or to P association with components

of the WTRs other than Fe or Al, which seems unlikely. Increased aqueous concentrations of metals were found in heat-treated (70 C) compared to the non-heated soil samples (Martinez et al., 2001). However, no parallel increase in oxalate extractable Fe or Al was observed. The authors attributed the increases in metal concentrations to organic matter decomposition.

In our case, it is unlikely that P would be significantly associated with the organic phase of the WTRs. Oxalate extraction (5 mM) is a milder extractant than the 200 mM and may be more selective in extracting P located externally or to easily accessible internal sorption sites. Potential P diffusion in micropores of the WTRs would have reduced P concentrations in sites accessed by the 5 mM oxalate, thus, the demonstrated reductions in oxalate-P.

WTRs exhibited considerable hysteretic water loss at 70 C that was also closely correlated with irreversible water losses. At time zero, isothermal TG water losses at 70 C of the WTRs were hysteretic suggesting the presence of micropore-bound water that demands significant amounts of activated energy to be slowly released. Thus, even air dried WTRs may still internally contain a significant amount of water, paralleling trends observed during heat incubation of the synthetic Al / Fe hydroxides. This may suggest minimal differences in P extractability in systems with water activity of one and systems with very low activity (our study). WTRs may behave as gels that contain significant amounts of internal water and would not inhibit potential P desorption from internal sorption sites.

However, heat incubations of the WTRs suggest decreased P extractability as evidenced by the 5 mM oxalate solution. No release of P was observed for all treatments

and temperatures with incubation time. This supports the conclusions drawn from the field study in Holland, MI, where no release of P was observed 5.5 years after WTR application.

Evaluation of the long-term stability of sorbed P in WTR-amended soils was also assessed by heat incubating soil samples from the Holland, MI sites. Both sites 1 and 2 exhibited no significant increase in the 5 or 200 mM extractable P and Al levels after 2 years of incubations at either 46 or 70 C. Absence of changes in oxalate extractable P levels was observed either for WTR-amended or unamended plots of sites 1 and 2. This data set results showed no release of P from the WTR-amended soil samples, corroborating data from the WTR heat incubations.

However, heat incubation of WTR-amended soil samples did not show the reduction in oxalate-P (5 mM) that was observed in the pure WTRs heat incubations. Increased complexity in the WTR-amended soil samples may be one of the reasons. WTRs are mixed with other soil components and they are in lower concentrations than the ones used for the pure WTR system. Also, P loads in the WTR-amended soil samples were much less than the loads used in the WTRs only incubations. Encouraging maybe the absence of P release from WTRs, and WTR-amended soils either in the field or heat incubated samples was common for all systems examined.

Further studies need to be conducted on predicting the time scales that P is stable and immobilized by WTRs. Inclusion of diffusion and thermodynamic models could be a good combination to tackle such a complicated issue. Non-linear fit of the long-term P sorption kinetics of the Fe-WTR, Tampa, FL to a diffusion model resulted in the calculation of a P diffusion coefficient in the order of 10^{-15} cm^2 s^{-1}. This value is in

accordance with slow P diffusion in microporous sorbents (Axe and Trivedi, 2001). There was an excellent agreement (94 %) in values between the electron microprobe relative P concentrations 60 μm inside the particle measured after 80 d, and the predicted sorbed P concentrations from the diffusion model, based on the above P diffusion coefficient.

However, the diffusion model is based on idealized case scenario where particles have unimodal particle and pore size distributions with a specific shape. It is also assumed that sorption and desorption have the same reaction rates; excluding any hysteretic effects. We also anticipate that P diffusion coefficients will vary from WTR to WTR depending on the ease by which phosphate molecules diffuse in the structure.

Factors that will influence the value of P diffusion coefficient could be the carbon content and the ratios of CO_2 / N_2 SSAs. The slower the P sorption kinetics, the smaller the value of the P diffusion coefficient. Accordingly, the greater the carbon content and the CO_2 / N_2 SSA ratio, the smaller the P diffusion coefficient could be. Experiments that will test the worst-case scenario (time-bomb WTRs), or at least may be more realistic should be evaluated. Incubation at room temperature after 160 d in aqueous solution WTR particles did not lose their rigidity or integrity. Microbial mediated WTR decomposition should also be evaluated to assess the P desorbability.

In conclusion, based on our work, we may say in confidence that WTRs' micropore bound P should be ultimately immobilized under ambient temperatures, pH, and pressures. Future work should focus on realistic models that take into account slow sorption P kinetics and hysteretic desorption phenomena that may take place during P reactions with WTRs. Dynamic models should be developed that accurately predict the

long-term fate of sorbed P by WTRs. Factors such as the redox potential and microbial degradation of WTRs should also be investigated.

LIST OF REFERENCES

Agbenin, J.O., and H. Tiessen, 1994. Phosphorus transformations in a toposequence of lithosols and cambisols from semiarid northeastern Brazil. Geoderma 62: 345-362.

Agbenin, J.O., and H. Tiessen, 1995. P sorption at field capacity and soil ionic strength: kinetics and transformation. Soil Sci. Soc. Am. J. 59:998-1005.

Ainsworth, C.C. and M.E. Sumner, 1985. Effect of aluminium substitution in goethite on P adsorption: II. Rate of adsorption. Soil Sci. Soc. Am. J. 49:1149-1153.

Ainsworth, C.C., J.L Pilon, P.L. Gassman, and W.G. Van Der Sluys, 1994. Cobalt, cadmium and lead sorption to hydrous iron oxide: Residence time effect. Soil Sci. Soc. Am. J. 58: 1615-1623.

Altin, O., O. Ozbelge, and T. Dogu, 1999. Effect of pH in an aqueous medium on the surface area, pore size, distribution, density and porosity of montmorillonite. J. Colloid Interf. Sci. 217: 19-27.

American Society of Civil Engineers, 1996. *Management of water treatment plant residuals*. American society of Civil Engineers, NY and American Water Works Association, Denver, CO.

Anderson, M.A., Tejedor-Tejedor, M.I. and R.R. Stanforth, 1985. Influence of aggregation on uptake kinetics of phosphate by goethite. Environ. Sci. Technol. 19: 632-637.

Anderson, S.J., K.E. Sanders and K.J. Steyer, 1996. Effect of colloidal goethite and kaolinite on colorimetric phosphate analysis. J. Environ. Qual. 25: 1332-1338.

Ann, Y., Reddy, K.R., and J.J., Delfino, 2000. Influence of chemical amendments on phosphorus immobilization in soils from a constructed wetland. Ecol. Engin. 14: 157-167.

Axe, L., and P. Trivedi, 2002. Intraparticle surface diffusion of metal contaminants and their attenuation in microporous amorphous Al, Fe, and Mn oxides. J. Colloid Interf. Sci. 247: 259-265.

Bache, B.W. 1963. Aluminum and iron phosphate studies relating to soil. I. Solution and hydrolysis of variscite and strengite. J. Soil Sci. 14: 113-123.

Bache, B.W., 1964. Al and Fe phosphate studies relating to soil. II. Reactions between phosphate and hydrous oxide. J. Soil Sci. 15: 110-116.

Baig, A.A., J.L Fox, J. Hsu, Z. Wang, M. Otsuka, W.I., Higushi, and R.Z. LeGeros, 1996. Effect of carbonate content and crystallinity on the metastable equilibrium solubility behavior of carbonated apatites. J. Colloid Interf. Sci. 179: 608-617.

Baltpurvins, K.A., R.C. Burns, and G.A. Lawrance, 1996. Effect of pH and anion type on the aging of freshly precipitated Iron (III) hydroxide sludges. Environ. Sci. Technol. 30: 939-944.

Barcelo J, Poschenrieder C, Vazquez MD, and Gunse B., 1996. Aluminium phytotoxicity- A challenge for plant scientists. Fert. Res. 43: 217-223.

Barnett, G.M., 1994. P forms in animal manure. Bioresource Tech. 49: 139-147.

Barrer, R.M., 1978. *Zeolites and clay minerals as sorbents and molecular sieves*. pp.272-275. Academic Press, London, U.K.

Barron, V., Galvez, N., Hochella, M.F. Jr., and Torrent, J., 1997. Epitaxial growth of goethite on hematite synthesized in phosphate media: A scanning force and transmission electron microscopy study, American Mineralogist 82: 1091-1100.

Barrow, N.J., 1985. Reactions of cations and anions with variable-charge soils. Adv. Agron. 38:183-230.

Basta, N.T., R.J. Zupancic and E.A. Dayton, 2000. Evaluating soil tests to predict bermudagrass growth in drinking water treatment residuals with P fertilizer. J. Environ. Qual. 29: 2007-2012.

Beek, J., F.A.M. de Haan, and W.H. van Riemsdijk, 1977. Phosphates in soils treated with sewage water: II. Fractionation of accumulated phosphates. J. Environ. Qual. 6: 7-12.

Bertrand, I., N. Grignon, P. Hinsinger, G. Souche, and B. Jaillard, 2000. The use of secondary ion mass spectrometry coupled with image analysis to identify and locate chemical elements in soil minerals: the example of phosphorus. Scanning 23: 279-291.

Bhadoria, P.B.S., J. Kaselowsky, N. Claassen, and J. Jungk, 1991. Soil phosphate diffusion coefficients: Their dependence on phosphorus concentration and buffer power. Soil Sci. Soc. Am. J. 55: 56-60.

Bhatti, J.S., 1995. Influence of soil organic matter on P and oxalate sorption and desorption in a spodic horizon. Ph.D Thesis. Univ. of Florida, Gainesville, 1995.

Bhatti, J.S., N.B. Comerford, and C.T. Johnston, 1998. Influence of oxalate and soil organic matter on sorption and desorption of phosphate onto a spodic horizon. Soil Sci. Soc. Am. J. 62: 1089-1095.

Biber, M.V., Dos Santos Afonso, M., and Stumm, W., 1994. The coordination chemistry of weathering: IV. Inhibition of the dissolution of oxide minerals. Geochim. Cosmochim. Acta 58: 1999-2010.

Bolan, N.S., N.J. Barrow, and A.M.M. Posner, 1985. Describing the effect of time on sorption of phosphate by iron and aluminium hydroxides. J. Soil Sci. 36: 187-197.

Bondietti, G., J. Sinniger, and W. Stumm, 1993. The reactivity of Fe(III) (hydr)oxides: effects of ligands in inhibiting the dissolution. Colloids Surf. 79: 157-167.

Bramley, R.G.V., Barrow, N.J., and T.C. Shaw, 1992. The reaction between phosphate and dry soil. 1. The effect of time, temperature and dryness. J. Soil Sci. 43: 749-758.

Brown, E.A., and J.B. Sartain, 2000. Phosphorus retention in USGA greens. Soil Crop Sci. Soc. Fl. Proc. 59: 112-117.

Burns, R.T., Moody, L.B., Walker, F.R., and D.R. Raman, 2001. Laboratory and in-situ reductions of soluble P in swine waste slurries. Environmental Technology 22: 1273-1278.

Burrell, L.S, C.T. Johnston, D. Schulze, J. Klein, J.L. White, and S.L. Hem, 2001. Aluminium phosphate adjuvants prepared by precipitation at constant pH. Part I: composition and structure. Vaccine 19: 275-281.

Butkus, M.A., D. Grasso, C.P. Schulthess, and H. Wijnja, 1998. Surface complexation modeling of phosphate adsorption by water treatment residual. J. Environ. Qual. 27: 1055-1063.

Cabrera, F., P. De Arambarri, L. Madrid, and G.G. Toca, 1981. Desorption of phosphorus from iron oxide in relation to pH and porosity. Geoderma 26:203-216.

Campbell, A.S., Schwertmann U., Stanjek H., Friedl J., Kyek A., and Campbell P.A. 2002. Si incorporation into hematite by heating Si-ferrihydrite. Langmuir 18: 7804-7809.

Carta G, and A. Ubiera, 2003. Particle-size distribution effects in batch adsorption. AIChE 49: 3066-3073.

Castillo, A.E., Conejo, P. Pedregal, R. García and N. Alguacil, 2001. *Building and Solving Mathematical Programming Models in Engineering and Science*. Pure and Applied Mathematics: A Wiley-Interscience Series of Texts, Monographs, and Tracts, New York, 2001.

Cavallaro, N., N. Padilla, and J. Villarrubia, 1993. Sewage sludge effects on chemical properties of acid soils. Soil Sci. 156: 63-70.

Chang, A.C., A.L. Page, F.H. Sutherland and E. Grgurevic, 1983. Fractionation of P in sludge affected soils. J. Environ. Qual. 12: 286-290.

Christmas, K.G., L.B. Gower, S.R. Khan, and H. El-Shall, 2002. Aggregation and dispersion characteristics of calcium oxalate monohydrate: Effect of urinary species. J. Colloid Interf. Sci. 256:168-174.

Chwirka, J.D., R. Narasimhan, N. Scheuer and G. Rousseau, 2001. The impact of residuals on the selection of an arsenic treatment process. WEF/AWWA/CWEA Joint Residuals and Biosolids Management Conference. Biosolids 2001: "Building Public Support".

Codling, E.E., R.L. Chaney and C.L. Mulchi, 2000. Use of aluminum and iron-rich residues to immobilize P in poultry litter and litter-amended soils. J. Environ. Qual. 29: 1924-1931.

Cornell and Schwertmann, 1979. Influence of organic anions on the crystallization of ferrihydrite, Clays Clay minerals 6:402-410.

Cornell, R.M., and R. Giovanoli, 1985. Effect of solution conditions on the proportion and morphology of goethite formed from ferrihydrite. Clays Clay Minerals 33: 424-432.

Cox, A.E., J.J. Camberato, and B.R. Smith, 1997. Phosphate availability and inorganic transformation in an alum sludge-affected soil. J. Environ. Qual. 26: 1393-1398.

Crank, J., 1975. *The mathematics of diffusion*, 2nd ed. Oxford, U.K. (Univ. Press).

Cussler, E.L., 1997. *Diffusion mass transfer in fluid systems*, 2nd ed. pp.47-48, 412. Cambridge University Press, Cambridge, UK.

Dao, T.H., 1999. Coamendments to modify phosphorus extractability and nitrogen / phosphorus ratio in feedlot manure and composted manure. J. Environ. Qual. 28: 1114-1121.

Davis, J.A., R.O. James and J.O. Leckie, 1978. Surface ionization and complexation at the oxide / water interface. J. Colloid Interf. Sci. 63: 480-499.

Dayton, E.A., N.T. Basta, C.A. Jakober, and J.A. Hattey, 2003. Using treatment residuals to reduce phosphorus in agricultural runoff. J. Am. Wat. Works Association 95: 151-158.

De Jonge, H., and M.C. Mittelmeijer-Hazeleger, 1996. Adsorption of CO_2 and N_2 on soil organic matter: nature of porosity, surface area and diffusion mechanisms. Environ. Sci. Technol. 30: 408-413.

Design-Expert, 2001. *Software for design of experiments*, version 6.0.5, Stat-Ease Inc. Minneapolis, MN.

Desroches, S., S. Daydé, and G. Berthon, 2000. Aluminum speciation studies in biological fluids. Part 6. Quantitative investigation of aluminum(III)–tartrate complex equilibria and their potential implications for aluminum metabolism and toxicity. J. Inorg. Biochem. 81: 301-312.

Diakonov, I., I. Khodakovsky, J. Schott, and E. Sergeeva, 1994. Thermodynamic properties of iron oxides and hydroxides. I. Surface and bulk thermodynamic properties of goethite (α-FeOOH) up to 500 K. Eur. J. Miner. 6: 967-983.

Dou, Z., Zhang, G.Y., Stout, W.L., Toth, J.D., and J.D., Ferguson, 2003. Efficacy of alum and coal combustion by-products in stabilizing manure phosphorus. J. Environ. Qual. 32: 1490-1497.

Dubinin, M.M., The potential theory of adsorption of gases and vapors for adsorbents with energetically nonuniform surfaces, Chem. Rev. 1959, 235-241.

Dzombak, D.A., and F.M.M. Morel. *Surface Complexation Modeling-Hydrous Ferric Oxide*; J. Wiley and Sons: NY, 1990. pp.22-26.

Eick, M.J., J.D. Peak, and W.D. Brady, 1999. The effect of oxyanions on the oxalate-promoted dissolution of goethite. Soil Sci. Soc. Am. J. 63: 1133-1141.

Elliott, H.A. and B.A. Dempsey, 1991. Agronomic effects of land application of water treatment sludges. J. A.W.W.A. 84: 126-131.

Elliott, H.A., and L.M. Singer, 1988. Effect of water treatment sludge on growth and elemental composition of tomato (*Lycopersicon esculentum*) shoots. Commun. Soil Sci. Plant Anal. 19: 345-354.

Elliott, H.A., B.A. Dempsey, D.W. Hamilton, and J.R. DeWolfe, 1990. Land application of water treatment sludges: Impacts and management. AWWA Res. Foundation and Am Water Works Association, Denver, CO.

Elliott, H.A., G.A. O'Connor, and S. Brinton, 2002. Phosphorus leaching from biosolids-amended sandy soils. J. Environ. Qual. 31: 1362-1369.

Elliott, H.A., G.A. O'Connor, P. Lu, and S. Brinton, 2002. Influence of water treatment residuals on phosphorus solubility and leaching. J. Environ. Qual. 31: 681-689.

Everett, D.H., and Powl, J., 1976. J. Chem. Soc. Faraday Trans. 72: 619.

Farrell, J., D. Grassian, and M. Jones, 1996. Investigation of mechanisms contributing to slow desorption of hydrophobic organic compounds from mineral solids. Environ. Sci. Technol. 33: 1237-1243.

Fendorf, S., M.J. Eick, P. Grossl, and D.L. Sparks, 1997. Arsenate and chromate retention mechanisms on goethite. 1. Surface structure. Environ. Sci. Technol. 31: 315-320.

Fischer, L., Muhlen, E., Brummer, G.W., and Niehus, H., 1996. Atomic force microscopy investigations of the surface topography of a multidomain porous goethite. Eur. J. Soil Sci. 47:329-334.

Flaig, E., and K.R. Reddy, 1995. Fate of phosphorus in the Lake Okeechobee ecosystem Florida, USA: overview and recommendations. Ecol. Eng. 5: 127-142.

Ford, R.G., 2002. Rates of hydrous ferric oxide crystallization and the influence on coprecipitated arsenate. Environ. Sci. Technol. 36: 2459-2463.

Ford, R.G., P.M. Bertch, and K.J. Farley, 1997. Changes in transition and heavy metal partitioning during hydrous iron oxide aging. Environ. Sci. Technol. 31: 2028-2033.

Fox, T.R., N.B. Comerford, and W.W. McFee, 1990b. Kinetics of P release from Spodosols: Effect of oxalate and formate. Soil Sci. Soc. Am. J. 54: 1441-1447.

Fuller, C.C., J.A. Davis, and Waychunas, G.A., 1993. Surface chemistry of ferrihydrite: Part 2. Kinetics of arsenate adsorption and precipitation. Geochim. et Cosmochim. Acta 57: 2271-2282.

Galarneau, E., and R. Gehr, 1997. P removal from wastewaters: experimental and theoretical support for alternative mechanisms. Wat. Res. 31: 328-338.

Gallimore, L.E., N.T. Basta, D.E. Storm, M.E. Payton, R.H. Huhnke, and M.D. Smolen, 1999. Water treatment residual to reduce nutrients in surface runoff from agricultural land. J. Environ. Qual. 28: 1474-1478.

Galvez, N., V. Barron and J. Torrent, 1999a. Effect of phosphate on the crystallization of hematite, goethite and lepidocrocite from ferrihydrite. Clays Clay Miner. 47: 304-311.

Galvez, N., V. Barron and J. Torrent, 1999b. Preparation and properties of hematite with structural P. Clays Clay Miner. 47: 375-385.

Garrido, J., A. Linares-Solano, J.M. Martin-Martinez, M. Molina-Sabio, F. Rodriguez-Reinoso, and R. Torregrosa, 1987. Use of N_2 vs. CO_2 in the characterization of activated carbons. Langmuir 3: 76-81.

Goldberg, S., I. Lebron, D.L. Suarez, and Z.R. Hinedi, 2001. Surface characterization of amorphous aluminum oxides. Soil Sci. Soc. Am. J. 65: 78-86.

Grathwohl, 1998. *Diffusion in natural porous media: Contaminant transport, sorption/desorption and dissolution kinetics*. Kluwer Academic Publishers, AH Dordrecht, the Netherlands.

Gregg, S.J., and K.S.W. Sing, 1982. *Adsorption, surface area, and porosity*. 2nd ed. London; New York: Academic Press, 1982.

Gregor, J.E., C.J. Nokes, and E. Fenton, 1997. Optimizing natural organic matter removal from low turbidity waters by controlled pH adjustment of aluminium coagulation. Wat. Res. 31: 2949-2958.

Guo, G., and A. Chong Lua, 2002. Microporous activated carbons prepared from palm shell by thermal activation and their application to sulfur dioxide adsorption. J. Colloid Interf. Sci. 251: 242-247.

Hano, T., H. Takanashi, M. Hirata, k. Urano, and S. Eto, 1997. Removal of phosphorus from wastewater by activated alumina adsorbent. Wat. Sci. Tech. 35: 39-46.

Harris, W.G., Wang, H.D., and K.R. Reddy, 1994. Dairy manure influence on soil and sediment composition - implications for phosphorus retention. J. Environ. Qual. 23, 1071-1081.

Harris-Pierce, R., K.A. Barbarick, and E.F. Redente, 1993. The effect of sewage sludge application on native rangeland soils and vegetation. Annual Report Meadow Springs Ranch, Fort Collins, CO.

Haustein, G.K., T.C. Daniel, D.M. Miller, P.A. Moore, Jr. and R.W. Mcnew, 2000. Aluminum-containing residuals influence high-P soils and runoff water quality. J. Environ. Qual. 29: 1954-1959.

Hawke D. J., Powell K. J. and Gregor J. E. (1996). Determination of the aluminium complexing capacity of fulvic acids and natural waters, with examples from five New Zealand rivers. *Mar. Freshwat. Res.* 47, 11-17.

He, Z.L., A.K. Alva, Y.C. Li, D.V. Calvert, and D.J. Banks, 1999. Sorption-desorption and solution concentration of P in a fertilized sandy soil. J. Environ. Qual. 28: 1804-1810.

Hedley, M.J., W.B. Stewart, and B.S., Chauhan, 1982a. Changes in inorganic and organic soil phosphorus fractions induced by cultivation practices and by laboratory incubations. Soil Sci. Soc. Am. J. 46: 970-975.

Heil, D.M., and K.A. Barbarick, 1989. Water treatment sludge influence on the growth of sorghum-sudangrass. J. Environ. Qual. 18: 292-298.

Hetrick, J.A., and A.P. Schwab, 1992. Changes in aluminum and phosphorus solubilities in response to long-term fertilization. Soil Sci. Soc. Am. J. 56: 755-761.

Hiemenz, P.C., and R. Rajagopalan. *Principles of Colloid and Surface Chemistry*, 3rd. Ed., New York: Marcel Dekker, 1997.

Hofmann, A., M. Pelletier, L. Michot, A. Strander, P. Schurtenberger, and R. Kretzschmar, 2004. Characterization of the pores in hydrous ferric oxide aggregates formed by freezing and thawing. J. Colloid and Interf. Sci. 271: 163-173.

Hoge, V.R., R. Conrow, M. Coveney, and J. Peterson, 2003. The application of alum residual as a phosphorus abatement tool within the lake Apopka restoration area. WEF proceedings conference Alexandria Va.

Horanyi, G., 2002. Specific adsorption of simple organic acids on metal(hydr)oxides: A radiotracer approach. J. Colloid Interf. Sci. 254: 214-221.

Hsu, P.H., 1979. Effect of phosphate and silicate on the crystallization of gibbsite from OH-Al solutions. Soil Sci. 127: 219-226.

Hsu, P.H., 1982a. Crystallization of variscite at room temperature. Soil Sci. 133: 305-313.

Huang, W., and W.J. Weber, Jr., 1996. A distributed reactivity model for sorption by soils and sediments. 5. The influence of near-surface characteristics of mineral domains. Environ. Sci. Technol. 30: 2993-3000.

Huang, W., and W.J. Weber, Jr., 1997. A distributed reactivity model for sorption by soils and sediments. 10. Relationships between desorption, hysteresis, and the chemical characteristics of organic domains. Environ. Sci. Technol. 31: 2562-2569.

Hue, N.V., 1991. Effects of organic acids / anions on P sorption and phytoavailability in soils with different mineralogies. Soil Sci. 152: 463-471.

Hunger, S., H. Cho, J.T. Sims, and D.L. Sparks, 2004. Direct speciation of phosphorus in alum-amended poultry litter: solid-state ^{31}P NMR investigation. Environ. Sci. Technol. 38: 674-681.

Ippolito, J.A., K.A. Barbarick, and E.F., Rendte, 1999. Co-application of water treatment residuals and biosolids on two range grasses. J. Environ. Qual. 28: 1644-1650.

Ippolito, J.A., K.A. Barbarick, D.M. Heil, J.P. Chandler, and E.F., Redente, 2003. Phosphorus retention mechanisms of a water treatment residual. J. Environ. Qual. 32: 1857-1864.

Jacobs, L.W. and B.J. Teppen, 2000. WTR as a soil amendment to reduce nonpoint source pollution from phosphorus-enriched soils. 9 p. In Proc. 14th Annual Residuals and Biosolids Management Conference, Feb. 27-29, 2000, MA. CD-ROM, Water Environment Federation, Alexandria, VA.

James, R.O., and T.W. Healy, 1972. Adsorption of hydrolysable metal ions at the oxide-water interface, adsorption on SiO_2 and TiO_2 as model systems. J. Colloid Interf. Sci. 40:42-52.

Jaroniec M, Gilpin R. K., Staszczuk P, and Choma J., 1994. Studies of surface and structural heterogeneities of microporous carbons by high-resolution thermogravimetry. Characterization of porous solids. III. Studies in surface science and catalysis 87: 613-622.

Kandori, K, and Ishikawa T., 1999. TPD-MS-TG study of hematite particles produced by the forced hydrolysis reaction. Physical chemistry chemical physics 3: 2949-2954.

Kudeyarova, A. Yu, 1981. Aluminium phosphates as products of transformations of fertilizer phosphorus in an acid soil. Geoderma 26: 195-201.

Lane, C.T. Water treatment residuals effects on phosphorus in soils amended with dairy manure. Master's Thesis, Soil and Water Science Dept., Univ. of Florida, Gainesville, FL, 2002.

Langmuir, D., 1971. Particle size effect on the reaction: goethite=hematite + water. Amer. J. Sci. 272: 972.

Lefcourt, A.M., and J.J. Meisinger, 2001. Effect of adding alum or zeolite to dairy slurry on ammonia volatilization and chemical composition. J. Dairy Sci. 84: 1814-1821.

Ler, A., and R. Stanforth, 2003. Evidence for surface precipitation of phosphate on goethite. Environ. Sci. Technol. 37: 2694-2700.

Li, L., and R.J. Stanforth, 2000. Distinguishing adsorption and surface precipitation of phosphate on goethite (alpha-FeOOH). J. Colloid Interf. Sci. 230: 12-21.

Li, Y., and C.J. Werth, 2004. Slow desorption mechanisms of volatile organic chemical mixtures in soil and sediment micropores. Environ. Sci. Technol. 38: 440-448.

Livesey, N.T., and P.M. Huang, 1981.Adsorption of arsenate by soils and its relationship to selected chemical properties and anions. Soil Sci. 131: 88-94.

Lookman, R., P. Grobet, R. Merckx, and W.H. Van Riemsdijk, 1997. Application of ^{31}P and ^{27}Al MAS NMR for phosphate speciation studies in soil and aluminum hydroxides: promises and constraints. Geoderma 80: 369-388.

Lu. P. and G.A. O'Connor, 2001. Biosolids effects on P retention and release in some sandy Florida soils. J. Environ. Qual. 30:1059-1063.

Ludwig, C. and W.H. Casey, 1996. The effect of different functional groups on the ligand-promoted dissolution of NiO and other oxide minerals. Geochim. Cosmochim. Acta 60: 213-224.

Ma, Y.B., and N.C. Uren, 1997. The effects of temperature, time and cycles of drying and rewetting on the extractability of zinc added to a calcareous soil. Geoderma 75: 89-97.

Madrid, L., and A.M. Posner, 1979. Desorption of phosphate from goethite. J. Soil Sci. 30: 697-707.

Madrid, L., and P. De Arambarri, 1985. Adsorption of phosphate by two iron oxides in relation to their porosity. J. Soil Sci. 36: 523-530.

Manning, B.A., and S. Goldberg, 1997. Adsorption and stability of As(III) at the clay mineral-water interface. Environ. Sci. Technol. 31: 2005-2011.

Martin, R.R., R. St.C. Smart, and K. Tazaki, 1988. Direct observation of phosphate precipitation in the goethite/phosphate system. Soil Sci. Soc. Am. J. 52:1492-1500.

Martinez, C.E. and M.B. McBride, 1998. Solubility of Cd, Cu, Pb, and Zn in aged coprecipitates with amorphous iron hydroxides. Environ. Sci. Technol. 32: 743-748.

Martinez, C.E. and M.B. McBride, 2000. Aging of coprecipitated Cu in alumina: Changes in structural location, chemical form, and solubility. Geochim. Cosmochim. Acta 64:1729-1736.

Martinez, C.E., and M.B. MacBride, 1998. Coprecipitates of Cd, Cu, Pb, and Zn in iron oxides: solid phase transformations and metal solubility after aging and thermal treatment. Clays and Clay Minerals 46: 537-545.

Martínez,C.E, A. Jakobson, and M.B. McBride, 2001. Thermally induced changes in metal solubility of contaminated soils is linked to mineral recrystallization and organic matter transformations. Environ. Sci. Technol. 35: 908-916.

Martínez,C.E. S. Sauvé, A. Jacobson, and Murray B. McBride, 1999. Thermally induced release of adsorbed Pb upon aging of Ferrihydrite and soil oxides, Environ. Sci. Technol. 33: 2016-2020.

Mason, R.L., Gunst, R.F., and J.L. Hess. *Statistical design and analysis of experiments with applications to engineering and science*. Wiley, NY, 1989.

Maurer, M., and M. Boller, 1999. Modeling of P precipitation in wastewater treatment plants with enhanced biological P removal. Water Sci. Technol. 39: 147-163.

McKeague, J.A., J.E Brydon and N.M. Miles, 1971. Differentiation of forms of extractable iron and aluminum in soils. Soil Sci. Soc. Am. Proc. 35:33-38.

Mishra T., Parida K.M., Rao S.B., 1998. Cation exchange and sorption properties of aluminum phosphate. Sep. Sci. Technol. 33: 1057-1073

Molis, E., F. Thomas, and J.Y. Bottero, 1997. Colloidal chemistry of mineral coagulants as influenced by organic ligands. *In Aqueous chemistry and geochemistry of oxides, oxyhydroxides, and related materials*. volume 432, pp. 357. Materials research society symposium proceedings, San Francisco, CA.

Moore, P.A., Jr., T.C. Daniel, D.R. Edwards, and J.T. Gilmour, 1998. *Effect of alum-treated poultry litter, normal litter and ammonium nitrate on aluminum availability and uptake by plants*. Proceedings of the 1998 National Poultry Waste Management Symposium.

Moore, P.A. Jr., 1998. *Reducing ammonia volatilization and decreasing phosphorus runoff from poultry litter with alum*. Proceedings of the 1998 National Poultry Waste Management Symposium.

Moore, P.A., Jr., T.C. Daniel, D.R. Edwards, and D.M. Miller, 1996. Evaluation of chemical amendments on ammonia volatilization from poultry litter. Poultry Sci. 75: 315-320.

Moore, P.A., Jr., T.C. Daniel, and D.R. Edwards, 1999. Reducing phosphorus runoff and improving poultry production with alum. Poultry Sci. 78:692-698.

Muljadi, D., A.M. Posner, and J.P. Quirk, 1966b. The mechanism of phosphate adsorption by kaolinite, gibbsite and pseudoboehmite. II. The location of the adsorption sites. J. Soil Sci. 17: 230-237.

Muljadi, D., A.M. Posner, and J.P. Quirk, 1966c. The mechanism of phosphate adsorption by kaolinite, gibbsite and pseudoboehmite. III. The effect of temperature on the adsorption. J. Soil Sci. 17: 238-246.

Ng Kee Kwong K., and P. M. Huang, 1981. Comparison of the influence of tannic acid and selected low molecular weight organic acids on precipitation products of aluminum. Geoderma 26: 179-193.

Nooney, M.G., A. Campbell, T.S. Murrell, X.-F. Lin, L.R. Hossner, C.C. Chusuei, and D.W. Goodman, 1998. Nucleation and growth of phosphate on metal oxide thin films. Langmuir 14: 2750-2755.

Norrish, K., and H. Rosser. *Mineral phosphate*: *In* Soils: An Australian Viewpoint. CSIRO Publisher, Melbourne (1983) 335-361.

O'Connor, G.A. and H.A. Elliott, 2000. *Co-application of biosolids and water treatment residuals*. Final Report. Florida Dep. of Environ. Protection, Tallahassee, FL.

O'Connor, G.A., H.A. Elliott, and P. Lu, 2001. Characterizing water treatment residuals Phosphorus retention. Soil Crop Sci. Soc. Fl. Proc. 61: 67-73.

O'Melia, C.R., 1989. Particle-particle interactions in aquatic systems. Colloids Surf. 39: 255-271.

O'Reilly, S.E., D.G. Strawn and D.L. Sparks, 2001. Residence time effects on arsenate adsorption / desorption mechanisms on goethite. Soil Sci. Soc. Am. J. 65: 67-77.

Ohno, T. and L.M. Zibilske, 1991. Determination of low concentrations of phosphorus in soil extracts using malachite green. Soil Sci. Soc. Am. J. 55: 892-895.

Omoike, A.I., and G.W. Vanloon, 1999. Removal of phosphorus and organic matter removal by alum during wastewater treatment. Wat. Res. 33: 3617-3627.

Ozacar, M., and I.A. Sengil, 2003. Enhancing phosphate removal from wastewater by using polyelectrolytes and clay injection. J.Haz. Mat.. B 100: 131-146.

Parfitt, R.L., 1979. The availability of P from phosphate-goethite bridging complexes. Desorption and uptake by ryegrass. Plant and Soil 53: 55-65.

Parfitt, R.L., R.J. Atkinson, and R. St. C. Smart, 1975. The mechanism of phosphate fixation by iron oxides. Soil Sci. Soc. Am. Proc. 39: 837-841.

Peak, D., J.T. Sims., and D.L. Sparks, 2002. Solid-state speciation of natural and alum-amended poultry litter using XANES spectroscopy. Environ. Sci. Technol. 36: 4253-4261.

Peters, J.M., and N.T. Basta, 1996. Reduction of excessive bioavailable phosphorus in soils by using municipal and industrial wastes. J. Environ. Qual. 25: 1236-1241.

Pierzynski, G.M., Logan, T.J., Traina, S.J., and J.M. Bigham, 1990. P chemistry and mineralogy in excessively fertilized soils: Quantitative analysis of P-rich particles. Soil Sci. Soc. Am. J. 54: 1576-1583.

Pignatello, J.J., F.J. Ferrandino, and L.Q. Huang, 1993. Environ. Sci. Technol. 27: 1563-1571.

Postma, D. and R. Jakobsen, 1996. Redox zonation: Equilibrium constraints on the Fe(III) / SO_4 reduction interface. Geochim. Cosmochim. Acta 60: 3169-3175.

Prakash, P., and A. K. Sengupta, 2003. Selective coagulant recovery from water treatment plant residuals using donnan membrane process. Environ. Sci. Technol. 37: 4468-4474.

Qureshi, R.H., Jenkins, D.A., Davies, R.I., and Rees, J.A. 1969. Application of microprobe analysis to study of phosphorus in soils. Nature 221: 1142-.

Ran, Y., W. Huang, P.S.C. Rao, D. Liu, G. Sheng, and J. Fu, 2002. The role of condensed organic matter in the nonlinear sorption of hydrophobic organic contaminants by a peat and sediments. J. Environ. Qual. 31: 1953-1962.

Rao, J.L., and Berner, R.A., 1995. Development of an electron-microprobe method for the determination of phosphorus and associated elements in sediments. Chem. Geology 125: 169-183.

Ravikovitch, P.I., A.V. Neimark, and B.W. Bogan, 2003. Characterization of porosity and distribution of organic matter in soils using high-resolution gas adsorption. Abstract presented before the division of environmental chemistry, American Chemical Society, New York, NY, September 7-11. vol. 43: 925-928.

Reddy, K.R., M.R. Overcash, R. Khaleel, and P.W. Westerman, 1980. P adsorption-desorption characteristics of two soils utilized for disposal of animal wastes. J. Environ. Qual. 9: 87-92.

Reynolds, R.C. Jr.. Diffraction by small and disordered crystals. In *Modern Powder Diffraction*; Bish, D.L., Post, J.E., Eds.; Reviews in Mineralogy Volume 20; Mineralogical Society of America: Washington, DC, 1989; pp. 145-181.

Rodriguez-Reinoso, F. and Linares-Solano, A., *In Chemistry and Physics of Carbon*, Vol. 21 (Thrower, P. A., Ed.) Marcel Dekker, New York, 1988.

Saito, A., and H.C. Foley, 1991. Curvature and parametric sensitivity in models for adsorption in micropores. AlChE J. 37: 429-436.

Sahu, B.B., and K. Parida, 2002. Cation exchange and sorption properties of crystalline α-titanium(IV) phosphate. J. Colloid Interf. Sci. 248: 221-230.

SAS Institute, 1985. SAS User Guide. Statistics. Version 5 ed. SAS Institute, Cary, NC.

Saunders, W.M.H., and E.G. Williams, 1955. Observations on the determination of total organic P in soils. J. Soil Sci. 6: 254-267.

Scheidegger, A.M., and D.L. Sparks, 1996. A critical assessment of sorption-desorption mechanisms at the soil mineral/water interface. Soil Sci. 161:813-831.

Schwertmann, U., J. Friedl, and H. Stanjek, 1999. From Fe (III) to ferrihydrite and then to hematite. J. Colloid Interf. Sci. 209: 215-223.

Schwertmann, U., R.M., Cornell. *Iron Oxides in the Laboratory*, Wiley-VCH: Wienheim, 1991; pp. 1-12.

Self-Davis, M.L., P.A. Moore, Jr., T.C. Daniel, and D.R. Edwards, 1998. Use of aluminum sulfate to reduce soil test P levels in soils fertilized with poultry litter. Proceedings of the 1998 National Poultry Waste Management Symposium.

Sharpley, A.N., 1996. Availability of residual P in manured soils. Soil Sci. Soc. Amer. J. 60: 1459-1466.

Sharpley, A.N., and B. Moyer, 2000. P forms in manure and compost and their release during simulated rainfall. J. Environ. Qual. 29: 1462-1469.

Shreve, B.R., P.A. Moore, Daniel, T.C., Edwards, D.R., and D.M., Miller, 1995. Reduction of phosphorus in runoff from field-applied poultry litter using chemical amendments. J. Environ. Qual. 24: 106-111.

Sims, J.T., and B.G. Ellis, 1983. Changes in P adsorption associated with aging of aluminium hydroxide suspensions. Soil Sci. Soc. Am. J. 47: 912-916.

Sims, J.T., and N.J. Luka-McCafferty, 2002. On-farm evaluation of aluminum sulfate (alum) as a poultry litter amendment: Effects on litter properties. J. Environ. Qual. 31: 2066-2073.

Sorensen, M.A., M.M. Stackpoole, A.I. Frenkel, R.K. Bordia, G.V. Korshin and T.H. Cristensen, 2000. Aging of iron (hydr)oxides by heat treatment and effects on heavy metal binding. Environ. Sci. Technol. 34: 3991-4000.

Sowder, A.G., S.B. Clark, and R.A. Fjeld, 1999. The transformation of uranyl oxide hydrates: The effect of dehydration on synthetic Metaschoepite and its alteration to Becquerelite. Environ. Sci. Technol., 33: 3552-3557.

Spadini, L., Manceau, A., Schindler, P.W., and Charlet, L., 1994. Structure and stability of Cd surface complexes on ferric oxides I. Results from EXAF spectroscopy. J. Colloid Interf. Sci. 168: 73-86.

Sparks, D.L., 1996. *Method of soil analysis: chemical methods*. SSSA Book Series (part 3). Soil Sci. Soc. Am. Inc. Madison, WI.

Stevenson, F.J., and Vance, G.F., 1989. Naturally occuring aluminum-organic complexes. *In*: G. Sposito (Ed). *The environmental chemistry of aluminum* (pp. 117-145). CRC Press Boca Raton, FL.

Strauss, R., G.W. Brummer, and N.J. Barrow, 1997. Effects of crystallinity of goethite: I. Preparation and properties of goethites of differing crystallinity. Eur. J. Soil Sci. 48: 87-99.

Strauss, R., G.W. Brummer, and N.J. Barrow, 1997. Effects of crystallinity of goethite: II. Rates of sorption and desorption of phosphate. Eur. J. Soil Sci. 48: 101-114.

Tamura, H., K. Mita, A. Tanaka, and M. Ito, 2001. Mechanism of hydroxylation of metal oxide surfaces. J. Colloid Interf. Sci. 243: 202-207.

Tejedor-Tejedor, M.I., and M.A. Anderson, 1990. Protonation of phoshate on the surface of goethite as studied by CIR-FTIR and electrophoretic mobility. Langmuir 6: 602-611.

Tessier, A., D. Fortin, N. Belzile, R.R. DeVitre, and G.G. Leppard, 1996. Metal sorption to diagenetic iron and manganese oxohydroxides and associated organic matter: narrowing the gap between field and laboratory measurements. Geochim. Cosmochim. Acta 60:387-404.

Torrent, J. U. Schwertmann, and V. Barron, 1992. Fast and slow phosphate sorption by goethite-rich natural minerals. Clays and Clay Minerals 40:14-21.

Torrent, J., 1987. Rapid and slow phosphate sorption by Mediterranean soils. Effect of iron oxides. Soil Sci. Soc. Am. J. 51: 78-82.

USEPA, 2000. Test Methods for Evaluating Solid Waste, Physical/Chemical Methods, USEPA-65 FR 70678, Draft Update IVB SW-846. U. S. Governmental Printing Office: Washington, DC.

Valenta, P., Maier, K., Kronmuller, H., and Freitag, K., 1981. Self-diffusion of phosphorus in the amorphous alloy $Fe_{40}Ni_{40}P_{14}B_6$. Phys. Status Solidi (b) 105: 537-542.

Van Der Zee, S.E.A.T.M., and van Riemsdijk, 1990. Model for the reaction kinetics of phosphate with oxides and soil. *In: Interactions at the Soil Colloid-Soil Solution Interface*, (eds. G.H. Bolt et al.), pp.205-239. Kluwer Academic Pubs.

Van Riemsdijk, W.H., and J. Lyklema, 1980. Reaction of phosphate with gibbsite beyond the adsorption maximum. J. Colloid Interf. Sci. 76: 55-66.

Van Riemsdijk, W.H., F.A. Weststrate and G.H. Bolt, 1975. Evidence for a new aluminum phosphate phase from reaction rate of P with aluminum hydroxide. Nature (London) 257: 473-474.

Vansant, E.F., 1990. *Pore size engineering in zeolites. pp. 29-31.* John and Wiley and Sons, England, 1990.

Violante, A., and P.M. Huang, 1985. Influence of inorganic and organic ligands on the formation of aluminum hydroxides and oxohydroxides. Clays and Clay Minerals 33: 181-192.

Vyas, S.N., S.R. Patwardhan, S. Vijayalakshimi, and K.Sri Ganesh, 1994. Adsorption of gases on carbon molecular sieves. J. Colloid Interf. Sci. 168: 275-280.

Waychunas, G.A., B.A. Rea, C.C. Fuller, and J.A. Davis, 1993. Surface chemistry of ferrihydrite: Part 1. EXAFS studies of the geometry of coprecipitated and adsorbed arsenate. Geochim. et Cosmochim. Acta 57: 2251-2269.

Weidler, P.G., 1997. BET sample pretreatment of synthetic ferrihydrite and its influence on the determination of surface area and porosity. J. Porous Mat. 4: 165-169.

Weidler, P.G., and H. Stanjek, 1998. The effect of dry heating of synthetic 2-line and 6-line ferrihydrite: II. Surface area, porosity and fractal dimension. Clay minerals 33: 277-284.

Werth, C.J., and M. Reinhard, 1997. Effects of temperature on trichloroethylene desorption from silica gel and natural sediments. 2. Kinetics. Environ. Sci. Technol. 31: 697-703.

Willett, I.R., and R.B. Cunningham, 1983. Influence of sorbed phosphate on the stability of ferric hydrous oxide under controlled Eh and pH conditions. Austr. J. Soil Res. 21: 301-308.

Willett, I.R., C.J. Chartres, and T.T. Nguyen, 1988. Migration of phosphate into aggregated particles of ferrihydrite. J. Soil Sci. 39: 275-282.

Wu S.C., and Gschwend P.M., 1988. Numerical modeling of sorption kinetics of organic-compounds to soil and sediment particles. Water Resources Res. 24: 1373-1383.

Xia, G., and W.P. Ball, 1999. Adsorption partitioning uptake of nine low-polarity organic compounds on a natural sorbent. Environ. Sci. Technol. 33: 262-269.

Xing, B., and J.J. Pignatello, 1997. Dual-mode sorption of low polarity compounds in glassy poly(vinyl chloride) and soil organic matter. Environ. Sci. Technol. 31: 792-799.

Yamaguchi, N.U., M. Okazaki, and T. Hashitani, 1999. Volume changes due to sulfate, selenate, and phosphate adsorption on amorphous iron (III) hydroxide in an aqueous suspension. J. Colloid Interf. Sci. 209: 386-391.

Yapp, C.J., 1983. Effects of AlOOH-FeOOH solid solution on goethite-hematite equilibrium. Clays and Clay Minerals 31: 239-240.

Zhang, T.Q. and A.F. MacKenzie, 1997. Changes in soil P fractions under long-term corn monoculture. Soil Sci. Soc. Am. J. 61: 485-493.

Zhao, H, and Stanforth, R., 2001. Competitive adsorption of phosphate and arsenate on goethite. Environ. Sci. Technol. 35: 4753-4757.

Zhou, M., R.D. Rhue, and W.G. Harris, 1997. P sorption characteristics of Bh and Bt horizons from sandy coastal plain soils. Soil Sci. Soc. Am. J. 61: 1364-1369.

BIOGRAPHICAL SKETCH

Konstantinos Christos Makris was born February 08, 1974 in Thessaloniki, Macedonia, Greece. He received his Bachelor's degree in Forestry and Natural Environment from Aristotle University in Thessaloniki in 1998. He also received his Master's degree in Agronomy from the University of Kentucky, Lexington, USA. He is currently finishing his Ph.D dissertation at the University of Florida, USA.